Studies on skeletal muscle stem cell biology of the apolipoprotein E deficient mice

Joseph James Barlow Bsc. MSc.

University of Hull

Hull York Medical School

Abstract

Skeletal muscle has tremendous adaptive and regenerative ability, this is achieved through a resource of stem cells which remain present in adults. These cells remain quiescent until activated by myogenic factors, at which point they proliferate and then differentiate into new fibres. To guide this process, the muscle stem cells express different transcription factors: Pax7 when quiescent, MyoD when activated and during proliferation, and Myogenin during differentiation. The present work focuses on the muscle stem cell function of the of the Apolipoprotein E deficient ($ApoE^{-/-}$) mouse, and aims to understand the influence of hyperlipidaemia, as well as senescence on muscle stem cell function.

This thesis uses the atherosclerotic ApoE deficient mouse model, to determine the muscle stem cell function. Muscles of wild type and ApoE deficient mice were dissected, and single fibres or stripped stem cells were cultured to determine the expression patterns of Pax7, MyoD and Myogenin or the proliferation and differentiation capacity respectively. Regeneration of injured muscle was also studied *in vivo* by staining injured muscle of wild type and ApoE mice to detect necrotic fibres, regenerating fibres, and macrophage infiltration. Experimental hyperlipidaemia was induced in cultured myoblasts by culturing with palmitate to determine the influence of oxidative stress in hyperlipidaemia by applying the antioxidant ebselen. Senescence was induced in cultured myoblasts by adding doxorubicin to culture media to determine the proliferation and differentiation capacity of senescent muscle stem cells. Releasate of activated human platelets was applied to senescent cells as a treatment to promote regeneration.

The thesis shows that hyperlipidaemia results in impaired myogenic progression, and muscle stem cells have reduced capacity for both proliferation and differentiation, this is underlined by the fact that the ApoE deficient mouse had impaired recovery after muscle injury. Furthermore, the influence of oxidative stress in hyperlipidaemia was highlighted as the antioxidant ebselen restored muscle stem cell function in culture. Senescence using doxorubicin greatly inhibited proliferation and differentiation of muscle stem cells, and application of growth factors released from activated platelets only partially restored function.

Contents

List of Figures

List of Tables

Thesis Outputs

Peer Reviewed Publication

Barlow, J., Sfyri, P.P., Mitchell, R., Verpoorten, S., Scully, D., Andreou, C., Papadopoulos, P., Patel, K., Matsakas, A., 2021. Platelet releasate normalises the compromised muscle regeneration in a mouse model of hyperlipidaemia. Exp. Physiol. 106, 700–713. https://doi.org/10.1113/EP088937

Conference Abstracts and Presentations

Barlow J, Sfyri P, Verpoorten S, Scully D, Matsakas A (2020). 'Hyperlipidaemic mice have deficits in skeletal myogenesis and impaired muscle regeneration which can be alleviated by antioxidant agents and growth factors' Allam lecture 2020, Hull UK.

Barlow J, Sfyri P, Verpoorten S, Scully D, Matsakas A (2020). 'Muscle stem cell function and skeletal muscle regeneration in a mouse model of experimental atherosclerosis and hyperlipidaemia: Novel insights into the role of ebselen and platelet secretome' British atherosclerosis society conference (BAS), Manchester, UK

Barlow J, Sfyri P, Verpoorten S, Scully D, Matsakas A (2019). 'Regulation of skeletal muscle stem cell functionin a mouse model of experimental atherosclerosis and hyperlipidaemia' British atherosclerosis society conference (BAS), Manchester, UK

Barlow J, Sfyri P, Verpoorten S, Scully D, Matsakas A (2019). 'Compromised skeletal muscle stem cell function in a mouse model of hyperlipidaemia and atherosclerosis' Physiology 2019, Aberdeen, UK

Barlow J, Sfyri P, Verpoorten S, Scully D, Matsakas A (2019). 'Muscle stem cell function in a mouse model of experimental atherosclerosis and hyperlipidaemia'. Allam lecture 2019, Hull, UK

Barlow J, Sfyri P, Verpoorten S, Scully D, Matsakas A (2018). 'The myogenic progression of skeletal muscle satellite cells in Apolipoprotein-E deficient mice' North of England Cell Biology forum (NEB) 2018, Huddersfield, UK

Barlow J, Sfyri P, Verpoorten S, Scully D, Matsakas A (2018). ‘The effect of apolipoprotein-E deficiency on stem-cell progeny of skeletal muscle’. HYMS conference 2018, Hull, UK

Acknowledgements

I would like to express my deepest gratitude to my supervisor Dr Antonios Matsakas for his valuable guidance, support, and advice throughout. My gratitude extends to The University of Hull and The Hull York Medical School for the opportunity and financial support.

I would like to place on record my best regards to Dr Peggy Sfyri for her guidance and assistance in lab experiments.

Special thanks to all my friends and family who have supported me along the way. This thesis is dedicated to my loving parents Paul Barlow and Siobhan Barlow. Thank you for all your support and love.

Declaration

I confirm that this work is original and that if any passage(s) or diagram(s) have been copied from academic papers, books, the internet or any other sources these are clearly identified by the use of quotation marks and the reference(s) is fully cited. I certify that, other than where indicated, this is my own work and does not breach the regulations of HYMS, the University of Hull or the University of York regarding plagiarism or academic conduct in examinations. I have read the HYMS Code of Practice on Academic Misconduct, and state that this piece of work is my own and does not contain any unacknowledged work from any other sources.

Abbreviations

ANOVA	Analysis of variance
ApoE	Apolipoprotein E
ApoE-/-	Apolipoprotein E deficient
ATP	Adenosine triphosphate
cDNA	Copy deoxyribose nucleic acid
CSA	Cross sectional area
Cyp	Cyclophilin
DAPI	4',6-diamidino-2-phenylindole
DHE	Dihydroethidium
DNA	Deoxyribonucleic acid
DNase I	Deoxyribonuclease I
dsDNA	Double stranded DNA
EDL	Extensor digitorum longus
EDTA	Ethylenediaminetetraacetic acid
FGF	Fibroblast growth factor
F4/80	EGF-like module-containing mucin-like hormone receptor-like 1
Gadd45a	Growth arrest and DNA-damage-inducible alpha
GPx	Glutathione peroxidase
H_2O_2	Hydrogen peroxide
HDL	High density lipoprotein
Hprt	Hypoxanthine guanine phosphoribosyl transferase
IDL	Intermediate density lipoprotein
Il1b	Interleukin 1b
iNOS	Inducible nitric oxide synthase
LDL	Low density lipoprotein
Ldlr	Low density lipoprotein receptor
Mhc	Myosin heavy chain
MhcI	Myosin heavy chain type I
MhcIIA	Myosin heavy chain type IIA

MhcIIB	Myosin heavy chain type IIB
MhcIIX	Myosin heavy chain type IIX
mRNA	Messenger ribonucleic acid
NADH	Nicotinamide adenine dinucleotide
NADPH	Nicotinamide adenine dinucleotide phosphate
NF-κB	Nuclear factor kappa beta
NO	Nitric Oxide
Nox	NADPH oxidase
Ogg1	Oxoguanosine DNA glycosylase 1
oxLDL	Oxidised low density lipoprotein
PAD	Peripheral arterial disease
PBS	Phosphate buffered saline
PCR	Polymerase chain reaction
PDGF	Platelet derived growth factor
PFA	Paraformaldehyde
QD	Quadriceps
qRT-PCR	Quantitative reverse transcription PCR
RNA	Ribonucleic acid
RNS	Reactive nitrogen species
ROS	Reactive oxygen species
SDS	Sodium Dodecyl Sulfate
SG	SYBR green
TA	Tibialis anterior
TEMED	Tetramethylethylenediamine
T_m	Melting temperature
Tnfα	Tumour necrosis factor alpha
VEGF	Vascular endothelial growth factor
Vegfa165	Vascular endothelial growth factor a 165
VLDL	Very low density lipoprotein
8-OHdG	8-hydroxy-2' -deoxyguanosine

Chapter 1 – General introduction

1.1 Skeletal muscle

Skeletal muscle, one of the largest tissues in the human body, comprises almost 40% of total body weight in non-obese men (Frontera and Ochala, 2015). The composition of muscle in the body is mainly water (75%), protein (20%) and other substances such as inorganic salts, minerals, fat, and carbohydrates (5%). Muscle mass is dependent on the balance between protein synthesis, and protein degradation, both of which can be altered by hormone balance, physical activity and exercise, injury or disease, and nutrition. Skeletal muscle primarily functions in movement, generating force by turning chemical energy into mechanical energy, generating force and power, maintaining posture, producing movement, and ultimately contributing to functional independence. This requires a great deal of metabolic demand, and accounts for up to 40% of the resting metabolic rate of humans and makes up 30-50% of the protein turnover in the whole body (Matsakas and Patel, 2009). This in turn generates several by-products such as lactic acid and reactive oxygen species. Metabolically, skeletal muscle contributes to basal energy metabolism, serves as storage for important substrates such as amino acids and carbohydrates, produces heat to maintain core temperature, and consumes the majority of oxygen and fuel used during physical activity and exercise. Furthermore skeletal muscle serves a number of metabolic functions such as glucose and lipid metabolism the deposition of fat in the adipose tissue, and the "browning" of the white adipose tissue, immune and redox effects, heat generation, and it has been recently been discovered that skeletal muscle is important to cognitive function (Barbalho et al., 2020; Chazaud, 2020; Pedersen and Febbraio, 2012; Severinsen and Pedersen, 2020; Sui et al., 2020). Furthermore, muscle has a high capacity for oxidative metabolism and is a major peripheral tissue in insulin mediated glucose uptake, glycogen storage and triglyceride storage (Hargreaves and Spriet, 2020; Merz and Thurmond, 2020). Skeletal muscle has a role in storage of amino acids needed by other tissues such as brain, skin, and heart for the synthesis of organ-specific proteins. The reservoir of amino acids is also used to maintain blood glucose levels during starvation conditions. A reduction in muscle mass impairs the ability of the body to respond to stress and chronic illness, therefore the roles of the skeletal muscle are of relevance to disease prevention and maintenance of health. Therefore, skeletal muscle function and homeostasis is important in health and disease, the balance of oxidative metabolism in a tissue with high oxygen consumption rates is one important factor which is closely regulated and may be imbalanced in disease (Beyfuss

and Hood, 2018; Roy et al., 2020, p. 1). The homeostasis between protein synthesis and protein degradation can regulate muscle mass and is affected by nutrient availability, exercise, hormonal profile, injury, and disease. Skeletal muscle is a highly robust and adaptable tissue, able to alter size and functional properties, and able to regenerate and repair throughout adulthood due to its resident population of stem cells (Relaix and Zammit, 2012).

1.1.1 Skeletal muscle composition

Skeletal muscle is composed of myofibres, nerve tissue, capillaries, and connective tissue. A detailed diagram of skeletal muscle structure is listed in figure 1.1. Individual myofibres are grouped together into clusters known as fascicles, which themselves form a muscle (Bottinelli and Reggiani, 2000; Frontera and Ochala, 2015). Each myofiber is surrounded by connective tissue known as the endomysium, and each fascicle is surrounded by connective tissue known as the perimysium (Morrissey and Sherwood, 2015). Muscles are separated from one another by connective tissue known as the fascia and surrounding this is the epimysium. A single individual muscle fibre is approximately 100 µM in diameter and 1 cm in length and is surrounded by a cell membrane known as the sarcolemma. The sarcolemma itself is associated with a complex of several proteins connected to the internal structure of myofilaments, attaching to actin present in the thin filament. Dysfunction or absence of these proteins can result in damage to the sarcolemma, muscle weakness and atrophy. Dystrophin is one protein in the sarcolemma involved in stabilizing the plasma membrane of striated muscle – in loss of function mutation of the dystrophin gene, sarcolemma instability and muscle loss are results, this is seen in neuromuscular disorders such as Duchenne and Becker muscular dystrophies (Thomas, 2013).

Each myofiber is a multinuclear muscle cell stabilised in a post-mitotic state, excluding their water content, single muscle fibres consist of 80% protein – including contractile, regulatory and cytoskeletal proteins, and of 8% sarcoplasm (Hoppeler et al., 1973). Nuclei are in control of the type of myosin heavy chain a specific region expressed in proximity to them in the myofiber, known as a nuclear domain (Frontera and Ochala, 2015). Adjacent nuclear domains of a single fibre appear to coordinate protein expression in order to produce a certain type of protein such as myosin similarly across the length of the muscle fibre, though cases of different expression of contractile proteins in adjacent myonuclear domains have been reported (Wilkins et al., 2001).

Contained in myofibres are myofibrils, consisting of thick filaments of myosin and thin filaments of actin, which function in force generation by pushing against one another – myosin converting chemical energy (ATP) to mechanical energy to pull the actin filaments (Clark et al., 2002). Each individual muscle fibre is estimated to be composed of thousands of myofibrils and billions of myofilaments these units of the muscle are assembled together to form sarcomeres – the basic contractile units of skeletal muscle. Myofibrils are divided into segments known as sarcomeres, which are each bookended by Z-lines – a cytoskeletal disk composed of proteins such as α-actinin, α-spectrin, tropomyosin-α (Al-Khayat et al., 2010; Clark et al., 2002). These Z-lines allow the actin to link to adjacent sarcomeres, which allows the fibre to contract. The sarcomere is composed of I bands – containing actin filaments, and A bands – containing myosin filaments. The main molecular motor of muscle contractility is myosin – eleven sarcomeric genes with their corresponding protein products have been described in mammals, though not all are expressed in humans. The A band is further divided into the H zone which is a region where actin and myosin filaments do not overlap while the muscle is at rest. Inside the H zone is the M line, which is composed mostly of M line protein (Al-Khayat et al., 2010; Clark et al., 2002). Thin and thick filaments comprise the majority of the protein content of myofibres, and other proteins in the myofiber are associated with sarcomere function such as titin, nebulin and desmin which are important for the stability and organization of filaments, (Li et al., 1997; Pappas et al., 2011; Tskhovrebova and Trinick, 2010). Titin, for example attaches to the Z disc of the sarcomere, and attaches to myosin to help stabilize and align the thick filament, whereas nebulin integrates with the thin filaments containing actin, and desmin connects the Z line to the sarcolemma and to the extracellular matrix (Ottenheijm and Granzier, 2010).

Myofibres also contain organelles aside from the sarcomere, such as the sarcoplasmic reticulum which functions in Ca^{2+} transport, uptake, storage, and release. As a tissue demanding high levels of energy production, the muscle also houses an extensive network of mitochondria and a transverse tubular system for the transmission of action potential in the interior of the myofiber (Schiaffino and Reggiani, 2011).

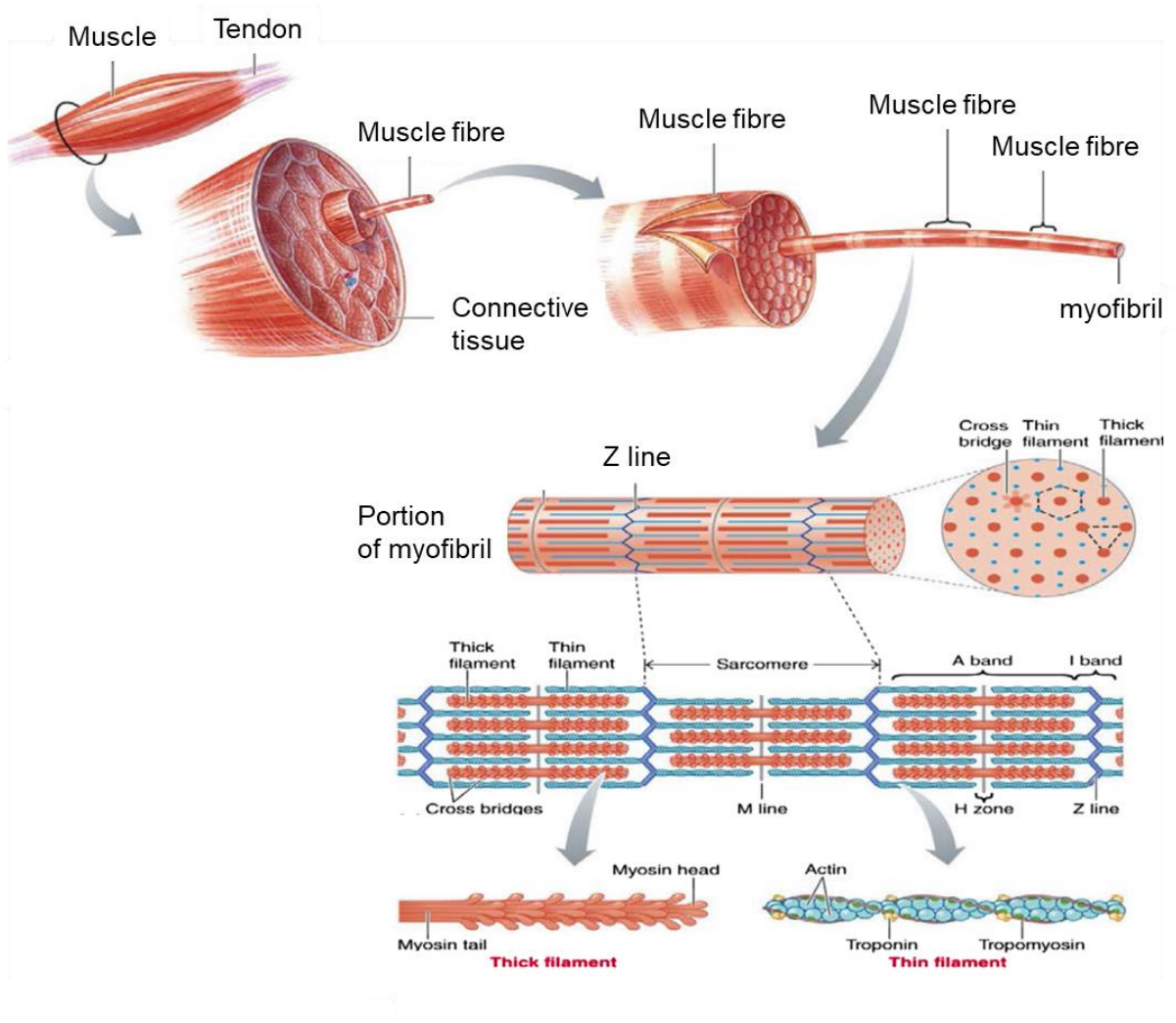

Figure 1.1 Structure of skeletal muscle (adapted from Frontera et al.)

1.1.2 Skeletal muscle plasticity

Skeletal muscle has a remarkable plasticity and myofibre transitions can occur as a result of significant changes in hormone levels, nerve activity or mechanical loading (Blaauw et al., 2013; Caiozzo et al., 1997; Pette and Staron, 2000). Hypothyroidism for example causes myofiber transition from a faster to a slower type (IIB→ IIX → IIA → I), while hyperthyroidism has inverse effects (Schiaffino and Reggiani, 2011; Westerblad et al., 2010). Nerve activity is also important in fibre type transition, with fast nerves generally innervating fast twitch muscle and slower nerves innervating slow twitch fibres (Schiaffino and Reggiani, 2011). Furthermore, cross-reinnervation of a muscle i.e. fast nerve innervating a slow twitch muscle or vice versa leads to an associated transition of myofiber type, and changes in neuronal activity due to cross-innervation, denervation or paralysis are associated with myofiber transitions

(Westerblad et al., 2010). Mechanical loading – exercise also induces functional adaptations and changes in metabolism and structure of muscle. The adaptations of skeletal muscle in response to exercise differ according to frequency, intensity, and duration of exercise (Egan and Zierath, 2013).

Endurance training for example enhances mitochondrial biogenesis, improves cellular aerobic fitness, and promotes transition to oxidative fibres (IIA and I), while resistance training induces muscle fibre hypertrophy, increases satellite cells and myonuclei count, enhances muscle net protein synthesis and decreases type IIAX fibres (Blocquiaux et al., 2020; Qaisar et al., 2016).

Despite the noted myofibre transitions in response to exercise, myofibre transition in regenerating and developing muscle is more extensive (Westerblad et al., 2010). Adaptations on a cellular level however are more frequent – such as mitochondrial biogenesis and respiration, oxidative metabolism, increased capillarization (Westerblad et al., 2010). Muscle myofiber composition is also influenced by diet, age and pathological conditions (Matsakas and Patel, 2009). An oxidative phenotype for example is induced by food restriction, with an increase of oxidative myofibres whereas a high fat diet will promote an oxidative phenotype initially, before leading to glycogen and lipid storage, decreasing metabolic function and muscle insulin resistance (Matsakas and Patel, 2009). Ageing is commonly associated with reduced force generation capacity and atrophy (Frontera and Ochala, 2015). Furthermore, a decrease in type IIX and IIB fibres is seen in elderly humans and rodents, regenerative capacity becomes reduced due to loss of muscle stem cells, metabolic efficiency is reduced and sarcoplasmic reticulum function is diminished (Frontera and Ochala, 2015).

Skeletal muscle fibre heterogeneity marks a significant variability in mechanical, biochemical, and metabolic phenotypes from fibre to fibre, with each fibre type representing a different phenotype(Salviati et al., 1982). Different muscles of the human body are comprised of different percentages of the various fibre types. The presence of different fibre types in the same muscle may be due to varying patterns of activity induced by motor neurons, imparting different properties to different fibres. The variability in physiological properties of fibres is important to enable various metabolic and mechanical abilities in the muscle, maintaining flexibility through

heterogeneity (Liu et al., 2012). Each muscle fibre type also responds differently to stimuli such as denervation, hormonal levels, aging, inactivity, and disease. Atrophy is particularly evident in fast type II fibres compared to slow type I fibres in conditions associated with muscle wasting such as cancer(Ciciliot et al., 2013). Muscle fibre contraction speed is determined by the extent of sarcoplasmic reticulum development, while mitochondrial content determines the oxidative capacity and fatigue tolerance. Human limb muscles are comprised of three fibre types: type I (slow, oxidative, fatigue-resistant), IIA (fast, oxidative, intermediate metabolic properties), and IIX (fastest, glycolytic, fatigable) (Vlahovic et al., 2017). Muscle protein isoforms have been used to identify and distinguish muscle fibre types including myosin heavy chain type I, IIA, IIX, which have been useful in determining muscle fibre types, and immunofluorescence antibodies allow investigators to determine muscle fibre type transitions. Muscle fibre transitions have been known to occur as a result of variations in the pattern of neural stimulation, exercise, availability of substrates, and hormonal signals. Myogenic transcription factors such as MyoD and myogenin play a significant role in muscle protein synthesis for the specific fibre type isoforms (Hu et al., 1997; Hughes et al., 1993).

1.1.3 Skeletal muscle action

In order to generate force, the muscle first receives transmission of the nerve stimulus to the triad, then calcium is released from the nerve cisternae of the sarcoplasmic reticulum, the whole process is known as excitation-contraction coupling (Costello et al., 1986; Ríos and Györke, 2009). The action potential arriving at the muscle fibre is conducted into the muscle fibre via the transverse tubular (T tubule) system (Calderón et al., 2014). The action potential reaches the triad where the T tubule is in close proximity to the terminal cisternae of the calcium storing sarcoplasmic reticulum (Al-Qusairi and Laporte, 2011). Stored calcium is released generating a calcium current in the muscle fibre, the calcium current then triggers the opening of ryanodine receptors in the terminal cisternae of the sarcoplasmic reticulum and releases large amounts of calcium into the sarcoplasm (Dulhunty et al., 2017; Woll and Van Petegem, 2022). The release of calcium to the sarcoplasm means calcium binding to troponin C on the actin thin myofilament, which displaces the tropomyosin blocking the active site of the actin filament which in turn allows the myosin head to bind actin, forming a cross-bridge (Fujita et al., 2004; Rayani et al., 2021). The myosin head then detaches

from actin through the action of ATP and ATPase in the myosin head. The ATPase hydrolyses ATP into ADP and Pi, and this results in the detachment of the cross-bridge (Kiani and Fischer, 2016). The myosin head then binds the new actin molecule forming a new cross-bridge. The release of Pi allows the myosin to push the actin filament passed it. Through this process the actin and myosin filaments pull against one another resulting in the generation of force.

As a high energy demanding tissue, the muscle demands a large amount of ATP in order to perform muscle contractions. The muscle fibre uses three different energy pathways to provide muscle action: through ATP and creatine phosphate stores, through anaerobic glycolysis, and through oxidative phosphorylation (Hargreaves and Spriet, 2020). Each energy pathway supports different activities, for example ATP and creatine phosphate is used in short burst high intensity activities of a few seconds, anaerobic glycolysis supports actions of a few minutes of activity by quickly generating ATP, though this produces lactate and H^+ (Gastin, 2001). Longer duration activities, however, are sustained by oxidative phosphorylation, which can support exercise from minutes to hours (Conley et al., 2001). Oxygen reaches active muscle fibres through a network of capillaries whose density is dependent on the metabolic demand of the muscle fibre.

Skeletal muscle actions may be either static – generation of force without movement of the limb, dynamic concentric – shortening of the muscle conferring movement, or dynamic eccentric – lengthening of the muscle conferring movement. Static muscle actions are actions which generate force without generating movement such as when the resistance is greater than the force generated (i.e., pushing against a wall). These muscle actions are supported by the generation of force under the sliding filament theory, the force generated by actin-myosin cross-bridges as discussed above is transmitted longitudinally and laterally along the length and breadth of the fibre (Powers et al., 2021). The transmission of this force across the Z disks of sarcomeres in series produces movement. The extent of the force generated by a skeletal muscle depends on the degree of activation at the neuromuscular junction, the size of the muscle, the space between myofilaments and the number of cross-bridges formed. The force produced by a muscle in relation to its size is the specific force, and this can be used as an indication of muscle functional quality. Specific force has been seen to be reduced in both overweight and older humans.

1.1.4 Skeletal muscle diseases, and current therapeutic approaches

The term ‘muscle disease’ relates to a large group of conditions, most of which are progressive, with muscles gradually weakening over time. Muscle weakness and impaired cardiorespiratory function are common in patients of muscle disease, alongside pain, and fatigue which contributed to a decrease in quality of life.

The most common muscular dystrophy in children is Duchenne muscular dystrophy, which is caused by mutation of the DMD gene which encodes dystrophin (Bushby et al., 2010). In DMD, type II fibres are the first fibres to degenerate and are the first fibres to be lost, while slow type I fibres are not effected until later on in the progression of DMD (Webster et al., 1988). Type I fibres remaining in the later stages of DMD are often abnormally expressing embryonic myosin heavy chain – indicating that these fibres have undergone degeneration and regeneration (Marini et al., 1991). The use of corticosteroids, non-invasive respiratory support, and active surveillance and management of associated complications have improved ambulation, function, quality of life and life expectancy.

Facioscapulohumeral muscular dystrophy is a progressive muscular dystrophy characterised by weakness and wasting of the facial, shoulder, and upper arm muscles. Facioscapulohumeral muscular dystrophy is strongly associated with aberrant activation of DUX4 – the gene encoding a double homeobox transcription factor which induces expression of many germline, stem cell, and other genes and is normally repressed in skeletal muscle (Tawil et al., 2014). Facioscapulohumeral muscular dystrophy results in loss of maximum force generating capacity in type II fibres, but not tupe I fibres(Celegato et al., 2006). There are no approved treatments that alter the course of facioscapulohumeral muscular dystrophy, one of the most common forms of muscular disease.

Myotonic dystrophies are among the most common adult-onset muscular dystrophies, and they involve multiple organ involvement, muscle atrophy and muscle weakness(Thornton, 2014). Myotonic dystrophies are caused by microsatellite expansions in DMPK or CNBP(Marsh et al., 2020). Active screening and management have been suggested as a clinical approach to treating myotonic dystrophies, and some genetic treatments have seen success *in vitro* and *in vivo*(Thornton et al., 2017).

Commonly, muscle related weakness and atrophy appear as a result of ageing. The prevalence of sarcopenia in the older population has been between 5% and 50% depending on the study, gender and country of subjects(Papadopoulou, 2020). Sarcopenia has been associated with the loss of muscle force in older people with mobility limitations, and in an individual fibre a reduced number of skeletal muscle stem cells may be seen, particularly in fibres expressing type II myosin heavy chain. Most of the motor unit and fibres lost with advanced age are type II fibres, and muscle stem cell activation in response to muscle damage is reduced in older men (McKay et al., 2013). Furthermore sarcopenia in muscle is characterised by segregated calcium stores of the sarcoplasmic reticulum which impairs excitation contraction coupling efficiency (Weisleder et al., 2006). Mitochondrial loss and reduced function of mitochondria is also associated with aging, though this can be reduced by exercise training(Marzetti et al., 2013).

1.1.5 Skeletal muscle stem cells

Muscles have tremendous adaptive and regenerative ability after injury and are capable of growth and regeneration in response to exercise. This is achieved through muscle stem cells, also known as satellite cells, which are muscle progenitor cells that reside in niches between the sarcolemma and the basal membrane of the myofibres (Collins et al., 2005). Abundant evidence suggests that muscle stem cells are an integral part of skeletal muscle growth and regeneration in response to injury (Relaix and Zammit, 2012). In adult skeletal muscle, these stem cells remain mitotically quiescent and are activated by myogenic factors when myofibre damage or hypertrophy occurs, during which muscle stem cells become activated to proliferate and then differentiate into myoblasts and fuse together for de novo myotube formation, or fuse to damaged myofibres for replacement of myonuclei (Collins et al., 2005; Yin et al., 2013). The fate of these satellite cells is influenced by extrinsic or intrinsic factors, these contribute to their proliferation and differentiation, or recycling back into satellite cells (Dumont et al., 2015). The recycling of satellite cells through asymmetric cell division is an important aspect of the continued plastic and regenerative ability of the muscle (Kuang et al., 2007). In several pathological conditions, such as muscular dystrophy and chronic obstructive pulmonary disease, muscle stem cells have impaired capacity for activation and differentiation (Girgenrath et al., 2005; Morgan and Zammit, 2010; Pomiès et al., 2015). In metabolic diseases, such as obesity,

muscle stem cells have been reported to exhibit decreased myogenic capacity after skeletal muscle injury (X. Fu et al., 2016; Xu et al., 2018). Muscle stem cells' reduced functional capacity may be due to insufficient cues for proliferation or differentiation or harmful extrinsic factors such as reactive oxygen species which in excess will influence muscle stem cell development.

More precisely, muscle stem cells are governed by their expression of transcription factors and myogenic factors. In quiescence, all muscle stem cells express Pax7, whereas muscle stem cells will be expressing MyoD when activated (Halevy et al., 2004, p. 7; Zammit et al., 2004). While expressing MyoD muscle stem cells proliferate – generating the material to regenerate muscle fibres before differentiation. After a period of proliferation, myoblasts halt their cell cycle and begin expressing myogenin which initiates the differentiation processes (Sabourin and Rudnicki, 2000). While myogenin expressing cells are committed to differentiation, some myoblasts will instead express Pax7 which allows the muscle to maintain a pool of muscle stem cells – meaning the muscle will be able to regenerate again (Collins et al., 2005; Sincennes et al., 2021). The differential expression of these transcription factors allows the myogenic progression and self-renewal of muscle stem cells to be modelled *ex vivo* by determining their relative expression in cultured single fibres. This process is summarised in *figure 1.2.*

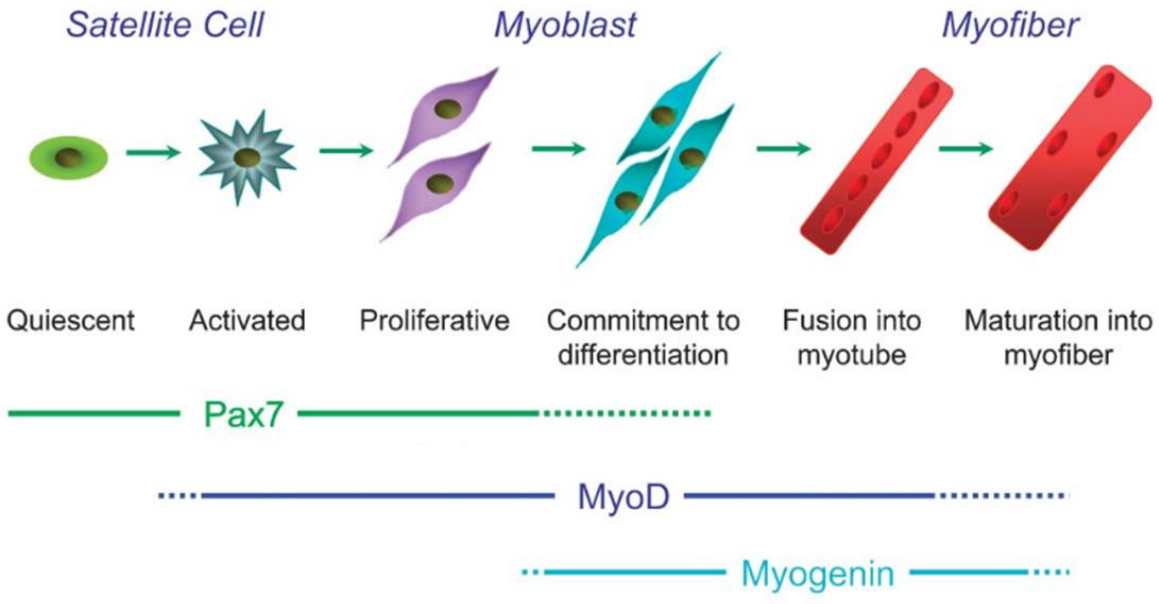

Adapted from Zammit et al, 2006

Figure 1.2. Commitment to myogenesis through transcription factors.

Adult muscle stem cells remain quiescent and express Pax7 until activated whereupon myoD expression begins(Zammit et al., 2006). While expressing MyoD muscle stem cells proliferate and eventually either become committed to differentiation or begin expressing Pax7 again in order to maintain the stem cell pool (Jin et al., 2007). After a period of proliferation, committed myoblasts halt their cell cycle and begin expressing myogenin which initiates the differentiation processes (Zammit, 2017).

1.2 Apolipoprotein E in health and disease

Apolipoprotein E is an important protein in lipid and lipoprotein metabolism, involved in clearance of remnants of triglyceride-rich lipoproteins from circulation into the liver. ApoE acts as the ligand for the LDL receptor family of proteins in order to clear these remnants. ApoE transfers lipids in the brain, influences adipogenesis and decreases fat absorption. The ApoE protein influences vascular function via its influence on inflammatory responses, platelet aggregation, and maintaining the blood-brain barrier integrity.

Apolipoproteins function in the transport of lipoprotein complexes through the lymphatic and circulatory system, as well as acting as enzymes and cofactors in cholesterol metabolism – mediating lipid catabolism and cholesterol esterification (Irshad and Dubey, 2005; Morita, 2016). Apolipoproteins are important factors in plasma lipid homeostasis due to their effects in lipid clearance and metabolism in roles as cofactors for lipid metabolism enzymes and are important in cellular cholesterol efflux and serve as markers of coronary artery disease (Chan and Watts, 2006; Mahley et al., 1984; Yokoyama, 1998).

Apolipoprotein E (ApoE) is a 34kDa glycoprotein of 299 amino acids, synthesized in the liver and in macrophages and is found in plasma at 3-5 mg/dl (Getz and Reardon, 2009; Huang et al., 2009; Imaizumi, 2011). The ApoE gene is located on human chromosome 19 and contains 4 exons, comprising 3.6kb (Greenow et al., 2005; Lee et al., 2010; Phillips, 2014). The first exon contains the translation start and the second exon contains a signal peptide, while the third and fourth exons contain the structural codons of ApoE and its copy deoxyribose nucleic acid (cDNA) comprises 1163 base pairs (Paik et al., 1985).

ApoE functions in lipid clearance – dietary fat transport, endogenous fat transport, and reverse cholesterol transport and is suggested to have an important function in cognition (Getz and Reardon, 2009; Mahley et al., 2009; Mahley and Rall, 2000). ApoE has 3 common isoforms occurring by variation at two amino acids – amino acids 112 and 158 which can be either ApoE2 (Cys112,Cys158), ApoE3 (Cys112,Arg158) or ApoE4 (Arg112,Arg158) (Greenow et al., 2005; Weisgraber, 1994). These substitutions affect the structure of ApoE isoforms and influence their function. This genetic variation at the ApoE locus (i.e. ApoE2 and ApoE4 variants vs the 'wild type' ApoE3) impacts lipid and amyloid-β clearance and are associated with increased risk of developing hypercholesterolaemia/atherosclerosis (in ApoE2) and Alzheimer's disease (in ApoE4) (Li and Liu, 2014; Lopez et al., 2014).

ApoE's function in cholesterol homeostasis is through a number of pathways including clearing chylomicron remnants, lipid fragments and lipoproteins from circulation by functioning as a ligand for low-density lipoprotein receptor (Go and Mani, 2012). ApoE acts as a ligand for two membrane bound receptors – the low-density lipoprotein (LDL) receptor and the chylomicron remnant receptor. ApoE functions primarily though Low density lipoprotein receptor (LDLR) as its primary physiological ligand to clear very low density lipoproteins (VLDL), LDL and intermediate density lipoproteins (IDL) or through the chylomicron remnant receptor to IDLs (Sacks, 2015). ApoE's main role in lipoprotein metabolism is through activating enzymes essential to lipoprotein breakdown. ApoE binds LDLR and is internalised through endocytosis, wherein lipoprotein complexes are released from the receptor in the endosomes and are transported to lysosomes, as the receptors return to the membrane (Go and Mani, 2012).

ApoE is a component of the reverse cholesterol transport pathway (the process by which cholesterol is cleared from lipid-loaded peripheral cells such as macrophage foam cells and is transported via the plasma to the liver), in cholesterol efflux from peripheral cells into the plasma and in uptake of cholesterol esters into the liver (Getz and Reardon, 2018). Initially, in reverse cholesterol transport, cholesterol must be secreted from cells in the arterial subintima such as macrophages and the high density lipoproteins (HDL) in the plasma takes up the cholesterol (Price et al., 2019). ApoE appears to facilitate both the process of cholesterol secretion and uptake into HDL (Mahley et al., 2006). While some evidence on the involvement of apoE in these

processes is conflicting, ApoE levels are greatly increased in cholesterol-loaded macrophages (Mahley et al., 2006). Less conflicting, however is evidence on the role of apoE in the transport of tissue cholesterol to the liver. After uptake into HDL, cholesterol is delivered to the liver via cholesterol ester transfer protein-mediated transfer to apoB-containing particles (VLDL, LDL, IDL, LDL receptor), where apoE acts as the primary ligand to remove apoB-containing lipoproteins (Ikewaki et al., 2004; Yakushkin and Tsibulsky, 1998). Cholesterol may also be delivered to the liver via selective uptake of HDL cholesterol ester and apoE may be required for cholesterol esters to diffuse from HDL to hepatocytes (Meyer et al., 2013). Furthermore, ApoE may mediate another process of cholesterol delivery to the liver in binding to specific hepatocyte receptors to allow hepatocytes to internalise HDL (Morton et al., 2019).

While ApoE is highly expressed in the liver and 90-95% of plasma ApoE is of hepatic origin, ApoE is widely expressed with functions beyond cholesterol efflux (Getz and Reardon, 2018; Klos et al., 2008). ApoE scavenges cell cholesterol chylomicron remnants and lipid clearance, and deficits are seen in ApoE deficient models and genetic variation at the ApoE locus is implicated in susceptibility to both atherosclerosis and Alzheimer's disease (Bejta et al., 2007; Getz and Reardon, 2009).

ApoE acts in an inflammatory capacity, inducing transformation of macrophages to M2 phenotype, inducing lymphocyte proliferation, and apoE has been suggested as a biomarker of Nasal mucosal inflammation, and ApoE3 and ApoE4 transfected macrophages show increased activity of redox sensitive transcription factor NF-κB as well as increased production of pro-inflammatory proteins TNF-a, Interleukin 1b (IL1b), IL6, MIP1a and decreased production of anti-inflammatory IL10 (Y. W. Chung et al., 2020; Jofre-Monseny et al., 2007b). Furthermore these macrophages have increased superoxide production and increased membrane oxidation (Jofre-Monseny et al., 2007b). Neuronal and cognitive effects of ApoE3 and ApoE4 transgenic mice include poor dendritic recovery of hippocampal neurons following innate immune response, impaired neuronal remodelling, and decreased cognitive performance in spatial learning and memory tasks (Bellosta et al., 1995; Maezawa et al., 2006; Raber et al., 2000).

1.2.1 Hyperlipidaemia and atherosclerosis

Hyperlipidaemia, an elevation of levels of total cholesterol concentration in the serum, as well as elevated levels of triglycerides, which may be caused by genetic or environmental causes, is a major risk factor for atherosclerosis and cardiovascular disease (Nelson, 2013). The development of atherosclerosis in the endothelium is contributed to by decreased bioavailability of nitric oxide and inhibition of endothelial NO synthase, the resulting increase in chemokines causes an increase in the amount of reactive oxygen species (Ellulu et al., 2016). Oxidised low density lipoprotein (oxLDL) forms through oxidization of LDL in the vessel wall which is phagocytosed by macrophages leading to the formation of foam cells as well as inducing proinflammatory response in macrophages leading to more ROS production (Gimbrone and García-Cardeña, 2016).

Obesity-independent hyperlipidaemia induces intramuscular lipid accumulation and skeletal muscle oxidative stress in ApoE deficient ($ApoE^{-/-}$) mice, an established model of atherosclerosis and hyperlipidaemia (Meyrelles et al., 2011). Moreover, previous evidence suggests that $ApoE^{-/-}$ mice have delayed skeletal muscle regeneration after injury (Arnold et al., 2015; Crawford et al., 2013; Kang et al., 2008; Pellegrin et al., 2014). This delay in skeletal muscle regeneration was attributed mainly to the perturbed accumulation of proinflammatory macrophages and decreased macrophage phagocytosis due to ApoE deficiency (Arnold et al., 2015; Crawford et al., 2013; Kang et al., 2008; Pellegrin et al., 2014). Specifically, Kang et al. showed that proinflammatory cytokines remained increased in $ApoE^{-/-}$ injured muscle even after 14 days of injury (Kang et al., 2008). Moreover, Arnold et al. reported that ApoE deficiency impacts negatively on macrophage phagocytic activity and is at least partially responsible for the impairment of skeletal muscle regeneration (Arnold et al., 2015).

Atherosclerosis is the accumulation of fatty or fibrous material in the innermost layers of arteries – the intima (Falk, 2006). Atherosclerotic plaque progressively becomes more fibrous, accumulating calcium, and encroaching on the lumen of the artery (Bailey et al., 2016; Vink and Pasterkamp, 2002). This can lead to reduced blood flow and tissue ischaemia, which can be particularly harmful to the muscle tissue, which demands high oxygen supply. Atherosclerosis causes ischaemic strokes, transient cerebral ischaemic attacks, formation of aneurysm, and in the peripheral arteries it can

lead to intermittent claudication, and ulceration (Herrington et al., 2016). Atherosclerosis occurs initially as a result of accumulation of LDL particles (Mineo, 2020). LDLs transport water-insoluble cholesterol through the blood and LDL-C concentrations in excess of physiological needs (10–20mg/dL) over a long duration of time. Furthermore, research has indicated that oxidized LDL particles can promote atherogenesis, which could be a contributing factor to the increased reactive oxygen species in the muscle of the atherosclerotic mouse, or vice versa (Park, 2014). Oxidized LDL particles in the initiation of atherosclerosis have been suggested to act as ligands for the scavenger receptors which facilitate foam cell formation (Luo et al., 2017). Once established, atherosclerotic plaques progress by continued accumulation of lipid and lipid-engorged cells.

1.2.1.2 Skeletal muscle deficits of the hyperlipidaemic and atherosclerotic mouse

The ApoE$^{-/-}$ mouse is used as a model for hypercholesterolemia, hyperlipidaemia and atherosclerosis. Apolipoprotein E in the wild type associates with triglyceride rich proteins such as chylomicrons and very low density lipoproteins, clearing them from the plasma as well as activating proteins essential for the breakdown of lipoproteins, and reduces the oxidation of LDL seen in mice with greater oxidative stress and systemic effects of ApoE deficiency are summarised in table 1 (Marais, 2019).

Evidence suggests that skeletal muscle specifically is impacted by ApoE deficiency in a number of ways, including decreased capillary density, increased H_2O_2, decreased myogenin levels post ischemia/reperfusion, increased lipid deposition and calcification, decreased fibre size and delayed muscle regeneration (Arnold et al., 2015; Kang et al., 2008; Pereira et al., 2012; Stapleton et al., 2010). Recent evidence suggests a variety of effects of ApoE deficiency on skeletal muscle, including muscle fibre transitions from IIB fibres to IIX fibres which can rely on oxidative metabolism rather than glycolytic metabolism in IIB fibres which are less able to obtain energy from fat (Sfyri et al., 2018). ApoE deficiency furthermore has been shown to increase intramuscular fat accumulation which has been associated with redox imbalance in wild type mice on high fat diet. Redox imbalance was confirmed in ApoE deficient mouse skeletal muscle with higher mRNA levels of Nox2, Tumour necrosis factor alpha (Tnfα) and Il1b detected in gastrocnemius muscle alongside elevated levels of

reactive oxygen species (ROS), protein carbonylation, tyrosine nitration, lipid peroxidation and Deoxyribonucleic acid (DNA) damage (Sfyri et al., 2018).

ROS including superoxide anion, hydrogen peroxide and hydroxyl free radicals function in intracellular signalling to prevent tissue injury and promote angiogenesis at low levels, however at higher concentrations they are deleterious to cells due to their action in lipid peroxidation, protein oxidation and DNA damage, resulting in their role in the aforementioned diseases (Batna et al., 1997; Carbone et al., 2015; Farmer and Mueller, 2013; Sies and de Groot, 1992). ROS have been implicated in a variety of pathologies including cardiovascular disease, neurological diseases, and cancer, and could be an important factor in the muscle deficits seen in hyperlipidaemia (Casas et al., 2015).

Table 1.1. Systemic effects of Apolipoprotein E deficiency

Reference	Findings
(Zhang et al., 1992)	5x total plasma cholesterol 0.45x HDL plasma cholesterol 1.86x plasma Triglyceride Multi-layered intimal foam cell deposits
(Plump et al., 1992)	Increased ApoA-I and ApoA-IV in -/- 8.2x total plasma cholesterol 1.7x triglycerides 17.8x VLDL + IDL-C 14x LDL-C ↔ HDL-C Mean lesion area of 3157 (chow) and 9200 (western)
(Gaudreault et al., 2012)	↑ lipid accumulation in circulating monocytes ↑ inflammatory molecules on monocytes and vascular endothelium
(Nunes et al., 2018)	synaptic loss cognitive dysfunction high plasma lipid levels Cholesterol precursors desmosterol and lathosterol were detected in apoE-KO mice plasma

	↓ cholesterol, desmosterol, campesterol and 24-hydroxycholesterol in apoE-KO brains ↓ 7α-hydroxycholesterol and 7β-hydroxycholesterol. ↓ Cholesterol content, synthesis rates (desmosterol) and export of 24-hydroxycholesterol in the apoE-KO brain
(Teng et al., 2017)	Loss of tight junction proteins 7d after controlled cortical impact (traumatic brain injury) ↑MMP-9 activity (BBB integrity, NFkB activity)
(Zheng et al., 2014)	↑ MMP-9 ↓Claudin-5, occluding (tight junction proteins) (brain injury)
(Zheng and Cai, 2019)	↑ capillary vessel area, number of junctions in peripheral retina ↓ Mean E Lacunaroty
(Zhao et al., 2018)	dyslipidemia and liver steatosis Significant atherosclerotic plaques were observed in the abdominal aorta mononuclear cell infiltration in early lesions ↑ expression of inflammatory cytokines, as well as macrophage accumulation in lesions

1.3 Cellular senescence and skeletal muscle

Cellular senescence is a product of ageing and cancer, involving indefinite cell cycle arrest of aged or damaged cells, which arises in response to a variety of environmental conditions, including increased oxidative stress, macromolecular damage or signalling from activated oncogenes (Barnes et al., 2019; Passos et al., 2007; Wei and Ji, 2018). Anthracycline antibiotic doxorubicin – used as a treatment in a variety of cancers, while effective against cancer cells, is nonselective and its toxicity limits it's use (Carvalho et al., 2009; Tacar et al., 2013). This toxicity has become evident in a variety of tissues including the heart, brain, liver, kidneys and skeletal muscle (Alhowail et al., 2019; Guigni et al., 2018; Lee and Harris, 2011; Prasanna et al., 2020; Songbo et al., 2019). Prominently, cardiotoxicity had been catalogued as a side effect of doxorubicin, however mounting evidence suggests that toxicity is seen in skeletal muscle and its resident stem cells (Hayward et al., 2013). Doxorubicin induces cell cycle arrest and

even cell death through a variety of pathways including apoptosis, autophagy, and necrosis (Kim et al., 2009; Ma et al., 2017).

Previous research suggests doxorubicin induces formation of reactive oxygen species (ROS) which induces cytochrome c release from mitochondria – leading to apoptosis and cell death (Kim et al., 2010). Furthermore, senescent cells may acquire apoptosis resistance, increased beta galactosidase activity and prooxidant activity, with reduced homeostatic compensation to alleviate oxidative stress (Songbo et al., 2019). The prooxidative environment induced in senescent cells further induces ROS and therefore feeds back into increased senescence. Reactive oxygen species are generated in normal cell function through mitochondrial respiration and energy generation, predominantly by contracting in skeletal muscle (Powers et al., 2020). These ROS function as essential mediators of cellular metabolism and gene regulators. Their detrimental effects, however, can accumulate when present in excess or ROS clearance is impaired. ROS mediated lipid peroxidation, synthesis of proteins damaging to the cell, and activation of stress signalling pathways can play a significant role in mitochondrial function, remodelling and repair pathways, protein turnover and gene expression which is particularly impactful in skeletal muscle and skeletal muscle stem cells (Diebold and Chandel, 2016; Moloney and Cotter, 2018; Ochoa et al., 2018; Su et al., 2019).

Skeletal muscle stem cells have a built-in pathway for cell cycle arrest, as after a phase of proliferation, growth is halted to initiate differentiation. Through myoD interacting with retinoblastoma tumour suppressor protein, cell cycle arrest is initiated via cyclin D1 and $p16^{ink4a}$, which allows differentiation to occur (Chen and Wang, 2000; Rajabi et al., 2014). Retinoblastoma tumour suppressor protein and $p16^{ink4a}$ however, also increase ROS, which in turn activates protein kinase C δ (PKCδ) to induce senescence. PKCδ further increases oxidative stress by increasing ROS itself and creating a positive feedback loop. In normal function, MyoD should signal through the Six1/4-Mef2-Pbx1 pathway to induce myogenin expression, however in cases of excessive ROS myogenin expression is inhibited, directly by ROS, and indirectly through p53 – which is upregulated by ROS and doxorubicin, and both inhibit myogenin expression and activate p21 to induce cell cycle arrest (Faralli and Dilworth, 2012; Sandiford et al., 2014; Yang et al., 2015, p. 53). The shared proteins in these pathways are summarised in figure 1.3 (Barbouti et al., 2020; Faralli and Dilworth,

2012; Harrington et al., 1998; Knudsen et al., 2000; Sandiford et al., 2014; Takahashi et al., 2006; Yang et al., 2015).

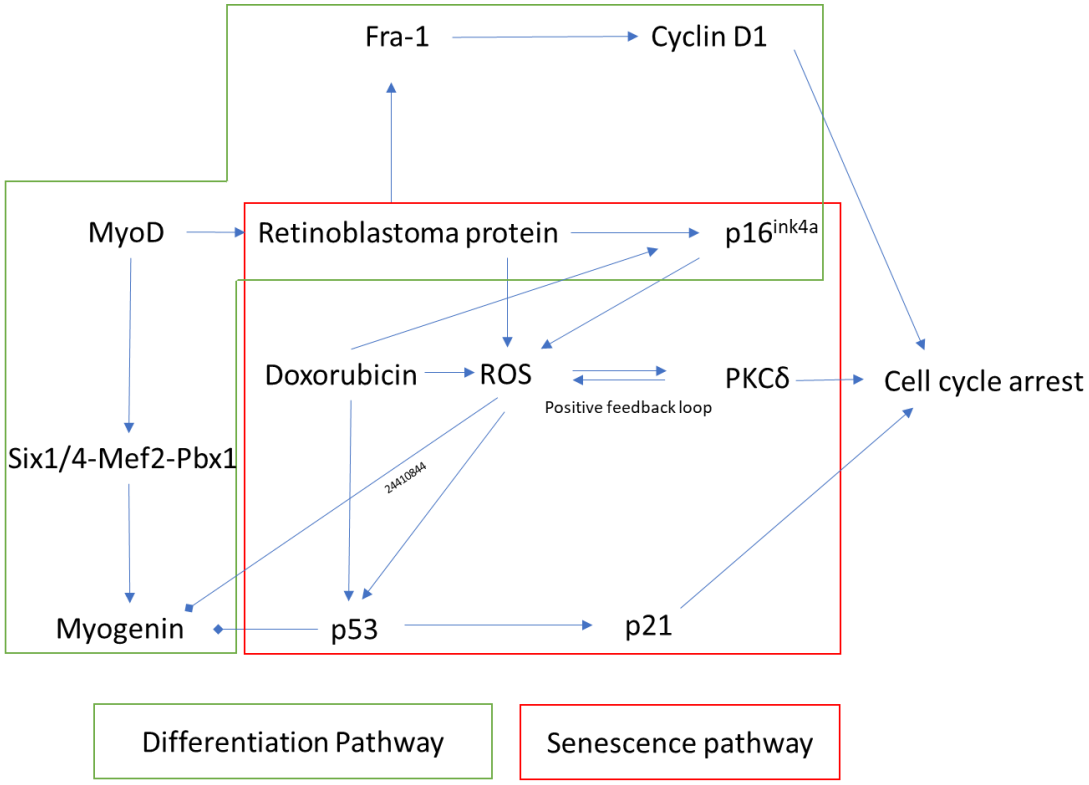

Figure 1.3: The shared processes between cell cycle arrest and senescence pathways in skeletal muscle stem cells. Green boxes highlight normal myogenic progression driven by MyoD and Myogenin. First MyoD acts through retinoblastoma protein and Fra-1 to activate cyclin D1 and begin cell cycle arrest (Chen and Wang, 2000; Rajabi et al., 2014). This allows differentiation to occur and myogenin to activate through the Six1/4-Mef2-Pbx1 pathway(Faralli and Dilworth, 2012). Red box highlights processes involved in senescence activated by doxorubicin and by elevated reactive oxygen species levels. ROS are increased by doxorubicin, retinoblastoma protein and p16, these go on to activate p53 which inhibits myogenin, inhibit myogenin directly, and arrest the cell cycle through protein kinase C δ(Faralli and Dilworth, 2012; Sandiford et al., 2014; Yang et al., 2015, p. 53).

In muscle stem cells the necessity for cell cycle arrest is governed by a number of important pathways. First MyoD interacts with retinoblastoma protein to bring about cell cycle arrest in order for differentiation to occur (Rajabi et al., 2014). Reactive oxygen species also bring about cell cycle arrest through protein kinase C δ and p53 signalling, but an excess of reactive oxygen species can also inhibit myogenin

expression and prevent proper differentiation (Yamaguchi et al., 2007; Yang et al., 2015).

Skeletal muscle retains a small population of stem cells throughout adulthood which enables it's strong capacity for regeneration (Relaix and Zammit, 2012). These muscle stem cells remain quiescent during adulthood unless activated by myofibre injury, at which point they proliferate and either return to quiescence (to retain a population of stem cells) or differentiate to support regeneration (Zammit, 2017). This regenerative ability may however come at a cost, such as incomplete functional recovery, stiffness, excessive inflammation, or fibrosis (Laumonier and Menetrey, 2016). There is currently an increasing interest in the field of skeletal muscle regenerative research. Many factors contribute to this interest such as the lack of effective treatments for myopathies, neuromuscular disease, and muscle related effects of sarcopenia, hyperlipidaemia as well as cancer therapies.

1.4 Platelets and platelet releasate

Platelets are intercellular communicators, which act as a conduit for inherent and endocytosed factors from the bone marrow to the blood stream, and while in circulation, act as sensors in the plasma which can be activated in response to injury. Upon activation at the site of injury, platelets release their powerful cocktail of soluble, cleaved, and vesicular factors, the platelet releasate, all of which can exert powerful paracrine effects on target cells (Edelstein, 2017; Etulain, 2018). Platelet activation leads to the degranulation of alpha granules (Rubenstein and Yin, 2018). Platelets may be activated exogenously by thrombin, calcium chloride, or as the result of mechanical trauma (Rubenstein and Yin, 2018). Therefore, it is possible to collect and activate platelets in order to use the releasate therapeutically to improve regeneration in injury (Pagel et al., 2017).

1.4.1 Platelet structure and function

Platelets are formed in the red bone marrow, through hematopoietic stem cells giving rise to common myeloid progenitor cells, which then differentiate into megakaryocytes (Boscher et al., 2020; Machlus and Italiano, 2013). These megakaryocytes migrate to the vascular niche and generate anucleate platelets through long extensions into vascular sinusoids. Platelets adhere to sites of vascular injury and become activated due to exposure of prothrombotic extracellular matrix proteins. The major functions of

platelets are to promote healing of damaged tissue, and to limit blood loss after injury (Holinstat, 2017). Platelets release cytokines, chemokines and growth factors from their granules at sites of injury to promote wound healing (Passaretti et al., 2014). Platelet structure is summarised in figure 1.5.

The platelet granules include α-granules – which contain growth factors and cytokines, dense γ-granules - which release calcium, serotonin, polyphosphates, pyrophosphates, ADP and ATP, and lysosomes, which contain a number of hydrolytic enzymes. The platelet is composed primarily of α-granules which are typically 200-500nm and platelets hold approximately 50-80 per platelet (Harrison and Cramer, 1993; Smith, 2022). The α-granules can be secreted intracellularly or extracellularly and their contents include a number of growth factors important to growth and regeneration including, but not limited to, platelet-derived growth factor (PDGF), vascular endothelial growth factor (VEGF), transforming growth factor beta (TGFβ), insulin-like growth factor (IGF), epithelial growth factor (EGF), and fibroblast growth factor (FGF) (Rendu and Brohard-Bohn, 2001). Once activated, platelets release trophic factors through degranulation, the aforementioned growth factors interact with injured tissue structures to improve the healing response. Aside from platelet degranulation, aggregation is another major function of platelets, for haemostatic plug formation and thrombosis (Hvas, 2016; Sang et al., 2021). Injured tissue and damaged cells release soluble platelet agonists such as thrombin and ADP which signal to platelets allowing for activation, platelet spreading and adhesion, then eventually granule secretion (Estevez and Du, 2017; Li et al., 2010). Exocytosis of the contents of α-granules, vesicle-associated membrane protein 8 (VAMP-8), synaptosomal-associated protein 23 (SNAP-23) and syntaxin 2 (a Q-SNARE proteins participating in exocytosis) activity causes platelet shape change, then granule exocytosis.

Platelets function in normal haemostasis in repair of damage to the endothelial cell layer, where collagen is exposed from the subendothelial space (Golebiewska and Poole, 2015). Platelets interact with collagen and von Willebrand factor through their glycoproteins, initiating platelet adhesion at the site of damage, and forming a monolayer (Li et al., 2010). Platelets aggregate and form a three-dimensional structure through glycoprotein IIb/IIIa integrins, more platelets are recruited through platelets secreting aggregatory signals such as thromboxane A2, ADP, ultra large von Willebrand factor multimers, serotonin, and thrombin (Fox, 1994). Further to collagen

recruitment and activation of platelets, tissue factor is another mediator of vascular homeostasis and thrombosis (Camera et al., 2015). Tissue factor is released from deeper tissue damage to smooth muscle, adventitial cells and pericytes, mediating conversion of pro-thrombin to thrombin, generation of fibrin and activation of the closing cascade. Arterial thrombosis can occur in atherosclerosis in the event of plaque rupture and clot formation leading to platelet aggregation, thrombus formation and vessel occlusion (Mackman, 2008). Thrombus formation has been linked to platelet secretion of protein disulfide isomerases, some of which react with reactive oxygen species and induce thrombus formation. Protein disulfide isomerases are essential for platelet aggregation and are used to regulate the increase of thrombin production on the surface of activated platelets(Essex and Wu, 2018).

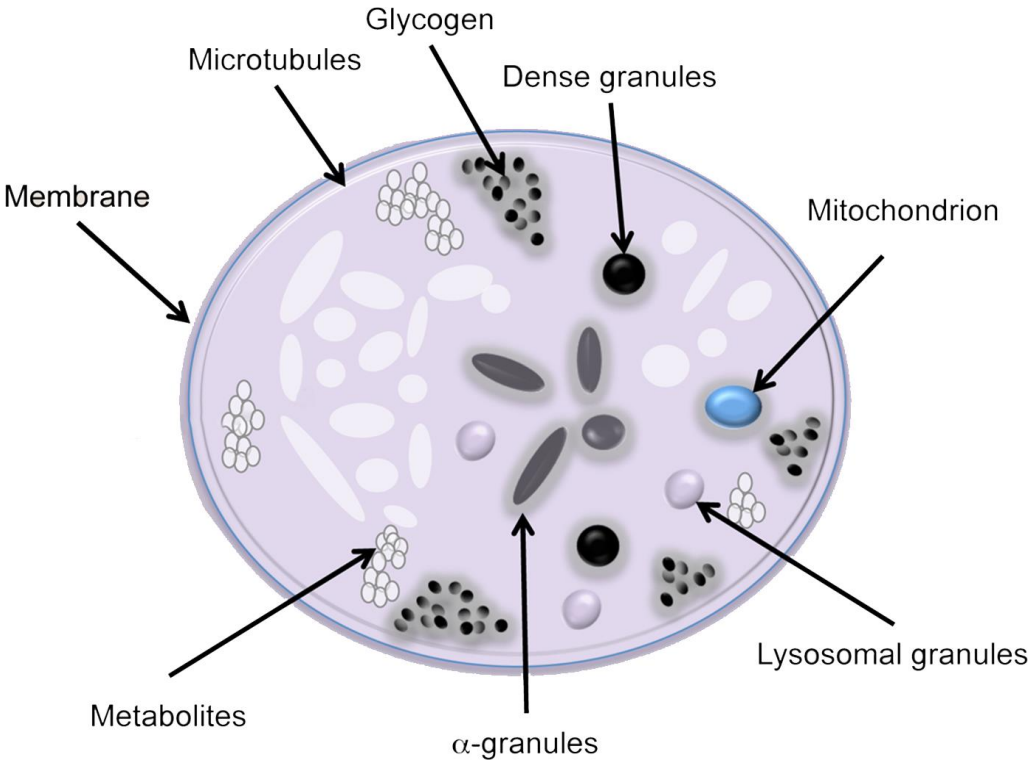

Figure 1.4. Platelet structure. *Adapted from Zapata et al (Zapata et al., 2014).*

1.4.2 Platelet based therapies

Platelet based therapies have been used in regenerative medicine for 50 years. Commonly platelet rich plasma (PRP) that is a solution of platelets generated through differential centrifugation of whole blood – collecting the upper yellow layer after the first centrifugation and the pellet after the subsequent centrifugation resuspending the platelet pellet in either the lower third of the supernatant or modified Tyrode's buffer

(Coppinger et al., 2007; Dhurat and Sukesh, 2014; Vélez et al., 2015). PRP products have been used in humans to treat a variety of medical conditions such as musculoskeletal disorders, osteoarthritis and central nervous system pain (de Mos et al., 2008; O'Connell et al., 2019). These whole platelet-based therapies do have potential disadvantages however, such as the potential to induce aggregation which may even occlude blood vessels. These drawbacks have led to the development of platelet lysates – which offer a method of delivering the many growth factors found in platelets without the cellular material (Meftahpour et al., 2021). These platelet lysates have demonstrated therapeutic value in the treatment of pain and in orthopaedic injuries (da Fonseca et al., 2021).

Recently the further refinement of platelet-based therapies has used activated platelets rather than lysed them using specific mediators of degranulation (such as PAR1) to release platelet secretome and discard cellular material via centrifugation (Huang et al., 2015; Jiang et al., 2017; Scully et al., 2020). The resulting platelet releasate is rich in numerous growth factors, cytokines, and myokines such as vascular endothelial growth factors (VEGFs), fibroblast growth factors (FGFs), Epidermal growth factors (EGFs), Hepatocyte growth factor (HGF), Transforming growth factor beta (TGFβ) and some studies have found ApoE precursor and ApoE (Pagel et al., 2017; Parsons et al., 2018; Vélez et al., 2015). This cocktail of useful growth factors serves as a powerful biomaterial for regenerative medicine and provides a great potential use in increasing myogenic potential in myoblasts. Such use has been demonstrated to promote differentiation *ex vivo* and *in vivo,* and in this study the effects of platelet releasate in skeletal muscle regeneration was determined in $ApoE^{-/-}$ mice, palmitate treated myoblasts and primary muscle stem cells(Scully et al., 2019).

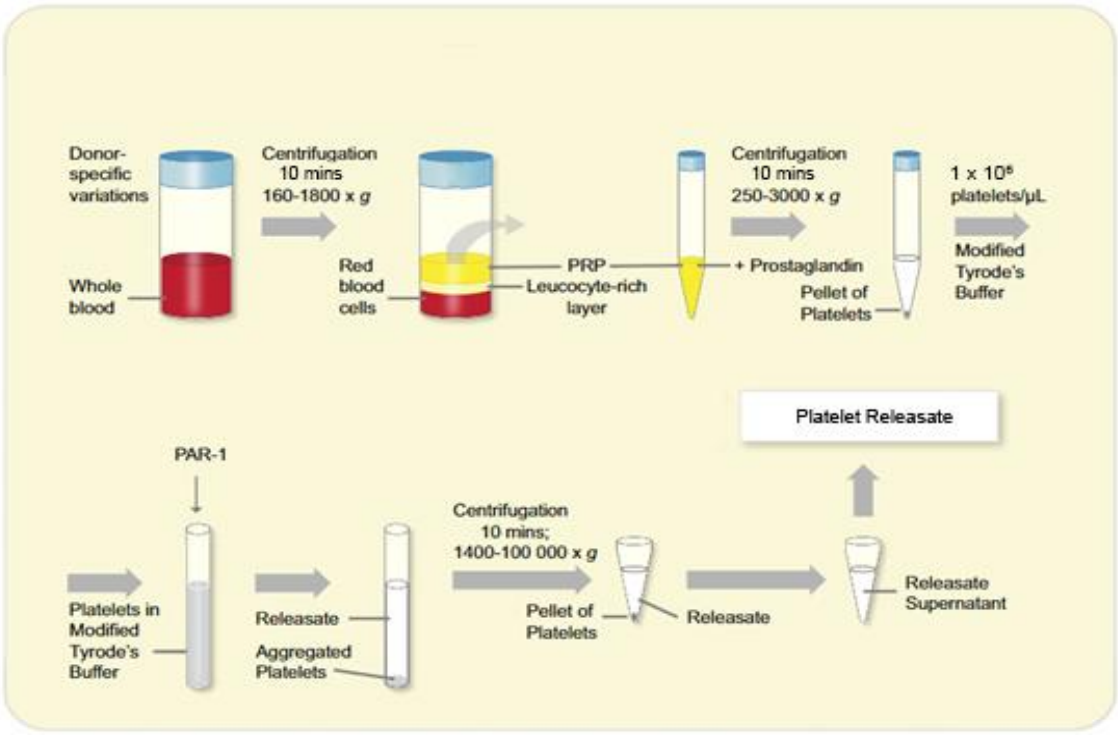

Figure 1.5: A schematic diagram showing the different stages in preparation of platelet-based applications. (Adapted from Scully et al. 2019).

1.4.3 Platelet releasate and PRP in animal, cell, and human studies

Platelet releasate and PRP have seen limited use in human trials, however a great deal more data has been recorded in animal studies of PRP and platelet releasate. Applications of PRP and platelet releasate in regenerative medicine are summarised in table 1.2. Initial studies using PRP showed promising results of increased cell proliferation, differentiation, and muscle stem cell recruitment of the regenerating mouse muscle (Dimauro et al., 2014). The suggested action of PRP was in downregulation of myo-miR-113 (a regulator of myoblast proliferation via serum response factor suppression), alongside increased Pax7, MyoD and myogenin (Nakasa et al., 2010). While one of the most abundant growth factors in PRP TGF-β is important to recovery, PRP supplemented with a TGF-β inhibitor has also been seen to enhance myofibre regeneration, and decrease fibrosis, indicating that the vast array of growth factors available in PRP together work to enhance regeneration (Kelc et al., 2015). Furthermore, muscle stem cell number increased in response to PRP with TGF-β inhibitor, further demonstrating the effectiveness of platelet-based therapies in enhancing muscle stem cell activity. In vivo study of PRP cultured human muscle derived progenitor cells saw a similar regeneration capacity to foetal bovine serum

cultured cells on transplantation into injured gastrocnemius muscle (Li et al., 2013). Furthermore, PRP has been used in rat models to improve recovery after local delivery of PRP to an injured muscle. In vitro data suggests that platelet releasate upregulates proliferation but inhibits myoblast fusion (Tsai et al., 2017). The role of ROS in myogenic differentiation is multifaceted, and cellular response to ROS depends upon a variety of factors such as ROS levels, ROS clearance and overall oxidative stress (L.-H. Chung et al., 2020; Li et al., 2021; Rajasekaran et al., 2020). PRP has been used to attenuate the oxidative stress resulting from muscle contusion – which increases levels of oxidative stress markers in the muscle (Martins et al., 2016). Antioxidant enzymatic defence is boosted by PRP in skeletal muscle, suggesting that platelet-based therapies could be an effective treatment for oxidative stress related muscle impairment. Platelet based therapies have further been used in cell studies, one such study treated primary rat gastrocnemius muscle cells with platelet releasate, finding that releasate increased proliferation of cells in a dose dependent manner (Tsai et al., 2017). The increased proliferation could indicate an increase in cell cycle progression from G1 to S phase. Another study found that in C2C12 cells the PRP enhanced proliferation and differentiation (McClure et al., 2016).

The use of platelet releasate has been effective in a variety of settings, such as improving angiogenesis (Chou et al., 2014; Huang et al., 2009; Jiang et al., 2017; Kakudo et al., 2014), nerve pain and injury (Akeda et al., 2017; Chuang et al., 2020; Obata et al., 2012), osteoarthritis (Kosmacheva et al., 2014), and proliferation and differentiation of various stem cells (He et al., 2017; Kark et al., 2006; McLaughlin et al., 2016; Suess et al., 2020; Tanaka et al., 2007) notably muscle cells (Kakudo et al., 2014; Scully et al., 2019; Tsai et al., 2017) presented in table 2. While the applications of releasate are wide and far reaching, this study focuses on the benefits to skeletal muscle regeneration and muscle stem cells. As early as 2006 releasate of thrombin activated platelets was demonstrated to increase proliferation and scratch wound closure of rat bone marrow derived cells, indicating a potential use during fracture healing to promote proliferation of osteogenic cells (Kark et al., 2006). Further study utilized releasate in mouse skin wounds showing accelerated regeneration (Tanaka et al., 2007), human adipose derived stem cells treated with releasate increased proliferation and maintained the capacity to differentiate along osteogenic, chondrogenic, and adipogenic lineages (McLaughlin et al., 2016), releasate was also

found to induce differentiation of mouse and human fibroblasts to myofibroblasts (Suess et al., 2020).

Tsai et al first identified platelet rich plasma as a source of various cytokines and growth factors beneficial to the process of muscle healing and investigated the effect of releasate on skeletal muscle cell proliferation (Tsai et al., 2017). The study found that rat platelet releasate enhances rat skeletal muscle cell proliferation by shifting cells from G1 to S phase and G2/M phase and that PRP releasate treated muscle cells expressed more cyclin A2, Cyclin B1, cdk1, cdk2 and PCNA in a dose dependent manner, whereas PRP releasate had no effect on cyclin E1 expression. Further work went to show that PRP releasate treatment could enhance the muscle-healing process and decrease CD68-positive cells and apoptotic cells – establishing the effectiveness of platelet releasate in treating muscle injury.

Further study by Scully et al. then refined the method of releasate generation by analysing the effect of releasate on C2C12 myoblast activation and differentiation using releasate from human platelets activated via collagen, TRAP6 (a PAR1 agonist) or thrombin, demonstrating greater proliferation when activated by collagen or TRAP6. This study demonstrated that platelet releasate promotes skeletal myogenesis through the Platelet derived growth factor (PDGF)/VEGF-CyclinD1–MyoD–Scrib-Myogenin axis and accelerates skeletal muscle regeneration after acute injury (Scully et al., 2019). Evidence of platelet releasate use in the promotion of proliferation and differentiation in cell progenitors as well as promotion of healing presents the possibility of skeletal muscle regeneration, as skeletal muscles house their own population of stem cells.

Stem cell capacity to proliferate, differentiate and maintain stemness decreases with age (Liu et al., 2014). PRP injections in aging cartilage have resulted in reversal of senescence processes and based on a number of studies demonstrating increased proliferation in response to PRP releasate treatment alongside decreased apoptosis evidence indicates that platelet releasate can counteract cell senescence (Chou et al., 2014; do Amaral et al., 2015; He et al., 2017; Jiang et al., 2017; Kakudo et al., 2014; Kark et al., 2006). Specifically in skeletal muscle regeneration, PRP and PPP were identified as potential biological treatments to aid muscle repair. While these

treatments aid in reducing senescence based attenuation of muscle regeneration, platelet releasate presents a superior alternative (Oberlohr et al., 2020).

Table 1.2. The applications of platelet releasate in regenerative medicine.

Reference	Species	Intervention	Findings
(Jiang et al., 2017)	Human	PAR1 or PAR4 activated Platelet releasate	↑ MCF-7 and MFA-MB-231 Breast cancer cell proliferation ↑ *in vivo* tumour growth
(He et al., 2017)	Human	SMCC.7721 and HepG2 treated with PR	↑ Proliferation ↓ apoptosis ↓ G0/G1 phase cells, ↑ S and G2/M phase cells
(Kakudo et al., 2014)	Human	HUVECs treated with PR	↑ proliferation, migration and tube formation
(Huang et al., 2015)	Human	Endothelial progenitor cells	↑ EPC migration ↑ capillary-like network formation of EPCs
(Chou et al., 2014)	Bovine	Corneal endothelial cells	↑ proliferation & viability
(do Amaral et al., 2015)	Human	nasoseptal chondrogenic cells	↑ proliferation
(van Buul et al., 2011)	Human	Human osteoarthritic chondrocytes	inhibits inflammatory processes
(Kosmacheva et al., 2014)	Human	multipotent mesenchymal stem cells	↑ osteogenic differentiation
(Akeda et al., 2017)	Human	PRP releasate injected into nucleus pulposus of patients with Lower back pain	↓ lower back pain No adverse effects
(Kark et al., 2006)	Rat	Releasate on osteogenic bone marrow derived cells	↑ Proliferation + scratch wound closure
(McLaughlin et al., 2016)	Human	Grown in media containing PR	↑Growth of human adipose derived stem cells, maintained ability to differentiate along chondrogenic, adipogenic and osteogenic lines
(El Bakly et al., 2020)	Rat	IP injection of releasate	↑ β1 integrin ↑ mTOR signaling ↓ apoptosis
(Yu et al., 2021)	Rat	Treated achilles tenotomy	↑ collagen synthesis ↓ apoptosis ↑ proliferation ↓ macrophage infiltration

(Tanaka et al., 2007)	Mouse	Releasate applied to excisional skin wounds in type 2 diabetic mice	↑ rate of skin wound area decrease. ↑ mean vascular density
(Scully et al., 2019)	Mouse and C2C12 cells	Treated with releasate	↑ myoblast proliferation ↓ myoblast fusion ↓ Differentiation
(Tsai et al., 2018)	Sprague-Dawley rats	Transverse incision injured rats were treated with PRP releasate	↑ Regeneration (accelerates healing) ↓ inflammation ↓ apoptosis ↑ Tetanic strength
(Tsai et al., 2017)	Sprague-Dawley rats	Treated with PRP releasate	↑ Proliferation ↑ cyclin A2, cyclin B1, cdk1, cdk2 and PCNA Shift to S and G2/M phase.
(Suess et al., 2020)	Primary human fibroblasts and NIH-3T3 cells	Treated with releasate	induced differentiation of cultured murine and human fibroblasts into a myofibroblast phenotype

1.4.3.2 Platelet releasate components and their function

In order to determine the potential use of platelet releasate, it is important to understand the composition of the variety of signals released on platelet activation. Releasate contains megakaryocyte-derived and endocytosed plasma components which play a role in hemostasis, wound healing, and inflammation (Machlus and Italiano, 2013). Recent evidence suggests that platelets actively sense their environment and release signals relevant to the environment i.e. inflammation, or wounds (Bye et al., 2016; Stalker et al., 2012). Platelet releasate generated for therapeutic use however may be easily replicated and is generated using Par1 agonist thrombospondin each time. To determine the composition of platelet releasate, various studies have used proteomic qualitative and quantitative approaches to characterise the contents of releasate, often yielding differing results due to inter-individual variability (Pagel et al., 2017; Parsons et al., 2018; Vélez et al., 2015). Therefore, the composition of platelet releasate should be taken as a whole – a collection of growth factors and cytokines, considering the specific effects of individual growth factors.

Parsons et al. undertook proteome profiling using label-free quantitative proteomics in 32 healthy adults in order to determine a core set of 277 proteins with low variance between healthy adults with high reproducibility when releasate is generated from human whole blood (Parsons et al., 2018). The study found that 177 of these core proteins were found in exosomes - both human and murine platelets release exosome-sized vesicles upon activation indicating they are a major contributor to intercellular communication. Of particular note the core set of proteins included PDGF, TGF, VEGF, CTGF, PF4, Actins – including actin alpha 1 which is found in muscle, as well as some cytoskeletal actins, and non-sarcomeric myosins.

Many of the growth factors from releasate have effects in skeletal muscle – PDGF and VEGF, induce angiogenesis which can improve blood flow to injured muscle, TGF, EGF, FGF, IGF, HGF and SDF-1α have been shown to improve muscle stem cell activation or differentiation; FGF, ang-1 and TNF attenuate atrophy; and TGF VEGF, FGF, IGF, and SDF-1α has been shown to improve injury regeneration (Benoit et al., 2017; Brzoska et al., 2012; Delaney et al., 2017; Gianni-Barrera et al., 2018; Sanchez-Encinales et al., 2015; Tidball and Spencer, 1993; Wagner, 2011; Wang et al., 2020). The effects of important individual proteins and growth factors found in releasate are summarised in table 1.3.

However, there are possible downsides to using platelet releasate as a therapy, chemokines found in releasate contribute to pathological conditions such as thrombosis, and atherogenesis (Bakogiannis et al., 2019; van der Meijden and Heemskerk, 2019). While soluble growth factors such as PDGF, VEGF and TGFβ promote tumour growth and metastasis anti-angiostatic factors such as PF-4, endostatin and TSP-1 are also released from platelets and serve a protective role against tumour survival and growth (Lazar and Goldfinger, 2021).

Table 1.3: releasate growth factors and proteins effects in skeletal muscle

Reference	PGF	Cell sources	Effect in skeletal muscle
(Gianni-Barrera et al., 2018)	PDGF	Platelets, endothelial cells, macrophages, smooth muscle cells	regulates splitting angiogenesis in skeletal muscle by limiting VEGF-induced endothelial proliferation.
(Tidball and Spencer,			induces phosphorylation of talin and cytoskeletal reorganization.

1993)			
(Delaney et al., 2017) (Weist et al., 2013)	TGF	Macrophages, T lymphocytes, keratinocytes	regulation of muscle repair via satellite cells activation, connective tissue formation, as well as regulation of the immune response intensity. enhances contractility in engineered skeletal muscle.
(Wagner, 2011) (Frey et al., 2012)	VEGF	Platelets, macrophages, keratinocytes, endothelial cells	Angiogenesis + blood flow. Improves regeneration after acute trauma.
(Wang et al., 2020)	EGF	Platelets, macrophages, monocytes	musculoskeletal tissue regeneration and activate the myogenic differentiation of satellite cells.
(Benoit et al., 2017) (Pawlikowski et al., 2017)	FGF	Platelets, macrophages, mesenchymal cells, chondrocytes, osteoblasts	regulates skeletal muscle mass and ameliorates muscle wasting in mice. essential for self-renewal of skeletal muscle stem cells (satellite cells) and required for maintenance and repair of skeletal muscle.
(Petrosino et al., 2019)	CTGF	Platelets, fibroblasts	ECM remodelling.
(Yoshida and Delafontaine, 2020) (Witt et al., 2017) (Song et al., 2013)	IGF	Platelets, plasma, epithelial cells, endothelial cells, fibroblasts, osteoblasts, bone matrix	regulates both anabolic and catabolic. improves myoblast activation. IGF-I is involved in increasing muscle mass and strength, reducing degeneration, inhibiting the prolonged and excessive inflammatory process due to toxin injury, and increasing the proliferation potential of satellite cells.
(Sanchez-Encinales et al., 2015) (Witt et al., 2017) (Proto et al.,	HGF	Platelets, mesenchymal cells	improves glucose homeostasis in diet-induced obese mice. improves myoblast activation. crucial for inflammation resolution and the completion of repair in dystrophic skeletal muscle.

2015)			
(Aravena et al., 2020) (Morales et al., 2016)	Ang-1	Platelets, neutrophils	Decreases Myostatin-Induced NF-kappaB Signaling and Skeletal Muscle Atrophy. attenuates disuse skeletal muscle atrophy in mice via its receptor, Mas.
(Brzoska et al., 2012) (Kowalski et al., 2017)	SDF-1α	Platelets, endothelial cells, fibroblasts	Sdf-1 (CXCL12) improves skeletal muscle regeneration via the mobilisation of Cxcr4 and CD34 expressing cells. Increases stem cell migration and fusion.
(Patel and Patel, 2017) (Li et al., 2020) (Meyer et al., 2015)	TNF	Macrophages, mast cells, T lymphocytes	TNF-alpha has a direct catabolic effect on skeletal muscle and causes wasting of muscle by the induction of the ubiquitin-proteasome system (UPS). Age based atrophy. Alpha. Inhibits SC differentiation (in opposition to IGF-1.

1.5 Ebselen

Ebselen is an antioxidant and anti-inflammatory drug with ROS reducing qualities which has not yet been approved for any treatment by the FDA, however they have allowed several clinical trials including phase III clinical trial for ebselen in the treatment of Meniere's disease, hearing loss, bipolar disorder and COVID-19 (ClinicalTrials.gov: NCT03013400, NCT01452607, NCT00762671, NCT04677972, NCT04483973 and NCT02603081). Ebselen was first recognised as an antioxidant and has superoxide scavenging qualities as well as a number of protein interactions involving the reduction of thiols (Müller et al., 1984; Smith et al., 2012). Glutathione peroxidase (GPx) is an endogenous antioxidant, which acts as a catalyst in reducing H_2O_2, and ebselen works in a similar fashion, as a glutathione peroxidase (GPx) mimetic (Sies, 1993). As a lipid-soluble compound, ebselen can permeate the cell membrane and has rapid absorption following oral administration, making ebselen a potentially useful drug candidate, and a lack of toxicity has been observed in clinical trials (Noguchi et al., 1992; Takasago et al., 1997). Ebselen induces transcriptional

expression of detoxifying and antioxidant genes. As a consequence of its antioxidant properties, ebselen has a variety of effects such as, anti-thrombotic, anti-atherosclerotic, cytoprotective and more (Azad et al., 2014; Chew et al., 2009; Schewe, 1995). As such, ebselen is being studied as a treatment of atherosclerosis, neurological diseases, and cancer, as well as a number of other potential uses. The well accounted for effect of ebselen in inhibition of NADPH oxidase (nox) dependant superoxide generation has the expected consequence of reduction in ROS, which themselves cause DNA damage and apoptosis in the cardiovascular system and the brain (Lee et al., 2012; Maulik and Yoshida, 2000). The rapid reaction of ebselen with peroxynitrite and other free radicals, protecting against ROS and reactive nitrogen species, good pharmacokinetic profile and wide array of beneficial interactions, makes it a potential therapy for ROS induced injuries (Guven et al., 2008; Masumoto and Sies, 1996).

Ebselen has also been effective in treating endothelial damage, and structural changes in the endothelium are ameliorated by ebselen treatment (Phinikaridou et al., 2013). ApoE$^{-/-}$ mice have a greater width of gap junctions and fewer gap junctions, causing a reduced structural stability, this is also alleviated by ebselen. An increase of collagen type 1, MMP1, MMP9 and TIMP1 protein expression in ApoE$^{-/-}$ UNX mice compared to wild type is reduced by ebselen. These metalloproteinases are involved in the breakdown of the extracellular matrix, alongside TIMP1, an inhibitor of matrix metalloproteinases, and Collagen 1, the protein which MMPs degrade (Baragi et al., 2009). Despite the altered expression of both counteractive proteins, this clearly demonstrates some level of altered matrix remodelling in ApoE$^{-/-}$ UNX mice which is resolved by treatment with ebselen. These UNX mice also had similar expression of VEGF receptor flt-1, which was alleviated by ebselen, preventing the proliferation of endothelial cells which leads to atherosclerotic lesions. The ApoE$^{-/-}$GPx1$^{-/-}$ double knockout studies confirm ebselen's effects on oxidative stress, lesion progression and endothelial reorganisation, as ebselen restores a lower expression of GPx3&4, MCP-1, Collagen IV, TGF-β signalling as well as Collagen I & IV (Chew et al., 2010). It's GPx-like action compensating for the ablation of GPx1. An attenuation of glomerulosclerosis and mesangial expansion as well as a reduction in matrix accumulation in the tubulointerstitium were also seen by ebselen treatment of the

ApoE$^{-/-}$GPx1$^{-/-}$ double knockout, implying a role for ebselen in treating diabetic complications (Tan et al., 2013).

Ebselen also causes a reduction in macrophage proliferation in ApoE$^{-/-}$GPx1$^{-/-}$ mice – a phentotype with reduced antioxidant capacity. In atherosclerosis macrophages phagocytose oxLDL, for slow degradation in the lysosome, this accumulates and foam cells form. The proliferation of macrophages acts through the MAP kinase, ERK 1/2 pathway by abrogating ERK phosphorylation (Cheng et al., 2013). In a study on oxLDL, ebselen essentially abolished the peroxides but not the aldehydes of oxLDL, and had no impact on oxLDL uptake by macrophages (Shen and Sevanian, 2001). There is also a decrease in alpha smooth muscle actin in the aortic sinus in response to ebselen treatment, which implies a reduction in myofibroblasts; ebselen is effective in treating the inflammatory aspects of atherosclerosis in the aorta. These data suggest a role for ebselen in tempering the inflammatory response as a response to an increase in ROS which leads to macrophage infiltration.

1.5.1 Ebselen in ApoE$^{-/-}$ mice

The ApoE protein shows antioxidant activity *in vitro*, although it's *in vivo* relevance remains to be established. Interestingly, the antioxidant activity appears to be allele specific. Miyata and Smith found that at physiological concentrations all three apoE proteins significantly reduced H_2O_2-induced cell death, but in the following order of effectiveness E2, E3, E4, with the E2 protein being approximately twofold more effective compared with E4 (Miyata and Smith, 1996; Pellegrin et al., 2014).However, evidence regarding the contribution of apoE genotype to oxidative stress-dependent processes is limited. In the Northwick Park Heart Study II the authors speculated that the 2.79-fold increased risk of CVD events in apoE4 smokers relative to the non-smoking group may be due to the different antioxidant capacity of the apoE protein isoform, although no direct evidence was provided (Talmud et al., 2006). Importantly, significantly higher (29%) circulating levels of F2-isoprostanes, a surrogate biomarker of lipid peroxidation, in mildly hypercholesterolemic(45.6 mmol/L) apoE4 as compared with non-apoE4 carriers have been observed (Sfyri et al., 2018). This finding is in line with other studies reporting higher plasma concentrations of oxidised LDL and malon-dialdehyde-modified LDL in apoE4versusnon-apoE4 allele carriers (Metso et al., 2003; Tsuda et al., 2004). In cell culture studies, apoE4 macrophages exhibited increased membrane oxidation and produced more reactive oxygen and

nitrogen species upon stimulation with the phorbol ester PMA and bacterial LPS, respectively (Jofre-Monseny et al., 2007a). A higher transactivation of the key redox sensitive transcription factor NF-kB was evident in apoE4 as compared with apoE3macrophages and was accompanied by a higher production of pro-inflammatory molecules (tumour necrosis factor a, interleukin 1b, macrophage inflammatory protein 1a). Amounts of the anti-inflammatory cytokine interleukin 10 produced inapoE4 macrophages were lower than in apoE3 cells (Huebbe et al., 2010). These data may indicate that apoE4 macrophages have an altered inflammatory response, which may contribute to the higher CVD risk observed in apoE4 carriers

As ebselen has a variety of effects on a number of different pathologies, it has been used to reduce oxidative stress in more rodents than simply $ApoE^{-/-}$ mice, as summarised in table 1.4. In cultured wistar rat brain cells, ebselen suppressed Hydrogen peroxide ($H_2O_{2)}$ induced release of cellular proteins heat shock protein (HSP) 90 and HSP110, (Ito et al., 2013). Malondialdehyde, the end product of lipid peroxidation, is elevated in oxidative stress and levels are decreased in the rat lung by treatment with ebselen, however ebselen was unable to inhibit Inducible nitric oxide synthase (iNOS) activity in the same study (Yaren et al., 2007). While other studies have seen a decrease in iNOS activity in response to ebselen each shows a reduction in oxidative stress.

A study on wild type mice neutrophils found an increase in microparticle expression after exposure to high pressure gas (Thom et al., 2014). These microparticles are small membrane encapsulated cell fragments, and they initiate a systemic inflammatory process that is related to neutrophil activation. Ebselen was able to decrease expression of microparticles after exposure to high pressure gas, indicating that the oxidative stress caused by periods of low oxygen availability can be alleviated by ebselen, making it potentially useful to deep sea divers and astronauts, similarly periods of low oxygen exposure during open heart surgery can be alleviated as tested by Maulik et al (Maulik and Yoshida, 2000). Furthermore, the same study saw a reduced actin turnover by ebselen, as in neutrophils a higher actin turnover can contribute to oxidative stress through activation of iNOS; ebselen has a multiplicity of action in relieving oxidative stress. Another study saw ebselen used to reduce osteogenic responses to oxidative stress in aortic myofibroblasts; it's abrogation of Msx2 after myofibroblast induction by TNF preventing aortic calcification (Lai et al.,

2012). These results suggest a role for ebselen in ischemia-reperfusion, where a tissue is without oxygen and the reperfusion of oxygen introduces a sharp rise of ROS. Therefore, ebselen is useful to help reintroduce oxygen without the ROS.

Ebselen prevents vasculopathy and prevents an increase in senescent endothelial cells in Zucker diabetic rats (Brodsky et al., 2004). Patients with metabolic syndrome develop premature senescence of the cardiovascular system; ebselen prevents the increase in advanced glycation end products – proinflammatory mediators upregulated under oxidative stress. Ebselen also decreases abundance of nitrotyrosine modified proteins in diabetic rats, prevents the increase of senescent endothelial cells and prevents vasculopathy, all of which contribute to an atherogenic phenotype and are elevated in oxidative stress.

Skeletal muscle is also affected by oxidative stress, exposure to hypoxic conditions, tissue trauma and even ageing can result in a production of ROS. The hypoxia-reperfusion response is well documented to cause an increase in ROS and can cause oxidative stress in skeletal muscle. Ebselen mitigates muscle fatigue and ROS generation in reperfusion after exposure to hypoxic conditions (Zuo et al., 2013). Mouse denervated muscle exhibits increased ROS production; ebselen has fatty acid hydroperoxide scavenging qualities and reduced H_2O_2 expression in denervated mouse muscle (Bhattacharya et al., 2009). Mechanical loading of skeletal muscle stimulates ROS production which activates AMP kinase and increases glucose uptake, ebselen decreases this by decreasing ROS (Chambers et al., 2009). After increase of ROS subject to soft tissue trauma in rats, ebselen restores disturbed microcirculation and reduces the inflammatory response which in turn prevents secondary injury due to leukocyte infiltration (Gierer et al., 2010). Ebselen has also been seen to have counteractive effects at differing concentrations, increasing high affinity binding of ryanodine to the skeletal muscle type ryanodine receptor at nanomolar concentrations, but inhibiting this at low micromolar concentrations (Xia et al., 2004). This effect is the result of ebselens oxidation of thiols, at lower concentrations fourteen free thiols of ryanodine receptor are oxidised, enhancing Ca2+ release; however greater concentrations oxidise more thiols to inhibit this. Ca2+ release initiates muscle contractions. The ryanodine receptor is a Ca2+ releasing channel which initiates muscle contractions by rapid release of sarcoplasmic reticulum Ca2+, therefore ebselen can modulate contractions of muscle.

Table 1.4. The effects of ebselen on ApoE$^{-/-}$ mice in regenerative medicine

Reference	Species	Intervention	Findings
(Chew et al., 2009)	Male ApoE$^{-/-}$ mice (8 wks), diabetic	Ebselen, dissolved in 5% CM-cellulose, was gavaged twice daily at 10 mg/kg body weight (i.e. 20mg/kg/day) For 10/20 wks	↓ diabetes induced weight loss ↓ total aortic plaque ↓ nitrotyrosine levels ↓ nox2 mRNA & protein levels in aorta ↓ RAGE mRNA & protein in aorta Ebselen attenuated diabetic induced VEGF increase in aorta ↓ α-SMA in aorta ↓F4/80 staining (macrophage marker) NO change in: SOD1, ↑ Glutathione peroxidase-1
(Chew et al., 2010)	Male apoe$^{-/-}$ GPx1$^{-/-}$ mice (8 wks), diabetic	Ebselen gavaged twice daily dissolved in 5% CM-cellulose (10gm/kg) at 10 weeks, maintained for 10/20 weeks	↓ diabetes induced weight loss ↓ Organic hydroperoxides in plasma ↓ total aortic plaque ↓ nox2 mRNA & protein levels in intimal and medial layers of diabetic aortas ↓ nitrotyrosine & 4-HNE levels, aorta ↓ GPx3, GPx4, aorta Ebselen attenuated diabetic induced VEGF increase, aorta ↓ MCP-1 & VCAM-1, aorta
(Tan et al., 2013)	Human aortic endothelial cells, normal rat kidney cells, ApoE$^{-/-}$ GPx1 dKO mice (8 wks)	Diabetes induced with 2 daily doses of streptozotocin, (100 mg/kg/day) At 10 weeks ebselen gavaged twice daily (10mg/kg) (i.e. 20mg/kg/day) for 12 weeks	↓ total aortic plaque, ↓ aortic lesions ↓ Aortic oxidative stress (nitrotyrosine staining) ↓ accumulation of matrix in the tubulointerstitium ↓ collagen IV protein mesangial expansion and glomerulosclerosis were attenuated in Ebselen ↓ Kidney oxidative stress ↓ TGF-β signalling in kidney ↓ Collagen I & IV expression in NRK52E cells
(Phinikaridou et al., 2013)	male ApoE$^{-/-}$ mice (8wks), ND or HFD (21% fat, 0.15%	Left untreated or treated with ebselen by daily gavage (5 mg/kg body weight dissolved in 5% CM-cellulose) for 12 weeks	↓ vessel wall enhancement (brachiocephalic artery) ↓ plaque burden ↓ endothelial damage, gap junction width ↓ monocyte/ macrophage content of endothelium

	cholesterol) for 12 wks.	(concurrent with HFD) MRI measured	
(Piecha et al., 2008)	ApoE$^{-/-}$ mice (8 wks), ND ad libintum,	At 10 wks, unilateral nephrectomy or sham operation, received either ebselen (30mg/kg body weight/day by gavage), tempol, or trandolapril	No effect on Systolic blood pressure, ↑ capillary length density, ↓ mean intercapillary distance in myocardium. UNX induced Aortic intima-media thickness increase prevented by ebselen, Atherosclerotic plaque formation prevented, Prevents increased deposition of collagen I, increase of MMP1,MMP9,TIMP1, No change in TGFβR1 or R1 ↓ VEGF, ↑ VEGF receptor - flt1 No change in nitrotyrosine vs untreated UNX, but Sham untreated had lower nitrotyrosine than sham ebselen No change in eNOS, ↓ iNOS
(Laursen et al., 2001)	ApoE$^{-/-}$ mice(6-18 months),	Treated with ebselen (although not main focus of paper and no intervention really listed)	↓ peroxynitrite
(Park et al., 2011)	Prdx2$^{-/-}$ ApoE$^{-/-}$ mice, HFD (0.15% cholesterol, 20% fat, and 0.05% sodium cholate), ApoE$^{-/-}$ mice,	Ebselen dissolved in 80% (v/v) DMSO administered via osmotic pump at a dose of 10 mg/kg/day Or aortic sections pretreated with 20 μmol/L ebselen.	Ebselen reduced atherosclerotic plaque, ↓ aortic H_2O_2 & VCAM-1 & iCAM-1. Ebselen blocked MCP-1, aorta effectively suppressed the transmigration of CD11b+ monocytes
(Cheng et al., 2013)	ApoE$^{-/-}$ GPx1$^{-/-}$ standard diet for 5 months or HFD for 8 wks for 12 wks	Macrophages from ApoE$^{-/-}$GPx1$^{-/-}$ mouse pretreated with 10 μM Ebselen for 1 h and incubated with 10 mg/ml oxLDL and BrdU for another 48 h. After preincubation with 10 ng/ml MCSF	Ebselen decreased macrophage proliferation in ApoE$^{-/-}$GPx1$^{-/-}$ mouse. Abrogated ERK phosphorylation in ApoE$^{-/-}$GPx1$^{-/-}$, but not ApoE$^{-/-}$.

		for 3 days, cells incubated with ebselen for 5 min.	
(Jeong et al., 2018)	ApoE$^{-/-}$ mice, ND 20 wks or HFD 10 wks (20% fat, 0.15% cholesterol)	Peritoneal macrophages isolated from Prdx1$^{-/-}$ mice were pretreated with 10mM ebselen	Restoration of lipophagic flux & cholesterol efflux.

1.5.2 Ebselen in cell studies

Cellular studies can be a powerful method of assessing the benefits of ebselen on oxidative stress. Oxidative stress has been simulated in these studies (summarised in table 1.5) through viral transfection of Nicotinamide adenine dinucleotide phosphate (NADPH) oxidases, overexpressing them, application of insulin to induce production of H_2O_2, direct exogenous application of H_2O_2, nitrogen mustard or t-butyl hydroperoxide (Lai et al., 2012; Müller et al., 1984; Sies, 1993; Smith et al., 2012). While these studies may not fully recapitulate the extent of oxidative stress - not simply a matter of increased production of ROS, free radicals, reactive nitrogen species (RNS), a decreased anti-oxidative capacity or a reduced ability to reduce ROS, but a combination of these factors, the positive effects of ebselen are clear. Cellular studies have seen ebselen improve myofibroblast expression of Msx2, inhibition of tau phosphorylation, induction of glioma cell death and alter wound healing (Datla et al., 2007; Lai et al., 2012; Sharma et al., 2008; Xie et al., 2012).

ROS function in intracellular signalling to prevent tissue injury and promote angiogenesis at low levels, however at higher concentrations they may be deleterious to cells due to their action in lipid peroxidation, protein oxidation and DNA damage, resulting in their role in the aforementioned diseases (Batna et al., 1997; Farmer and Mueller, 2013; Yang, 2019). The primary enzymatic sources of ROS production in the cell are Nicotinamide adenine dinucleotide phosphate (NADPH) oxidases (Nox), multimeric protein complexes which produce superoxide via their catalytic Nox subunit which is membrane bound and transfers electrons from cytosolic NADPH to molecular oxygen (Miller et al., 2006). Of the four Nox isomers, expression of Nox1, Nox2 and Nox4 has been reported in skeletal muscle, and Nox4 appears to have a greater

impact on the expression of ROS in skeletal muscles (Ferreira and Laitano, 2016). Nox inhibitors have a great deal of therapeutic potential in their ability to reduce ROS and restore homeostasis, their use has been shown to potentially alleviate atherosclerosis, asthma and ischemic stroke.

One such study in human microvascular endothelial cells found reduced tube formation and wound healing responses in Nox4 siRNA mediated gene silenced cells (Datla et al., 2007). This implicated the actions of NADPH oxidase in angiogenesis and wound healing, indicating a beneficial role for ROS after injury. The prevention of proliferation of cells by ebselen may not be useful in all cells, as satellite cells differentiation to regenerate muscle may be impaired as they need to be activated for a period of proliferation. This effect was further demonstrated in human microvascular endothelial cells with viral overexpression of Nox4 or the dominant negative form of Nox4 ($Nox4^{\Delta nadph}$) enhancing or attenuating these responses respectively (Datla et al., 2007). The exogenous application of H_2O_2 further enhanced tube formation and wound healing, while ebselen had an opposing effect (Sies, 1993). As ROS tend to induce an inflammatory response, the action of ebselen is counterintuitive at sites of injury as wound healing will be inhibited.

Msx2-Wnt signalling has been suggested as a pro arteriosclerotic pathway, initially discovered as an important osteogenic pathway in craniofacial skeletal development. The pathway also contributes to arteriosclerotic calcification and the process of ROS activation of TNF induces this osteogenic action. The study of aortic myofibroblasts saw a reduction of TNF induced Msx2-Wnt signalling when treated with ebselen, reducing the oxidative stress causing the osteogenic reaction (Lai et al., 2012).

Interestingly, in glioblastoma cells ebselen has been found to have opposite effects, sensitizing cells to TNF-α rather than preventing its activation (Smith et al., 2012). In cell lines U87MG, A172 and T98G, cell viability was unchanged at low concentrations, however at a higher concentration of 50μM, a ~35% reduction in cell viability was seen (Smith et al., 2012). These cell lines used were resistant to TNF-α induced apoptosis, and the viability when exposed to both ebselen and TNF-α was further reduced to around 50%, decreasing the expression of TNFR1 and inhibiting Nuclear factor kappa beta (NF-κB) activity and gene expression in these glioma cell lines (Smith et al., 2012). This suggests a role for ebselen in inducing apoptosis in resistant tumour cells,

suggesting ebselen as a candidate to overcome a major problem in anticancer therapy.

A study in neuroblastoma SH-SY5Y cells, treated with ebselen for 12 hours and treated with iron to induce tau phosphorylation (Müller et al., 1984). Ebselen abrogated the effects, reducing tau phosphorylation and the decrease in ROS production decreases cellular iron influx too. Furthermore, the activity of CDK5 and GSK3β responsible for tau phosphorylation were reduced by ebselen. As tau phosphorylation is implicated in a number of neurodegenerative diseases such as Alzheimer's disease the counteractive ability of ebselen could be important in preventing these degenerative diseases.

While many effects of ebselen in relation to atherosclerosis and cancer are beneficial, it remains to be seen if the effects are positive in all tissue types. Skeletal muscle satellite cells for example, which would begin to proliferate in response to injury could be impeded by abrogation of MSX2, or the decrease in collagen IV, both of which are important to differentiation of satellite cells. As there are muscular aspects of atherosclerosis, it would be important to determine ebselen's effect on satellite cells in order to prevent an exacerbation of this symptom.

Table 1.5. Studies concerning ebselen treated cells

Reference	Cell Type	Intervention	Findings
(Lai et al., 2012)	mouse aorta adventitial myofibroblasts of WT, TNFR1$^{-/-}$, TNFR2$^{-/-}$, and p47phox$^{-/-}$	Cultures were pretreated with ebselen 100μM for 30 min before treatment with TNF.	Ebselen treatment almost completely abrogates TNF induction of Msx2
(Müller et al., 1984)	Human neuroblastoma SH-SY5Y cells	After treatment with 5 lM ebselen for 12 h, cells were incubated with 0.5 lM calcein-AM (Dojindo Laboratories, Japan) for 30 min at 37 ºC.	↓ Tau phosphorylation ↓ ROS production, cellular ion efflux ↓CDK5 and GSK3β activity in iron treated cells
(Smith et al., 2012)	Glioblastoma cell lines U87MG, A172 and T98G	On attaining semiconfluence, cells were switched to serum free media	Sensitized to TNFa-induced apoptosis Affects the expression

		and after 12 hr, cells were treated with different concentration of Ebselen (in Dimethyl sulfoxide, DMSO) in the presence or absence of TNFa (50 ng/ml) in serum free media for 24 hr	of molecules associated with TNFa induced signaling events ↓ TNFR1 expression ↑ TRADD and ↓ TRAF2 levels in the TNFR1-TRADD-TRAF2 signaling complex in TNFa treated cells Inhibits NF-κB activity in TNFa treated gliomas Inhibits TNFa-induced NF-κB reporter gene expression in glioma cells Affects molecules associated with cell cycle progression
(Sies, 1993)	Human microvascular endothelial cells (HMECs)	Exogenous H_2O_2 (0.1,0.3,3,10μmol/L) and ROS scavenger ebselen (10μmol/L).	wound healing and tube formation responses were enhanced by exogenous H_2O_2 but attenuated by ebselen

1.6 Aim, hypothesis, objectives of the thesis

The project is focusing on the skeletal muscle stem cell function of the Apolipoprotein E deficient ($ApoE^{-/-}$) mouse, aiming to understand the effects of hyperlipidaemia with increased oxidative stress between the wild type and $ApoE^{-/-}$ mice. The $ApoE^{-/-}$ mouse has a hypercholesterolemic and atherogenic phenotype, which in humans can lead to intermittent claudication so the increase of ROS seen in other tissues in this model is likely also seen in skeletal muscle and could be a factor in the impaired muscle function. Some evidence suggests that obesity is a risk factor to attenuate skeletal muscle stem cell activity; therefore the present work intends to see if this is as a result of increased oxidative stress (Sfyri et al., 2018). Here the work examines the differences in total satellite cell number and number of satellite cells expressing

specific transcription factors: Pax7 – highly expressed ubiquitously in quiescent and activated satellite cells, myogenic differentiation 1 (MyoD) – expressed in myogenic proliferating cells and Myogenic factor 4 (myogenin) – expressed in committed differentiating myogenic cells. Only Pax7 is expressed in quiescent cells (Zammit et al., 2006). This will help to determine if the ApoE$^{-/-}$ mouse has impaired proliferation or differentiation of satellite cells, impairing muscle growth. While the full on Pax7 knockout is viable, mice usually die within 2 weeks after birth. They produce fibres with smaller diameter, but the organisation of fibres is unchanged despite deficient postnatal muscle growth.

The effect of ApoE deficiency on skeletal muscle stem cell myogenic capacity and function remains unknown so far. Therefore, the present work aimed to determine whether hyperlipidaemia followed by increased oxidative stress in skeletal muscle of ApoE$^{-/-}$ mice would affect muscle stem cell myogenic progression, independently of their niche in the whole muscle. To achieve this, ApoE deficient muscle stem cell myogenesis was evaluated in two different experimental settings, i.e. on single muscle fibres and isolated muscle stem cells. Firstly, Myofibres from ApoE$^{-/-}$ mice were isolated and cultured *ex vivo* to investigate the myogenic progression and self-renewal of muscle stem cells. Secondly, muscle stem cells were removed from their microenvironment, i.e. myofibres, and their myogenic potential was studied in cultures *in vitro*. The present study took advantage of the differential expression patterns of transcription factors and myogenic regulatory factors as follow: in adult skeletal muscle, quiescent stem cells express Pax7, activated stem cells switch on MyoD expression, proliferating stem cells co-express Pax7 and MyoD, stem cells committed to differentiation are Pax7-negative and MyoD-positive, whereas differentiated stem cells give rise to new myonuclei that express myogenin (Füchtbauer and Westphal, 1992; Grounds et al., 1992; Yablonka-Reuveni et al., 1999; Yablonka-Reuveni and Rivera, 1994; Zammit et al., 2004, 2002). It was hypothesised that muscle stem cell function may be perturbed in atherosclerotic mice with systemic hyperlipidaemia and skeletal muscle oxidative stress and this may explain the impaired muscle regeneration seen *in vivo*.

Reactive oxygen species (ROS) including superoxide anion, hydrogen peroxide and hydroxyl free radicals have been implicated in a variety of pathologies including cardiovascular disease, neurological diseases, and cancer (Carvalho et al., 2017;

Galanis et al., 2008; Kennedy et al., 2012; Sugamura and Keaney, 2011). Contracting muscles generate ROS, these ROS are important in normal insulin signalling, and contribute to wound healing (Steinbacher and Eckl, 2015). Increased production of ROS however, is a major contributor to atherosclerosis that leads to muscle fatigue – in peripheral artery disease this manifests as intermittent claudication, reduced exercise tolerance and ambulation (Kattoor et al., 2017). Overall, the impact of an excess of ROS outweighing the antioxidant capacity has a negative effect on the body.

1.7 Aims and objectives

Given the lack of evidence on the role of skeletal muscle stem cell involvement in impaired muscle function in the ApoE$^{-/-}$ mouse, the aim of this thesis was to characterise for the first time the muscle stem cell capacity for proliferation and differentiation in the ApoE deficient mouse. The thesis further aims to determine the extent to which this may be alleviated through ebselen or platelet releasate.

It was hypothesised that

1. The hyperlipidaemic and atherosclerotic mouse would have skeletal muscle stem cells with impaired function.
2. Experimental hyperlipidaemia induced via palmitate would disrupt muscle stem cell function and increase oxidative stress, while the use of antioxidant ebselen would restore muscle stem cell function.
3. The injured ApoE deficient mouse would have a delayed or impaired regeneration.
4. Administration of platelet releasate generated from isolated and activated human platelets would improve muscle stem cell function and regeneration in senescence induced muscle stem cells.

These hypotheses were tested by addressing the following objectives:

- To characterise the progression of muscle stem cells (i.e. development of activated, proliferating and committed to differentiation cells) of the ApoE$^{-/-}$ mouse model.
- To determine the impact of experimental hyperlipidaemia on muscle stem cell reactive oxygen species levels, and their function with and without antioxidants.
- To establish whether functional changes in muscle stem cells follow an impairment in injury regeneration.
- To examine doxorubicin induced senescence and its effects on muscle stem cell proliferation and differentiation, and to determine the impact of platelet releasate on senescent cells.

Chapter 2 – General Materials and Methods

2.1 Practical Methods

2.1.1 Animal Maintenance

Mice were purchased from Charles river, both genotypes and were maintained in the animal facility of the University of Hull. Mice homozygous for deletion of apolipoprotein E (ApoE$^{-/-}$) on a C57Bl/6J background (Charles River, Kent, UK) and wild type (C57Bl/6J) mice were used in accordance with UK Animals (Scientific Procedures) Act 1986. Male C57Bl/6J (wild-type, WT) and ApoE deficient (ApoE$^{-/-}$) mice on the same genetic background were housed at the University of Hull under standard environmental conditions (20–22 °C, 12–12 h light–dark cycle) and were provided standard chow (normal diet, ND) and water *ad libitum*. The experiments were performed under a project license from the United Kingdom Home Office in agreement with the revised Animals (Scientific Procedures) Act 1986. Animals were humanely sacrificed via Schedule 1 killing under terminal anaesthesia.

2.1.2 Tissue harvesting and freezing

Tissue was harvested at the University of Hull. Liver, Extensor Digitorum Longus (EDL), Tibialis Anterior (TA), Gastrocnemius (Gas), Quadriceps (QDs) and soleus muscles were excised from both limbs. The connective tissue surrounding the EDL, TA and soleus muscles was removed and the muscles were flattened and subsequently frozen in isopentane (2-methylbutane) cooled in liquid nitrogen in order to avoid freezing artefacts, autolysis, or putrefaction. Quadriceps and gastrocnemius were snap frozen in liquid nitrogen for molecular analysis. All the experimental procedures were performed on frozen specimens.

2.1.3 Single myofibre isolation and culture

Murine C57Bl/6J single myofibres were isolated from the extensor digitorum longus (EDL) and biceps brachii muscle. EDL and biceps brachii muscles were dissected as described in chapter 2.1.2, but instead of freezing muscles were chemically digested with collagenase (0.2%; Sigma Aldrich; cat. C2674) for 3-4 hours with gentle shaking every 20 minutes at 37°C and 5% CO_2. Muscles were transferred to horse serum coated 3.5cm petri dishes in serum free media (Dulbecco's modified Eagle's Medium (DMEM; HyClone) and 1% penicillin-streptomycin (Sigma-Aldrich)). A glass pipette was used to gently triturate each muscle individually in until fibres began to dissociate from the muscle, living fibres were transferred to a new petri dish, while dead fibres,

hypercontracted fibres and debris were discarded. Isolated myofibres were cultured for 24, 48 and 72 hours in single fibre media containing 10% Horse Serum, 0.5% chick embryo extract and 1% penicillin-streptomycin. Single myofibres were isolated from the extensor digitorum longus or biceps brachii muscle and studied at different time points (T0, T24, T48 and T72 hours) to determine quiescent, proliferating and differentiating satellite cells, by means of Pax7, MyoD and Myogenin staining. This is a common method to determine skeletal muscle stem cell function and the differential expression of these transcription factors allows for the determination of proliferative function, activation, and commitment to differentiation.

2.1.4 Muscle stem cell isolation from single myofibres

Muscle stem cells were islolated from the EDL and biceps brachii of wild-type and ApoE$^{-/-}$ mice. Muscle stem cells were collected from myofibres isolated as described in chapter 2.1.3 by trypsinisation in 0.125% trypsin-Ethylenediaminetetraacetic acid (EDTA) solution and seeded in Matrigel *(*1mg mL-1; Corning Matrigel; cat. 354234*)*-coated 24-well cell culture plates, in muscle stem proliferation media (30% FBS, 1.5% chick embryo extract and 1% penicillin-streptomycin). Differentiation of muscle stem cells was achieved through culturing for 3 days in appropriate proliferation medium as per experimental condition before switching to differentiation medium (5% Horse Serum, 0.5% chick embryo extract, 1% penicillin-streptomycin and 0.1% amphotericin B) for a further 5 days. This allows for determination of proliferation and differentiation independent of the muscle fibre niche, and a greater control of the environment (e.g. palmitate was applied to cultured cells to simulate a hyperlipidaemic environment).

2.1.5 *In Vivo* cardiotoxin-induced muscle injury.

On day 1, wild-type mice and ApoE$^{-/-}$ mice (12 week old) were injected with a total of 30µL, 50µM Naja pallida cardiotoxin (CTX; Latoxan, Valence France) into the tibialis anterior (TA) muscle (n=5 per group). At 5 and 10 days, mice were sacrificed, the TA muscles were collected, immediately frozen and 12µM cryo-sections were processed for immunohistochemistry. CTX is a myotoxic substance often used to induce chemical injury in order to study muscle recovery. This is a suitable model as the regeneration process occurs relatively efficient due to a proper blood supply and the preservation of basal lamina and microvasculature (Czerwinska et al., 2012; Harris, 2003). CTX-injection is also less harmful for the animal compared to mechanical injuries (Couteaux et al., 1988). The CTX-induced regeneration model establishes

similarities with diverse myopathies and therefore serves as a tool to study these pathologies (Pessina et al., 2014; Sunitha et al., 2016).

2.1.6 Releasate treatments *in vivo*, *ex vivo* and *in vitro*.

For C2C12 studies on proliferating cells, 100µl releasate was added to 900µl growth media at the time of seeding, then again after 24 hours, before cells were fixed at 48 hours. Initial experiments on differentiating C2C12 cells used 2 doses of 100µl releasate on day 5 then day 6. Subsequently differentiation experiments used 2 doses of 100µl releasate on day 2, day 3 and day 4. Experiments on muscle fibres *ex vivo* added 100µl releasate to the media for 24h prior to fixation at all time points. For *in vitro* studies Mice were administered a 100µl dose of human releasate, on the day of injury, 1-, and 3-days post injury by intraperitoneal injections.

2.1.7 Tissue embedding and cryosectioning

To assess skeletal muscle morphology and potential pathophysiological features, EDL, TA, soleus and the heart were assessed by histological and immunohistochemical procedures. Specimens were embedded in optimal compound temperature tissue mounting medium (OCT) and 100% ethanol on dry ice. A cryomold was filled with OCT and was subsequently submerged in cooled ethanol. Once the OCT began freezing, the tissues were transferred, oriented for cryosectioning and fully submerged in the OCT. The frozen blocks (tissue in OCT) were stored at -80ºC. Prior to cryosectioning, blocks were equilibrated to -21ºC for 20 minutes in the cryostat chamber. Transverse sections (10µm thickness) from the mid-belly of the muscles were obtained and mounted on microscopy glass slides coated with Poly-L-lysine. The microscopy glass slides were air dried for 20-30 minutes at room temperature and stored at -80ºC until further analysis.

2.2 Technical Methods

Histology/Histochemistry for regenerating/injured/inflammation muscle

2.2.1 Muscle stem cell proliferation and viability analysis.

Muscle stem cell proliferation was evaluated by the pyrimidine analogue EdU incorporation assay using the fluorescent Click-iT® EdU Cell Proliferation Assay (Invitrogen, Life Technologies, Grand Island, NY, USA) according to the manufacturer's instructions. Proliferating cells were measured as a percentage of EdU

positive divided by 4',6-diamidino-2-phenylindole(DAPI) -stained (Dako))-stained nuclei.

2.2.2 Immunohistochemistry & morphometrics

Isolated primary muscle stem cells were seeded on coverslips in 1mL of media in 24-well plates (Corning® Costar® TC-Treated 24-Well Plates). Media was removed at the end of experiments with 4% paraformaldehyde in phosphate buffered saline (PBS) added for 15 minutes, followed by two washes in phosphate-buffered saline. Permeabilisation buffer (0.2% Triton X-100 in PBS) was then added for 20 minutes followed by two washes in wash buffer (5% FBS and 0.05% Triton X-100 in PBS) before applying onto optical slides. Primary antibodies for Pax7, MyoD, Myogenin, anti-myosin heavy chain 3 (Santa Cruz; cat. sc-81648, sc-760, sc-52903, sc-53091 respectively) and EGF-like module-containing mucin-like hormone receptor-like 1 (F4/80) (R&D Biosystems; cat MBA3249) were used. Cells were measured by the intensity of myogenin fluorescence per cell divided by DAPI-stained nuclei as a percentage. Morphometric analysis was performed on an AxioImager fluorescence microscope equipped with an Axiocam digital camera using the ZEN imaging software (Zeiss, Germany). The relative myofibre cross sectional area (CSA) was calculated from the diameter assuming fibre cylindrical shape and normalised to wild-type. Senescence was measured via staining of senescence associated-β-galactosidase using a commercially available staining kit according to the manufacturer's protocol (abcam - ab102534). Cells were fixed for 15 minutes in fixative solution, followed by PBS washes and incubation overnight with beta-galactosidase staining solution in a dry incubator with 0% CO_2. Cells were observed at x40 magnification under microscope for blue colour development and imaged for analysis. Images were then deconvoluted using ImageJ to determine the area of positive staining per image.

2.2.3 RNA extraction and real-time PCR analysis

Quantitative polymerase chain reaction (PCR) was performed on differentiated muscle stem cells. Muscle stem cells were seeded in 6-well plates in proliferation media (30% FBS, 1.5% chick embryo extract and 1% penicillin-streptomycin) and total RNA was isolated on day 4 of differentiation using the EZNA Total RNA Kit I (Omega Biotek, USA). The differentiated muscle stem cells were collected in 400µL trizol. Using a cell scraper, cells were detached from plates and collected into 1.5ml Eppendorf tubes. Tubes were transferred on ice and 80µL of 100% chloroform was added per 400µL

trizol for separation of molecules. This mixture was left at room temperature for 2 minutes and subsequently centrifuged at 4ºC for 15 minutes at 12,000 x g. The upper aqueous phase (containing RNA) was carefully transferred in a new tube and 500μL of 100% isopropyl alcohol was added and incubated for 5 minutes at room temperature for precipitation of nucleic acids. The mixture was loaded on a HiBand RNA Column and centrifuged at 4ºC for 1 minute at 10,000 x g and the flow through was discarded. RNA Wash Buffer I (500μL) was added in the HiBand RNA Column and centrifuged at 4ºC for 1 minute at 10,000 x g and the flow through was discarded. RNA Wash Buffer II (500μL) was subsequently added in the HiBand RNA Column and centrifuged at 4ºC for 1 minute at 10,000 x g and the flow through was discarded. The procedure was repeated once more, and the HiBand RNA Column was centrifuged at 4ºC for 2 minutes at 13,000 x g in order to dry. To elute RNA, 20μL of ultrapure water was added in the HiBand RNA Column, left for 1 minute at room temperature and centrifuged at 4 o C for 2 minutes at 12,000 x g. The elution step was repeated once more and the concentration (ng·μL -1) and purity (A 260 /A 280) of RNA isolated was determined on a NanoDrop spectrometer (ThermoFisherScientific, USA) prior to sample storage at -20ºC. Total RNA (1.5 μg) was reverse-transcribed to cDNA and analysed by quantitative real-time RT-PCR on a StepOne Plus cycler (Applied Biosystems, UK). Primers were designed using the software Primer Express 3.0 (Applied Biosystems, UK). Relative expression was calculated using the ΔΔCt method with normalisation to the reference genes encoding cyclophilin-B (*Cyp*) and hypoxanthine-guanine phosphoribosyltransferase (*Hprt*). mRNA levels of *MyoD,* Scribble planar cell polarity protein (*Scrib1)*, myogenic factor 6 (myf6), *Myogenin*, transmembrane protein 8c (*Tmem8c*), brain expressed X-linked 1 (*Bex1*), Serum response factor (*Srf*), myosin heavy chain 1 (*Mhc1*), myosin heavy chain 2a (mhc2a), actin alpha 1 (*Acta1*), vascular endothelial growth factor α 165 (vegfα165) and platelet derived growth factor α (pdgfα) for wild-type and ApoE$^{-/-}$ myotubes or C2C12 myoblasts. Primers are listed in appendix I.

2.2.3.1 cDNA synthesis

Global complementary DNA (cDNA) synthesis was performed by reverse transcription. Prior to cDNA synthesis, the RNA samples were treated with Deoxyribonuclease I (DNase I) (ThermoFisher Scientific, USA). According to the manufacturer's instructions the following mix was prepared per RNA sample;

Amount of RNA 10μg

10x Reaction Buffer

2μL DNase I

RNase-free 5μL (5U)

Ultrapure Water to 20μL

The mixture was incubated at 37ºC for 30 minutes after which 2μL of 50mM EDTA was added and the mixture was subsequently incubated at 65oC for 10 minutes. The RNA that was DNase I treated was placed on ice for cDNA synthesis. The reverse transcription was performed with the RevertAid H Minus First Strand cDNA Synthesis Kit (ThermoFisher Scientific, USA). As per manufacturer's instructions, a mix per RNA sample was prepared that included 1μL of 100μM Oligo(dT)18 Primer, 3μL of ultrapure water and a volume of 8μL and concentration of 0.46μg·μL-1 of RNA sample. In addition the following Reverse Transcription master mix per RNA sample was prepared;

5x Reaction Buffer 4μL

RiboLock RNase Inhibitor 1μL

10mM dNTP mix 2μL

Ultrapure Water to 20μL

Revertaid Reverse Transcriptase 1μL (200 U/μL)

In each mix containing RNA template, 8μL of the Reverse Transcription master mix was added giving a final volume of 20μL and following a brief pulse spin, reverse transcription was performed using a Veriti thermal cycler (Applied Biosystems, USA) in accordance with the below reaction;

42ºC 60 minutes

70ºC 10 minutes

cDNA was diluted in ultrapure water by a factor 1:18 to correct for further loading on qPCR and prior to the dilution 3μL of cDNA were kept for evaluation of the primers.

Similarly, the concentration (µg·µL-1) and purity (A260/A280) of cDNA was determined on a NanoDrop spectrometer (ThermoFisher Scientific, USA) prior to dilution and sample storage at -20ºC.

2.2.3.2 Primer design

Primers were designed using NCBI/Primer-Blast software. Exon spanning murine specific primers were used whenever possible. The primers used to quantify gene expression are listed in Appendix I.

2.2.3.3 Quantitative real time PCR assay

To measure gene expression differences, qPCR was employed. The Primer Master Mix was prepared on ice and the optimal final volumes for the most efficient reactions were the following per well;

SYBR Green PCR Master Mix 7.5µL

Forward primer 0.15µL

Reverse primer 0.15µL

Ultrapure water 3.2µL

cDNA template 4µL

Three technical replicates were performed per sample in PCR grade 96well plates (ThermoFisher Scientific, UK) and covered with corresponding adhesive covers (ThermoFisher Scientific, UK). No template controls (NTCs) for each gene were included on each experimental plate to control for unspecific binding. Plates were pulse centrifuged and subsequently loaded onto a Step-onePlus Real-Time PCR machine (Applied Biosystems, USA). The cycling programme that was adopted throughout the experiments was;

Holding Stage	50ºC for 2min	
	95ºC for 10min	
Cycling Stage	95ºC for 15sec	*Denaturation*
	61ºC for 1min	*Annealing/Extension*

Melt Curve Stage	95ºC for 15sec
	60ºC for 15sec
	95ºC for 15sec

Holding stage and melt curves were performed in a single cycle while the cycling stage was set at 40 cycles. The annealing and extension steps were consolidated in a single step. Melt curves were performed to determine the specificity of amplification. A melt curve shows the decrease in fluorescence when double-stranded DNA with incorporated dye molecules dissociates into single-stranded DNA as the temperature of the reaction is raised. The melting point depicts the temperature at which 50% of the DNA has dissociated and is proportional to the size of DNA (Gundry et al., 2003).

2.2.3.4 qRT-PCR analysis and interpretation by the comperative CT method (2-ΔΔCT method)

SYBR green (SG) is an asymmetric cyanine dye, with two aromatic systems containing nitrogen, that interacts in three different ways with the double stranded DNA (dsDNA), through intercalation between base pairs, electrostatic interaction and entering the minor groove (Dragan et al., 2012; Kubista et al., 2006; Zipper et al., 2004). SG binding to dsDNA leads to an increase of the quantum yield about 1,000-fold and the excitation and emission of the SG/dsDNA complex is 497nm and 520nm respectively (Dragan et al., 2012; Monis et al., 2005). The increase in the amount of dsDNA product due to qPCR thermal cycles is depicted by the increase in the fluorescence signal which can be detected in real time (Kubista et al., 2006). Detection of differences in gene expression among groups was conducted by relative quantification to reference genes. To achieve this, the baseline threshold cycle values were determined automatically from the relative rate of amplification using StepOne software V2.0 (Kubista et al., 2006; Livak and Schmittgen, 2001). Furthermore, reference (housekeeping) genes Cyp and Hprt (Appendix I) were used as normaliser genes for correcting any variability in the RT-qPCR process and they displayed similar expression pattern in all groups with coefficient of variation (CV) 3.26 for Cyp and CV 4.1 for Hprt respectively that was calculated dividing the standard deviation by the mean and multiplying by 100. All gene expression data presented were determined with the use of the comparative CT method according to following published

recommendations (Livak and Schmittgen, 2001). Briefly, the CT of the sample for the gene of interest (target) is initially normalised to the mean CT of the reference genes (ref) both for the sample (CTtarget) and for the calibrator sample (CTcal), according to the following equation;

Equation 2.1: $\Delta C_{Tsample} = C_{Ttarget,sample} - C_{Tref,sample}$ and

$\Delta C_{Tcal} = C_{Ttarget,cal} - C_{Tref,cal}$

In this case, the calibrator sample was the mean of the wild type mice group on a standard chow diet. Secondly, the ΔCT of the sample is normalised to the ΔCT of the calibrator sample with the following equation;

Equation 2.2: $\Delta\Delta CT = \Delta C_{Tsample} - \Delta C_{Tcal}$

Finally, the fold change in gene expression of a sample relative to the calibrator sample and the reference genes is calculated by the equation;

Equation 2.3: Fold Change= $2^{-\Delta\Delta C}$

2.2.4.1 Tissue homogenisation and quantification of protein extracts

Protein extracts in RIPA lysis buffer were prepared from homogenisation of tissues. RIPA lysis buffer contained 1% v/v Nonidet P 40 substitute (NP-40, Sigma-Aldrich, UK), 0.1% w/v sodium dodecyl sulfate (SDS) (Fisher Scientific, UK) and 0.5% w/v sodium deoxycholate (Sigma-Aldrich, UK) in 50mL PBS. SDS and sodium deoxycholate are ionic detergents as opposed to NP-40 which is a non-ionic detergent. RIPA lysis buffer is used for solubilisation of all membranes of the cells so as proteins from all subcellular compartments can be released. Briefly, whole frozen quadriceps and 40-60mg of frozen liver tissue were resuspended in 1mL of pre-chilled RIPA Buffer supplemented with protease inhibitors (1:50, ThermoFisher Scientific, USA) and dispersed for 30 to 40sec at 18,000 x rpm with an IKA Ultra-Turrax T-25 (SigmaAldrich, UK). The procedure was repeated till tissues were completely homogenised. The protein extracts were centrifuged at 4ºC for 15 minutes at 14,000 x g. The pellet containing undissolved tissue fractions was discarded and protein quantification was performed. Quantification of the protein extracts was performed with the Pierce BCA protein assay kit (ThermoFisher Scientific, USA). The Pierce BCA protein assay kit was used due to its compatibility with many detergents. In this assay proteins in an

alkaline environment reduce Cu+2 into Cu+1 (Biuret reaction) and the cuprous cation is detected colorimetrically through a reagent that contains bicinchoninic acid (BCA). The purple-coloured reaction product is formed by the chelation of one cuprous cation with two molecules of bicinchoninic acid and is detected by absorbance at 562nm. The colour formation seems to be determined by the macromolecular structure of protein, the number of peptide bonds and the presence of four particular amino acids (cysteine, cystine, tryptophan and tyrosine). The absorbance is almost linear when protein concentrations range between 20-2,000µg/mL. According to the manufacturer's instructions the protocol is as follows: For determination of protein concentrations, bovine serum albumin (BSA) was used as the reference protein. A series of dilutions of 2mg/mL BSA Stock solution in RIPA lysis buffer ranging from 25 to 2,000µg/mL were prepared to make the standard curve.

Protein extracts were diluted 1:5 in RIPA buffer and assayed alongside with the standards in two replicates and incubated at 37ºC for 30 minutes. The absorbance of the u-shaped 96well plates was measured at 562nm in a Tecan plate reader (Tecan Trading AG). All values were corrected for background noise prior to calculation of protein concentration according to the standard curve.

2.2.4.2 SDS-PAGE

Protein extracts (20-30µg of protein) for protein synthesis studies or from differentiated C2C12 cells were diluted in a 1:1 ratio with Laemmli's sample buffer (0.025M Tris-HCl, 20% glycerol, 0.002% bromophenol blue, 4% w/v SDS and 10% 2-mercaptoethanol, all reagents from Fisher Scientific, UK) and boiled at 95ºC for 10 minutes to break disulphide bonds and denature proteins so separation by molecular weight could be performed (Mahmood and Yang, 2012). For SDS-Page, 10% separating gel (3.25mL deionised water, 2.65mL 30% Bis/Tris Acrylamide, 2mL of 1.5M Tris Buffer with pH 8.8 and 0.4% SDS, 37.5µL 10% APS and 5µL Tetramethylethylenediamine (TEMED)) was prepared. After the gel set, methanol was removed and 3% stacking gel (2.435mL deionised water, 750µL 30% Tris/Bis Acrylamide, 935µL of 1.5M Tris-HCl Buffer with pH 6.8 and 0.4% SDS, 37.5µL 10% APS and 5µL TEMED) overlaid the resolving gel. The stacking gel is slightly acidic and has lower concentration of acrylamide to allow proteins to form thin and defined bands whereas the resolving gel is basic with a higher concentration of acrylamide to allow protein separation according to size (Mahmood and Yang, 2012). Once the stacking gel was set, the gel was secured in a casting

stand and was subsequently placed into a Mini Protean Tetra 108 Cell tank (Biorad, UK). Running buffer (0.25mM Tris base, 193mM glycine and 0.1% w/v SDS) was added to the tank until all wells were fully submerged. Following addition of molecular weight marking protein ladder (10-250 kDa, Fisher Scientific, UK) in the first well, samples were loaded in the subsequent wells and separated at 100 Volt for 120 minutes i.e. until the dye was visible at the bottom of the resolving gel. 20µg of protein extracts were loaded.

2.2.4.2 Transfer of proteins by Wet Blotting

Foam pads and precut blot paper (12cm x 8cm) were soaked with Transfer Buffer (25mM Tris base, 192mM glycine and 20% pure methanol) and polyvinylidene membrane (Amersham Hybond 0.45µm PVDF) was activated for 1 minute in pure ethanol and subsequently soaked with Transfer buffer for 2-5 minutes. In a holder cassette the gel and the PVDF membrane were placed between blot papers and foam pads. To ensure homogenous transfer of proteins, the membrane was rolled when was placed onto gel so as to remove any air bubbles. The holder cassette was placed into a Mini Trans-Blot Module (Biorad, UK) ensuring that the PVDF membrane was between the gel and a positive electrode. Transfer Buffer was added to the Mini Protean Tetra Cell gel tank until the holder cassettes were submerged and electro-transferred at 100 Volt for 80 minutes. Following that the membrane was rinsed in TBS Buffer pH 7.6 for 5 minutes on an agitator. After protein was resolved in 10% SDS-PAGE, immunoblotting was performed with the following antibodies: H2AX (1:1000, abcam - ab22551), p21 (1:1000, abcam - ab188224), p53 (1:1000 dilution, abcam - ab252388) β tubulin (1:1000; EMD Millipore; cat. 05-661). Primary antibodies for p21 (1:1000, abcam - ab188224) was used to evaluate cell cycle arrest in injured muscle sections of 12µm. Immunoblotting analysis was performed by probing the membranes with each antibody or β-tubulin and analysed using the Odyssey Infrared Imaging System (LI-COR Biosciences). Band density was measured using Li-cor image studio software. The band densities were normalized to β tubulin content.

2.2.5 Detection of superoxide

Skeletal muscle stem cells were incubated with 10µM of dihydroethidium (DHE) in PBS, for 30 min at 37°C in a 5% CO_2 incubator for 30 min and were subsequently fixed with 4% PFA in PBS. DHE is a fluorogenic dye specifically targeted to superoxides and whose oxidation by superoxide produces red fluorescence which was

imaged under fluorescence microscopy. The detection for superoxide in skeletal muscle stem cells gives insights into the potential oxidative stress under certain conditions.

2.2.6 Palmitate production

BSA conjugated palmitate was prepared as previously reported by Chavez and Summers (Chavez and Summers, 2003). Palmitate was dissolved in 50% (v/v) ethanol by heating at 60°C and then added at a concentration of 200mM to DMEM containing 20%(w/v) fatty acid free BSA at a ratio of 1:3 (BSA:PA). For conjugation, the solution was placed in shaker incubator for 1h and then sonicated for 30 min before treating the cells.

2.2.7 Palmitate challenge to stem cells

Primary skeletal muscle stem cells proliferated until confluent, then differentiated. 24h before fixation ebselen or vehicle control was applied, palmitate was then applied after 30 mins. Skeletal muscle stem cells were incubated with 10μM of dihydroethidium (DHE) in PBS, for 30 min at 37°C in a 5% CO_2 incubator for 30 min and were subsequently fixed with 4% paraformaldehyde (PFA) in PBS. Palmitate challenge to muscle stem cells allowed for study of hyperlipidaemia in a controlled cell culture environment.

2.2.8 Human platelet releasate

Human blood was collected from healthy donors in acid citrate dextrose (ACD) to whole blood at a ratio of 1:5, centrifuged at 190 *g* for 15 minutes followed by PRP collection and inactivation of platelets using prostaglandin I_2 (534 nmol/L; Cayman Chemical). The PRP was then centrifuged in a swing-out rotor at 800 *g* for 12 minutes and the platelet-poor plasma (PPP) supernatant was then removed. Modified Tyrode's buffer (NaCl, HEPES, NaH_2PO_4, $NaHCO_3$, KCl, $MgCl_2$ and D-Glucose) was used to re-suspend the platelet pellet to a concentration of 1×10^9 platelets mL^{-1}(unless otherwise stated) using a cell counter (Beckman Coulter; Z1-Series Coulter® Particle Counter). The platelet preparation was activated using a PAR1 agonist (TRAP6; 20μmol/L; AnaSpec; cat. AS-60679, Cambridge Bioscience, Cambridge, UK), in an aggregometer (CHRONO - LOG® Model 490 4 + 4 Optical AggregationSystem, USA). Platelets were centrifuged at 9500 *g* for 10 minutes, and the releasate supernatant was aliquoted and stored at −80°C until further use.

2.2.9 Doxorubicin

ApoE$^{-/-}$ mice were administered a 20mg/kg cumulative dose over 17 days in 4 doses of 5mg/kg every 4 days. Doxorubicin is a cytotoxic anthracycline antibiotic isolated from cultures of Streptomyces peucetius var. caesius. Doxorubicin is used a cancer treatment, which causes cytotoxicity, is linked with myopathy, and dysfunction of skeletal muscle. As doxorubicin leads to cell cycle arrest and senescence, the potential for damage to muscle stem cells is great, therefore the present work sought to determine it's effects on muscle stem cells and seek options to alleviate damage.

2.3 Statistical analysis

Data are reported as mean±SD for the *in vitro* muscle stem cell experiments and Mean±SEM the *ex vivo* muscle stem cell myogenic progression. Cell culture experiments were conducted with n=6-9 technical replicates and n=2-3 independent experiments as indicated in figure legends. Statistical differences between experimental groups were determined by the one-way analysis of variance (ANOVA) test and were considered as significant for $p<0.05$. Statistical analysis was performed with the SPSS software (IBM SPSS Statistics version 24).

2.3.1 Analysis of Variance

Two way ANOVA was employed in order to detect significant differences in response to genotype (wild type, WT versus ApoE$^{-/-}$ mice) and followed by the Bonferroni post hoc test. Two way anova was chosen in WT vs ApoE$^{-/-}$ experiments to determine how the two variables of genotype effect muscle stem cell progression, or how they effect muscle regeneration.

2.3.2 Bonferroni post hoc

The Bonferroni is one of the most commonly used post hoc test. The Bonferroni correction is used to reduce the chances of obtaining false-positive results (type I errors) when multiple pair wise tests are performed on a single set of data. The Bonferroni adjustment is based on a familywise error rate that is calculated by dividing the alpha level (critical value p) with the number of hypotheses. The limitation of the Bonferroni procedure is that the result tends to be too conservative and do not have enough power when the set of tests is large (Kim, 2015). Bonferroni was used to specifically compare between groups.

Chapter 3 - The impact of ApoE deficiency on skeletal muscle stem cell function

3.1 Overview

Skeletal muscle is a tissue which demands great energy expenditure to cope with mechanical loading and unloading, as well as rapid response to stimuli as in innervation (Hargreaves and Spriet, 2020; Lieber et al., 2017). The response to individual stimuli may result in changes in energy metabolism, changes in mitochondrial content, alterations of gene expression and oxidative metabolism, and changes in structural proteins involved in muscle contraction (Kuo and Ehrlich, 2015; Matsakas and Patel, 2009). Furthermore, the tissue must remain adaptable throughout adult life in order to respond to injury. In pathophysiological conditions, such as muscular atrophies, obesity and type II diabetes, and peripheral artery disease, changes in muscle function and adaptability have been characterized (Blaauw et al., 2013; Kruse and Højlund, 2018; Tallis et al., 2018). However, obesity independent hyperlipidaemia and atherosclerosis have muscular effects including atrophy, intermittent claudication, and loss of strength (Askew et al., 2014; Mauer et al., 2015; McDermott et al., 2007; Sfyri and Matsakas, 2017). So far, the effects on skeletal muscle stem cells and the regenerative capacity of skeletal muscle in hyperlipidaemia and atherosclerosis has not been characterized.

Type II diabetic patients exhibit skeletal muscle atrophy, have decreased content of type I myofibres and decreased capillarisation (D'Souza et al., 2013). Obese patients with metabolic syndrome, i.e. coexistence of several cardiovascular risk factors (e.g. hyperlipidaemia, hypertension, insulin resistance) have increased intramyocellular triglyceride accumulation and exhibit muscle insulin resistance (Jornayvaz et al., 2010). On the other hand, patients with peripheral arterial disease (PAD) in advanced disease stage demonstrate decreased content of glycolytic myofibres, increased fat accumulation and high oxidative stress in the muscle (Koutakis et al., 2014; Weiss et al., 2013). Patients of atherosclerosis in the peripheral arteries exhibit myofibre degeneration, fatty acid deposition, fibrosis and decreased capillarization. Obesity-independent hyperlipidaemia induces intramuscular lipid accumulation and skeletal muscle oxidative stress in ApoE deficient ($ApoE^{-/-}$) mice, an established model of atherosclerosis and hyperlipidaemia.

There is sparse scientific evidence on the effect of hyperlipidaemia (independently of obesity and insulin resistance) and central atherosclerosis on skeletal muscle (Stapleton et al., 2010; Wang et al., 2012). Stapleton et al. reported that ApoE deficient

mice on a chow diet had decreased capillary density in the gastrocnemius compared to wild type mice (Stapleton et al., 2010). Wang et al. reported that ApoE deficient mice on a high fat diet (21% w/w fat) gained less body weight and displayed better glucose tolerance than wild type mice (Wang et al., 2012). Moreover, ApoE deficient mice had decreased intramyocellular triglycerides and insulin sensitivity in skeletal muscle was not impaired compared to wild type mice (Wang et al., 2012). Sfyri et al. reported that ApoE deficiency induces a mild transition to oxidative myofibres, an increase in capillary density, intramyocellular fat content and increases oxidative stress (Sfyri et al., 2018). The impact of these outcomes on skeletal muscle stem cell function and skeletal muscle regeneration after injury however, has not been investigated.

Muscle stem cells, also known as satellite cells, are muscle progenitor cells that reside in niches between the sarcolemma and the basal membrane of the myofibres (Yin et al., 2013, Relaix and Zammit, 2012). Abundant evidence suggest that muscle stem cells are an integral part of skeletal muscle growth and regeneration in response to injury (Relaix and Zammit, 2012). In adult skeletal muscle, these stem cells remain mitotically quiescent and are activated when myofibre damage or hypertrophy occurs, during which muscle stem cells differentiate into myoblasts and fuse together for *de novo* myotube formation, or fuse to damaged myofibres for replacement of myonuclei (Yin et al., 2013, Relaix and Zammit, 2012). In several pathological conditions, such as muscular dystrophy and chronic obstructive pulmonary disease, muscle stem cells have impaired capacity for activation and differentiation (Pomies et al., 2015, Girgenrath et al., 2005, Morgan and Zammit, 2010). In metabolic diseases, such as obesity, muscle stem cells have been reported to exhibit decreased myogenic capacity after skeletal muscle injury (Fu et al., 2016, Xu et al., 2018).

Recently Sfyri et al. showed that obesity-independent hyperlipidaemia induced intramuscular lipid accumulation and skeletal muscle oxidative stress in ApoE deficient ($ApoE^{-/-}$) mice, an established model of atherosclerosis and hyperlipidaemia (Meyrelles et al., 2011). Moreover, previous evidence suggests that $ApoE^{-/-}$ mice have delayed skeletal muscle regeneration after injury (Kang et al., 2008, Arnold et al., 2015, Pellegrin et al., 2014, Crawford et al., 2013). This delay in skeletal muscle regeneration was attributed mainly to the perturbed accumulation of proinflammatory macrophages and decreased macrophage phagocytosis due to ApoE deficiency

(Crawford et al., 2013, Pellegrin et al., 2014, Kang et al., 2008, Arnold et al., 2015). Specifically, Kang et al. showed that proinflammatory cytokines remained increased in ApoE$^{-/-}$ injured muscle even after 14 days of injury (Kang et al., 2008). Moreover, Arnold et al. reported that ApoE deficiency impacts negatively on macrophage phagocytic activity and is at least partially responsible for the impairment of skeletal muscle regeneration (Arnold et al., 2015).

The effect of ApoE deficiency on skeletal muscle stem cell myogenic capacity and function remains unknown so far. Therefore, this chapter aims to determine whether hyperlipidaemia followed by increased oxidative stress in skeletal muscle of ApoE$^{-/-}$ mice affects muscle stem cell myogenic progression, independently of the proinflammatory environment. To achieve this, ApoE deficient muscle stem cell myogenesis was evaluated in two different experimental settings, i.e. on single muscle fibres and isolated muscle stem cells. Firstly, Myofibres from ApoE$^{-/-}$ mice were isolated and cultured *ex vivo* to investigate the myogenic progression and self-renewal of muscle stem cells. Secondly, muscle stem cells were removed from their microenvironment, i.e. myofibres, and their myogenic potential was studied in cultures *in vitro*. The present study takes advantage of the differential expression patterns of transcription factors and myogenic regulatory factors as follows: in adult skeletal muscle, quiescent stem cells express Pax7, activated stem cells switch on MyoD expression, proliferating stem cells co-express Pax7 and MyoD, stem cells committed to differentiation are Pax7-negative and MyoD-positive, whereas differentiated stem cells give rise to new myonuclei that express myogenin (Zammit et al., 2002, Fuchtbauer and Westphal, 1992, Grounds et al., 1992, Yablonka-Reuveni and Rivera, 1994, Yablonka-Reuveni et al., 1999, Zammit et al., 2004). It was hypothesised that muscle stem cell function is perturbed in atherosclerotic mice with systemic hyperlipidaemia and skeletal muscle oxidative stress and this may explain the impaired muscle regeneration seen *in vivo*.

3.2 Aims

The principal aim of this chapter was to investigate skeletal muscle stem cell function in the atherosclerotic ApoE deficient mouse model compared to wild type mice. It was hypothesized that muscle stem cell function would be perturbed in atherosclerotic mice with systemic hyperlipidaemia and this would contribute to impaired muscle regeneration *in vivo*. To achieve this, the following objectives were set:

- To study the genotype effect on relative expression of transcription factors involved in satellite cell proliferation and differentiation
- To determine the myogenic potential of isolated primary myoblasts from ApoE deficient mice.
- To determine the gene expression patterns in differentiating myotubes derived from cultured EDL muscle stem cells from ApoE deficient mice

3.3 Results

3.3.1 Muscle stem cell function proliferation and differentiation profiles of apolipoprotein deficient single fibres.

It has been recently shown that ApoE$^{-/-}$ mice have increased myofibre cross-sectional area(Sfyri et al., 2018). Therefore, the present work sought to determine the myonuclear domain, defined as the cytoplasmic area of a myofibre controlled by a single myonucleus using the single fibre model in EDL muscle(Allen et al., 1999). There were no significant differences in total myonuclear number per fibre between genotypes. However, the relative myofibre cross sectional area (CSA) was significantly higher by 63% in ApoE$^{-/-}$ compared to WT EDL myofibres (Figure 3.1A). Consequently, the relative myonuclear density was significantly lower in ApoE$^{-/-}$ myofibres compared to WT myofibres (64.20%±4.97 vs. 100%±6.52, respectively, Figure 3.1A). Next, the proliferation and differentiation profiles of muscle stem cells during myogenic progression were determined. Therefore, muscle stem cells retained in their niche on isolated EDL myofibres were immunostained for Pax7 at baseline (T0), Pax7 and MyoD (T24, T48) and Myogenin (T72) (Figure 3.1B). No significant differences in total muscle stem cell numbers between ApoE$^{-/-}$ and WT mice were seen at any time point (Figure 3.1C). ApoE$^{-/-}$ muscle stem cells exhibited the same proliferation patterns as in WT EDL myofibres at 24 and 48 hours, despite a transient delay in MyoD activation at 24 hours (Figure 3.1C). Specifically, at T24 the majority of muscle stem cells had become activated in both genotypes (78.67%±2.7 in WT and 73.10%±2.7 in ApoE$^{-/-}$ muscle stem cells) as shown by the expression of MyoD and co-expression of Pax7/MyoD (Figure 3.1C). Similarly, at T48, 94.96%±1.6 of WT and 93.77%±1.2 of ApoE$^{-/-}$ muscle stem cells were proliferating. However, at T72 ApoE$^{-/-}$ muscle stem cells exhibited a differential pattern of myogenin expression compared to WT fibres (Figure 3.1C). ApoE$^{-/-}$ muscle stem cells had a significantly lower expression of myogenin by 12.5% compared to WT (i.e. 59.9%± 1.9 in ApoE$^{-/-}$ vs. 68.1%± 1.9 in WT, Figure 3.1C). This data indicates that despite the absence of significant differences in muscle stem cell activation and proliferation profiles between ApoE$^{-/-}$ and WT muscle stem cells, there is compromised differentiation of muscle stem cells in ApoE$^{-/-}$ fibres.

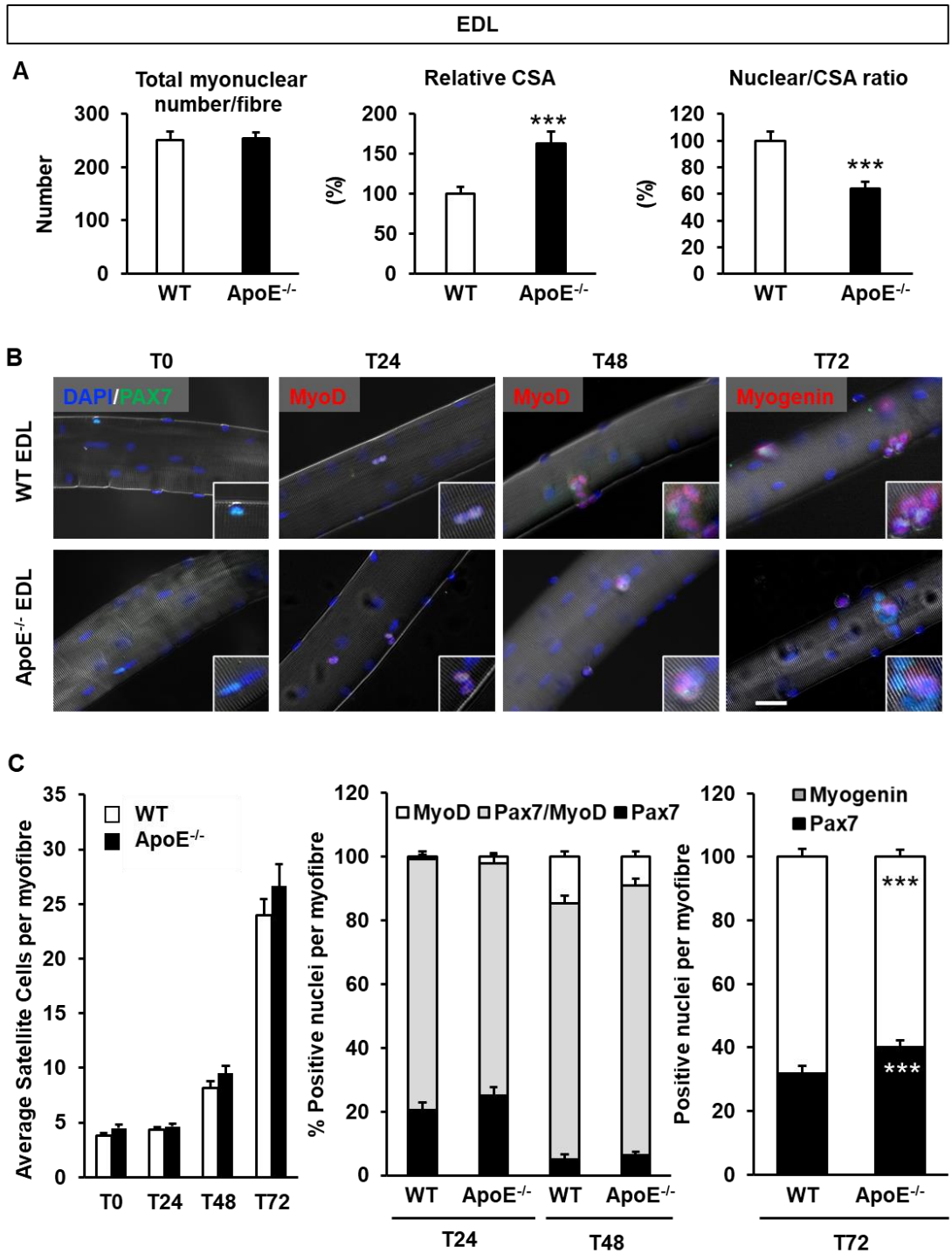

Figure 3.1. Impaired differentiation of muscle stem cells of EDL myofibres from ApoE$^{-/-}$ mice *ex vivo*. (**A**) Baseline differences in total nuclear number per myofibre, relative cross sectional area (CSA), (i.e. normalised to the CSA of the WT myofibres) and Nuclear/CSA ratio in isolated EDL myofibres from WT and ApoE$^{-/-}$ mice. (B) Single myofibres were isolated from the EDL muscle and studied at different time points (T0, T24, T48 and T72 hours) to determine quiescent, proliferating and differentiating satellite cells, by means of Pax7, MyoD and Myogenin staining. Representative

images of immunofluorescent detection of Pax7 (T0), Pax 7 and MyoD (T24 & T48) and Pax7 and Myogenin (T72, x40 magnification, scale bar=50μm, inset images depict enlarged satellite cell clusters). (C) Average number of satellite cells per myofibre and relative quantification of expression of Pax7, MyoD and Myogenin. Data are mean±SEM (n=70-85 myofibres from n=4 mice/group). Statistical analysis was performed by one way ANOVA, *p<0.05 and ***p<0.001 $ApoE^{-/-}$ vs WT.

To corroborate and strengthen the above results from the EDL muscle, the same battery of experiments was conducted on the biceps brachii muscle from $ApoE^{-/-}$ and WT fibres. $ApoE^{-/-}$ myofibres also had a significantly lower myonuclear density at baseline and a larger myofibre diameter, indicating that in both muscles single myonuclei are in control of a larger cytoplasmic area in the $ApoE^{-/-}$ mice (Figure 3.2A). Muscle stem cell numbers at baseline (T0) as well as proliferation (T24, T48) and differentiation (T72) profiles were also examined in the biceps brachii (Figure 3.2B). The average muscle stem cell number was not different between genotypes at any time point for the biceps brachii (Figure 3.2C**).** $ApoE^{-/-}$ muscle stem cells had different activation and proliferation patterns compared to WT muscle stem cells at 24 but no differences at 48 hours (Figure 3.2C). In particular, Pax7 was expressed in more $ApoE^{-/-}$ muscle stem cells by 27% and Pax7/MyoD was significantly lower by 9% compared to WT muscle stem cells (Figure 3.2C). However, these rather transient differences at T24 were not evident at T48, where $ApoE^{-/-}$ muscle stem cells displayed a similar profile of proliferation to WT stem cells (Figure 3.2C). However, similarly to the findings obtained in the EDL muscle stem cells, at T72 $ApoE^{-/-}$ biceps brachii muscle stem cells exhibited a significantly lower expression pattern of myogenin by 20% compared to WT muscle stem cells (i.e. 65.3%± 2.5 vs. 52.2%± 2.3, Figure 3.2C). Thus, $ApoE^{-/-}$ muscle stem cells in the biceps brachii have an impaired differentiation profile compared to WT muscle stem cells. Taken together these data from EDL and biceps brachii robustly suggest an impact of ApoE deficiency on the muscle stem cell progeny in terms of myogenic differentiation.

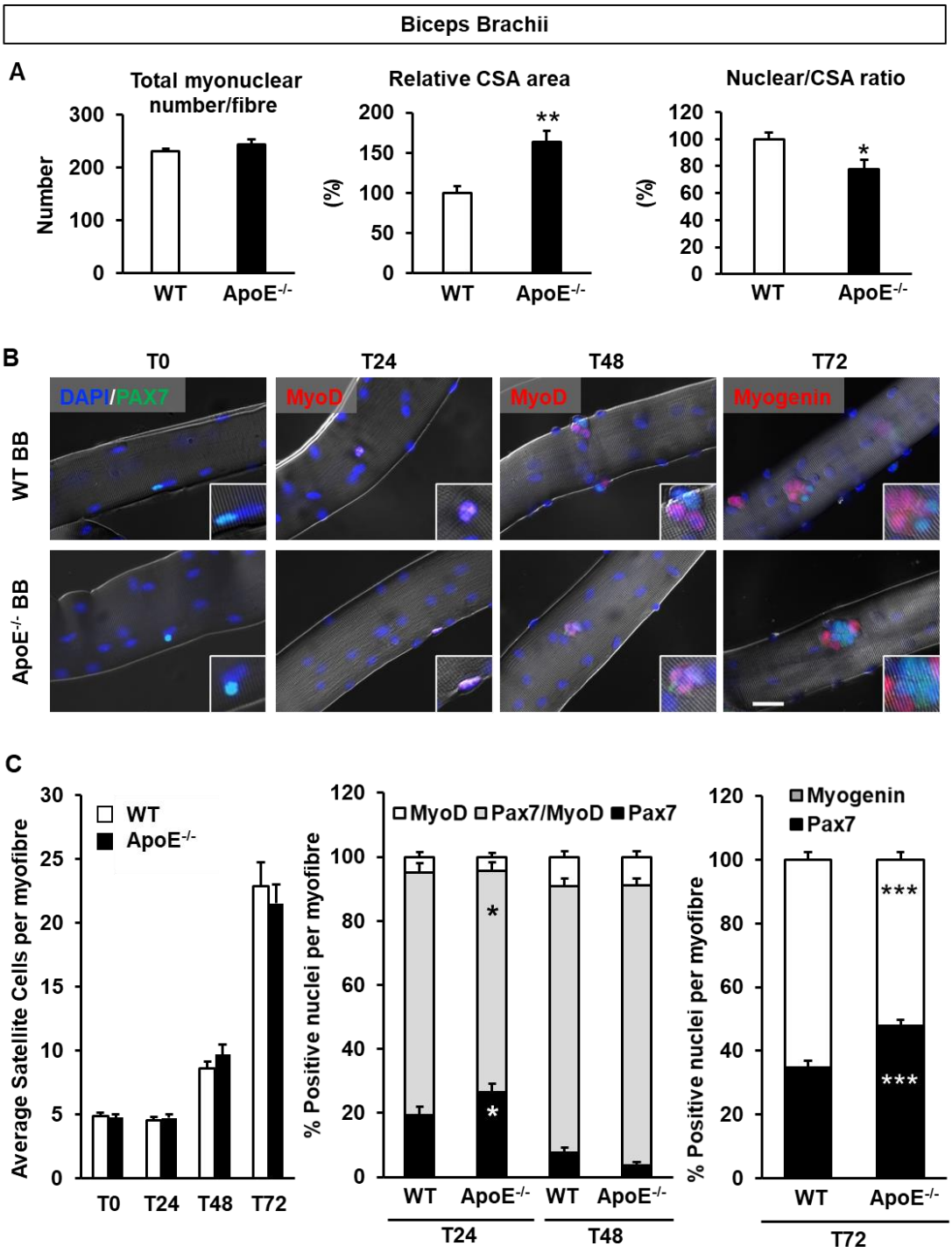

Figure 3.2. Impaired differentiation of muscle stem cells of Biceps Brachii myofibres from ApoE$^{-/-}$ mice *ex vivo*. (**A**) Baseline differences in total nuclear number per myofibre, relative cross sectional area (CSA), (i.e. normalised to the CSA of the WT myofibres) and Nuclear/CSA ratio in isolated biceps brachii myofibres from WT and ApoE$^{-/-}$ mice. (**B**) Single myofibres were isolated from the biceps brachii muscle and studied at different time points (T0, T24, T48 and T72 hours) to determine quiescent, proliferating and differentiating satellite cells, by means of Pax7, MyoD and Myogenin

staining. Representative images of immunofluorescent detection of Pax7 (T0), Pax 7 and MyoD (T24 & T48) and Pax7 and Myogenin (T72, x40 magnification, scale bar=50µm, inset images depict enlarged satellite cell clusters). (**C**) Average number of satellite cells per myofibre and relative quantification of expression of Pax7, MyoD and Myogenin. Data are mean±SEM (n=60-70 myofibres; n=4 mice/group). Statistical analysis was performed by one way ANOVA, *p<0.05 and ***p<0.001 $ApoE^{-/-}$ vs WT.

3.3.2 Compromised proliferative capacity of isolated muscle stem cells from $ApoE^{-/-}$ mice

Given the compromised muscle stem cell differentiation in both EDL and biceps brachii at T72 *ex vivo*, *in vitro* the proliferation patterns of isolated muscle stem cells from $ApoE^{-/-}$ and WT fibres from EDL and biceps brachii were then determined. Isolated muscle stem cells were cultured for 24 hours and cell proliferation was measured by the EdU incorporation assay before cells were fixed and imaged (Figure 3.3A). Proliferating cells were measured as a percentage of EdU positive cells normalised to total cell number (DAPI). Muscle stem cells from the EDL of $ApoE^{-/-}$ mice showed significantly reduced proliferation by 21% compared to WT muscle stem cells (i.e. 48.6%±10.7 vs. 35.5%±11.04, Figure 3.3B). Furthermore, $ApoE^{-/-}$ muscle stem cells from the biceps brachii had significantly decreased proliferation by 30% compared to WT muscle stem cells (i.e. 49.1%±14.6 and 34.0%±13.4, Figure 3.3B). Taken together, these findings indicate that ApoE deficiency impacts on the proliferative capacity of isolated muscle stem cells when the local niche of the myofibre is eliminated.

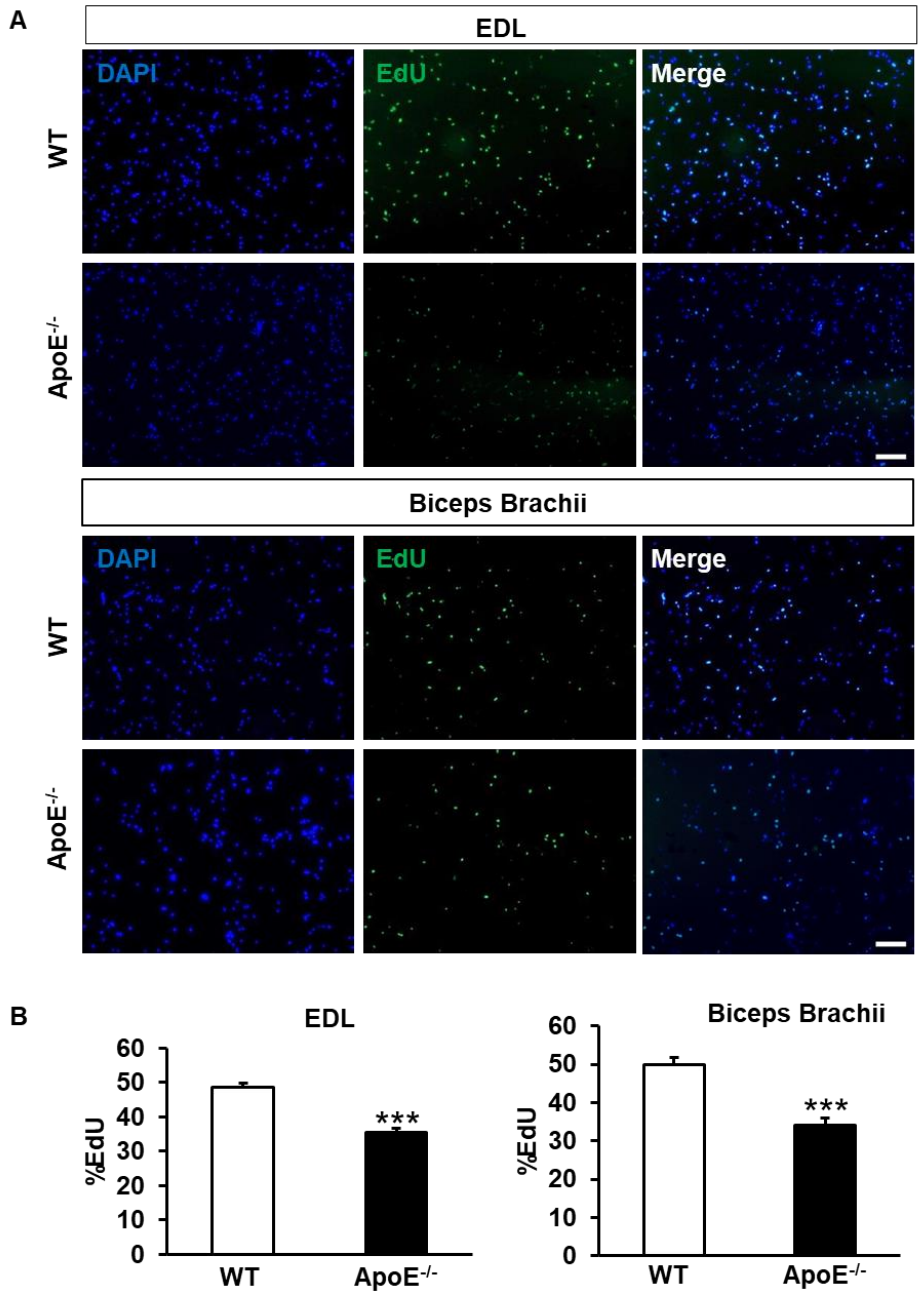

Figure 3.3. Impaired proliferation of isolated muscle stem cells from ApoE$^{-/-}$ mice *in vitro*. Proliferation of muscle stem cells isolated from EDL and Biceps Brachii of wild-type and ApoE$^{-/-}$ mice was detected by EdU staining. (**A**) Representative images of proliferating cells stained for DAPI (blue) and EdU (green) from the EDL and Biceps Brachii myofibres (x5 magnification, scale bar 200µm). (**B**) Quantification of the percentage of proliferating cells (EdU positive) per total number of nuclei from EDL and Biceps Brachii. Data are mean±SEM (40=images per group, n=9 technical replicates from 3 independent experiments). Statistical analysis was performed by one way ANOVA, ***p<0.001 vs WT.

3.3.3 Impaired differentiation and fusion of isolated muscle stem cells from ApoE$^{-/-}$ mice

Given the *ex vivo* finding that a lower proportion of ApoE$^{-/-}$ muscle stem cells express myogenin, the present work hypothesised that this would impair the myogenic differentiation *in vitro*. Therefore, the following experiments determined whether there were any deficits in the capacity of isolated muscle stem cells from the ApoE$^{-/-}$ mice to fuse and form myotubes as compared to wild-type muscle stem cells after 4 days of differentiation. To this aim, differences in total nuclear number, fusion index, overall number of myotubes, myotube length and width were determined in differentiated muscle stem cells (Figure 3.4A-D). There was a significantly lower total nuclear number by 35% in ApoE$^{-/-}$ EDL culture as compared to WT. The fusion index – an indicator of the ability of muscle stem cells to form myotubes, was significantly decreased by 46% in the ApoE$^{-/-}$ myotubes as compared to WT (Figure 3.4A-B). Most importantly, ApoE$^{-/-}$ muscle stem cells from the EDL muscle, formed significantly fewer myotubes by 50% per viewing field (Figure 3.4A-B). The present work also found that the myotube length was significantly smaller by 11% in ApoE$^{-/-}$ compared to WT cultures, without any significant differences in myotube width.

In order to corroborate and strengthen the above findings from the EDL, the same battery of experiments was conducted on the isolated muscle stem cells of the biceps brachii muscle from ApoE$^{-/-}$ and WT mice. Consistent to the findings from the EDL muscle stem cells, the study found that the fusion index was significantly lower by 52% in the ApoE$^{-/-}$ myotubes formed from biceps brachii muscle stem cells (Figure 3.4D). Furthermore, ApoE$^{-/-}$ muscle stem cells from the biceps brachii muscle formed significantly fewer (by 50%) and shorter myotubes (by 20%) compared to WT (Figure 3.4C-D). Taken together, these findings indicate that the myogenin deficit in ApoE$^{-/-}$ muscle stem cells from two different muscles results in impaired fusion and myotube morphology compared to WT.

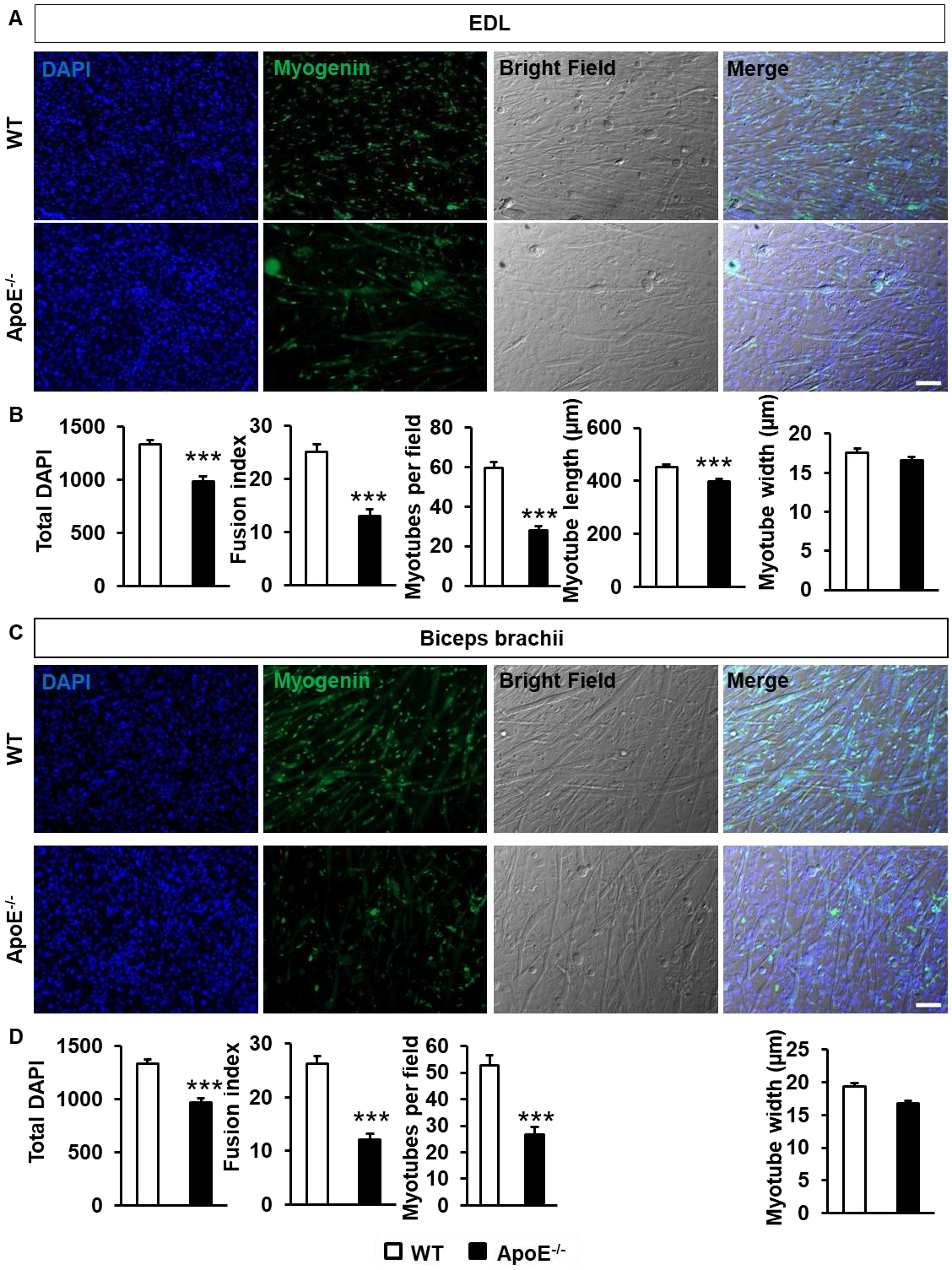

Figure 3.4. Impaired myotube formation of isolated muscle stem cells from ApoE$^{-/-}$ mice *in vitro*. Myotube number and morphology from differentiated muscle stem cells isolated from the EDL and Biceps Brachii of wild-type (WT) and ApoE$^{-/-}$ mice. (A) Representative immunofluorescence images for nuclei (DAPI) and myogenin in the EDL (x10 magnification, scale bar 100µm). Myotube formation is shown with bright

field images. (B) Quantification of total number of nuclei, fusion index (number of myogenin positive nuclei within myotubes divided by total number of nuclei), the number of myotubes per field, myotube length and myotube width in the EDL of WT and ApoE$^{-/-}$ mice. (C-D) Data from the Biceps Brachii. For legend details see above (A-B).Data are mean±SEM (n=9 technical replicates from 3 independent experiments). Statistical analysis was performed by one way ANOVA, **p<0.01 and ***p<0.001 vs WT.

3.3.4 Muscle stem cells from ApoE$^{-/-}$ mice exhibit reduced expression of genes regulating muscle stem cell fate, fusion and contractile proteins

Isolated ApoE$^{-/-}$ muscle stem cells from the EDL exhibited significantly reduced capacity to form myotubes *in vitro*. Thus, the present work next sought to determine whether this decrease was at least partially due to impaired myoblast differentiation. To this aim, isolated muscle stem cells were differentiated for 4 days to form myotubes and mRNA levels of genes involved in muscle stem cell fate (i.e. *MyoD*, *Scrib1* and *Myogenin*), myoblast fusion (i.e. *Bex1*, *Tmem8c* and *Srf*) and genes coding for contractile proteins (i.e. *Mhc1, Acta1*) were measured. Significantly lower mRNA levels were found of all studied genes in ApoE$^{-/-}$ myotubes (Figure 3.5). These findings indicate that both differentiation and fusion are impaired at the transcriptional level in ApoE$^{-/-}$ muscle stem cells.

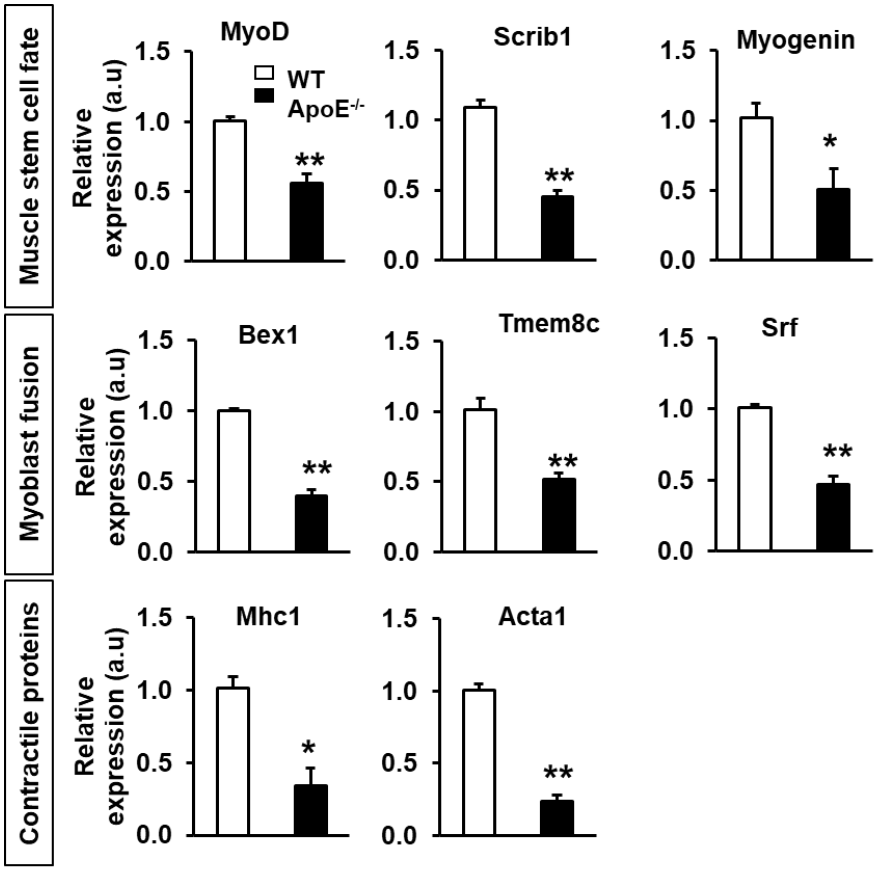

Figure 3.5. Gene expression patterns in differentiating myotubes derived from cultured EDL muscle stem cells from ApoE$^{-/-}$ and WT mice. mRNA levels of genes involved in differentiation and muscle stem cell fate (*MyoD, Scrib1 and Myogenin), myoblast* fusion (*Bex1, Tmem8c* and *Srf*) and contractile proteins (*Mhc1* and *Acta1*) were assessed in differentiating muscle stem cells from the EDL of WT and ApoE$^{-/-}$ mice. Data are shown as mean±SEM (n=6 technical replicates from 2 independent experiments). Statistical analysis was performed by one way ANOVA tests with *p<0.05, **p<0.01 and ***p<0.001 vs WT.

3.4 Discussion

Skeletal muscle has a remarkable intrinsic regenerative capacity mainly brought about by skeletal muscle stem cells; these are muscle-specific progenitor cells essential for skeletal muscle maintenance and regeneration (Relaix and Zammit, 2012). Recent evidence suggests that muscle stem cell function may be abnormal or impaired in the context of obesity both after skeletal muscle injury as well as various experimental conditions *in vitro* and *in vivo* (Akhmedov and Berdeaux, 2013; D'Souza et al., 2015; J. Fu et al., 2016; Nguyen et al., 2011; Verpoorten et al., 2020). Recently it was found found that CD36-deficient mice another diet-independent mouse model of systemic hyperlipidaemia have impaired muscle stem cell function and delayed muscle regeneration (Verpoorten et al., 2020). However, the function of muscle satellite cells in ApoE deficient mice has not received much attention so far.

Hyperlipidaemia is a major risk factor for atherosclerosis and cardiovascular disease as well as an independent risk factor for PAD. PAD is a chronic disease characterised by restriction and finally blockage of the arteries of the lower extremities (Haas et al., 2012; Varu et al., 2010). PAD is a risk factor of cardiovascular morbidity and mortality (Haas et al., 2012; Varu et al., 2010). Patients with PAD exhibit skeletal myopathy that is characterised by altered myofibre morphology, increased oxidative damage, inflammation, mitochondriopathy and poor muscle regeneration impacting on the patients' quality of life (Fu et al., 2008; Koutakis et al., 2015, 2014; Weiss et al., 2013). Although our understanding about the function of muscle stem cells in obesity and diabetes is still evolving, the obesity-independent impact of systemic hyperlipidaemia followed by increased oxidative stress on muscle stem cell myogenic progression and self-renewal is largely unknown (Sfyri et al., 2018). Therefore, this study determined the muscle stem cell myogenic proliferation and differentiation profiles in ApoE$^{-/-}$ mice, an established mouse model of obesity-independent hyperlipidaemia and atherosclerosis. Moreover, this work took advantage of cutting-edge platelet-based applications as biomaterials in order to deliver a cocktail of growth factors in order to boost the regenerative capacity of the skeletal muscle from ApoE deficient mice after injury (Scully et al., 2020, 2019, 2018). The present work found that the muscle stem cell progeny numbers were similar between genotypes for all timepoints, indicating that muscle stem proliferation is normal in ApoE$^{-/-}$ mice. The present work also reports a transient impairment of muscle stem cell myogenic progression (i.e. activation) at

T24 shown by decreased expression of Pax7/MyoD co-expression. More strikingly, impaired myogenin expression at T72 in the stem cells of EDL myofibres from ApoE$^{-/-}$ mice *ex vivo*. This finding is in line with the decreased expression of myogenin found in the gastrocnemius of ApoE$^{-/-}$ mice after hindlimb ischemia (Kang et al., 2008). Taken together, these findings indicate that ApoE deficiency may delay *ex vivo* myogenic progression of muscle stem cells and perturb myogenic differentiation. Beyond hyperlipidaemia, ApoE$^{-/-}$ mice have elevated intramuscular reactive oxygen species (ROS) production and oxidative stress (Sfyri and Matsakas, 2017; Sfyri et al., 2018). The previous work from Sfyri et al. reports excessive levels of ROS in the injured TA muscle of ApoE$^{-/-}$ mice independent of the presence of platelet releasate. Studies have reported that elevated ROS production impairs myogenic differentiation *in vitro* through inhibition of MyoD and MyoD-dependent transcription (Ardite et al., 2004; Barbieri and Sestili, 2012; Catani et al., 2004). Evidence suggests that the major pathways that may lead to reduction of MyoD levels, are through the increase of NF-κB activity or TNFα expression (Guttridge et al., 2000) Thus, the delayed myogenic progression in this study may be attributed to the impact of increased ROS from the myofibre environment that is possibly due to elevated intramuscular lipid content (Sfyri et al., 2018). However, the role of apolipoprotein E on muscle stem cell myogenic progression is not well established. Although it has been shown that apolipoprotein E protein is expressed in differentiating human muscle stem cells, its function has yet to be investigated (Le Bihan et al., 2015). Hence, another possible explanation for the delayed muscle stem cell differentiation could be that apolipoprotein E plays a role in muscle stem cell activation and differentiation. To further investigate the above findings, muscle stem cells were isolated from single fibres and subjected them to cell culture experiments *in vitro* as described previously (Omairi et al., 2016; Scully et al., 2018; Verpoorten et al., 2020). Interestingly, ApoE$^{-/-}$ muscle stem cells stripped from their niche and myofibre environment exhibited impaired proliferation compared to wild-type. The impaired proliferation and differentiation could be attributed to oxidative stress altering their ability to self-renew and differentiate (Chen et al., 2017; Sriram et al., 2019). Furthermore, it has been shown that satellite cells from diet-induced obese mice have impaired proliferation *in vitro* (D'Souza et al., 2015). The above finding suggests that muscle stem cells have perturbed activation that is more prominent in the *in vitro* environment, highlighting the role of myofibre stem cell niche (Takemoto et al., 2019). The present work reports here novel findings that muscle stem cells from

ApoE$^{-/-}$ mice exhibit compromised myogenic differentiation as shown by severely impaired myotube formation, fusion index and myotube length *in vitro*. To verify that the impairment in differentiation and fusion was not a consequence of the fewer number of myotubes, expression of genes involved in the above process were determined. Indeed, the present work found decreased mRNA levels of genes involved in muscle stem cell fate (MyoD, Scrib1 and Myogenin) fusion (i.e. Bex1, Tmem8cand Srf) as well as late myogenesis (i.e. Mhc1 and Acta1), suggesting that this impairment was due to muscle stem cell functional capacity. Studies have shown that oxidative stress as well as lipotoxicity lead to reduced C2C12 - an immortalised myoblast line - proliferation and differentiation *in vitro* (Bosutti and Degens, 2015; Grabiec et al., 2016; Lee et al., 2012; Pomiès et al., 2015). Thus, the hyperlipidaemic environment of the myofibres may have rendered muscle stem cells susceptible to impaired proliferation and differentiation. Recent evidence showed that ApoE$^{-/-}$ mice have ectopic fat deposition in skeletal muscle leading to elevated intramuscular triacylglycerol contents followed by evidence of perturbed antioxidant capacity and increased oxidative stress (Sfyri et al., 2018). Taken together, these findings suggest that ApoE$^{-/-}$ muscle stem cells have perturbed myogenic progression in two different experimental settings (i.e. *ex vivo* and *in vitro*) and this may be attributed to impaired muscle stem cell functional capacity, probably secondary to oxidative stress and increased lipid accumulation or ApoE deficiency per se. However, further research is needed to determine the impact of hyperlipidaemia on potential satellite cell epigenetic modifications.

Chapter 4 – Mechanistic insights about the role of experimental hyperlipidaemia on primary muscle stem cell function and the effect of antioxidant agents

4.1 Overview

Hyperlipidaemia, an elevation of levels of total cholesterol concentration in the serum, as well as elevated levels of triglycerides, which may be caused by genetic or environmental causes, is a major risk factor for atherosclerosis and cardiovascular disease (Casino et al., 1994; Reddy et al., 1994). Experimental hyperlipidaemia is addressed using a number of mouse models such as $ldlr^{-/-}$ which lacks an important orchestrator of cholesterol homeostasis has been used to study endothelial dysfunction, cardiovascular disease risk, inflammation, and oxidative stress, and $ApoE^{-/-}$ mice which lacks the ligand for the same process as discussed in chapter 3 (Abu-Saleh et al., 2021; Ishibashi et al., 1993; Josefs et al., 2020; Mehta et al., 2007; Plump et al., 1992; X. Sun et al., 2020; van Leent et al., 2021; Zhang et al., 1992). Small models of atherosclerosis have been reviewed by Zhao et al. who concluded that the current primary platforms - $ApoE^{-/-}$ and $Ldlr^{-/-}$ transgenic mice provide an ease of breeding, low maintenance and short generation time, however these models imperfectly reflect the human lipoprotein metabolism (Zhao et al., 2020). Given the pivotal role of hyperlipidaemia in atherosclerosis it is important to understand it's effects in muscle stem cell function. Hyperlipidaemia may also be modeled *in vitro* by treating cells with the fatty acid palmitate to identify the role of hyperlipidaemia more closely.

Previous data indicates that a fatty acid rich environment could have severe impacts on the muscle phenotype, in particular obese mice fed a high-fat diet have impaired regeneration after muscle damage compared to those on a control diet (Brown et al., 2015; Hu et al., 2010). Saturated fatty acids contribute to muscle atrophy in diabetes, atherosclerosis and sarcopenia (Boden, 2008; DeFronzo and Tripathy, 2009), and are known to attenuate anabolic signaling pathways which causes a downregulaion of protein synthesis in myofibres, as well as cause increases of intramuscular ROS leading to mitochondrial dysfunction and apoptosis (Costford et al., 2007; Rachek et al., 2007; Yuzefovych et al., 2012).

Palmitate is a saturated fatty acid which is known to induce oxidative stress, mitochondrial DNA damage, and apoptosis (Yuzefovych et al., 2010, 2012). Palmitate is commonly used *in vitro* to simulate a high fat environment and has been used extensively on C2C12 myoblasts - immortalized myoblasts which are capable of rapid proliferation under high serum conditions and differentiation into myotubes under low

serum conditions, and these uses in C2C12 cells and some others have been summarized in table 4.1. C2C12 studies demonstrate induced expression of musclin, TNF-α, and myostatin, increases oxygen consumption rate and reduces viability of C2C12 cells in culture (Covington et al., 2016; Gu et al., 2015; Haghani et al., 2015; Schuh et al., 2012).

While evidence suggests increased ROS is an aspect of skeletal muscle stem cell impairments in hyperlipidaemia and fatty acid treatment *in vitro*, the specific impact of ROS has not yet been studied. Ebselen is a powerful antioxidant and has been used in various mouse and cell studies, however to date it's effects in skeletal muscle stem cells have not yet been studied (Chambers et al., 2009; Gierer et al., 2010; Zuo et al., 2013). The specific effects of palmitate and ebselen on skeletal muscle proliferation and differentiation therefore remain to be studied, though studies using palmitate in C2C12 cells are listed in the table below. This chapter addresses the *in vitro* and *ex vivo* effects of both palmitate and ebselen on skeletal muscle stem cells in both wild type and ApoE$^{-/-}$ mice.

Table 4.1: The use of palmitate in myoblast cells

Ref	Cell Type	Intervention	Outcome
(Gu et al., 2015)	C2C12	0.5 mM palmitate or oleate/1% BSA Cells differentiated for 10 days, were then treated for 6 or 12 h.	induced the gene expression of musclin, GRP78 and CHOP
(Park et al., 2015)	C2C12	Exposure to various concentrations of palmitate for 16 h Cells were treated with 1 to 200 μM hispidin or 100 μM Vitamin C for 8 h, and then 1 mM	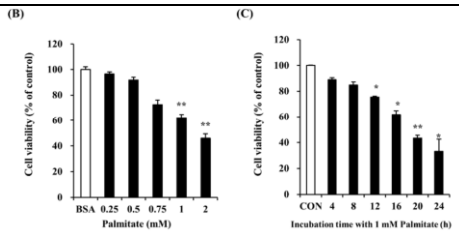

		palmitate was added for 16 h	Hispidin reduced effects of palmitate on intracellular ROS concentration
(Masuda et al., 2018)	C2C12 & SCs	palmitate 1 mmol/L and BSA of and 1% (w/v) 24h	Palmitate loading promoted the secretion of CXCL1
(Abu Bakar and Tan, 2017)	C2C12	Differentiated for at least 4 days. 0.75mM palmitate, 2%(w/v) BSA	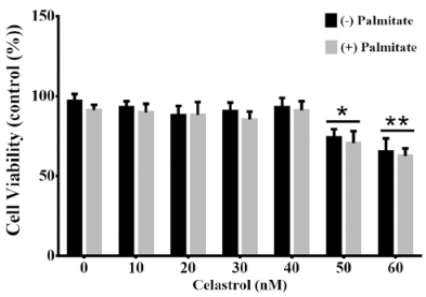 0.75mM Palmitate, 24h
(Jing et al., 2017)	C2C12	cells were differentiated 6 days. 2% BSA 0.5 mM palmitate for 16 h.	GDF11 decreased in palmitate-induced insulin resistance in C2C12 myotubes
(Haghani et al., 2015)	C2C12	Four days after fusion, the differentiated myotubes were used. Palmitate 0.75mM for 8,16,24h 1% BSA	Increase TNF-α protein levels.
(Pierre et al., 2016)	C2C12	After 96 h differentiating, C2C12 myotubes were incubated for 17 h with palmitate. To investigate the insulin pathway, C2C12	↑ ATF4, CHOP, TRB3, XBP1s, BiP, GRP94 mRNA (ER Stress)

		myotubes were stimulated with 100 nM insulin (Actrapid, Novo Nordisk) for 10 min. Palmitate 1 mM 2% (w/v) BSA	
(Covington et al., 2016)	Myotubes	4d differentiation	mRNA levels of IL-6, IL-8, and CTGF ↑, returned to baseline after 24h. Myostatin ↑did not return to baseline.
(Schuh et al., 2012)	200 µM Sodium Palmitate	WT & mdx fibres	↑ Oxygen consumption rate ↑ extracellular acidification rate

4.2 Aims

The principal aim of this chapter was to investigate skeletal muscle stem cell function and C2C12 cell function in experimental hyperlipidaemia. It was hypothesized that proliferation and differentiation would be disrupted by fatty acid in both skeletal muscle stem cells and C2C12 cells, and that these effects would be alleviated by antioxidant ebselen. To achieve this, the following objectives were set:

- To study the impact of experimental hyperlipidaemia on stem cell proliferation and differentiation in primary muscle stem cells and single fibres in Wild type and AopE$^{-/-}$ mice.

- To determine the effects of antioxidant ebselen in Wild type and AopE$^{-/-}$ mice on proliferation and differentiation.

4.3 Results

4.3.1 Palmitate and ebselen in *ex vivo* WT and ApoE$^{-/-}$ fibres

It has previously been shown that ApoE$^{-/-}$ mice have increased intramyocellular fat content, and the previous chapter demonstrated that the ApoE deficient phenotype alone was enough to induce impairment in skeletal muscle stem cell function. Therefore, the present work sought to determine the proliferation and differentiation profiles of muscle stem cells during myogenic progression in both wild type and ApoE$^{-/-}$ muscle fibres treated with palmitate to simulate experimental hyperlipidaemia. Muscle stem cells retained in their niche on isolated EDL myofibres were immunostained for Pax7 and MyoD (T48) (Figure 4.1) or Pax7 and Myogenin (T72) (Figure 2). At each timepoint, fibres were cultured with palmitate and ebselen for the 24 hours prior to harvest. At 48 hours, wild type fibres treated with 0.5mM palmitate had significantly increased numbers of muscle stem cells, and treatment with 15µM Ebselen normalised this effect. In contrast ApoE$^{-/-}$ muscle fibres treated with 0.5mM palmitate showed no significant increase, while treatment with both 0.5mM palmitate and 15µM Ebselen resulted in a significant increase of total stem cells per fibre. Wild type fibres exhibited a significant decrease in muscle stem cell activation when cultured with palmitate when compared to without (91.32%±2.25 without vs 73.53%±3.3 with palmitate), but a strong significant increase in proliferating (MyoD^{+}/Pax7^{-}) (29.67%±4.0 without vs 59.43%±4.54 with palmitate). Both effects were reversed when cultured with both palmitate and ebselen. Interestingly in the ApoE$^{-/-}$ the palmitate group were not significantly different in total activated stem cells(MyoD^{+}), however the percentage of proliferating activated stem cells (Pax7^{-}/MyoD^{+}) were increased in ApoE$^{-/-}$ fibres cultured with palmitate (33.58%±6.41 without vs 66.72%±5.74 with palmitate). Despite showing an increase in total stem cell number per fibre, ApoE$^{-/-}$ fibres cultured with ebselen and palmitate had no significant difference in activation profile compared to ApoE$^{-/-}$ fibres cultured in growth media alone. These results indicate that the functional impairments of muscle stem cells in

experimental hyperlipidaemia can be effectively alleviated using antioxidant ebselen.

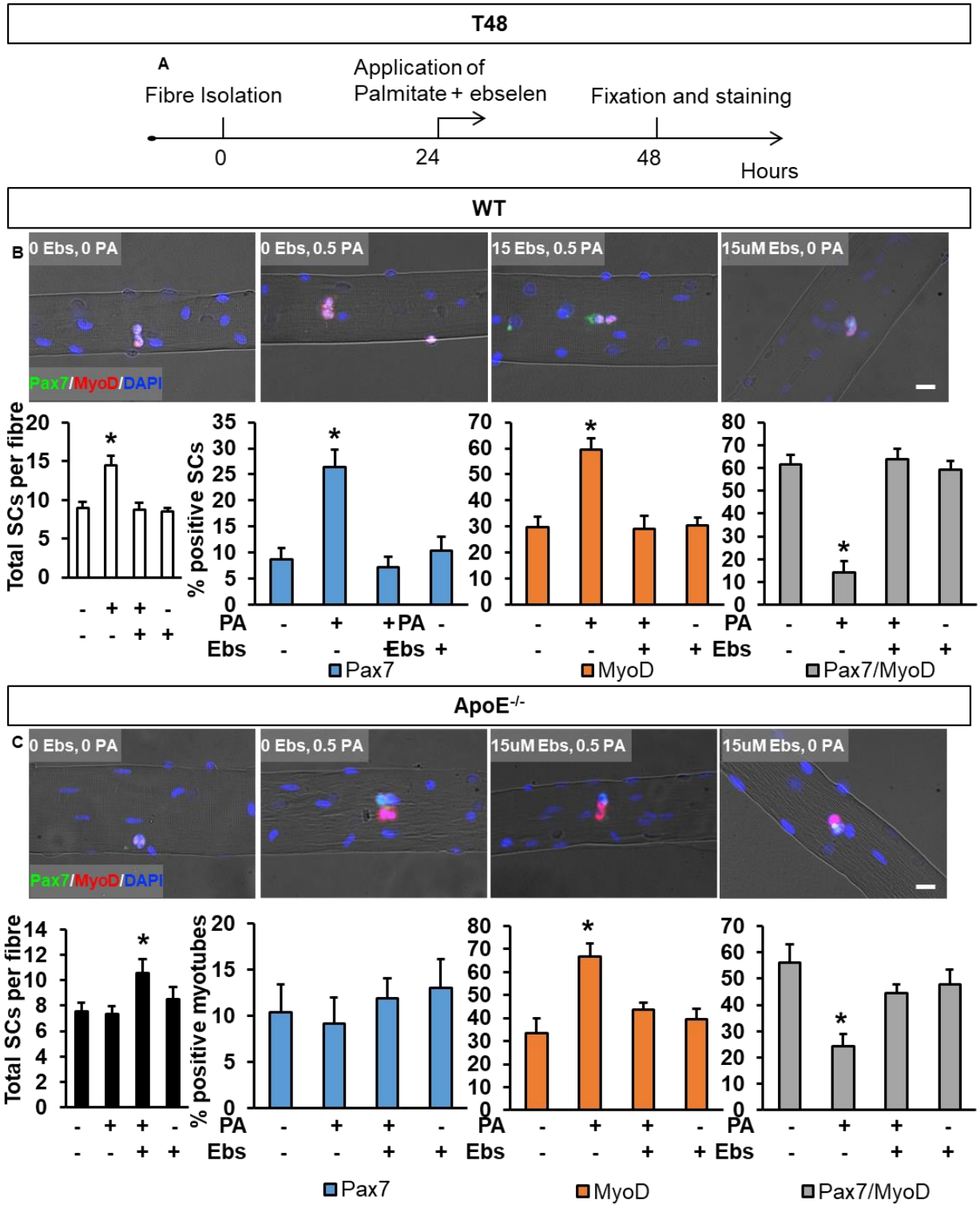

Figure 4.1. Impaired differentiation of muscle stem cells of WT and ApoE$^{-/-}$ myofibres from mice *ex vivo*. (**A**) Experimental timeline. Single myofibres were isolated from (**B**) wild-type and (**C**) ApoE-/- EDL muscle and studied at T48 hours cultured with or without 0.5mM palmitate (PA) for the latter 24h, with or without 15μM ebselen (Ebs), to determine quiescent, proliferating and differentiating satellite cells, by means of Pax7, MyoD staining. Representative images of immunofluorescent detection of Pax7 and MyoD (x40 magnification, scale bar=200μm). (**C**) Relative quantification of expression of Pax7 and MyoD. Data are mean±SEM. Statistical analysis was performed by Two way ANOVA and tukey post-hoc test. *p<0.05, vs all others. #p<0.05, vs 0.5mM palmitate and 30μM ebselen, †p<0.05, vs everything except for 0.5PA 60Ebs.

At 72 hours, neither wild type fibres nor ApoE$^{-/-}$ fibres had significantly different number of muscle stem cells per fibre when cultured for 24h with palmitate or palmitate and ebselen. Wild type fibres exhibited a significant increase in muscle stem cell differentiation (Myogenin^{+}) when cultured with palmitate when compared to without (61.34%±2.05 without vs 75.1%±2.27 with palmitate), this effect was normalised when cultured with both palmitate and ebselen (55%±2.95). Interestingly in the ApoE$^{-/-}$ the palmitate group as well as the ebselen group displayed significantly greater differentiation (Myogenin^{+}) than ApoE$^{-/-}$ in growth media alone (53.14%±2.05 without vs 70.02%±3.74 with palmitate and 68.04%±2.27 with palmitate and ebselen). These results further demonstrate the effects of experimental hyperlipidaemia, confirming that antioxidant ebselen improves retention of stemness in wild type, however in ApoE$^{-/-}$ fibres ebselen isn't enough to improve Pax7 expression.

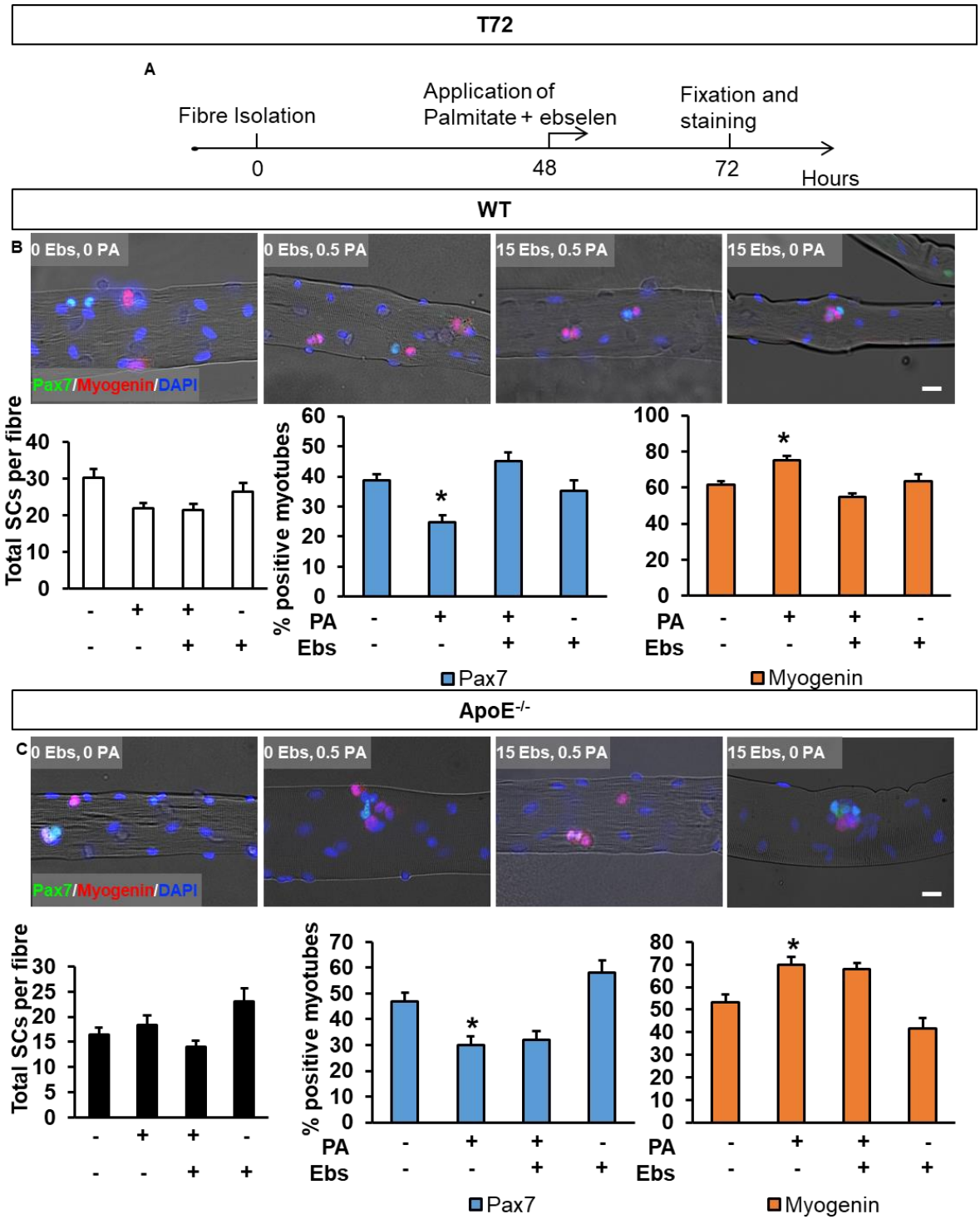

Figure 4.2: Impaired differentiation of muscle stem cells of WT and ApoE$^{-/-}$ myofibres from mice *ex vivo*. (**A**) Experimental timeline. Single myofibres were isolated from (**B**) wild-type and **(C)** ApoE$^{-/-}$ EDL muscle, and studied at T72 hours - cultured with or without 0.5mM palmitate for the latter 24h, with or without 15µM, 30µM, 60µM ebselen, to determine quiescent, proliferating and differentiating satellite cells, by means of Pax7 and Myogenin staining. Representative images of immunofluorescent detection

of Pax 7 and Myogenin (x40 magnification, scale bar=200µm). Relative quantification of expression of Pax7 and Myogenin. Data are mean±SEM. Statistical analysis was performed by Two way ANOVA and tukey post-hoc test. *p<0.05 vs all others, \p<0.05 vs 0.5 ; #p<0.05 vs 0 Palmitate, 0 ebselen.

4.3.2 Impaired differentiation and fusion of isolated muscle stem cells from ApoE$^{-/-}$ and WT mice treated with palmitate

Given the *ex vivo* finding that palmitate increases proliferation and differentiation in WT and ApoE$^{-/-}$ muscle stem cells, the study hypothesised that this may be due to elevated ROS which may be used as a positive signal to induce proliferation and differentiation. Therefore, the present work sought to determine the differentiation capacity *in vitro*, and the extent of oxidative stress of cultured WT and ApoE$^{-/-}$ muscle stem cells treated with palmitate and with palmitate and ebselen. To this aim, WT and ApoE$^{-/-}$ muscle stem cells were cultured to confluence, then differentiated and either left untreated, treated with palmitate, or treated with palmitate and ebselen. Dihydroethidium fluorescence intensity of DHE dyed myotubes was measured to determine oxidative stress levels, and myogenin staining was used to determine myofiber area and myofusion index. WT myotubes with palmitate had significantly higher oxidative stress (1116.6a.u. ±213.9 vs 741.44±156.8) which was not significantly alleviated by ebselen (1032.3±147.6). The ApoE$^{-/-}$ myotubes however started at a point of higher oxidative stress without treatment (1058.3 a.u.±164.0) and the application of palmitate significantly increased oxidative stress, an effect which was reversed by ebselen (1437.1±212.2 vs 1076.2±120.9). The average area of myotubes in all groups was significantly lower than the untreated wild type (12802µM^2±2792) indicating that both ApoE deficiency (7269µM^2±2026) and palmitate (4141µM^2±1309) impair the differentiation of muscle stem cells. In both cases ebselen was unable to improve average myofibre area. These data indicate that ebselen is an effective alleviator of oxidative stress, and its use partially restores the function of muscle stem cells.

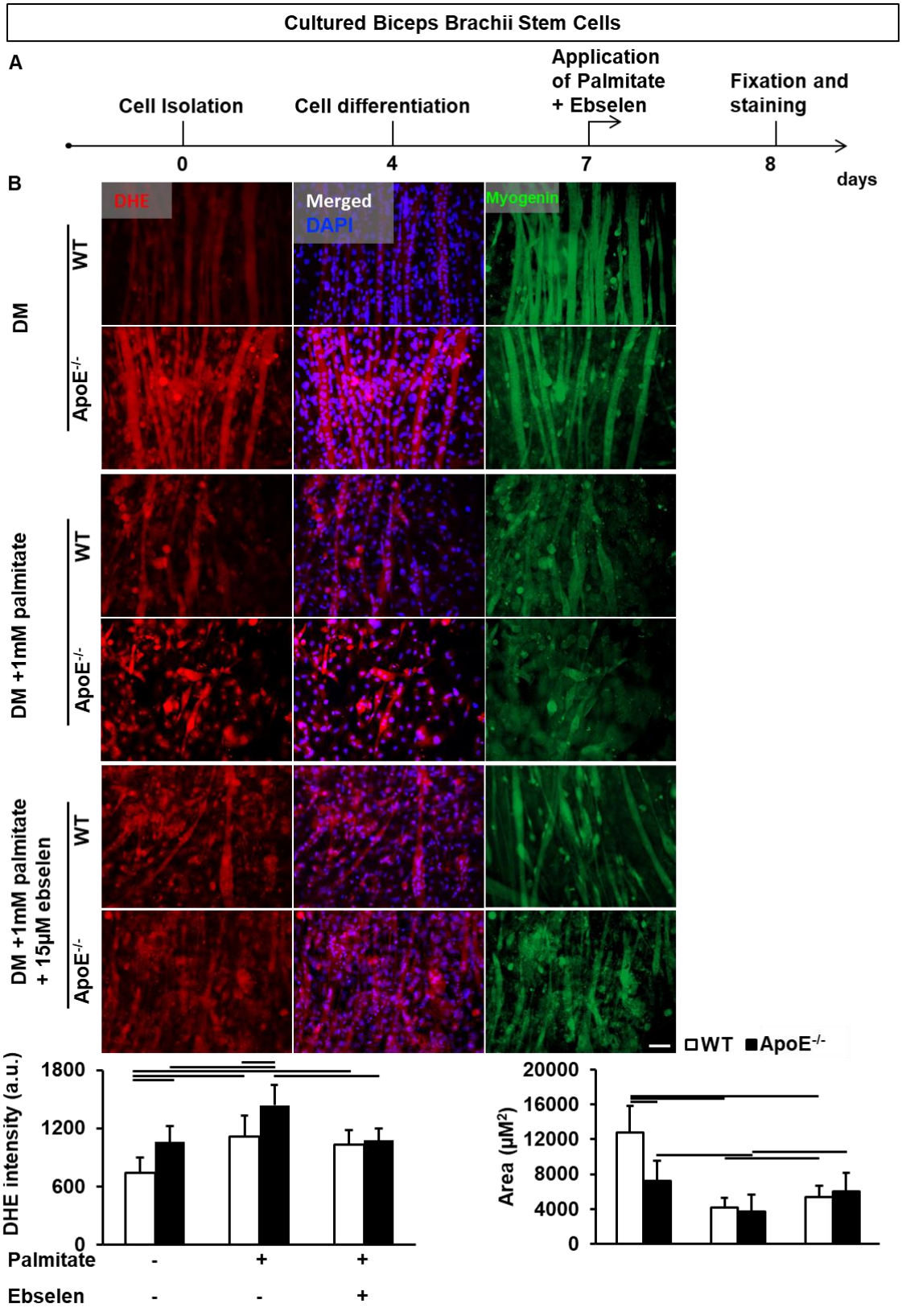

Figure 4.3. Impaired proliferation of isolated muscle stem cells from WT and ApoE$^{-/-}$ mice treated with palmitate *in vitro*. Myotube morphology from differentiated muscle stem cells isolated from the BB of wild-type (WT) and ApoE$^{-/-}$ mice with and without

24h 1mM palmitate treatment prior to fixing. (**A**) Representative immunofluorescence images for nuclei (DAPI) and DHE in the BB (x20 magnification, scale bar 200µm). (**B**) Quantification of DHE positive nuclei per fibre. (**C**) Quantification of myotube length and myotube width in the BB of WT and ApoE$^{-/-}$ mice. Statistical analysis was performed by two-way ANOVA and bonferroni post-hoc test, lines between bars denote $p<0.05$.

4.4 Discussion

Experimental hyperlipidaemia is one potential method of determining the effects of hyperlipidaemia on specific cell types in culture. Here, experimental hyperlipidaemia was induced using palmitate in the culture media of differentiating myoblasts and *ex vivo* muscle fibres. This allowed for the effects of hyperlipidaemia to be detected and the specific influence of antioxidant ebselen could be determined when added to media.

The present work determined the function of muscle stem cells *ex vivo* on fibres. While there was an overall decrease in MyoD expressing cells per fibre, there was an increase of cells expressing MyoD alone. While this may indicate a greater commitment to differentiation, the reduction in cells expressing Pax7 and MyoD together may indicate a dysfunction in functional activation of muscle stem cells which instead of increasing proliferation could result in growth arrest, the suggested pathway through this action may occur is listed in figure 4.4.

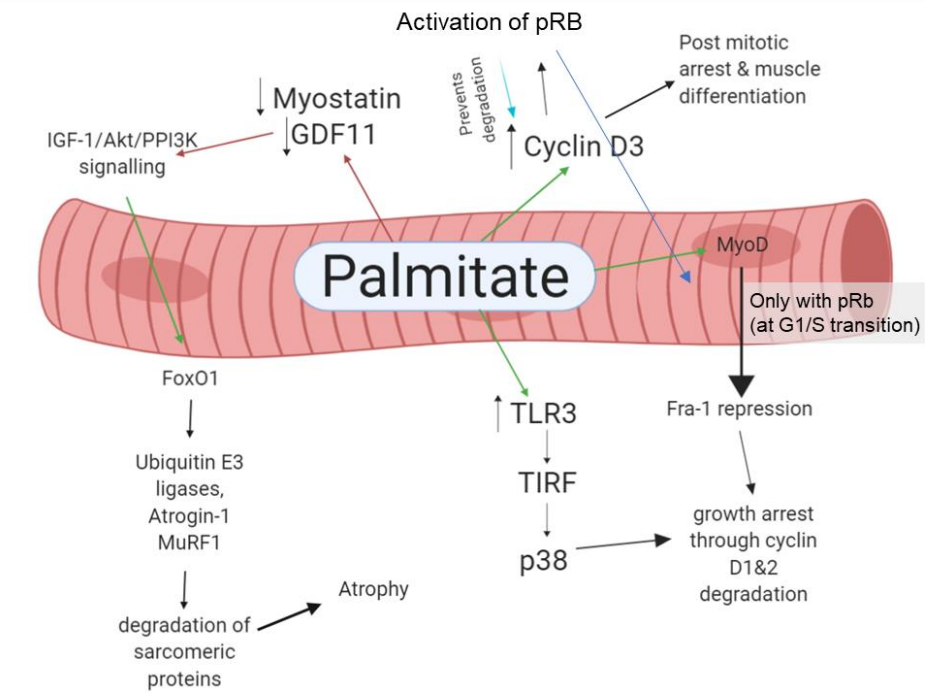

Figure 4.4: The effects of Palmitate on cell cycle and differentiation pathways in skeletal muscle stem cells. Green arrows are activation, while red arrows are inhibition. Palmitate has direct and indirect interactions which can lead to cell cycle arrest and atrophy. Palmitate directly activates cyclin D3 which leads to cell cycle arrest and differentiation (Grabiec et al., 2016). Palmitate also leads to arrest indirectly through MyoD and TLR3 activation which are both parts of the cell cycle arrest

pathways(Yang et al., 2013). Furthermore Palmitate has been seen to decrease levels of growth differentiation factor 11 (GDF11) as well as it's analogue myostatin in C2C12 cells, both of which are the start point of signalling pathways leading to atrophy (Jing et al, 2017; Grabiec et al, 2016).

A recent study treating C2C12 myoblasts with palmitate found increases in myogenin, α-actinin, and myosin heavy chain, protein markers of myogenesis (Grabiec et al., 2016). Interestingly, palmitate was also seen to alter cell cycle proteins, in this case increasing levels of Cyclin D3, which regulates the G1/S phase transition and this increase leads to post mitotic arrest and allows for differentiation to occur (Grabiec et al., 2016).

Furthermore, palmitate has been seen to alter the cell cycle in rodent pancreatic β-cells, in increasing protein and gene expression of TLR3, palmitate leads to growth arrest through degradation of cyclin D1 and Cyclin D2 (Yang, 2019). In β-cells, this arrest leads to reduction of mass, however this thesis posits that in skeletal muscle stem cells palmitate will serve to halt the initial proliferation and therefore accelerate differentiation. Furthermore, palmitate has been seen to decrease levels of growth differentiation factor 11 (GDF11) as well as it's analogue myostatin in C2C12 cells (Grabiec et al., 2016; Jing et al., 2017). GDF11 is another regulator of the G1/S phase transition, which when inhibited increases muscle mass and strength as well as halts progression to the S phase (Jin et al., 2019, p. 11; Shi and Liu, 2011). A study using an antibody blocking the myostatin receptor found increased differentiation (Lach-Trifilieff et al., 2014). All of which may be aligned by the following results which demonstrated that differentiation was impaired in myoblasts in experimental hyperlipidaemia. As the MyoD expression induction had been demonstrated *ex vivo,* the impairment in differentiation is likely due to the action of these pathways in cell cycle arrest, which is normally necessary for differentiation to occur, but in this case the activation of cycle arrest occurs without the activation of differentiation pathways.

Chapter 5 – Injury in the hyperlipidaemic ApoE KO mouse

5.1 Overview

There is sparse scientific evidence on the effect of hyperlipidaemia (independently of obesity and insulin resistance) and central atherosclerosis on skeletal muscle (Stapleton et al., 2010; Wang et al., 2012). Stapleton et al. reported that ApoE deficient mice on a chow diet had decreased capillary density in the gastrocnemius compared to wild type mice (Stapleton et al., 2010). Wang et al. reported that ApoE deficient mice on a high fat diet (21% w/w fat) gained less body weight and displayed better glucose tolerance than wild type mice (Wang et al., 2012). Moreover, ApoE deficient mice had decreased intramuscular triacylglycerol and insulin sensitivity in skeletal muscle was not impaired compared to wild type mice (Wang et al., 2012). Sfyri et al. reported that ApoE deficiency induces a mild transition to oxidative myofibres, an increase in capillary density, intramyocellular fat content and increases oxidative stress. The impact of these outcomes on skeletal muscle stem cell function and skeletal muscle regeneration after injury however, has not been investigated.

Recently Sfyri et al. showed that obesity-independent hyperlipidaemia induced intramuscular lipid accumulation and skeletal muscle oxidative stress in ApoE deficient ($ApoE^{-/-}$) mice, an established model of atherosclerosis and hyperlipidaemia (Meyrelles et al., 2011). Moreover, previous evidence suggests that $ApoE^{-/-}$ mice have delayed skeletal muscle regeneration after injury (Arnold et al., 2015; Crawford et al., 2013; Kang et al., 2008; Pellegrin et al., 2014). This delay in skeletal muscle regeneration was attributed mainly to the perturbed accumulation of proinflammatory macrophages and decreased macrophage phagocytosis due to ApoE deficiency (Crawford et al., 2013, Pellegrin et al., 2014, Kang et al., 2008, Arnold et al., 2015). Specifically, Kang et al. showed that proinflammatory cytokines remained increased in $ApoE^{-/-}$ injured muscle even after 14 days of injury (Kang et al., 2008). Moreover, Arnold et al. reported that ApoE deficiency impacts negatively on macrophage phagocytic activity and is at least partially responsible for the impairment of skeletal muscle regeneration (Arnold et al., 2015).

The effect of ApoE deficiency on skeletal muscle stem cell myogenic capacity and function remains unknown so far. Therefore, this chapter aims to determine whether hyperlipidaemia followed by increased oxidative stress in skeletal muscle of $ApoE^{-/-}$ mice affects muscle stem cell myogenic progression, independently of the proinflammatory environment. To achieve this, ApoE deficient muscle stem cell

myogenesis was evaluated in two different experimental settings, i.e. on single muscle fibres and isolated muscle stem cells. Firstly, Myofibres from ApoE$^{-/-}$ mice were isolated and cultured *ex vivo* to investigate the myogenic progression and self-renewal of muscle stem cells. Secondly, muscle stem cells were removed from their microenvironment, i.e. myofibres, and their myogenic potential was studied in cultures *in vitro*. This work took advantage of the differential expression patterns of transcription factors and myogenic regulatory factors as follows: in adult skeletal muscle, quiescent stem cells express Pax7, activated stem cells switch on MyoD expression, proliferating stem cells co-express Pax7 and MyoD, stem cells committed to differentiation are Pax7-negative and MyoD-positive, whereas differentiated stem cells give rise to new myonuclei that express myogenin (Zammit et al., 2002, Fuchtbauer and Westphal, 1992, Grounds et al., 1992, Yablonka-Reuveni and Rivera, 1994, Yablonka-Reuveni et al., 1999, Zammit et al., 2004). It was hypothesised that muscle stem cell function may be perturbed in atherosclerotic mice with systemic hyperlipidaemia and skeletal muscle oxidative stress and this may explain the impaired muscle regeneration seen *in vivo*.

5.2 Aims

The principal aim of this chapter was to investigate skeletal muscle regeneration in the atherosclerotic ApoE deficient mouse model compared to wild type mice. It was hypothesised that perturbed muscle stem cell function in hyperlipidaemic mice would result in impaired muscle regeneration in response to injury. The impaired muscle stem cell function and increased oxidative stress discussed in chapters 3 and 4 respectively would contribute to impaired muscle regeneration *in vivo*. To achieve this, the following objectives were set:

- To evaluate the degree to which muscle regeneration is impaired *in vivo* after chemically induced injury in ApoE deficient mice.
- To evaluate the degree to which muscle injury progresses over the course of 14 days in ApoE deficient and wild type mice.
- To evaluate the degree to which muscle stem cells function *in vivo* after chemically induced injury.

5.3 Results

5.3.1 Impaired skeletal muscle regeneration of ApoE$^{-/-}$ mice 5 and 10 days post injury

Having shown that ApoE deficiency had an impact on function of skeletal muscle stem cells, muscle hindlimbs were injured with Cardiotoxin, and the regeneration of wild-type and ApoE$^{-/-}$ mice TA muscles was examined after 5 and 10 days of recovery. TA muscles of ApoE$^{-/-}$ display more exaggerated injury than wild-type after 5 days post injury(**Figure 5.1**), this is evident in a significantly higher frequency of low cross sectional area regenerating fibres by 80%(expressing eMHC) indicating a further progression in recovery from injury by the wild-type(**Figure 5.1 B,C**). Furthermore the damaged and dying fibres (identified through the presence of IgG inside muscle fibres) were more frequently found by 200% in the ApoE$^{-/-}$, indicating escalated injury in the hyperlipidaemic mouse(**Figure 5.1 D,E**). The ApoE$^{-/-}$ mouse also displayed more macrophage infiltration as seen by F4/80 staining (**Figure 5.1F,G**). After 10 days, recovery had progressed to an extent where regenerating fibres were less visible in the wild-type, however the TA of ApoE$^{-/-}$ mice were still recovering, with evidence of eMHC expressing muscle fibres remaining(**Figure 5.2 B,C**). No difference in IgG infiltration into injured fibres was evident, indicating that the muscle had recovered from the damaged and dying fibres, however the ApoE$^{-/-}$ had not regenerated to the same extent as wild-type(**Figure 5.2 D,E**). The ApoE$^{-/-}$ mouse also displayed more macrophage infiltration as seen by F4/80 staining (**Figure 5.2F,G**).

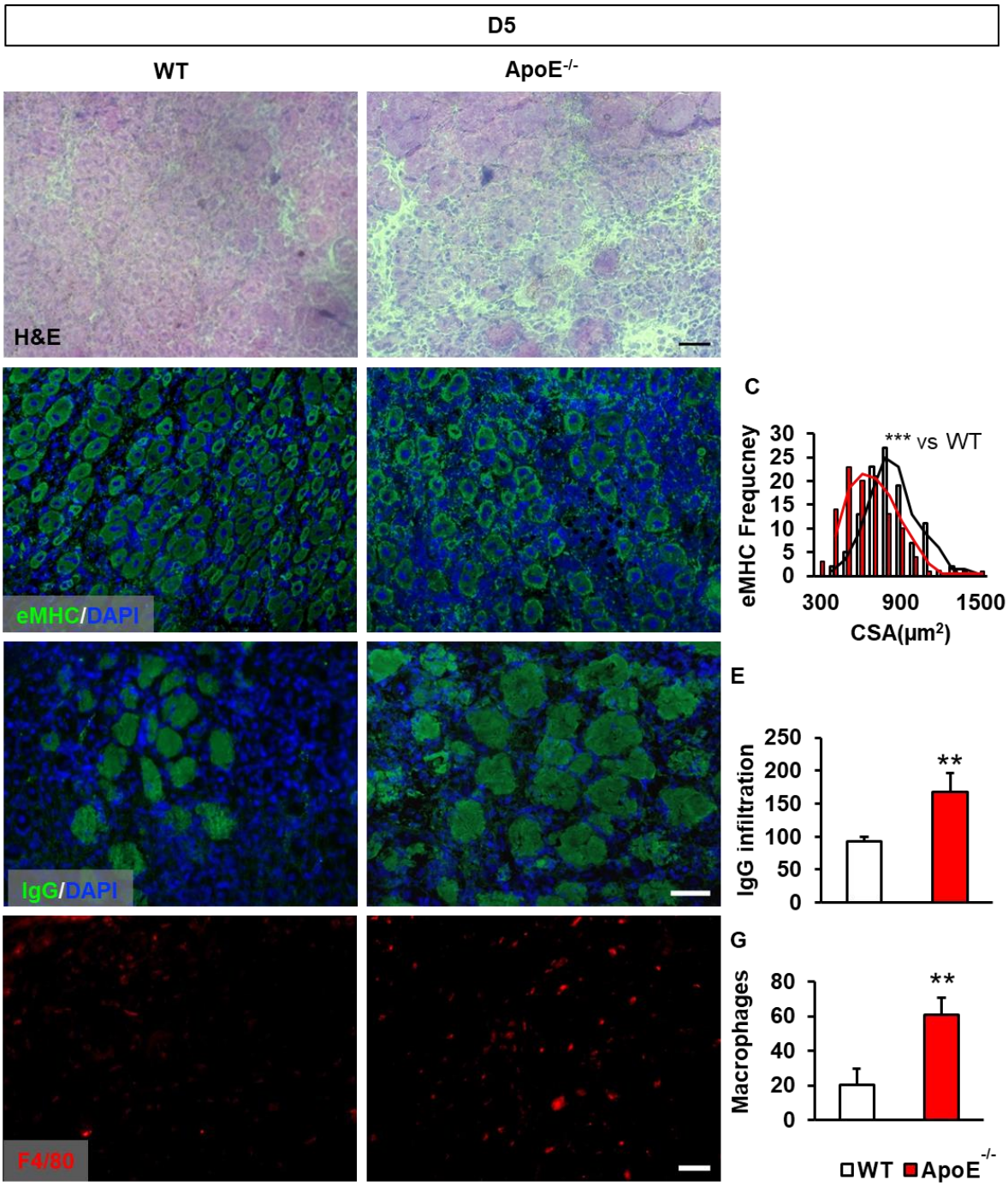

Figure 5.1. Impaired skeletal muscle regeneration of ApoE$^{-/-}$ mice 5 days after injury. Representative images of (**A**) H&E staining (x20) (**B**) the identification of regenerating muscle fibres (through the expression of embryonic myosin heavy chain (eMHC), x20), (**D**) damaged and dying fibres (identified through the presence of IgG inside muscle fibres, x20), and (**F**) macrophages (identified through F4/80 staining, x40) on day 5 after cardiotoxin injury and platelet releasate treatment. Quantification of (**C**) cross sectional area of fibres expressing eMHC, (**E**) number of fibres with IgG infiltration per muscle and (**G**) number of macrophages are displayed. Scale bar: 20μm at x40, 50μm

at x20. Data are mean ±SD. Statistical analysis was performed by student's T test. Differences are **p<0.01, ***p<0.001 vs WT.

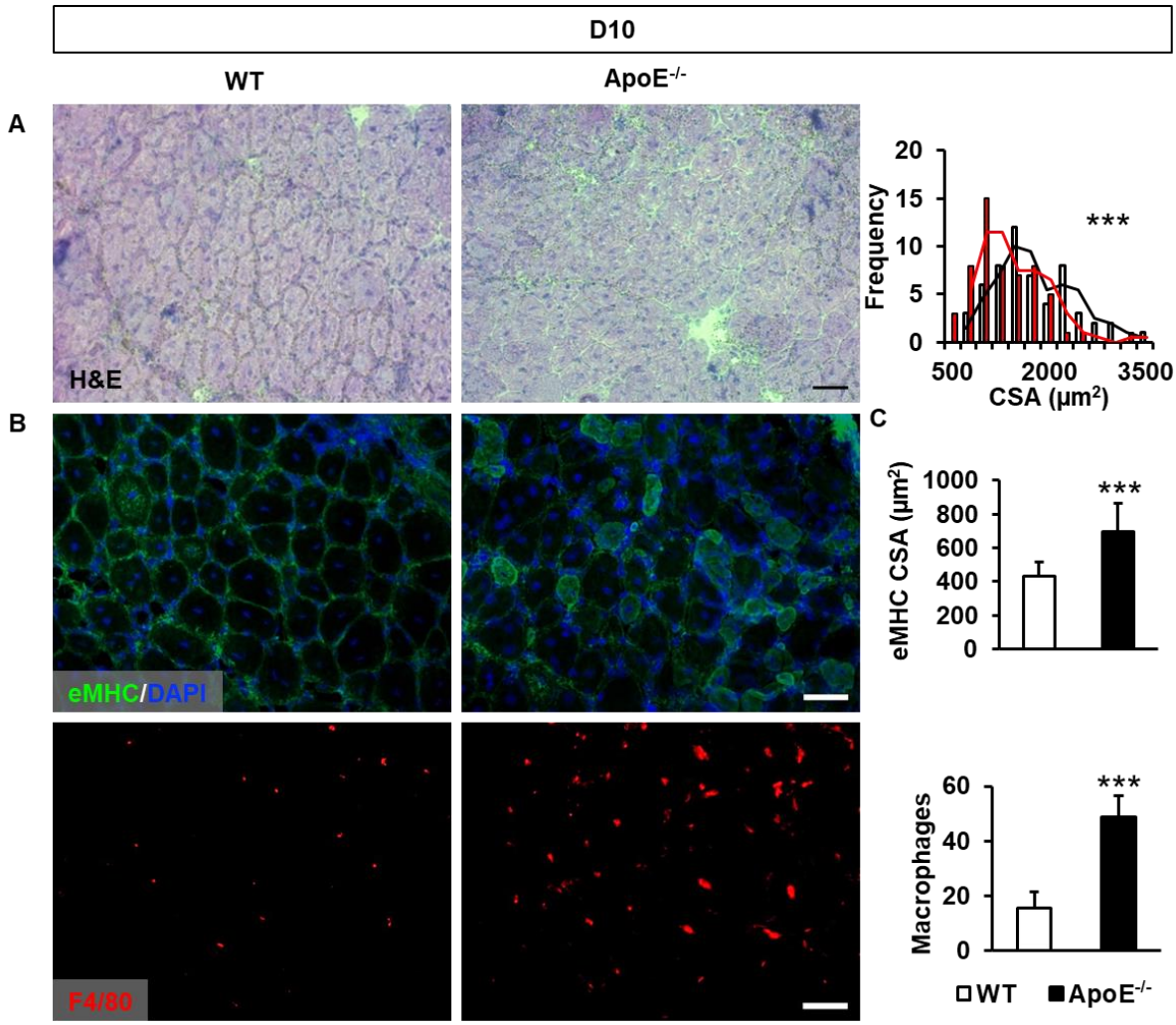

Figure 5.2. Impaired skeletal muscle regeneration of ApoE$^{-/-}$ mice 10 days after injury. Representative images of (**A**) H&E staining (x20) (**B**) the identification of regenerating muscle fibres (through the expression of embryonic myosin heavy chain (eMHC) x20), (**D**) damaged and dying fibres (identified through the presence of IgG inside muscle fibres, x20), and (**F**) macrophages (identified through F4/80 staining, x40) on day 5 after cardiotoxin injury and platelet releasate treatment. Quantification of (**C**) cross sectional area of fibres expressing eMHC, (**E**) number of fibres with IgG infiltration per muscle and (**G**) number of macrophages are displayed. Scale bar: 20µm at x40, 50µm at x20. Data are mean ±SD. Statistical analysis was performed by student's T test. Differences are *p<0.05, ***p<0.001 vs WT.

5.4 Discussion

To determine the effect of impaired skeletal muscle stem cell function on muscle regeneration, ApoE-and wild-type mice were subjected to an acute injury protocol with cardiotoxin *in vivo*. Here is reported impaired muscle regenerative capacity in the injured ApoE$^{-/-}$ mice on days -5 and -10 post injury as evidenced by eMHC expression and IgG infiltration (i.e. indicating fibre necrosis); and the size of regenerating fibres respectively compared to wild-type. These findings are in line with previously published data showing deficits in muscle regeneration in ApoE$^{-/-}$ mice 14 days post ischaemic injury, however at day 14, our injury model showed no difference in recovery, this may be due to the method of injury (cardiotoxin vs ischaemic) (Kang et al., 2008). Furthermore, intramuscular macrophage infiltration in injured TA muscle was significantly higher in the ApoE$^{-/-}$ mice, indicating a delay in the temporal sequence of inflammatory and regerative events following muscle injury(Ciciliot and Schiaffino, 2010). Most importantly, the muscle stem cell myogenic deficits in the *in vitro* and *ex vivo* settings of this work (chapter 3) were validated *in vivo* by showing a deficit in muscle stem cell activation and differentiation in injured ApoE$^{-/-}$ muscle due to impaired myoD and myogenin expression respectively. Taken together, the present study links for the first time the delayed skeletal muscle regeneration of the ApoE$^{-/-}$ mouse to impaired muscle stem cell function.

Platelet-based therapies have been used for almost 50 years since the first developed of platelet rich plasma (PRP) (Andia and Abate, 2013). A number of commercial enterprises have arisen that each market PRP products to treat a spectrum of human medical conditions ranging from osteoarthritis to central nervous system pain management (Behroozi et al., 2021; Centeno et al., 2017; Cohen and Lee, 2015). The use of PRP has a number of disadvantages most based on the notion that preparations containing platelets may induce aggregation and potentially occlude blood vessels, as PRP is administered intravenously, the possibility of developing a blood clot exists (Ramaswamy Reddy et al., 2018). This and other issues have led in part to the development of platelet lysates, rich in growth factors but devoid of cellular material. Indeed, these have been shown to have therapeutic value especially in the treatment of pain and orthopaedic injuries (Centeno et al., 2017). Recently platelet-based therapies have been refined by developed secretomes that produced in a cell-regulated manner (rather than lysis of platelets) using specific mediators of

degranulation (El Bakly et al., 2020; He et al., 2017; Scully et al., 2018; Tsai et al., 2018).

Chapter 6 –The impact of growth factors on cell senescence of the hyperlipidaemic ApoE KO mouse

6.1 Overview

Cellular senescence is a product of ageing and cancer, involving indefinite cell cycle arrest of aged or damaged cells, which arises in response to a variety of environmental conditions, including increased oxidative stress, macromolecular damage or signalling from activated oncogenes (Barnes et al., 2019; Passos et al., 2007; Wei and Ji, 2018). Anthracycline antibiotic doxorubicin – used as a treatment in a variety of cancers, while effective against cancer cells, is nonselective and its toxicity limits it's use (Carvalho et al., 2009; Tacar et al., 2013). This toxicity has become evident in a variety of tissues including the heart, brain, liver, kidneys and skeletal muscle (Alhowail et al., 2019; Guigni et al., 2018; Lee and Harris, 2011; Prasanna et al., 2020; Songbo et al., 2019). Prominently, cardiotoxicity had been catalogued as a side effect of doxorubicin, however mounting evidence suggests that toxicity is seen in skeletal muscle and its resident stem cells (Hayward et al., 2013). Doxorubicin induces cell cycle arrest and even cell death through a variety of pathways including apoptosis, autophagy, and necrosis (Kim et al., 2009; Ma et al., 2017).

Previous research suggests doxorubicin induces formation of reactive oxygen species (ROS) which induces cytochrome c release from mitochondria – leading to apoptosis and cell death. Furthermore senescent cells may acquire apoptosis resistance, increased beta galactosidase activity and prooxidant activity, with reduced homeostatic compensation to alleviate oxidative stress (Songbo et al., 2019). The prooxidative environment induced in senescent cells further induces ROS and therefore feeds back into increased senescence. Reactive oxygen species are generated in normal cell function through mitochondrial respiration and energy generation, predominantly by contracting in skeletal muscle (Powers et al., 2020). These ROS function as essential mediators of cellular metabolism and gene regulators. Their detrimental effects, however, can accumulate when present in excess or ROS clearance is impaired. ROS mediated lipid peroxidation, synthesis of proteins damaging to the cell, and activation of stress signalling pathways can play a significant role in mitochondrial function, remodelling and repair pathways, protein turnover and gene expression which is particularly impactful in skeletal muscle and skeletal muscle stem cells (Diebold and Chandel, 2016; Moloney and Cotter, 2018; Ochoa et al., 2018; Su et al., 2019).

Given the increased oxidative stress in skeletal muscle of the atherosclerotic mouse, and the impaired skeletal muscle stem cell function in experimental hyperlipidaemia with increased ROS, patients taking doxorubicin may similarly be suffering from oxidative stress and therefore are likely to have impaired skeletal muscle stem cell function. Therefore, subsequent experiments investigated the impact of doxorubicin on skeletal muscle stem cell function; and used platelet releasate to attempt to restore function. While Studies using ebselen had restored function to skeletal muscle stem cells, senescence is a much more complex scenario. With increased DNA damage, apoptosis, inhibition of proliferation and impairment of mitochondria all being outcomes of doxorubicin use, platelet releasate is a cocktail of growth factors which could have positive effects on each of these outcomes. Releasate was therefore selected as a treatment most likely to demonstrate positive results.

Skeletal muscle stem cells already have a built-in pathway for cell cycle arrest, as after a phase of proliferation, growth is halted to initiate differentiation. Through myoD interacting with retinoblastoma rumour suppressor protein, cell cycle arrest is initiated via cyclin D1 and $p16^{ink4a}$, which allows differentiation to occur (Chen and Wang, 2000; Rajabi et al., 2014). Retinoblastoma tumour suppressor protein and $p16^{ink4a}$ however, also increase ROS, which in turn activates protein kinase C δ (PKCδ) to induce senescence. PKCδ further increases oxidative stress by increasing ROS itself and creating a positive feedback loop. In normal function, MyoD should signal through the Six1/4-Mef2-Pbx1 pathway to induce myogenin expression (Faralli and Dilworth, 2012), however in cases of excessive ROS myogenin expression is inhibited, directly by ROS (Sandiford et al., 2014), and indirectly through p53 – which is upregulated by ROS and doxorubicin, and both inhibits myogenin expression and activates p21 to induce cell cycle arrest (Yang et al., 2015). The shared proteins in these pathways are summarised in figure 6.1 (Barbouti et al., 2020; Faralli and Dilworth, 2012; Harrington et al., 1998; Knudsen et al., 2000; Sandiford et al., 2014; Takahashi et al., 2006, p. 53; Yang et al., 2015).

Skeletal muscle retains a small population of stem cells throughout adulthood which enables it's strong capacity for regeneration (Relaix and Zammit, 2012). These muscle stem cells remain quiescent during adulthood unless activated by myofibre injury, at which point they proliferate and either return to quiescence (to retain a population of stem cells) or differentiate to support regeneration (Zammit, 2017). This regenerative

ability may however come at a cost, such as incomplete functional recovery, stiffness, excessive inflammation, or fibrosis (Laumonier and Menetrey, 2016). There is currently an increasing interest in the field of skeletal muscle regenerative research. Many factors contribute to this interest such as the lack of effective treatments for myopathies, neuromuscular disease, and muscle related effects of sarcopenia, hyperlipidaemia as well as cancer therapies.

Due to the nonspecific cytotoxicity of doxorubicin, patients of cancer can experience myopathy, and this study proposes tissue specific treatment with platelet releasate to alleviate myotoxicity induced by this anticancer drug which causes cell senescence. Platelet based therapies including platelet rich plasma and platelet releasate are an easily generated method of delivering cytokines and growth factors in a tissue-specific manner to act as cell cycle regulators and promote regeneration and wound healing (Scully et al., 2018). Platelet secretomes have already been used for muscle specific regeneration such as in Barlow et al., and in Scully et al. revealing that releasate improves proliferation and differentiation of muscle stem cells in hyperlipidaemic mice, furthermore our lab has demonstrated the beneficial effects on muscle stem cells (Barlow et al., 2021; Scully et al., 2019). Collectively this data has demonstrated the ability of platelet releasate to promote myoblast proliferation and improve efficiency of differentiation when administered during fusion. The role of PDGF and VEGF present in platelet releasate in both processes is instrumental, as these act through the Akt/mTOR pathway, inducing skeletal muscle stem cell proliferation. While specific administration of platelet releasate has yielded positive results in hypercholesterolemic, and injured mouse skeletal muscle, it is not yet known to what extent releasate can improve cell cycle progression in senescent myoblasts.

This study harnesses the therapeutic potential of platelet releasate to induce cell cycle progression in senescent skeletal muscle stem cells. To determine the effect of platelet releasate on doxorubicin induced senescence in muscle stem cells, C2C12 cells were used to determine the proliferation and differentiation profiles as well as the level of senescence, the effects on senescence in mouse skeletal muscle regeneration and on *ex vivo* muscle fibres were further determined. C2C12 cells are an immortalized myoblast cell line capable of proliferation and differentiation into myoblasts, similar to primary muscle stem cells, this cell line was selected for some of the following experiments subsequent to study being disrupted by the COVID-19 global pandemic

and the loss of access to animals used for the remainder of experiments in this thesis. The C2C12 cells are a widely used muscle cell line offering the opportunity to generate data quickly while reducing the use of animals. The present work shows for the first time that releasate alleviates the cell cycle arrest of doxorubicin induced senescence in C2C12 cells and furthermore increases commitment to differentiation. Furthermore, this work shows that releasate improves the situation in muscle injury and in *ex vivo* fibres. These findings depict an improved cell cycle progression in senescence induce muscle stem cells, and a developed ability of muscle regeneration.

6.2. Aims

The principal aim of this chapter was to investigate the impact of platelet releasate on cell senescence in the hyperlipidaemic ApoE KO mouse. It was hypothesized that senescence could be induced in muscle stem cells by application of doxorubicin in culture, while application of platelet releasate in culture would reverse senescence and restore normal function. To achieve this, the following objectives were set:

- To determine the extent to which doxorubicin could induce senescence in differentiating muscle stem cells.
- To determine the proliferation and differentiation capacity of Doxorubicin-treated muscle stem cells
- To study the extent to which platelet releasate can reverse the effects of doxorubicin-induced senescence.
- To determine the effects of doxorubicin and platelet releasate on DNA damage and repair mechanisms in muscle stem cells.

6.3 Results

6.3.1 Doxorubicin induces senescence in culture

As anthracycline cancer treatment doxorubicin's effects include DNA damage (Silva et al., 2017) and induction of senescence(Bashiri Dezfouli et al., 2020), the present work sought to determine its impact on muscle stem cell function and to test the effects of platelet releasate to resolve the effects. To confirm that senescence was induced by doxorubicin, cells were cultured with 0-2μM of doxorubicin in growth media for 2 days before being fixed and stained for β-Gal or trypan blue (Figure 6.1A). Peak senescence associated β-galactosidase was detected in culture at 0.5μM doxorubicin (23.28μm^2 per unit area at 0.5μM DOX vs 1.25μm^2 per unit area at 0μM DOX) (Figure 6.1B). Surprisingly, higher concentrations of doxorubicin yielded lower levels of senescence-associated β-galactosidase, so trypan blue dye was used to detect cell death which became elevated at higher concentrations of doxorubicin. These data indicated that 0.5μM DOX induced peak senescence before cell death was induced, therefore 0.5μM DOX was selected for subsequent experiments.

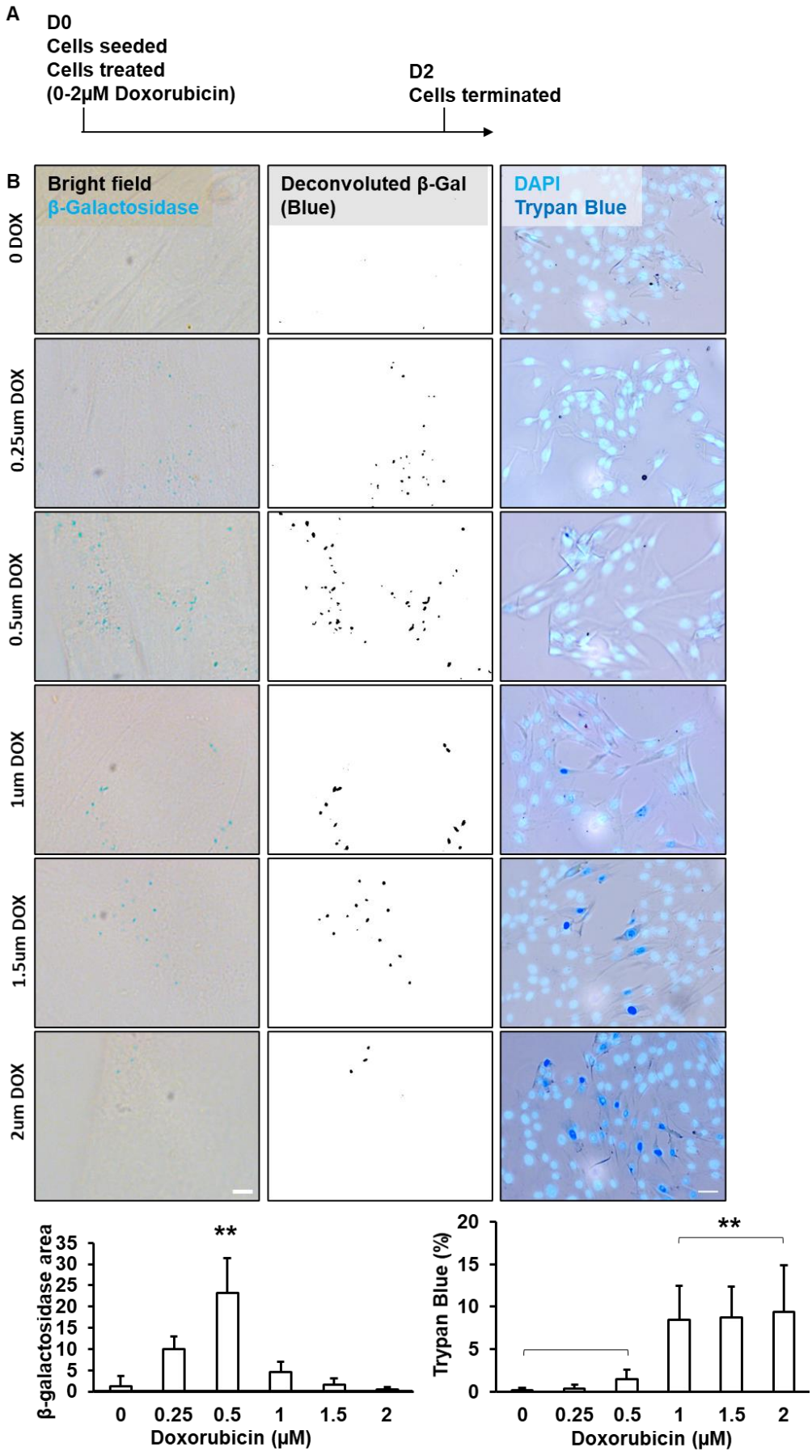
A
D0
Cells seeded
Cells treated
(0-2μM Doxorubicin)
D2
Cells terminated
B
Bright field
β-Galactosidase
Deconvoluted β-Gal
(Blue)
DAPI
Trypan Blue
0 DOX
0.25um DOX
0.5um DOX
1um DOX
1.5um DOX
2um DOX
β-galactosidase area
Doxorubicin (μM)
Trypan Blue (%)
Doxorubicin (μM)
**
**

Figure 6.1. Senescence-associated β-galactosidase in differentiated C2C12 cells. (A) experimental setup: C2C12 seeded cells were seeded in growth media (GM) for 2 days, with one treatment of 0-2μM doxorubicin (DOX) when seeded. (B) Bright field images of senescence associated β-galactosidase are presented alongside deconvoluted images of blue staining to provide a clearer contrast (magnification x100, scale bar = 5μm). Trypan blue stain detected cell death in culture (magnification x20, scale bar 50μm) (C) Quantification of area of senescence associated β-galactosidase staining per image and percentage of trypan blue dyed (dead) cells. Statistical analysis was performed by one way ANOVA and Bonferroni post-hoc test. n=6 ** $p<0.005$.

6.3.2 Doxorubicin induced senescence impairs myoblast proliferation capacity

Having defined 0.5 μM as the peak concentration to induce senescence in myoblasts in culture without significant cell death, this model was used to measure the proliferation capacity of C2C12 cells. Initially proliferation was measured in C2C12 cells by the EdU incorporation assay. Cells were seeded in serum free media and treated with DOX and releasate at 0h, then releasate groups received a second dose at 24h before all groups were fixed at 48h (figure 6.2A). While releasate alone improved the proliferation, Doxorubicin was found to induce great cell death in serum free media, so the following experiments were performed using growth media. C2C12 cell proliferation is almost entirely halted by doxorubicin (4.8% EdU) compared to untreated cells (47.5% EdU) while releasate has a small corrective effect (13.9% EdU) the levels of proliferation were still low (Figure 6.2B). These data indicate that DOX has a severe impact on proliferation of C2C12 cells which is not reversible via platelet releasate.

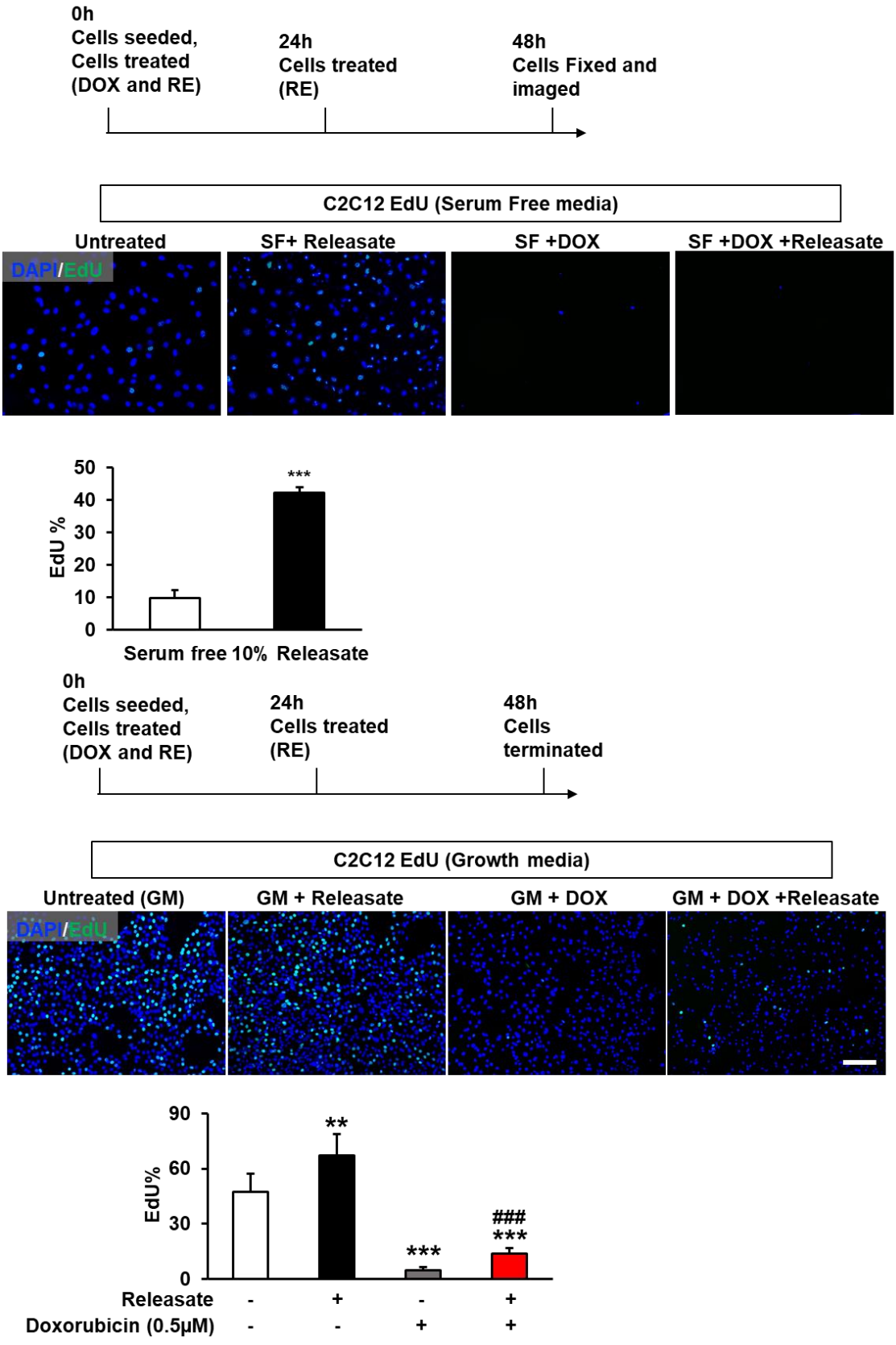

Figure 6.2. Platelet releasate improves proliferation of C2C12 cells treated with Doxorubicin (DOX). Proliferation of C2C12 cells treated with releasate and DOX was

detected by EdU staining. (A) Representative images of proliferating C2C12 cells stained for DAPI (blue) and EdU (green) (x10 magnification, scale bar 50μm). (B) Quantification of the percentage of proliferating cells (EdU positive) per total number of nuclei from EDL. Data are mean±SD. Statistical analysis was performed by one way ANOVA, **p<0.01, ***p<0.001 vs untreated ###p<0.001 vs DOX.

6.3.3 Doxorubicin-induced senescence impairs differentiation that is alleviated by platelet releasate

Given previous data (Scully et al., 2018) utilising platelet releasate to promote skeletal myogenesis via commitment to differentiation and evidence that releasate may be used to deliver robust tissue-specific regeneration, this study sought to determine the potential of releasate to improve differentiation of doxorubicin treated myotubes. C2C12 were first grown to 80% confluency, then differentiated in differentiation media for 7 days either untreated or with 2 treatments of doxorubicin (day 5&6), or 2 treatments of doxorubicin and releasate (day5&6) (Figure 4A). Doxorubicin impaired myotube formation to an extent that very few large myotubes were seen and a much greater proportion of myotubes with an area below 6000μM^2 (Figure 6.3B,C). Untreated myotubes had an average area of more than twice that of doxorubicin treated myotubes, while cells treated with both doxorubicin and releasate had a wider spread of large and small fibres and an intermediate average size (figure 6.3).

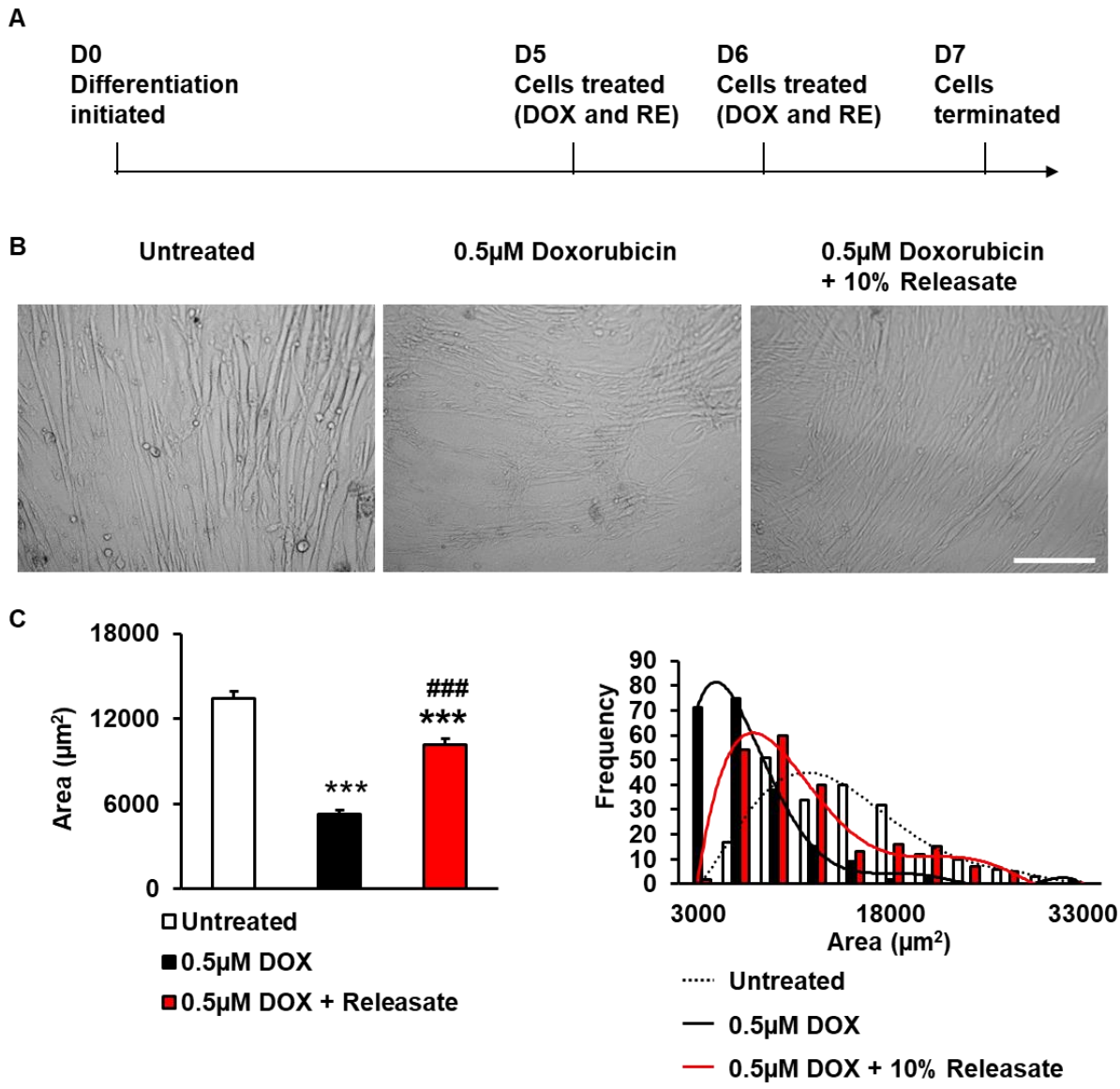

Figure 6.3. Myotube morphology of doxorubicin and releasate treated differentiating C2C12 cells. (A) Experimental setup: C2C12 seeded cells were seeded in growth media (GM) for 5 days before 5 days in differentiation media, then two treatments of 0.5μM doxorubicin (DOX) and 2 treatments of 10% releasate on consecutive days, changing media on the second day. (B) Morphometrics displaying myotubes in untreated, DOX, and DOX + Releasate groups. Scale bar 200μm, x10 magnification. (C) Quantification of myotube area, data are mean±SEM n=213. Statistical analysis was performed by one-way ANOVA followed by tukey's post-hoc test. Differences are *p<0.05 **p<0.01 ***p<0.001 vs the control group.

To further improve the differentiation capacity of C2C12 cells, the differentiation experiment was repeated with increased releasate treatment. Cells were this time

issued 3 releasate treatments (D2,3,4), and 2 DOX treatments (D3,4), earlier in the differentiation phase (timeline: figure 6.4A). This yielded normalised morphology of myotubes (10022µm^2 untreated vs 9545µm^2 DOX + Releasate) when comparing releasate and DOX to DOX alone (3705µm^2) (Figure 6.4B,C). Cells were then also stained for myogenin to determine the fusion index, doxorubicin treated cells had significantly lower fusion index by 33.7% and platelet releasate entirely rescued this condition, indicating that releasate reverses the impaired effects of doxorubicin on myoblast differentiation (Figure 6.4D). These data indicate that while proliferation of myoblasts is not improved by platelet releasate, the differentiation of myotubes is improved by releasate.

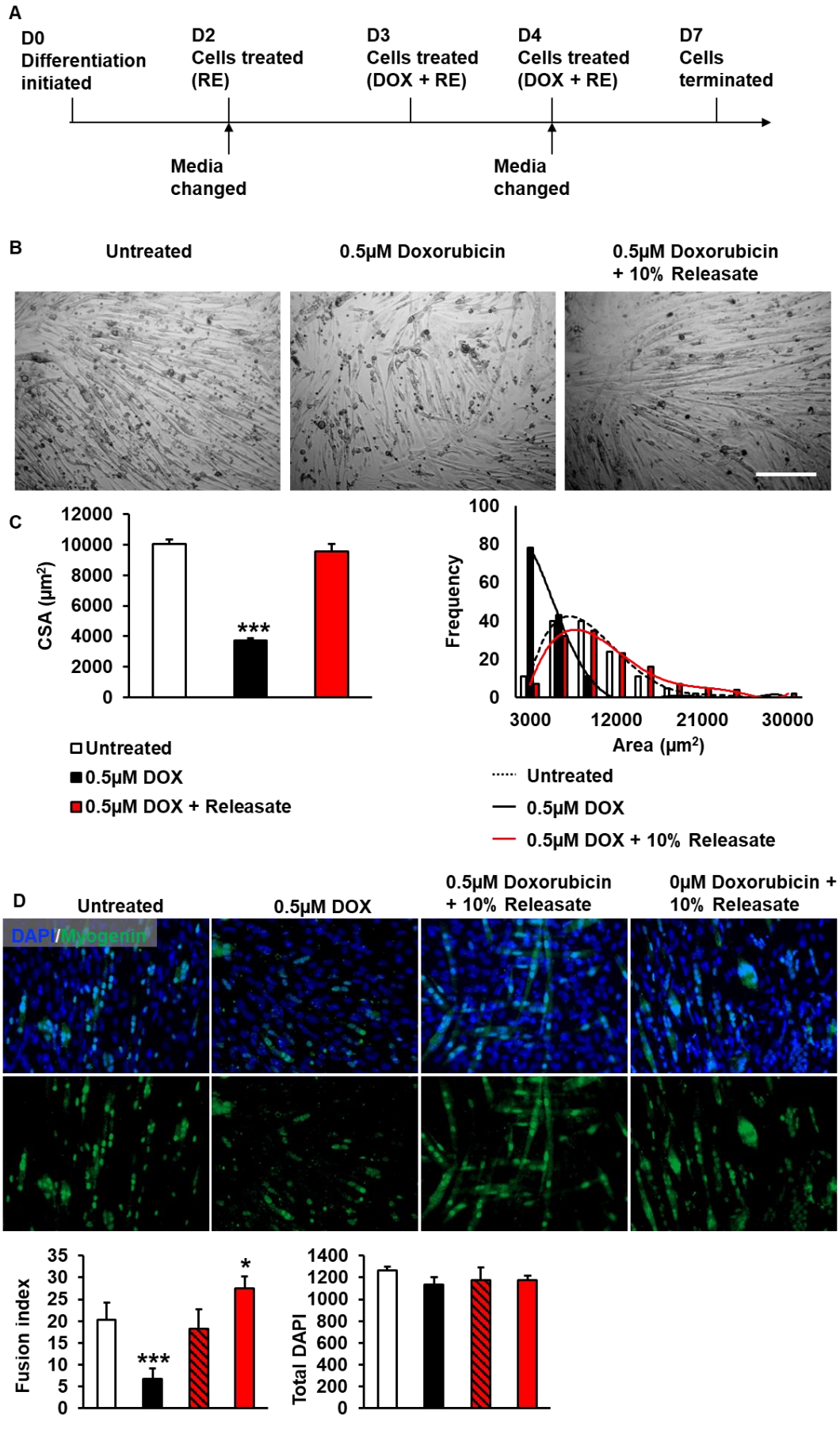
A
D0
Differentiation
initiated
D2
Cells treated
(RE)
D3
Cells treated
(DOX + RE)
D4
Cells treated
(DOX + RE)
D7
Cells
terminated
Media
changed
Media
changed
B
Untreated
0.5μM Doxorubicin
0.5μM Doxorubicin
+ 10% Releasate
C
CSA (μm²)
12000
10000
8000
6000
4000
2000
0
***
Untreated
0.5μM DOX
0.5μM DOX + Releasate
Frequency
100
80
60
40
20
0
3000
12000
21000
30000
Area (μm²)
Untreated
0.5μM DOX
0.5μM DOX + 10% Releasate
D
Untreated
0.5μM DOX
0.5μM Doxorubicin
+ 10% Releasate
0μM Doxorubicin +
10% Releasate
DAPI/Mybogenin
Fusion index
35
30
25
20
15
10
5
0
***
*
Total DAPI
1400
1200
1000
800
600
400
200
0

Figure 6.4. Pretreatment of releasate further improves myotube morphology. (A) Experimental setup: C2C12 seeded cells were seeded in growth media (GM) for 5 days before 3 days in differentiation media. Cells were then treated with 10% releasate on 3 consecutive days, with a treatment of 0.5µM doxorubicin (DOX) on the second day of releasate treatment. On the third day, media was replaced with fresh differentiation media and 0.5µM DOX. Cells were imaged and collected after 7 days of differentiation. (B) Morphometrics displaying myotubes in untreated, DOX, and DOX + Releasate groups. Scale bar 200µm, x10 magnification. (C) Quantification of myotube area. data are mean±SEM n=150. (D) Fibres were stained for myogenin, and fusion index and total nuclei were quantified. Statistical analysis was performed by one-way ANOVA followed by tukey's post-hoc test. Differences are *p<0.05 **p<0.01 ***p<0.001 vs the control group.

6.3.4 Gene expression is altered in senescent C2C12 cells, releasate does not resolve.

As the capacity for differentiation was significantly reduced by DOX, and releasate was able to improve this deficit, the work next sought to determine the impact of DOX on gene expression and whether the addition of releasate impacts gene expression itself or is alone sufficient to improve differentiation through addition of key factors. To this aim, C2C12 at 80% confluency were differentiated for 7 days and received DOX and releasate treatment on D5 and D6. After differentiation, mRNA was extracted from myotubes and gene expression analysis was performed for muscle stem cell fate (MyoD, Myogenin, Scrib1 and Myf6), fusion genes (Bex1, tmem8c, srf), contractile proteins (Mhc1, Mhc2a, Acta1), and growth factors of releasate (Vascular endothelial growth factor a 165 (VEGFa165), PDGFa, PDGFb, VEGFR1) were performed. Expression of growth factors from releasate all significantly increased after releasate treatment. A stark drop in expression of all muscle stem cell fate related genes was detected in myotubes harvested from DOX treated cells, while releasate did not significantly recover this. Furthermore, fusion genes were decreased by DOX treatment, though releasate did not reverse this effect. Surprisingly no significant differences were detected in contractile proteins mhc1, mhc2a and acta1. These findings indicate that differentiation and fusion are impaired at a transcriptional level by doxorubicin, and while releasate improves differentiation the transcriptional profile of C2C12 cells is not altered which could be due to DNA damage.

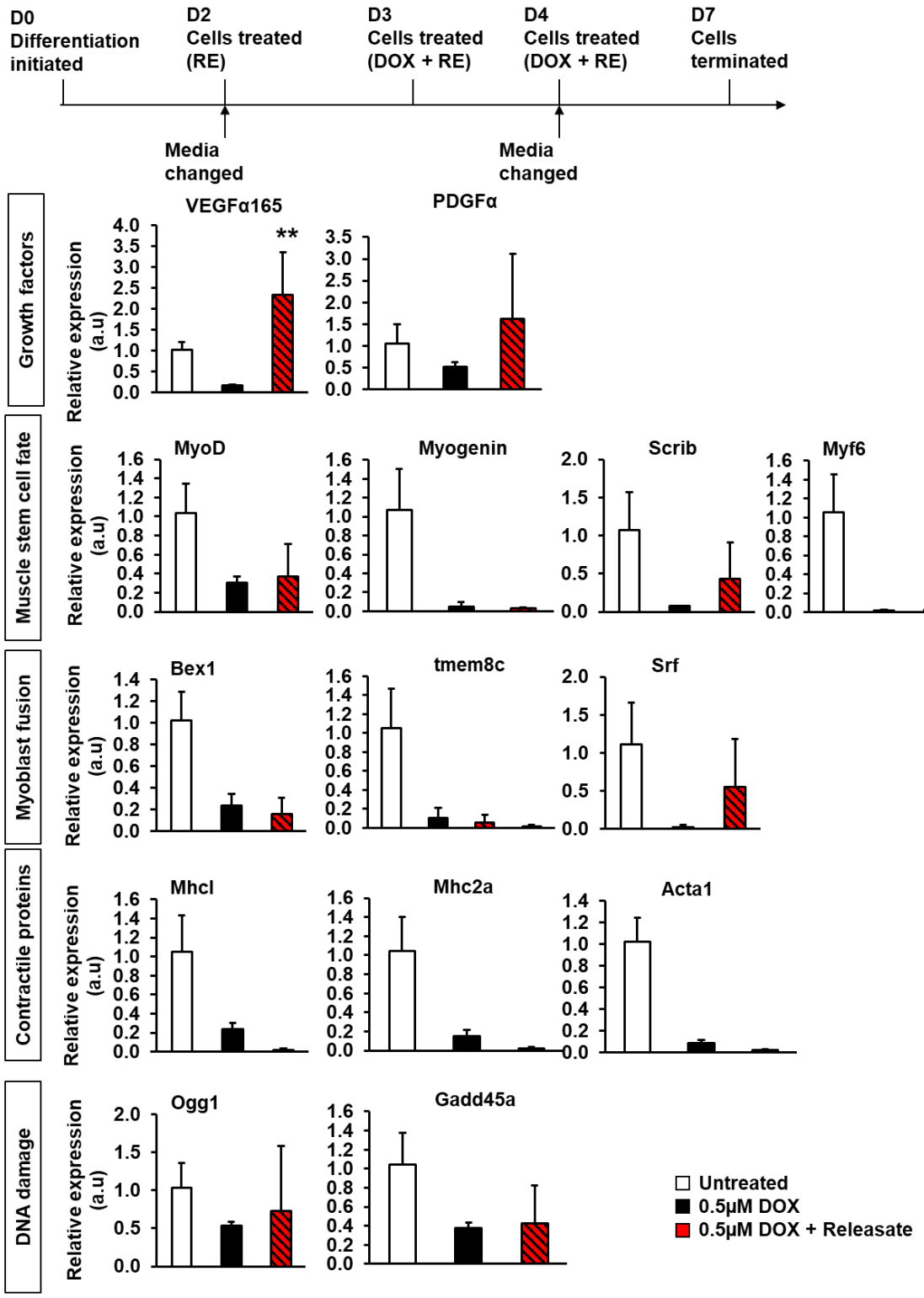

Figure 6.5. Gene expression patterns in differentiating C2C12 myotubes. Quantifications of mRNA levels of genes involved in differentiation and muscle stem cell fate (MyoD, Myogenin, Myf6, and Scrib1), myoblast fusion (Bex1, Tmem8c and Srf), contractile proteins (Mhc1, Mhc2a, and Acta1), and DNA damage (Oxoguanosine

DNA glycosylase 1 (OGG1), gadd45a) were assessed in differentiating C2C12 cells treated with doxorubicin and releasate by qPCR. Data are shown as mean±SD (n=6 technical replicates). Statistical analysis was performed by one way ANOVA with *p<0.05, **p<0.01 vs untreated.

6.3.5 Senescence induced in differentiating C2C12 by DOX can be alleviated by releasate

The effects of doxorubicin and releasate on C2C12 cell function were evident in proliferation and differentiation assays, so the following research sought to determine the impact of releasate on doxorubicin induced senescence. Cells were differentiated for 7 days and treated 3 times with 0.5µM releasate (D2,3,4), and twice with DOX (D3,4). Doxorubicin induced senescence in C2C12 cells detected by β-galactosidase staining (figure 6.5B), the average area of β-galactosidase per unit area decreased by 82.7% (22µm^2 DOX vs 3.8µm^2 releasate) in response to platelet releasate. This indicates that releasate can be used to prevent cellular senescence.

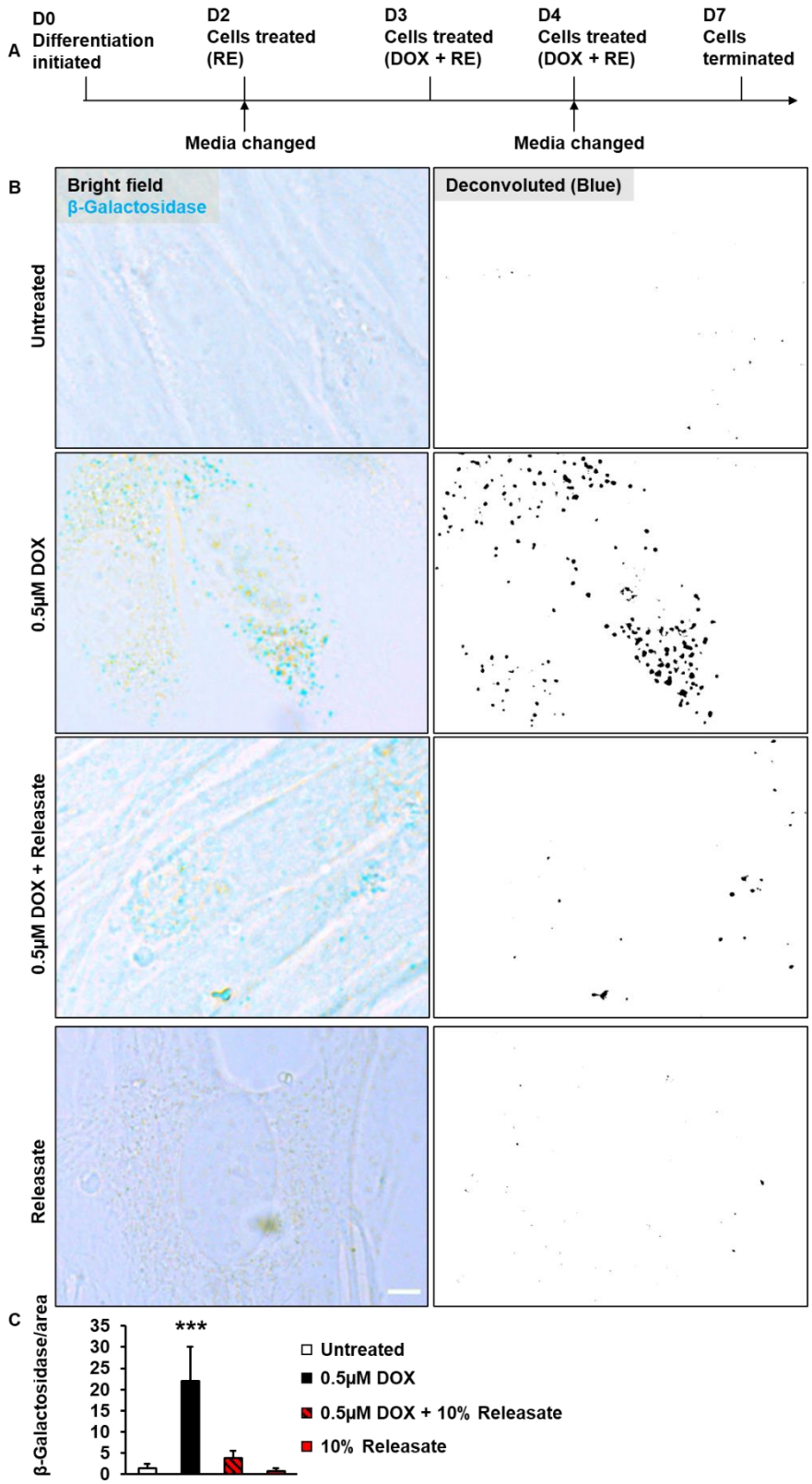

Figure 6.6. Senescence-associated β-galactosidase in differentiated C2C12 cells. (**A**) Experimental setup: C2C12 seeded cells were seeded in growth media (GM) for 5 days before 3 days in differentiation media. Cells were then treated with 10% releasate

on 3 consecutive days, with a treatment of 0.5µM doxorubicin (DOX) on the second day of releasate treatment. On the third day, media was replaced with fresh differentiation media and 0.5µM DOX. Cells were collected and stained for senescence associated β-galactosidase after 7 days of differentiation. (**B**) Bright field images of senescence associated β-galactosidase are presented alongside deconvoluted images of blue staining to provide a clear contrast. (**C**) Quantification of area of senescence associated β-galactosidase staining per image. n=12 scale bar = 5µm

6.3.6 DNA damage and DNA repair mechanisms induced by doxorubicin in C2C12 cells

Due to the effects of doxorubicin on DNA, the present work sought to determine the extent of DNA damage in C2C12 cells treated with doxorubicin and the potential impact of releasate to alleviate this. Cells were cultured for 48h, treated with DOX when seeded (0h) and treated with releasate twice (0h,24h) (timeline: figure 6.6A). Cells were then harvested and stained for H2AX - an indicator of DNA damage when nuclei have a greater number of foci, and p53 – an indicator of DNA repair mechanisms, both of which are increased on DOX treatment (Figure 6.6B). Each individual foci of H2AX indicates a double strand break, and overall fluorescence intensity isn't expected to vary, therefore H2AX foci were counted per nucleus to determine the extent of DNA damage in cultured cells. DOX increased average foci per nucleus number from 7±0.67 to 55±3.7, significantly inducing DNA damage. Treatment with releasate however, partially rescued the DNA damage, resulting in an average of 36.4±1.66 foci per nucleus. A low level of H2AX staining is to be expected, therefore the level of rescue may be enough reduce significant impairments (Mah et al., 2010). Similarly, p53 in significantly induced by DOX, with a 46% increase in fluorescence intensity, while releasate reduces this to merely 16% (346±11.4 in untreated vs 508±19.7 in Doxorubicin and 404±15.65 in doxorubicin + releasate). As DNA repair mechanisms are reduced by releasate as well as DNA damage, these data indicate that releasate resolves the cellular impairment and the impact of DOX on DNA damage is reduced.

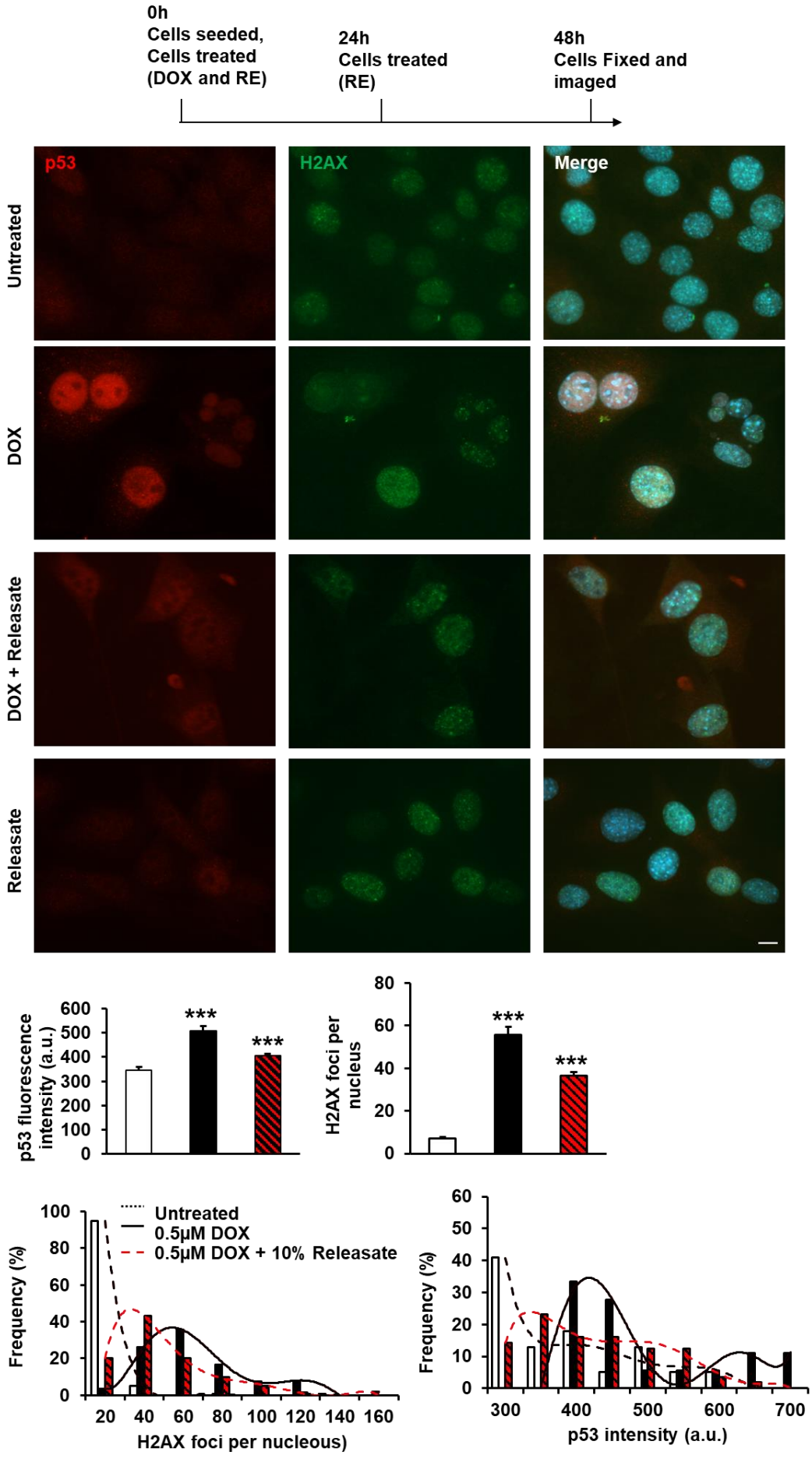
0h
Cells seeded,
Cells treated
(DOX and RE)
24h
Cells treated
(RE)
48h
Cells Fixed and
imaged
p53
H2AX
Merge
Untreated
DOX
DOX + Releasate
Releasate
p53 fluorescence intensity (a.u.)
H2AX foci per nucleus
***
Untreated
0.5μM DOX
0.5μM DOX + 10% Releasate
Frequency (%)
H2AX foci per nucleous)
p53 intensity (a.u.)

Figure 6.7. senescence and DNA damage in C2C12 cells. (**A**) experimental setup: C2C12 seeded cells were seeded in growth media (GM) for 2 days, with one treatment of 0.5µM doxorubicin (DOX) when seeded and 2 treatments of 10% releasate on consecutive days. (**B**) C2C12 cells were proliferated for 2 days with either doxorubicin treatment, releasate treatment or both. DNA damage and senescence were detected via H2AX and p53 staining respectively. (100x magnification, 10µm) (**C**) Quantification of number of H2AX foci and p53 fluorescence. Data are mean±SEM n=100. Statistical analysis was performed by Two way ANOVA and tukey post-hoc test. ***p<0.001 vs all other groups.

6.3.7 DNA damage and repair in C2C12 cells

Given the DNA damage and reduced proliferation seen in differentiating myotubes and proliferating cells respectively, the protein expression of H2AX, p21 and p53 was determined in differentiating C2C12 cells treated with DOX and releasate. C2C12 cells were seeded in growth media for 5 days before 5 days in differentiation media, then two treatments of 0.5µM DOX and 2 treatments of 10% releasate on consecutive days, changing media on the second day (figure 6.7A). DOX induced H2AX expression by 244% and releasate reduced this treatment to only 166%. DOX induced no significant changes in either p21 or p53 expression. These data indicate that DOX induces DNA damage and arrests proliferation, while releasate partially improves this on a protein level.

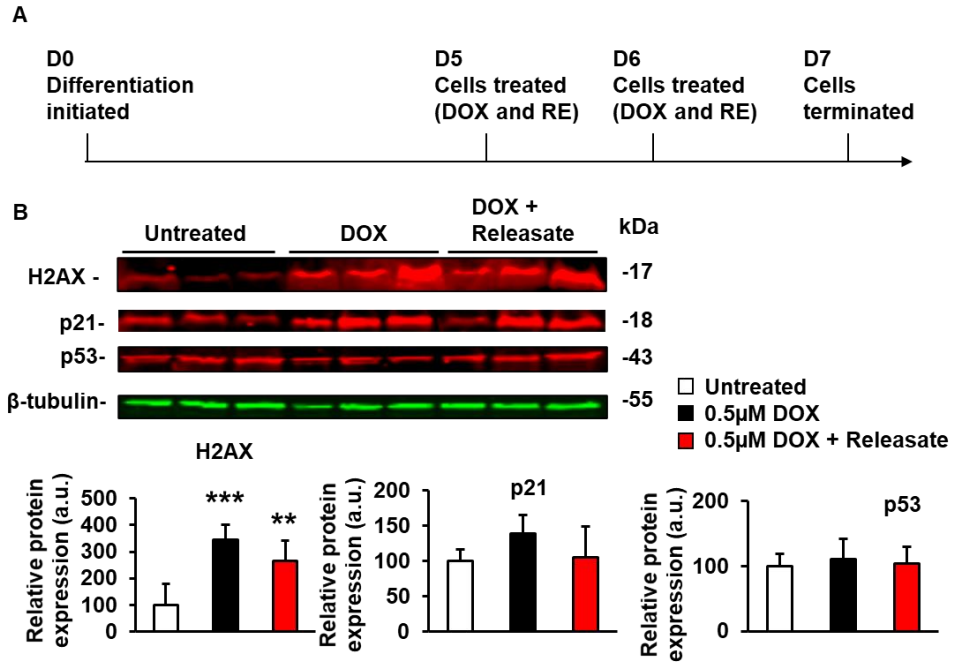

Figure 6.8. Senescence induced proteins are partially alleviated by releasate. (**A**) Experimental setup: C2C12 seeded cells were seeded in growth media (GM) for 5 days before 5 days in differentiation media, then two treatments of 0.5μM doxorubicin (DOX) and 2 treatments of 10% releasate on consecutive days, changing media on the second day. (**B**) Western blots and quantification of H2AX, p21 and p53 in C2C12 cells. N=6, **p<0.01, ***p<0.001 vs control.

6.3.9 p21 – an inhibitor of cyclin dependent kinase is upregulated in muscle tissue by DOX and alleviated by releasate

To further determine the level of DNA damage induced by DOX p21 expression in muscle sections was determined. P21 promotes cell cycle arrest in response to a number of stimuli. WT and ApoE$^{-/-}$ mice were administered a 20mg/kg cumulative dose doxorubicin over 17 days in 4 independent doses of 5mg/kg, and those receiving releasate were administered 100μl releasate. Mice were then sacrificed and hindlimbs dissected, TA muscles were frozen in liquid nitrogen, sectioned, and stained for p21. The percentage of p21 expressing nuclei increased from 13.6% in the untreated WT mouse to 66.6% in the DOX treated mouse, while mice treated with both DOX and releasate expressed p21 in 28.4% of their nuclei. For the ApoE$^{-/-}$ mouse, without treatment 37% of nuclei expressed p21, the DOX treated ApoE$^{-/-}$ mouse expressed p21 in 58% and the ApoE$^{-/-}$ mouse receiving both treatments expressed p21 in 20.8%

of nuclei. The anti-proliferative effects of DOX include induction of p21 expression in WT and ApoE TA muscle, while platelet releasate reverses this action. The ApoE$^{-/-}$ mouse expressed p21 in a greater percentage of nuclei than the WT, which corroborates the impaired proliferation of ApoE$^{-/-}$ muscle stem cells as reported in Chapter 3 and by Barlow et al. (Barlow et al., 2021). These data indicate that DOX does in fact induce anti-proliferative factors in the mouse muscle, and that releasate treatment can alleviate this effect, to potentially allow for muscle stem cell proliferation.

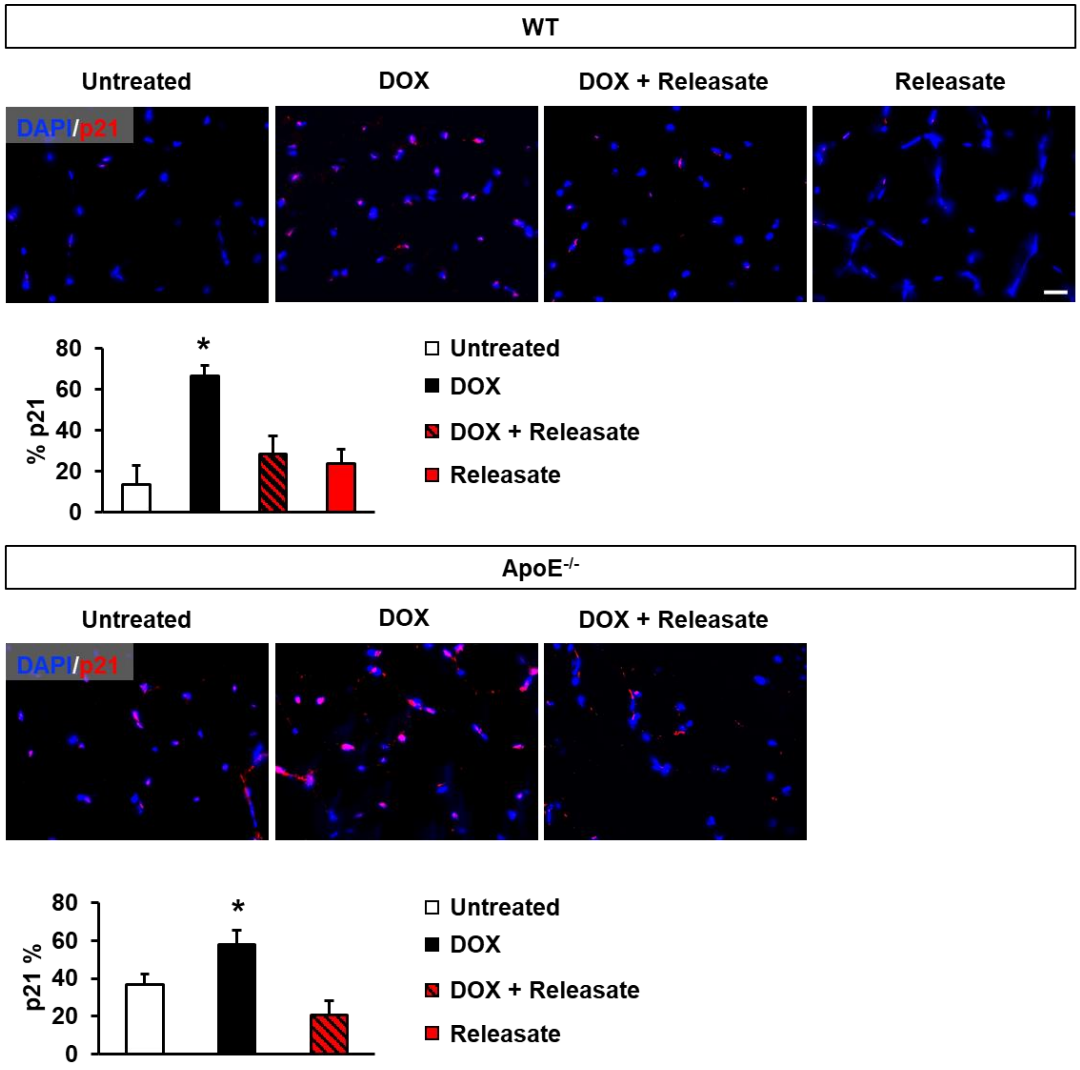

Figure 6.9. Senescence induced by Doxorubicin is alleviated by platelet releasate. P21 staining in TA muscle of mice injected with doxorubicin, releasate or both (x40 magnification, Scale bar 20µm). Quantification of the percentage of p21 positive nuclei. *p<0.05 vs all other groups.

6.3.10 Muscle and body weights of WT and ApoE mice with and without releasate

To determine the effects of platelet releasate on the muscle of WT and ApoE$^{-/-}$ mice, mice were administered a 100µl dose of human releasate by intraperitoneal injection on the day of injury and twice subsequently – one- and three-days post injury. Body weights and muscle weights were recorded after 5, 10 and 14 days. At 5 days releasate made no significant differences in relative muscle weight, however injury made a significant impact on the relative weights of TA muscle in all groupsFigure 6.10). By day 10 the effect of injury on muscle weights was reduced, but still significant in the wild type muscles alone. At day 14 there were no significant differences detected in relative muscle weight in any group.

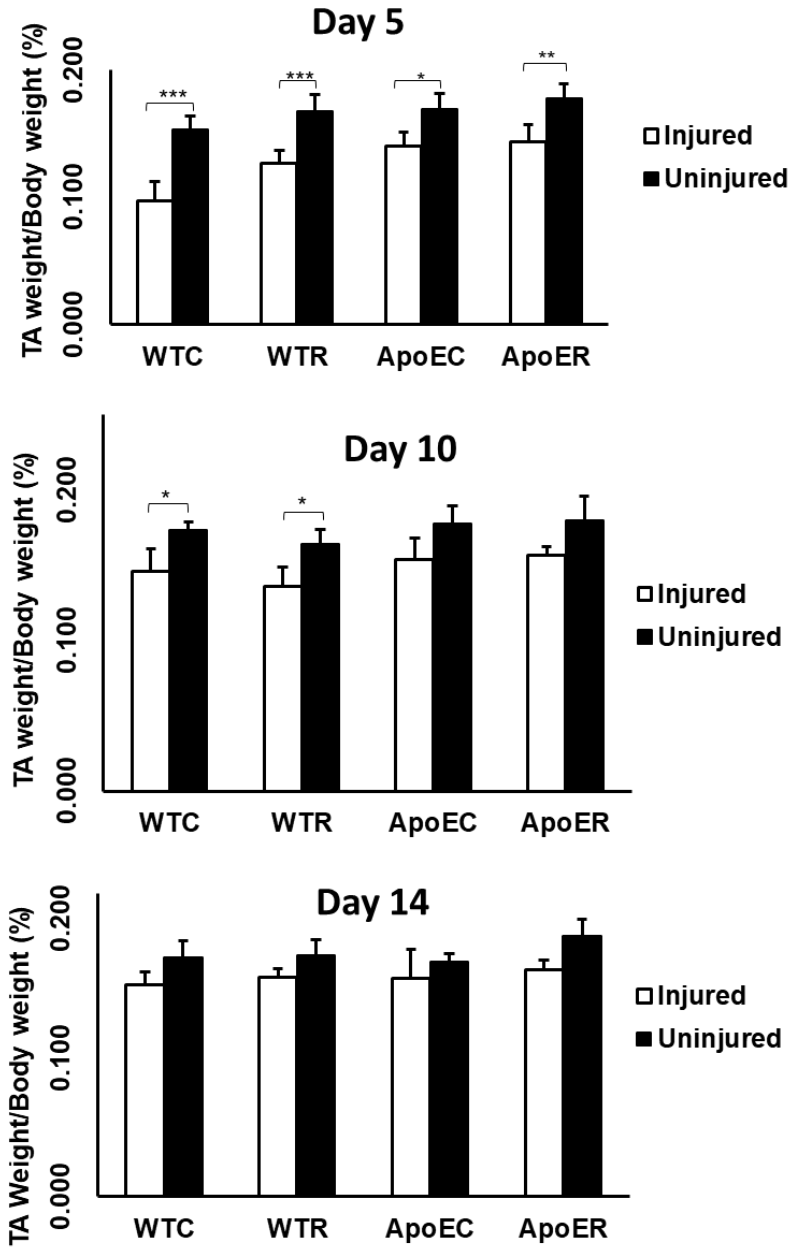

Figure 6.10 Relative weight of mouse TA muscle. Relative weight of mouse TA muscle as a percentage of full body weight in WT and ApoE$^{-/-}$ mice with or without releasate treatment including the injured and the uninjured muscle. Data are expressed as mean ± SD (n=6 per group). Statistical analysis was performed by two-way ANOVA, *p<0.05, **p<0.01, **p<0.001.

6.3.11 Protein synthesis in Quadriceps and Heart of wild type mice with and without releasate

To further determine the effects of platelet releasate on WT mice, western blotting studies on the quadriceps and heart of mice administered releasate to determine if this resulted in changes in protein synthesis. Puromycin is incorporated into the nascent polypeptide chain of newly synthesized proteins in the sunset method, therefore in detecting the puromycin content of mice, it is possible to determine the rate of mRNA translation. Puromycin content was not significantly different between treated and untreated mice in the quadriceps and heart, therefore AKT and S6 phosphorylation were detected in the quadriceps and AKT phosphorylation was detected in the heart. These experiments also saw no significant difference in expression; therefore, these data indicate that platelet releasate does not significantly alter protein synthesis or signaling pathways important to muscle stem cell function are not significantly altered.

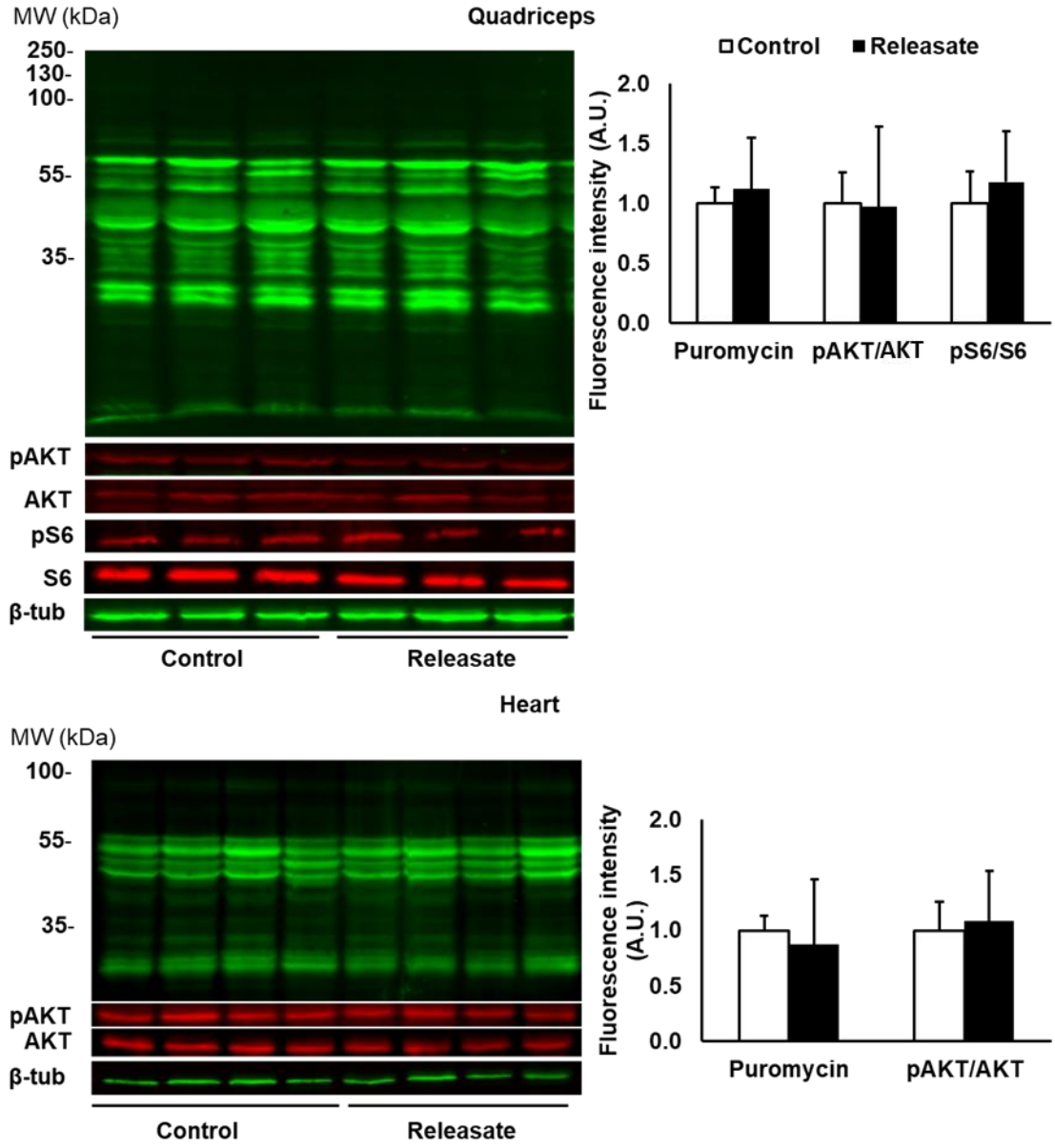

Figure 6.11 Protein synthesis in Quadriceps and Heart. Protein synthesis was detected in wild type mice with and without releasate treatment via the SUnSET method and determining the expression of Puromycin in the quadriceps and heart. Furthermore pAKT, AKT pS6 and S6 levels were detected.

6.3.12 Doxorubicin induced senescence in ApoE$^{-/-}$ mice is alleviated by releasate injection.

Given the compromised proliferation of both *ex vivo* and cultured satellite cells of ApoE$^{-/-}$ mouse muscles (chapter 3), the following work aimed to determine the impact of doxorubicin induced senescence on the expression patterns of transcriptional factors and myogenic regulatory factors involved in myogenic progression of skeletal

muscle stem cells. Single fibres were isolated from ApoE$^{-/-}$ mice which had been treated with doxorubicin, and cultured for up to 72 hours, fibres were fixed and stained for Pax7 at T0, Pax7 and MyoD at T24 and T48 and Pax7 and Myogenin at T72. Releasate treated fibres were found to express less Pax7 and more myogenin than those with only Doxorubicin. Releasate increases average number of SCs, but not to levels of untreated ApoE$^{-/-}$ fibres, as seen in Figure 6.12C. As reported previously in muscle stem cells of ApoE$^{-/-}$ single fibres, these stem cells proliferate to the same level of WT after 72h, so it is unlikely that the ApoE$^{-/-}$ genotype contributes to senescence (Barlow et al). ApoE$^{-/-}$ muscle stem cells exhibited altered exhibition patterns when treated with doxorubicin, significantly fewer muscle stem cells became activated at 24h (Pax7^{+ve}/Myod^{+ve}) by 30.4% (74.752%±2.8 in control vs 52.1±6.0 in doxorubicin treated and 75.5±6.2 in doxorubicin + releasate treated, figure 6.12). Similarly, at T48 a significantly greater amount of muscle stem cells by 25.1% were activated or proliferating (MyoD^{+ve}) when not treated with doxorubicin (93.0%±1.0) than those treated with doxorubicin (69.7%±4.3) and the releasate treatment reversed this almost entirely (90.4%±3.5). The expression of Pax7^{-ve}MyoD^{+ve} cells however was significantly increased by releasate treatment (21.9%±4.1 for doxorubicin vs 38.9%±5.0 for doxorubicin + releasate). This indicates that releasate disposes satellite cells towards activation. At T72, doxorubicin treated ApoE$^{-/-}$ muscle stem cells exhibited a differential pattern of myogenin expression compared to untreated ApoE$^{-/-}$ muscle stem cells. Skeletal muscle stem cells from doxorubicin treated ApoE$^{-/-}$ mice had a significantly lower level of myogenin by 65.02% compared to untreated, and partially alleviated by releasate(56.52%±1.8 for untreated vs 19.77%±3.0 for doxorubicin treated vs 41.2%±3.8 for doxorubicin + releasate). Taken together these data indicate that doxorubicin impairs both the proliferation and differentiation of skeletal muscle stem cells, and while the expression patterns appear to be rescued by releasate, the proliferation does not continue to the same extent.

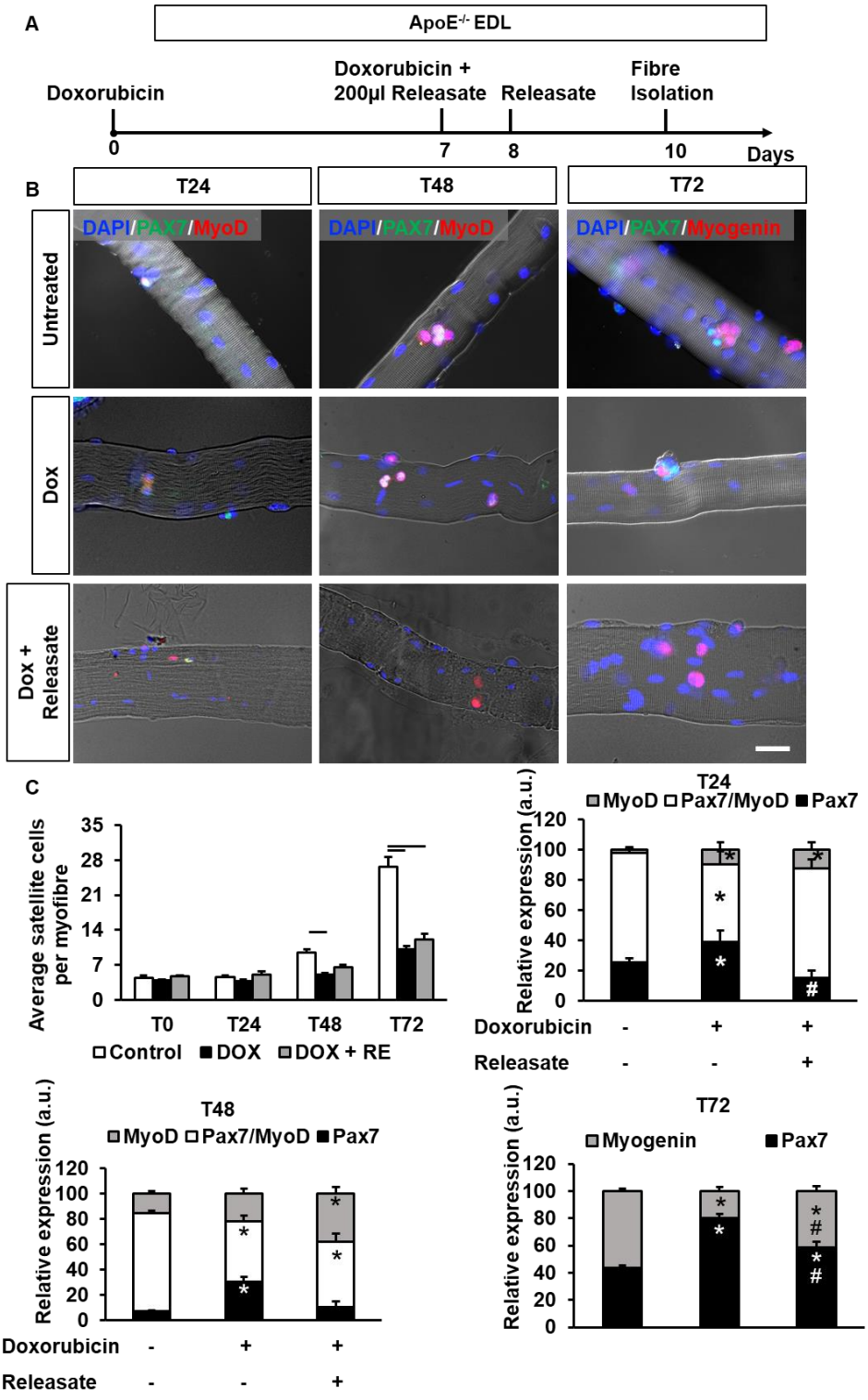

Figure 6.12. Doxorubicin induced senescence is alleviated by platelet releasate in ApoE$^{-/-}$ mouse single fibres of the extensor digitorum longus (EDL). Single fibres of ApoE$^{-/-}$ mice with increased senescence may be rescued by platelet releasate. (A) Experimental timeline. ApoE-/- mice were injected with doxorubicin, after 7 days mice were again injected with doxorubicin, injured with CTX and injected with releasate. 1

day post injury mice were injected again with releasate, and muscles were taken 3 days post injury. Single myofibres were isolated from the EDL muscle and studied at T24, T48 and T72 hours, to determine quiescent, proliferating and differentiating satellite cells, by means of Pax7 and Myogenin staining. (B) Representative images of immunofluorescent detection of Pax 7 and Myogenin (x40 magnification, scale bar=200µm). (C) Relative quantification of expression of Pax7 and Myogenin. Data are mean±SEM n=40. Statistical analysis was performed by Two way ANOVA and bonferroni post-hoc test. *p<0.05, ***p<0.001 vs Doxorubicin treated.

The same battery of experiments was performed for the biceps brachii to corroborate and strengthen this data. Similar to the EDL, $ApoE^{-/-}$ muscle stem cells of the biceps brachii exhibited altered exhibition patterns when treated with doxorubicin, significantly fewer muscle stem cells became activated ($Pax7^{+ve}$/$Myod^{+ve}$) by 39.2% (68.52%±2.81 in control vs 41.67%±5.78 in doxorubicin treated and 62.48±4.84 in doxorubicin + releasate treated). Similarly, at T48 a significantly greater amount of muscle stem cells by 25.1% were activated or proliferating ($MyoD^{+ve}$) when not treated with doxorubicin (93.7%±1.1) than those treated with doxorubicin (72.3%±6.9) and the releasate treatment reversed this almost entirely (85.45%±2.8). The expression of $Pax7^{-ve}MyoD^{+ve}$ cells however was significantly increased by releasate treatment (20.36%±4.5 for doxorubicin vs 37.2%±5.15 for doxorubicin + releasate). This indicates that releasate disposes satellite cells towards activation. At T72, doxorubicin treated $ApoE^{-/-}$ muscle stem cells exhibited a differential pattern of myogenin expression compared to untreated $ApoE^{-/-}$ muscle stem cells. Skeletal muscle stem cells from doxorubicin treated $ApoE^{-/-}$ mice had a significantly lower level of myogenin by 62.8% compared to untreated, and partially alleviated by releasate (63.67%±2.1 for untreated vs 23.69%±2.7 for doxorubicin treated vs 43.9%±2.4 for doxorubicin + releasate). Taken together these data closely resemble evidence provided in the EDL and further demonstrate the impaired proliferation and differentiation impairments induced by doxorubicin injection into the mouse. These data further indicate that platelet releasate can be of use to treat myopathy in patients receiving doxorubicin as it proved beneficial to expression of transcription factors regulating proliferation and differentiation.

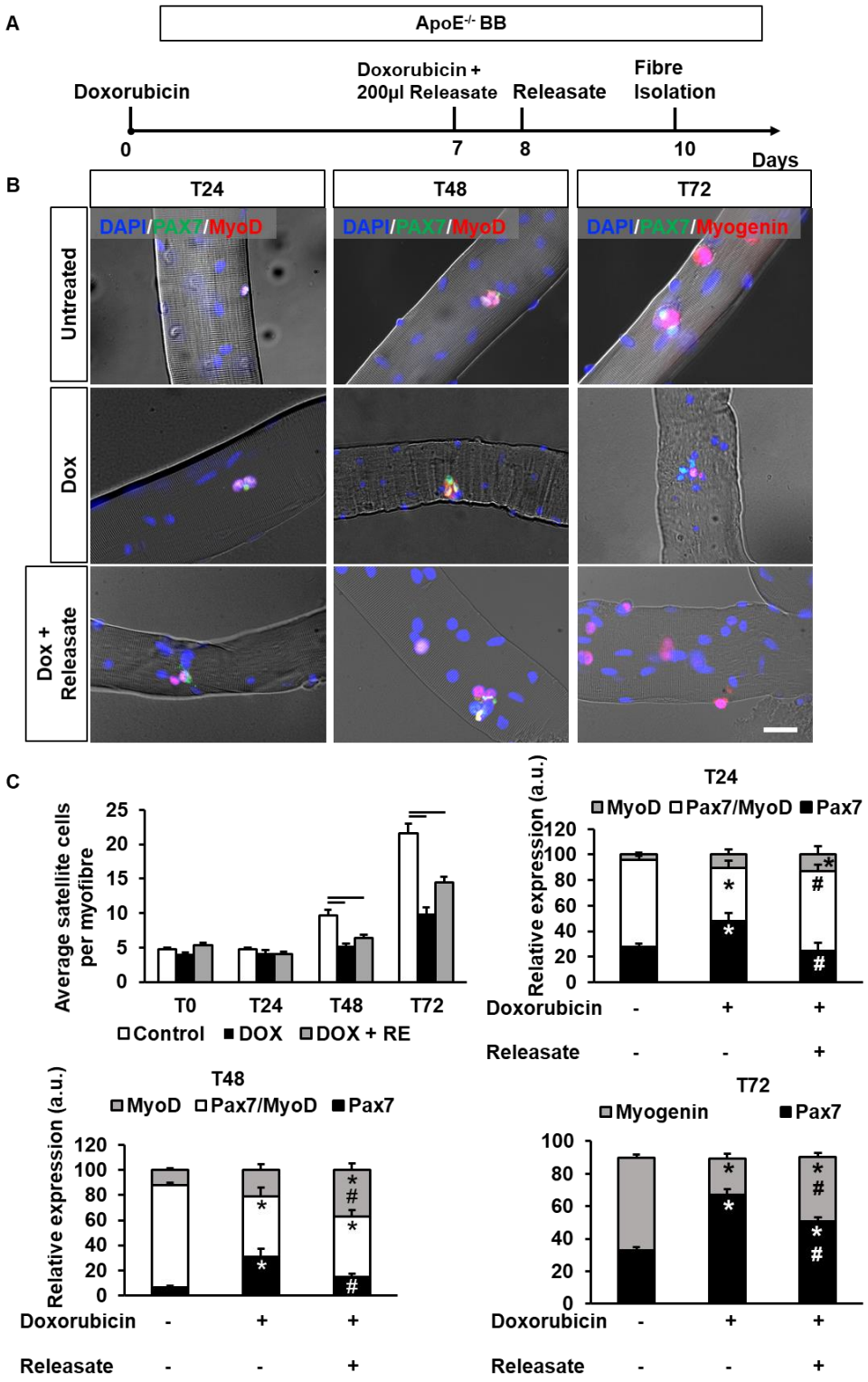

Figure 6.13. Doxorubicin induced senescence is alleviated by platelet releasate in ApoE$^{-/-}$ mouse single fibres of biceps brachii. (**A**) Experimental timeline. ApoE$^{-/-}$ mice were injected with doxorubicin, after 7days mice were again injected with doxorubicin, injured with CTX and injected with releasate. 1 day post injury mice were injected again with releasate and muscles were taken 3 days post injury. Single myofibres were

isolated from the biceps brachii muscle and studied at T24, T48 and T72 hours, to determine quiescent, proliferating and differentiating satellite cells, by means of Pax7 and Myogenin staining. (**B**) Representative images of immunofluorescent detection of Pax 7 and Myogenin (x40 magnification, scale bar=200µm). (**C**) Relative quantification of expression of Pax7 and Myogenin. Data are mean±SEM n=40. Statistical analysis was performed by Two way ANOVA and bonferroni post-hoc test. *p<0.05, **p<0.01, ***p<0.001 vs Doxorubicin treated.

6.5 Discussion

Skeletal muscle stem cells maintain quiescence throughout adult life until activated (generally by injury) allowing skeletal muscle to repair and regenerate when necessary, however the crossover between the pathways between differentiation and senescence makes muscle stem cells susceptible to senescence – which makes the necessary state of quiescence irreversible (Sincennes et al., 2021; Sousa-Victor et al., 2014).

Doxorubicin is a cancer treatment, which causes cytotoxicity, is linked with myopathy, and dysfunction of skeletal muscle(Bielack et al., 1989; Courneya et al., 2003; DeFina et al., 2016). Doxorubicin induces senescence in rat cardiomyocytes, skeletal muscle, and fibroblasts, however low doses of doxorubicin (10nM) proved to be not enough to significantly increase senescence-associated eta-galactosidase (Casella et al., 2019; Gibson et al., 2014; Piechota et al., 2016; Spallarossa et al., 2009). The present work therefore sought to determine the dose necessary to induce senescence in C2C12 myoblasts. Figure 6.1 demonstrates how senescence is induced by cancer treatment doxorubicin in myoblasts. Surprisingly, higher concentrations of doxorubicin yielded lower levels of senescence-associated β-galactosidase, so trypan blue dye was used to detect cell death which became elevated at higher concentrations of doxorubicin. The present study further develops the picture of senescence in myoblasts as doxorubicin treatment entirely halts proliferation – however platelet releasate marginally improves proliferation (figure 6.2 – proliferation determined via EdU stain). These data suggest that doxorubicin induces senescence and releasate can partially reverse it. Platelet releasate includes several pro-proliferative factors including VEGF, PDGF, which could contribute to the partial improvement in proliferation, however doxorubicin effectively halts proliferation and releasate only has a minor effect.

Differentiation is also impaired by doxorubicin, this work found that myotubes formed in DOX treated C2C12s had a greatly reduced surface area compared to untreated – indicating that senescence pathways prevent proper differentiation pathways. Furthermore, doxorubicin greatly reduces the fusion index of differentiating myotubes, while releasate restores it, as seen in figure 6.3. As p53 is induced by both doxorubicin and ROS, and p53 directly represses transcription of myogenin, this suggests that doxorubicin acts to arrest the cell cycle through p53, which in turn prevents myogenin expression, impairing muscle stem cell differentiation. Platelet releaste however,

entirely restores differentiation. These data indicate that while proliferation of myoblasts is not improved by platelet releasate, the differentiation of myotubes is improved by releasate. This is not entirely unexpected, as doxorubicin is used to directly prevent proliferation, and proliferation must halt before differentiation begins, therefore it is likely that doxorubicin disrupts fusion pathways, while releasate is able to restore them.

The present work further develops this by showing that stem cell fate and fusion genes expression are impaired by doxorubicin, however releasate does not ameliorate the expression. This indicates that the improved differentiation capacity is due to exogenous application of releasate rather than changes in gene expression. Growth factors found in releasate may be acting downstream of cell fate and fusion genes. Gene expression is reduced by doxorubicin and not restores via releasate, this is likely due to excessive DNA damage which prevents cells from being transcriptionally active.

Having developed an understanding of the effects of senescence in C2C12 myoblasts, the following work sought to determine the effect of releasate on senescence per se. Senescence-associated-beta-galactosidase levels were determined in doxorubicin and releasate treated C2C12 myotubes, resulting in a decrease of senescence in response to releasate. This indicates that the reduction in proliferation in C2C12 cells by DOX is reversible and an adequate dose of releasate may be a potential treatment to reverse senescence. Previous evidence shows that senescence can be reversed by inactivation of the p53, p16 and retinoblastoma protein pathway, furthermore, senescent cells are able to renter the cell cycle in cells with up-regulated survivin – which is the smallest member of the human inhibitor of apoptosis protein family and associates with Cdc2/Cdk1 to re-enter the cell cycle as a determinant of cancer therapy resistance (Beauséjour et al., 2003; Wang et al., 2011). These data indicate that senescence can be reversible, however Beauséjour et al. determined that though cells re-entered the cell cycle, those expressing high levels of p16 did entered the cell cycle without growth – this could be an example of why proliferation is entirely prevented by doxorubicin, but differentiation can be restored (Beauséjour et al., 2003).

As doxorubicin is purported to function by DNA fragmentation, the present work sought to determine the extent of DNA damage and DNA repair mechanism(Silva et al., 2017;

Yang et al., 2014). Increased p53 staining demonstrates that DNA repair mechanisms are upregulated in response to doxorubicin treatment. The DNA damage and repair in C2C12 merited further study, therefore, to determine the influence of DOX on a protein level, differentiated cells were treated with DOX for western blotting experiments. These protein experiments provided further evidence that DNA damage and repair are elevated in DOX treated cells, as well as DNA repair signals, with increases in H2AX, p21 and p53 protein levels. P53 also functions in repression of myogenin transcription, indicating that doxorubicin induced p53 mediated G1 arrest, while preventing differentiation – likely to reduce post-mitotic nuclear abnormalities, this contributes so skeletal muscle stem cell senescence (Yang et al., 2015). These pathways are suggested to increase time for cell repair, by arresting the cell cycle, allowing increased chances of survival. With greater levels of stress however, p53 facilitates increased levels of cellular stress by DNA fragmentation, this prevents aberrant cell proliferation, however caused unwanted cellular damage (Beyfuss and Hood, 2018). H2AX foci in these same experiments indicate that the level of overall DNA damage is greatly reduced by releasate. Our data indicates that releasate can be used to resolve the impact on DNA damage and allow p53 to function as intended in lower levels.

The present work next sought to determine the impact of doxorubicin and releasate on cell cycle arrest in WT and ApoE$^{-/-}$ mouse tibialis anterior muscle, by staining p21. In mice treated with DOX, cell cycle arrest was greatly increased, however releasate treatment reversed this, indicating that *in vivo* the effects of DOX on the cell cycle can be reversed by the tissue specific treatment of muscle with releasate, highlighting releasate as a potential treatment for myopathy in cancer. H2AX protein levels were also induced at protein level in C2C12 cells, indicating the expected levels of DNA damage, however they were not themselves alleviated by releasate. This may indicate that the beneficial effects of releasate do not protect from DNA damage, however p53 and p21 are not increased at a protein level, this may be due to DOX inducing too much cytotoxicity to turn on repair mechanisms. Other studies however have demonstrated that p53 is increased in iPSCs and human carcinoma cells treated with low doses of DOX, which could indicate that the double dose of DOX was in excess of this, inhibiting DNA repair mechanisms (Kannappan et al., 2018; Zurer et al., 2004).

The present study developed the potential use of platelet releasate by determining that releasate administration to the mouse *in vivo* has no significant effect on the relative weight of muscles alone, therefore it can be assumed that releasate treatment alone has no negative effects (i.e. muscle atrophy). Furthermore, protein expression was not significantly altered in the quadriceps or heart of mice treated with releasate *in vivo*.

In single fibres DOX irreversibly impaired proliferation for 72 hours, however the number of muscle stem cells at 72 hours were equivalent to untreated at 48 hours indicating a delayed recovery. Furthermore, the decreased expression of MyoD at 24 and 48 hours indicate an impaired ability of skeletal muscle stem cells to activate and therefore proliferate. This change in MyoD expression was reversed by releasate – indicating that releasate is enough to overcome the damage of DOX in some instances. Similarly, myogenin expression was greatly reduced by doxorubicin at T72, however releasate was able to restore myogenin expression. Taken together these data indicate that doxorubicin impairs both the proliferation and differentiation of skeletal muscle stem cells, and while the expression patterns appear to be rescued by releasate, the proliferation does not continue to the same extent.

6.5.1 Conclusions

This is the first study to investigate the impact of doxorubicin on senescence in skeletal muscle stem cells and its impact on myogenic function. This work provides evidence that muscle stem cells treated with doxorubicin have impaired capacity not only for proliferation but also for differentiation and proposes an autologous easily generated treatment to reduce these deficits. The present work demonstrates that doxorubicin not only increases senescence, but also induces DNA damage and results in upregulated DNA repair mechanisms, and the deleterious effects of doxorubicin are seen in impaired gene expression for muscle stem cell fate, myoblast fusion and contractile proteins. These results have implications based on the nonselective toxicity of cancer treatment doxorubicin and indicate that a tissue specific treatment of releasate may alleviate side effects in patients treated with doxorubicin.

Chapter 7-General Discussion

7.1 Overview

In skeletal muscle ApoE is required to contribute to lipoprotein homeostasis, and errors in lipoprotein homeostasis contribute to impaired hypertrophy signalling (Agergaard et al., 2021). ApoE is furthermore important to attenuate oxidative damage, and to promote myokine responses in response to high intensity interval training With increased ROS seen in skeletal muscle of ApoE deficient mice (Sfyri et al., 2018; Wang et al., 2021). Importantly, skeletal muscle ApoE deficiency is already known to cause impaired muscle healing after ischemia-reperfusion injury (Kang et al., 2008). In the ApoE deficient skeletal muscle, recent findings have shown a mild transition to oxidative myofibres, increased capillary density, increased intramyocellular fat content, increased oxidative stress, increased macrophage infiltration (inflammation) (Sfyri et al., 2018). Stem cell function of ApoE deficient skeletal muscle however remains to be studied.

The impaired skeletal muscle regeneration after injury in ApoE deficient mouse may be an indicator of skeletal muscle stem cell impairment. However, the function of skeletal muscle stem cells in ApoE deficient mice has not been studied in injury or independent of injury. Furthermore, the increased oxidative stress evident in skeletal muscle will likely have an impact upon muscle stem cells – which may use reactive oxygen species as an activator of proliferation, therefore it is not yet know whether the ApoE deficient muscle environment will impair stem cell function (Förstermann et al., 2017). Furthermore the ApoE deficient muscle is known to have increased intramyocellular fat content, and diet induced obesity has recently resulted in skeletal muscle stem cell function, therefore it can be assumed that impaired skeletal muscle stem cell function contributes to the impaired skeletal muscle regeneration in ApoE deficient mice(Verpoorten et al., 2020).

The purpose of this study was i) to investigate the effect of hyperlipidaemia on muscle stem cell function in proliferation and differentiation by using the atherosclerotic ApoE deficient mouse model, ii) to establish the function of skeletal muscle stem cells, their proliferative and differentiation capacity and the impact of oxidative stress in experimental hyperlipidaemia, using palmitate to induce experimental hyperlipidaemia, iii) to determine the extent to which hyperlipidaemia impairs skeletal muscle repair after muscle injury in the ApoE deficient model, iv) to examine if treatment with an autologously generated cocktail of growth factors from activated

platelets improves skeletal muscle stem cell function and reverses induced senescence by doxorubicin in ApoE deficient and wild type mice. To the best of my knowledge this thesis is the first to characterise the impact of hyperlipidaemia and atherosclerosis on skeletal muscle stem cell function. The key findings of the thesis are:

- ApoE deficiency impaired proliferation of skeletal muscle stem cells *in vitro* and *ex vivo*. (Chapter 3)
- ApoE deficiency impaired differentiation of skeletal muscle stem cells *in vitro* and *ex vivo. (Chapter 3)*
- Palmitate induced experimental hyperlipidaemia also impaired skeletal muscle stem cell function, and resulted in oxidative stress, which when treated with antioxidant ebselen partially improved muscle stem cell function. (Chapter 4)
- ApoE deficiency impaired skeletal muscle recovery after chemically induced injury, while platelet releasate improved recovery in both ApoE deficient and wild type mice (Chapter 5).
- Lastly, the present work demonstrated the beneficial effects of platelet releasate on doxorubicin induced senescence (Chapter 6).

7.2 Skeletal muscle stem cell function

Skeletal muscle stem cells are the resident population of stem cells, which lie between the basal lamina and the plasma membrane (Relaix and Zammit, 2012). Skeletal muscle stem cells are essential to generate new material for muscle recovery via their proliferation phase when activated by injury stimulus (Dumont et al., 2015). After a period of proliferation, the new cellular material can then differentiate and form new muscle to replace the injured muscle (Füchtbauer and Westphal, 1992). As muscle fibres are multinuclear, the period of proliferation is especially important, as the myonuclear domain – the area of cytoplasm surrounding each nucleus within a proximity of its transcriptional activity has an upper limit (Allen et al., 1999; Schwartz et al., 2016). The myonuclear domain is also strictly regulated in health, as decreased myonuclear domain is generally followed by atrophy and increased myonuclear domain by hypertrophy (Allen et al., 1999; Taylor-Weiner et al., 2020). However other evidence refutes the correlation between atrophy or hypertrophy and myonuclear domain, as disuse atrophy studies have shown no decrease in total stem cell numbers,

furthermore disuse atrophy also does not induce any changes in muscle stem cell content, though it has been suggested that changes in myonuclear loss may occur at a different timescale to hypertrophy (Bruusgaard et al., 2012; Bruusgaard and Gundersen, 2008; Snijders et al., 2014; van der Meer et al., 2011). Furthermore, evidence suggests that products of myonuclei remain localised close to their myonucleus of origin, this could indicate that muscle fibres with a higher myonuclear domain do not meet the transcriptional demand for the whole fibre (Pavlath et al., 1989). In the present work, ApoE deficient mice muscle fibres exhibited a greater myonuclear domain compared to wild type fibres despite having the same average number of nuclei overall. These findings indicate that ApoE is necessary to restrict the size of fibre and therefore myonuclear domain. While differences in myonuclei number per fibre were not different between wild type and ApoE deficient mice at T0 – the day of dissection, numbers of muscle stem cells were counted at 0h, 24h, 48h and 72h. No significant difference was found between numbers of stem cells on muscle fibres at any timepoint – therefore the capacity for stem cell proliferation was not entirely lost, though a functional impairment could still be enough to cause an overall difference in injury recovery.

Table 7.1: Myonuclear Density

Reference	Model	Application	Result
(Tseng et al., 1994)	soleus and plantaris muscles of adult rats	The relationships between fiber size, and the cytoplasmic volume per myonucleus were determined.	High MND = low succinate dehydrogenase activity (MND inversely related to oxidative capacity)
(Jaspers et al., 2006)	*Xenopus* iliofibularis muscle	Myonuclear density was determined in high- and low-oxidative fibres of freshly frozen muscle. (type 1 and type 3 fibres selected on basis of SDH activity). Nuclei were counted with H&E staining.	High oxidative muscle fibres had lower MND (reported as higher myonuclear density)
(van der Meer et al., 2011)	Type II fibres of rat plantaris muscle	Cross sections of muscle were counted in the deep and superficial region of the muscle, other serial sections were stained for succinate dehydrogenase (SDH) as a marker for oxidative capacity.	Muscle in superficial glycolytic region (low oxidative) ↑ MND ↓ SDH Deep oxidative region ↓ MND ↑ SDH

Hikida, et al. (1998).	Human young and aged muscle	The responses of young (22.5±5.8) and elderly (65±6) men to strength training were compared. The Muscle fiber hypertrophy in young and old men training was similar, although the elderly men underwent 16 weeks of training compared to 8 weeks for the young. Muscle biopsies taken from the vastus lateralis were examined to determine the changes in muscle fiber size before and after strength training, and the myonuclear and satellite cell compositions were determined	Hypertrophy did not affect MND in young (nuclei number increased with fibre size). Hypertrophy increased MND in elderly (nuclei number remained the same while fibre size increased) *This could be down to smaller initial fibre size (24% larger in the elderly) as a threshold for maximum transcriptional activity may not be reached, the addition of more nuclei may not be necessary.*
(Ross et al., 2018)	Mice with SIRT1 muscle KO, Mice with inducible overexpr	Myofibres isolated from mice with either a skeletal muscle-specific inactivation (mKO) or inducible overexpression (imOX) of SIRT1. Myonuclear organisation was electron microscopy and confocal microscopy subject to nuclei staining.	SIRT1 overexpression ↓ MND, Knockout ↑ MND

	ession of SIRT1		
(Moore et al., 2018)	Human old (~71) muscle	old (~71 years) male adults underwent 14 days of step reduction (<1500 steps/day) while performing six sessions of LLRE (~30% maximal strength) with one leg (SR + EX) while the contralateral leg served as an untrained control(SR). Seven healthy ambulatory age-matched male adults (~69 years) served as a comparator group (COM). Muscle biopsies taken from vastus lateralis after 14 days, and immunohistochemical analysis was performed to determine (CSA), myonuclear content, SC content, and total (C:F) and fibre type-specific (C:Fi)capillary-to-fibre ratios.	Restricted exercise ↓ MND, ↓ SC number. Exercise ↑ CSA, ↑ MND while nuclei number (and SC number vs COM) is maintained. *This follows Hikida's impression that threshold for maximum transcriptional activity may not be reached?*
(Murach et al., 2018)	Healthy young men (23±1)	CSA Nuclei counted,	Restricted exercise: ↓ CSA, ↓ MND, ↓nuclei/fibre Return to exercise: ↑ CSA, ↑ MND, ↑ nuclei/fibre, ↑ SCs. ↑ myogenesis markers,

			↑ autophagosome markers.
(Schwartz et al., 2016)	*Manduca sexta*	Intersegmental muscle (ISM) used in caterpillar, but not moth form, which undergoes program of atrophy before programmed cell death. ISM were extracted and fixed for histology, data collected on CSA and nuclear number.	Atrophic ↓ CSA, = nuclei, ↓ MND Dying ↓↓ CSA, = nuclei, ↓↓ MND
(Hikida et al., 1997)	Rat soleus	immunohistochemical method to determine myonuclear distribution in relation tomuscle fiber size. This report examines the nucleocyto-plasmic relationship between type I and type II fibers ofthe soleus muscles of rats. These fibers are compared inanimals that had been in the microgravity conditions of space for 10 days vs. ground-based control animals	↓ Fibre size in space muscles = MND
(Duddy et al., 2015)	MDX and WT mice EDL	Measured the main cellular components of muscle growth and regeneration over the period of postnatal growth and early pathology in mdx and wild-type (WT) mice;	In mdx ↓ Nuclei per fibre, ↓ MND postnatal hypotrophy

	phalloidin binding is used as a measure of fibre size, myonuclear counts and BrdU labelling as records of myogenic activity.	↓ Fibre size

To determine the functional capacity of muscle stem cells reports have used the differential expression of transcription factors Pax7, MyoD and Myogenin in quiescence ($Pax7^+/Myod^-$), activation ($Pax7^+/MyoD^+$), proliferation ($Pax7^+/MyoD^-$), and differentiation ($Pax7^-/Myogenin^+$). Differences in quiescent vs activated stem cells can be detected at 24h and expressed as a percentage of cells expressing Pax7 only vs Pax7 and MyoD respectively, at 48h a greater percentage of proliferating cells is expected and after 72h Myogenin expression is detected, which detects the muscle stem cells' capacity for differentiation. This method has previously been used to demonstrate the effectiveness of platelet releasate in increasing proliferation as well as differentiation in muscle stem cells when administered to single myofibres (Scully et al., 2020). The present work demonstrated through this method that muscle stem cells of fibres derived from ApoE deficient mice have a minor impairment to activation as well as an impairment in differentiation. This demonstrates that ApoE deficient mice have a functional impairment, it has previously been demonstrated that muscle in ApoE deficient mice have increased macrophage content, oxidative stress and fat content (Sfyri et al., 2018). This study however, used single muscle fibres separated from their environment in a muscle, though retained on a single fibre their functional capacity was not entirely isolated. Therefore, the present work went on to isolate single fibres to determine the functional effects of ApoE deficiency on isolated muscle stem cells.

While differentiational expression of transcription factors may be used to determine proliferation and activation of muscle stem cells in single fibres, isolated stem cells may take advantage of other methods. In culture, isolated stem cells proliferate in high serum conditions, therefore proliferation capacity can be directly studied via proliferation assay – in this case EdU staining of proliferating cells. Whereas muscle stem cells begin to differentiate in low serum conditions, myogenin expression may

also be used to determine cells committed to differentiation and a percentage of cells expressing myogenin may be used as a fusion index, determining the capacity for differentiation. Furthermore, the culture of isolated muscle stem cells provides the opportunity for morphological study, and the present work was able to determine the ability of stem cells to form myotubes by measuring their size. Previous evidence showed that LDL mediated lipotoxicity toxicity reduces the ability of cultured myoblasts to fuse, furthermore cisplatin induced ROS exposure in C2C12 myoblasts impairs proliferation (Tamilarasan et al., 2012; Zhou et al., 2021). Both lipotoxicity and oxidative stress have been detected in ApoE deficient muscle, ectopic accumulation of lipids in muscle tissue induces pathological changes and oxidative stress has a variety of harmful effects including DNA damage, therefore it was important to determine if these effects were also hallmarks of isolated skeletal muscle stem cells and not merely as a result of the muscle niche (Cole et al., 2011; Sfyri et al., 2018). The present work reveals that isolated muscle stem cells of ApoE deficient mice had impaired proliferation as well as differentiation, and the myotubes created from stem cells of ApoE deficient mice were smaller. This indicates that independent of the extracellular environment and the muscle fibre niche muscle stem cells of ApoE deficient mice are functionally impaired.

The present work went on to look into the gene expression of genes which regulate three processes: I) deciders of muscle stem cell fate, ii) regulators of myoblast fusion and iii) contractile proteins. As MyoD and Myogenin expression in stem cells have already been used to indicate commitment to differentiate into muscle cells, here scrib was used as an additional indicator of stem cell fate as it has previously been acknowledges to control stem cell fate and reduction in expression of all muscle stem cell fate genes was seen (Ono et al., 2015). Indicators of myoblast fusion bex1, tmem8c and srf were also reduced indicating a transcriptional impairment in myoblast fusion. Interestingly, Bex1-deficiency has been associated with prolonged proliferation and delayed differentiation following recovery after myotrauma, however this was not necessarily accompanied by reduction in proliferation as myogenin was reduced, myoD was not measured (Koo et al., 2007). Skeletal muscle-specific deletion of SRF causes severe muscle hypoplasia, and deletion of SRF in adult mice leads to loss of muscle mass and sarcopenia (Lahoute et al., 2008; Li et al., 2005). This loss of srf gene expression in mouse muscle stem cells could be a contributing factor to the

increased myonuclear domain in ApoE deficient mice. Myosin heavy chain and actin gene expression were also reduced in muscle stem cells of ApoE deficient mice, indicating that these stem cells have a reduced capacity to generate contractile proteins – an essential component of myogenesis. Taken together these results indicate that hyperlipidaemic mice have functionally impaired skeletal muscle stem cells, however the impact of this on skeletal muscle repair in injured muscle has not been defined.

Previous evidence has already demonstrated that ApoE deficient mice have delayed or impaired skeletal muscle regeneration after injury, however the extent of impaired regeneration remains to be seen (Arnold et al., 2015; Kang et al., 2008). Kang et al. first demonstrated that 7 days post ischemia-reperfusion injury that myogenin protein levels, were reduced in the ApoE deficient mouse calf muscle, but not MyoD levels (Kang et al., 2008). Furthermore after 14 days of recovery ApoE mice had a greater percentage of fibres with centrally located nuclei – indicating a slower progression in recovery (Kang et al., 2008). Moreover, Arnold et al. reported that in notexin induced injury of the tibialis anterior, ApoE deficiency impacts negatively on macrophage phagocytic activity and is at least partially responsible for the impairment of skeletal muscle regeneration (Arnold et al., 2015). Despite these studies however, the impact of ApoE deficiency on skeletal muscle regeneration were unclear. Therefore, the present work quantified the number of injured fibres per muscle, the number of regenerating fibres per muscle and the cross-sectional area of regenerating fibres per muscle, furthermore the extent of macrophage infiltration in injured muscle. These data were collected at three timepoints – 5 days, 10 days, and 14 days post injury, building the clearest picture of the extent of muscle injury in the hyperlipidaemic mouse to date. At 5 days clear differences in injury progression were already detected, with a much greater number of damaged fibres per muscle, and more small regenerating fibres than larger ones in the hyperlipidaemic mouse. Macrophage infiltration was also 3 times greater in the hyperlipidaemic mouse, although macrophage infiltration was already known to be increased in the uninjured muscle of ApoE deficient mouse (Sfyri et al., 2018). After 10 days of regeneration the extent of injury was improved in both hyperlipidaemic and wild type mice, where injured muscle fibres were detected at no more than two per fibre. The regenerating fibres had mostly fully regenerated, however more regenerating fibres were present in the hyperlipidaemic muscle and with greater

cross-sectional area. This was likely due to a greater progression in the wild type mouse as what fibres were regenerating were small minor additions, whereas the hyperlipidaemic muscle still had clearly regenerating fibres. At 14 days of regeneration no differences were detected between the two muscles, as both had fully recovered from injury. Taken together this builds a much clearer picture of skeletal muscle regeneration in the hyperlipidaemic mice, which take longer to clear damaged fibres, as well as develop regenerating fibres much slower. This would indicate that the impaired regeneration is at least in part due to already discussed stem cell impairments, as the repair mechanisms in regenerating fibres are much slower in the hyperlipidaemic mouse. The present work has been the first to relate delayed muscle regeneration to muscle stem cell function.

Previous work has indicated that the hyperlipidaemic mouse muscle microenvironment is one of increased oxidative stress due to increased production of reactive oxygen species (Sfyri et al., 2018). The present work therefore sought to determine the extent of oxidative stress in experimental hyperlipidaemia, and its effect on skeletal muscle stem cells. Previous studies have reported that increased production of reactive oxygen species impairs myogenic differentiation through MyoD inhibition and inhibition of MyoD-dependent transcription (Ardite et al., 2004; Barbieri and Sestili, 2012; Catani et al., 2004). The major pathway leading to reduced levels of MyoD in muscle with oxidative stress is likely through increase of NF-κB activity or TNFα expression (Guttridge et al., 2000). Therefore, the likelihood of reactive oxygen species as a contributing factor to muscle stem cell impaired function and reduced muscle regeneration capability is high, and the elevated intramuscular lipid content likely contributes to the increased ROS. Considering this, the present work used palmitate to simulate hyperlipidaemia in cultured muscle stem cells and single fibres.

Palmitate has previously been shown to induce reactive oxygen species accumulation (Wang et al., 2018; Wei et al., 2013; Yu et al., 2019). Previous work concerning palmitate treated C2C12 cells however, has yielded mixed results. For example, while many studies found that palmitate induces apoptosis or atrophy, grabiec et al. found that palmitate treatment actually increased myogenin, α-actinin, and myosin heavy chain, protein markers of myogenesis (Grabiec et al., 2016; Meshkani et al., 2014; Peterson et al., 2008; Y.-N. Sun et al., 2020, p. 19). Interestingly, palmitate was also seen to alter cell cycle proteins, in this case increasing levels of Cyclin D3, which

regulates the G1/S phase transition, and this increase leads to post mitotic arrest and allows for differentiation to occur (Grabiec et al., 2016). Therefore, a pilot study was implemented to determine the concentration of palmitate necessary to impair muscle stem cell function and 1mM palmitate was chosen as stem cell function was impaired without serious cell death. Experiments in cultured muscle stem cells revealed that palmitate does in fact induce reactive oxygen species production in cells of both wild type and ApoE deficient mice as indicated by the increased number of DHE expressing nuclei. Under conditions of oxidative stress in palmitate treated muscle stem cells of both wild type and ApoE deficient mice myoblast fusion and differentiation was inhibited. Ebselen however, was able to improve differentiation in wild type cells with experimental hyperlipidaemia, but not in ApoE deficient cells with experimental hyperlipidaemia. Following these experiments in single fibres found that palmitate vastly decreased the activation of muscle stem cells at 48h, and that ebselen fully reversed this effect in both wild type and ApoE deficient mice. At 72h however, differentiation is impaired in both wild type and ApoE deficient fibres, but ebselen only reverses this for wild type fibres, not ApoE deficient fibres. This data suggests that experimental hyperlipidaemia does in fact induce oxidative stress in skeletal muscle stem cells, impairing proliferation and differation capability, and that antioxidant ebselen can be used to restore proliferation, but not differentiation in muscle fibres of ApoE deficient mice.

The surprising increase of muscle fibre stem cells expressing MyoD and not Pax7 in response to palmitate at t48 could be due to the influence of reactive oxygen species on cell cycle proteins. Palmitate has been seen to alter the cell cycle in rodent pancreatic β-cells, in increasing protein and gene expression of TLR3, palmitate leads to growth arrest through degradation of cyclin D1 and Cyclin D2 (Yang et al., 2013). In β-cells, this arrest leads to reduction of mass, however the present work posits that in skeletal muscle stem cells palmitate will serve to halt the initial proliferation and therefore accelerate differentiation. Furthermore, Palmitate has been seen to decrease levels of growth differentiation factor 11 (GDF11) as well as it's analogue myostatin in C2C12 cells (Grabiec et al., 2016; Jing et al., 2017). GDF11 is another regulator of the G1/S phase transition, which when inhibited increases muscle mass and strength as well as halts progression to the S phase (Jin et al., 2019; Shi and Liu,

2011). A study using an antibody blocking the myostatin receptor found increased differentiation (Lach-Trifilieff et al., 2014).

ablation of FAS activity causes a dramatic down-regulation of Skp2, a component of the E3 ubiquitin ligase that controls the turnover of p27Kip1 (a CDK inhibitor) (Knowles et al., 2004).

7.3 Skeletal muscle senescence and treatment

One of the most important attributes of skeletal muscle stem cells is their dynamic ability to maintain quiescence through adult life, but retain the ability to proliferate when activated, with the capacity to self-renew, generating new quiescent stem cells as well as cells which differentiate to become new muscle. The muscle must retain this ability through severe and repetitive injuries, however aging muscle has a reduced capacity for self-renewal and quiescence is progressively lost (García-Prat et al., 2016; Hwang and Brack, 2018; Sousa-Victor et al., 2014). Senescence is induced in ageing muscle via upregulation of p16(INK4a) which irreversibly prevents the normal function of stem cell proliferation. Failure of the regeneration machinery of sarcopenic muscle to replace damaged myofibres is one of the major causes of the physical incapacitation and loss of independence in the geriatric population (Arthur and Cooley, 2012; Jang et al., 2011; Renault et al., 2002). Regeneration after cardiotoxin induced muscle injury reduces regeneration efficiency in old mice, and greatly reduces regeneration in geriatric mice. While there is a difference in stem cell number between adult mice and old mice, the number id not further reduced in geriatric mice, indicating the impaired regeneration is not due to reduced numbers of muscle stem cells. Furthermore, FACS sorted stem cells of geriatric mice transplanted into injured muscle of young mice produced fewer myofibres than the resident population of stem cells (Sousa-Victor et al., 2014).

Senescence in muscle is also evident in patients of cancer who are treated with chemotherapy. While anthracycline cancer therapies such as doxorubicin are used to limit the spread of cancer, they are nonspecific and their cytotoxicity causes side effects such as cardiomyopathy, myopathy, and skeletal muscle dysfunction – reducing the quality of life of those living with cancer. Doxorubicin treatment has demonstrated a reduction in overall muscle stem cell number in the extensor digitorum longus and soleus of Sprague-Dawley rats (D'Lugos et al., 2019). The antitumour

effects of doxorubicin are attributed to its inhibition of topoisomerase II, which is essential for the replication of DNA, changes in RNA transcription and importantly the generation of reactive oxygen species, leading to oxidation of lipid membranes and cellular proteins (Bredahl et al., 2021; Gewirtz, 1999; Sawyer et al., 2010). Similar to the case of hyperlipidaemia, the effects of doxorubicin induced myopathy have been attributed to excessive generation of reactive oxygen species.

Doxorubicin treatment has been shown to induce senescence in skeletal muscle, cardiomyocytes, and fibroblasts, though low doses of doxorubicin (10nM) proved to be not enough to significantly increase senescence-associated eta-galactosidase (Casella et al., 2019; Gibson et al., 2014; Piechota et al., 2016; Spallarossa et al., 2009). The present work sought to determine the dose necessary to induce senescence in C2C12 myoblasts. Using immunohistochemistry of senescence-associated β-galactosidase with various concentrations of doxorubicin in culture showed that senescence is induced by cancer treatment doxorubicin in myoblasts. Surprisingly, higher concentrations of doxorubicin yielded lower levels of senescence-associated β-galactosidase, therefore the experiment was repeated using trypan blue dye to detect cell death which became elevated at higher concentrations of doxorubicin. This initial data on doxorubicin treatment of cultured myoblasts confirmed the toxicity of doxorubicin and furthermore confirmed that at a concentration of 0.5µM doxorubicin, maximal senescence could be induced with minimal cell death.

Following confirmation of senescence in experimental culture, proliferation assay was used to determine the capacity for cell growth in doxorubicin treated culture. Initially C2C12 were cultured in serum free conditions with or without doxorubicin and releasate, however all groups incurred excessive cell death, therefore growth medium was selected for the proliferation experiment. In this case doxorubicin almost entirely halted proliferation, and releasate was able to induce a minor amount of proliferation. These data suggest that doxorubicin induces senescence and releasate can partially reverse it. Platelet releasate includes several pro-proliferative factors including VEGF, PDGF, which could contribute to the partial improvement in proliferation, however doxorubicin effectively halts proliferation and releasate only has a minor effect. The minor effect is likely due to doxorubicins effects on pro-proliferative factors ie. it has been shown toassociate with VEGF and direct inhibition may be a factor in it’s anti-

tumour effects, furthermore PDGF has been used to improve doxorubicin efficacy (Bilgen and Persil Çetinkol, 2020; Liu et al., 2011; Rotkrua et al., 2021).

To further characterise the effects of doxorubicin treatment on myoblasts, differentiation experiments were run, determining that doxorubicin also impairs differentiation. Myotubes formed by C2C12 cells cultured with doxorubicin had a greatly reduced surface area compared to those that were not treated and the fusion index was also reduced – indicating that doxorubicin reduces the capacity for muscle stem cell regeneration. Previous data has shown that doxorubicin inhibits differentiation in chondrocytes by stimulating ROS, and differentiated H9c2 cells were more susceptible to doxorubicin induced cytotoxicity (Branco et al., 2012; Wu et al., 2021). There has not yet been any evidence indicating that doxorubicin induced cytotoxicity can be alleviated in differentiating muscle, however the present study demonstrated that pre-treatment with platelet releasate improves differentiation. As p53 is induced by both doxorubicin and ROS, and p53 directly represses transcription of myogenin, it is suggested that doxorubicin acts to arrest the cell cycle through p53, which in turn prevents myogenin expression, impairing muscle stem cell differentiation (Ebata et al., 2017). Platelet releasate however, entirely restores differentiation. These data indicate that while proliferation of myoblasts is not improved by platelet releasate, the differentiation of myotubes is improved by releasate which could potentially mean that releasate is more effective after doxorubicin treatment has ceased, as it would likely have a better effect on proliferation.

The present work further develops this by showing that stem cell fate and fusion genes expression are impaired by doxorubicin, however releasate does not ameliorate the expression. This indicates that the improved differentiation capacity is due to exogenous application of releasate rather than changes in gene expression. Growth factors found in releasate may be acting downstream of cell fate and fusion genes, or DNA damage may prevent normal gene expression.

Having developed an understanding of the effects of senescence in C2C12 myoblasts, the effect of releasate on senescence per se was determined. Senescence-associated β-galactosidase levels were determined in doxorubicin and releasate treated C2C12 myotubes, resulting in a decrease of senescence in response to releasate. This indicates that the reduction in proliferation in C2C12 cells by DOX is reversible and an

adequate dose of releasate may be a potential treatment to reverse senescence. This is another indicator that platelet releasate could be a useful treatment for the muscle after cancer treatment has ceased.

As doxorubicin is purported to function by DNA fragmentation, the present work then sought to determine the extent of DNA damage and DNA repair mechanism. This work demonstrates via increased p53 staining in nuclei of doxorubicin treated C2C12 cells that DNA repair mechanisms are upregulated in response to doxorubicin treatment. P53 also functions in repression of myogenin transcription, indicating that doxorubicin induced p53 mediated G1 arrest, while preventing differentiation – likely to reduce post-mitotic nuclear abnormalities, this contributes so skeletal muscle stem cell senescence (Yang et al., 2015). These pathways are suggested to increase time for cell repair, by arresting the cell cycle, allowing increased chances of survival. With greater levels of stress however p53 facilitates increased levels of cellular stress by DNA fragmentation, this prevents aberrant cell proliferation, however caused unwanted cellular damage (Beyfuss and Hood, 2018). H2AX foci were used as a reliable indicator of double strand breaks and is the most sensitive method of detecting double strand breaks (Mah et al., 2010). H2AX foci in these same experiments indicate that the level of overall DNA damage is greatly reduced by releasate. These data indicate that releasate can be used to resolve the impact on DNA damage and allow p53 to function as intended in lower levels.

The success in demonstrating the extent of DNA damage and DNA repair responses to doxorubicin prompted further study to gain insights on the impact of doxorubicin and releasate on cell cycle arrest. The present work looked at the wild type and $ApoE^{-/-}$ mouse tibialis anterior muscle p21 expression – a key regulator of cell cycle progression at the G_1 to S phase transition whose action is utilised in chemotherapy. P21 promotes cell cycle arrest in response to many stimuli and expression of p21 is increased in differentiating myoblasts (Fujio et al., 1999; Liu et al., 2017). In mice lacking p21, the differentiation of myoblasts is decreased, and cell proliferation is increased (Chinzei et al., 2015; Hawke et al., 2003). Therefore, there is overlap between the intended cellular mechanisms of cell cycle arrest in order to promote differentiation and the cell cycle arrest generally induced by doxorubicin, however irreversible senescence as already discussed is detrimental to the muscle and it is

important to determine if cell cycle arrest induced in muscle by doxorubicin is reversible.

In mice treated with doxorubicin, cell cycle arrest was greatly increased, however releasate treatment reversed this, indicating that *in vivo* the effects of doxorubicin on the cell cycle can be reversed by the tissue specific treatment of muscle with releasate, highlighting releasate as a potential treatment for myopathy in cancer. Importantly, this data proves that cell cycle arrest can be reversed in muscle treated with doxorubicin and presents a potential quality of life benefit to patients of cancer. Furthermore, this data was supported at protein level *in vitro* as p21 expression was greatly induced by doxorubicin and alleviated by releasate treatment in C2C12 cells. H2AX protein levels were also induced, indicating the expected levels of DNA damage, however they were not themselves alleviated by releasate, likewise p53 was increased in all doxorubicin treated cells. This may indicate that the beneficial effects of releasate do not protect from DNA damage, but instead boost repair mechanisms, as p53 is increased in cells treated with both doxorubicin and releasate. These data indicate that releasate can be a useful treatment for myopathy in patients of cancer, without counteracting the beneficial antitumour effects of the therapy.

After determining the effects of doxorubicin and releasate on cell cycle arrest, DNA damage, and DNA repair mechanisms, it was important to determine the activation and differentiation profiles of single fibres under the same conditions. Previous research has discovered that doxorubicin selectively inhibits muscle specific expression of myogenic regulatory factors to prevent terminal differentiation in skeletal muscle stem cells (Puri et al., 1997). Furthermore, doxorubicin prevents both myoblast fusion and expression of muscle specific proteins and muscle regulatory factors without significantly altering non-muscle gene transcripts (Kurabayashi et al., 1993). Additionally, doxorubicin inhibits the ability of MyoD to trans-activate muscle-specific reporter genes (Kurabayashi et al., 1994). Doxorubicin has also seen to have negative effects on differentiation with studies reporting differentiation is blocked by doxorubicin in c2c12 cells and myogenin expression in h9c2 cardiomyocytes is reduced (Kurabayashi et al., 1994, 1994, 1993; Liu et al., 2015). Therefore, the present work determined the proliferation profiles of doxorubicin and releasate treated single fibres. In single fibres doxorubicin irreversibly impaired proliferation for 72 hours, however the number of muscle stem cells at 72 hours were equivalent to untreated at 48 hours

indicating a delayed recovery. Furthermore, the decreased expression of MyoD at 24 and 48 hours indicate an impaired ability of skeletal muscle stem cells to activate and therefore proliferate. This change in MyoD expression was reversed by releasate – indicating that releasate is enough to overcome the damage of doxorubicin in some instances. Similarly, myogenin expression was greatly reduced by doxorubicin at T72, however releasate was able to restore myogenin expression. Taken together these data indicate that doxorubicin impairs both the proliferation and differentiation of skeletal muscle stem cells, and while the expression patterns appear to be rescued by releasate, the proliferation does not continue to the same extent. These differences could be due to the previously stated ability for doxorubicin to prevent MyoD from trans-activating muscle specific reporter genes and inducing the terminal cell cycle arrest pathways through MyoD/pRB.

7.4 Limitations

Some aspects of the present study are considered to be limitations, for example in chapter 3 muscle stem cell myogenesis was evaluated in two different experimental settings: on single muscle fibres, and isolated muscle stem cells. Firstly, myofibres from ApoE$^{-/-}$ mice were isolated and cultured *ex vivo* to determine the expression profiles of myogenic transcription factors to determine the functional myogenic capacity of muscle stem cells. Secondly, muscle stem cells were isolated from fibres and cultured *in vitro* apart from their microenvironment. While this yielded data and new knowledge on the function of muscle stem cells in the ApoE$^{-/-}$ mice, the same study was not conducted *in vivo*, and while chapter 5 demonstrates decreaced capacity for recovery after injury in the ApoE$^{-/-}$ mice, myoD and myogenin expression *in vivo* would be a useful avenue of further study.

Further to this, Muscle stem cells behave differently, interacting with macrophages and the proinflammatory environments created by injury. For this reason it would be useful to have more *in vivo* data and even more data in primary cells in chapter 6, as the C2C12 cells used in most experiments are used as a standard model of myoblasts, however as they are an immortalized cell line they may be prone to function differently to primary muscle stem cells. These experiments relied on C2C12 cells more often due to the halt of experimentation during the COVID-19 lockdown, and the subsequent loss of access to animal models.

One limitation of the present work is that ROS production was measured in cultured cells via DHE staining. DHE staining is a commonly used method of evaluating levels of superoxide, DHE freely permeates the cell membrane and when oxidized by cellular superoxide to generate red fluorophores which intercalate with DNA, becoming highly fluorescent in the nucleus. For this reason, the present work used the number of fluorescent nuclei and the overall fluorescence intensity as measurements of ROS production (Wang and Zou, 2018). Furthermore, the present work demonstrates superoxide levels in myoblasts, but does not determine the hydrogen peroxide levels or the levels of other reactive oxygen species in culture beyond the stated superoxide levels. Therefore, further investigation into the overall abundance of ROS with more specific dyes such as Cyto-HyPer dye for hydrogen peroxide would be useful to improve our understanding of oxidative stress in hyperlipidaemia. (Pearson et al., 2014)

In determining the functional impairment in muscle stem cell proliferation and differentiation in experimental hyperlipidaemia the cell culture data mimicking hyperlipidaemia have not been expanded *in vivo* on mice, i.e. through the use of a pump to administer palmitate. While chapter 4 was a success in demonstrating the benefits of antioxidant usage in experimental hyperlipidaemia, and the involvement of oxidative stress in the negative effects of hyperlipidaemia, more quantitative data, such as the qPCR used in chapter 3 would be a useful metric to determine the functional effects of gene expression in high oxidative stress environments. Furthermore, the prospect of determining the gene expression of muscle related genes and myogenesis related genes in response to both superoxide and antioxidants is particularly interesting.

While platelet releasate is used in a variety of experiments in the present study, releasate from the same donor could not be assured. Due to policy limiting donations to once a month each donor, and due to privacy, a donation could not be stored from month to month to use the same donor. This presents a limitation, in that several studies have demonstrated that the composition of platelet releasate varies across individuals, while maintaining many of the same components (Pagel et al., 2017; Parsons et al., 2018; Vélez et al., 2015). Therefore, the composition of platelet releasate should be taken as a whole – a collection of growth factors and cytokines, considering the specific effects of individual growth factors. To limit the variability

between releasate produced from different donors, each individual experiment in the present study uses releasate from a single donor, which may be a different donor to other experiments (i.e. proliferation experiment uses releasate from one donor, while differentiation experiment uses releasate from another). Another limitation in releasate composition in the present study was that proteomics were not performed on the releasate used, as the resources for proteomics were not available, and each donor would have a different proteomic profile, as discussed previously (Pagel et al., 2017; Parsons et al., 2018; Vélez et al., 2015).

7.5 Future work

This project is the first to my knowledge to characterise the skeletal muscle stem cell biology of the atherosclerotic ApoE deficient mouse model. This work addressed not only the baseline capacity for skeletal muscle stem cells of the ApoE deficient mouse to generate new muscle, but also the capacity for the ApoE deficient mouse muscle to regenerate after injury. Furthermore, the work determined its response to senescence and two potential therapies were examined to improve muscle stem cell function in two contexts – hyperlipidaemia, and senescence. Ebselen – an antioxidant proved successful in restoring function to muscle stem cells in experimental hyperlipidaemia, and platelet releasate improved muscle stem cell function in response to doxorubicin induced senescence.

Although this work addressed the capacity for antioxidant ebselen and platelet releasate to alleviate the symptoms of hyperlipidaemia and doxorubicin induced senescence in muscle, both cases have seen positive outcomes in response to exercise. In ApoE deficient mice, studies have shown that exercise attenuates oxidative damage, and promotes myokine expression, furthermore exercise has the additional benefit of reduction in aortic lesions (Jakic et al., 2019; Wang et al., 2021). Studies of skeletal muscle outcomes in doxorubicin treated subjects have shown that exercise can preserve skeletal muscle mass, improve the maximal twitch rate and maximal rate of force in some muscles and prevents loss of muscle function overall (Bredahl et al., 2016; Dickinson et al., 2017; Mackay et al., 2021). It would be beneficial to determine the effects of exercise independent of the two treatments in the present work, as well as to determine the potential combined effect.

In addition to addressing the aforementioned limitations, it would be useful to determine the maximal twitch rate and maximal force capacity in the mouse muscle to determine the functional impact of reduced stem cell function in injured and uninjured hyperlipidaemic mice. Furthermore, exercise has been suggested to have protective effects in hyperlipidaemic as well as doxorubicin treated muscle, however it's precise impact on skeletal muscle stem cells is yet to be determined, therefore exercise based studies would be an important line of research to follow (Dickinson et al., 2017; Powers et al., 2019; Yang et al., 2017).

7.6 Concluding remarks

Hyperlipidaemia is a major risk factor for atherosclerosis and cardiovascular disease. Recently it was showed that obesity-independent hyperlipidaemia induced intramuscular lipid accumulation and skeletal muscle oxidative stress as well as delayed regeneration after injury in ApoE deficient ($ApoE^{-/-}$) mice, an established model of atherosclerosis and hyperlipidaemia (Meyrelles et al., 2011, Arnold et al., 2015; Crawford et al., 2013; Kang et al., 2008; Pellegrin et al., 2014). Nevertheless, the obesity-independent impact of hyperlipidaemia and atherosclerosis on skeletal muscle and skeletal muscle stem cells is largely unknown. This thesis reveals for the first time that skeletal muscle stem cells of the ApoE deficient mouse model have impaired function with reduced capacity for proliferation and differentiation, and this is reflected in the reduced ability to regenerate after muscle injury. Specifically, muscle stem cells expressed MyoD and myogenin less often in the hyperlipidaemic mouse, and this impaired myogenic progression was accompanied by a reduced capacity to proliferate and to generate myotubes. Furthermore, this thesis reveals the effects of cancer therapy doxorubicin on muscle stem cells and indicates that due to the nonspecific cytotoxicity of doxorubicin damaging the muscle, treatment of cancer patients with platelet releasate could benefit their muscle regeneration. This thesis has demonstrated the ability of platelet releasate to promote myoblast proliferation and improve efficiency of differentiation when administered during fusion which could be applied to not only cancer treatment but any kind of myopathy.

The present study relates to humans with obesity as obesity leading to hyperlipidaemia and atherosclerosis is recognised to induce morphological and metabolic changes in a variety of tissues, including the skeletal muscle. However, hyperlipidaemia can occur in the absence of obesity, and the extent to which hyperlipidaemia in the absence of

obesity effects the skeletal muscle and its resident stem cells is not fully understood (23073871, 27581063). In this regard, the present study used the ApoE$^{-/-}$ mouse model, an established model of hyperlipidaemia and atherosclerosis, that does not become obese when subjected to a high-fat diet, to determine the impact of and ApoE deficiency on skeletal muscle stem cell function.

This study provides pivotal evidence on the adverse effect of hyperlipidaemia and atherosclerosis on skeletal muscle stem cell function. It also identifies potential therapeutic targets for decreasing oxidative stress in skeletal muscle and for improving muscle stem cell function. This study positions ebselen and platelet releasate as potential treatments of muscle disease in oxidative stress related diseases. Both proposed treatments could be administered in a muscle-specific manner toward the site of myopathy to provide a functional increase in muscle stem cell functional capacity. While ebselen is currently in clinical trials it's benefits could improve the quality of life of those experiencing oxidative stress related myopathy such as in hyperlipidaemia, and platelet releasate is an autologous, easily, and quickly generated therapy to potentially accelerate regeneration after injury. Furthermore, as reported by Sfyri et al. obesity linked hyperlipidaemia results in muscle morphological changes as well as oxidative stress, therefore these treatments could be useful in restoring a functional microenvironment to the skeletal muscle in obesity (Sfyri et al., 2018). Overall, the present study provides evidence to the impairment of skeletal muscle stem cells in the hyperlipidaemic and atherosclerotic mouse and important insights into the potential therapeutic avenues.

Appendix I

Primers

Gene	Direction	Sequence (5’ to 3’)
Acta1	Forward	CCCAAAGCTAACCGGGAGAAG
	Reverse	GACAGCACCGCCTGGATAG
Bex1	Forward	ATGGAGTCCAAAGATCAAGGCG
	Reverse	CTGGCTCCCTTCTGATGGTA
F4.80	Forward	CTGCACCTGTAAACGAGGCTT
	Reverse	GCAGACTGAGTTAGGACCACAA
gadd45a	Forward	TGCTGACGAAGACGACGAC
	Reverse	CTGACCCGCAGGATGTTGAT
Hprt	Forward	GCTCGAGATGTCATGAAGGAGAT
	Reverse	AAAGAACTTATAGCCCCCCTTGA
MhcI	Forward	AGTCCCAGGTCAACAAGCTG
	Reverse	TTCCAACCTAAAGGGCTGTTG
Mhc2a	Forward	AGTCCCAGGTCAACAAGCTG
	Reverse	GCATGACCAAAGGTTTCACA
Myf6	Forward	GCTAAGGAAGGAGGAGCAAA
	Reverse	GAAGAAAGGCGCTGAAGACT
MyoD	Forward	AGGAGCACGCACACTTCTCT
	Reverse	TCTCGAAGGCCTCATTCACT
Myogenin	Forward	GAGACATCCCCCTATTTCTACCA

	Reverse	GCTCAGTCCGCTCATGCC
OGG1	Forward	CAACAACATTGCTCGCATTACTG
	Reverse	TCAAGCTGAATGAGTCGAGGT
Scrib1	Forward	CCTGGGCATCAGTATCGCAG
	Reverse	GCCCTCGTCATCTCCTTTGT
Srf	Forward	CTGCCTCAACTCGCCAGAC
	Reverse	TCAGATTCCGACACCTGGTAG
Tmem8c	Forward	GTGATGGGCCTGGTTTGTCT
	Reverse	GCATTGTGAAGGTCGATCTCTG

References

Abu Bakar, M.H., Tan, J.S., 2017. Improvement of mitochondrial function by celastrol in palmitate-treated C2C12 myotubes via activation of PI3K-Akt signaling pathway. Biomed. Pharmacother. Biomedecine Pharmacother. 93, 903–912. https://doi.org/10.1016/j.biopha.2017.07.021

Abu-Saleh, N., Yaseen, H., Kinaneh, S., Khamaisi, M., Abassi, Z., 2021. Combination of hyperglycaemia and hyperlipidaemia induces endothelial dysfunction: Role of the endothelin and nitric oxide systems. J. Cell. Mol. Med. 25, 1884–1895. https://doi.org/10.1111/jcmm.15787

Agergaard, J., Zillmer, M.C.F., Castro-Mejía, J.L., Mertz, K., Kot, W., Højfeldt, G., van Hall, G., Nielsen, D.S., Schjerling, P., Holm, L., 2021. Impaired skeletal muscle hypertrophy signaling and amino acid deprivation response in Apoe knockout mice with an unhealthy lipoprotein distribution. Sci. Rep. 11, 16423. https://doi.org/10.1038/s41598-021-96000-8

Akeda, K., Ohishi, K., Masuda, K., Bae, W.C., Takegami, N., Yamada, J., Nakamura, T., Sakakibara, T., Kasai, Y., Sudo, A., 2017. Intradiscal Injection of Autologous Platelet-Rich Plasma Releasate to Treat Discogenic Low Back Pain: A Preliminary Clinical Trial. Asian Spine J. 11, 380–389. https://doi.org/10.4184/asj.2017.11.3.380

Akhmedov, D., Berdeaux, R., 2013. The effects of obesity on skeletal muscle regeneration. Front. Physiol. 4, 371. https://doi.org/10.3389/fphys.2013.00371

Alhowail, A.H., Bloemer, J., Majrashi, M., Pinky, P.D., Bhattacharya, S., Yongli, Z., Bhattacharya, D., Eggert, M., Woodie, L., Buabeid, M.A., Johnson, N., Broadwater, A., Smith, B., Dhanasekaran, M., Arnold, R.D., Suppiramaniam, V., 2019. Doxorubicin-induced neurotoxicity is associated with acute alterations in synaptic plasticity, apoptosis, and lipid peroxidation. Toxicol. Mech. Methods 29, 457–466. https://doi.org/10.1080/15376516.2019.1600086

Al-Khayat, H.A., Kensler, R.W., Morris, E.P., Squire, J.M., 2010. Three-dimensional structure of the M-region (bare zone) of vertebrate striated muscle myosin filaments by single-particle analysis. J. Mol. Biol. 403, 763–776. https://doi.org/10.1016/j.jmb.2010.09.025

Allen, D.L., Roy, R.R., Edgerton, V.R., 1999. Myonuclear domains in muscle adaptation and disease. Muscle Nerve 22, 1350–1360. https://doi.org/10.1002/(sici)1097-4598(199910)22:10<1350::aid-mus3>3.0.co;2-8

Al-Qusairi, L., Laporte, J., 2011. T-tubule biogenesis and triad formation in skeletal muscle and implication in human diseases. Skelet. Muscle 1, 26. https://doi.org/10.1186/2044-5040-1-26

Andia, I., Abate, M., 2013. Platelet-rich plasma: underlying biology and clinical correlates. Regen. Med. 8, 645–658. https://doi.org/10.2217/rme.13.59

Aravena, J., Abrigo, J., Gonzalez, F., Aguirre, F., Gonzalez, A., Simon, F., Cabello-Verrugio, C., 2020. Angiotensin (1-7) Decreases Myostatin-Induced NF-κB Signaling and Skeletal Muscle Atrophy. Int. J. Mol. Sci. 21, E1167. https://doi.org/10.3390/ijms21031167

Ardite, E., Barbera, J.A., Roca, J., Fernández-Checa, J.C., 2004. Glutathione depletion impairs myogenic differentiation of murine skeletal muscle C2C12 cells through sustained NF-kappaB activation. Am. J. Pathol. 165, 719–728. https://doi.org/10.1016/s0002-9440(10)63335-4

Arnold, L., Perrin, H., de Chanville, C.B., Saclier, M., Hermand, P., Poupel, L., Guyon, E., Licata, F., Carpentier, W., Vilar, J., Mounier, R., Chazaud, B., Benhabiles, N., Boissonnas, A., Combadiere, B., Combadiere, C., 2015. CX3CR1 deficiency promotes muscle repair and regeneration by enhancing macrophage ApoE production. Nat. Commun. 6, 8972. https://doi.org/10.1038/ncomms9972

Arthur, S.T., Cooley, I.D., 2012. The effect of physiological stimuli on sarcopenia; impact of Notch and Wnt signaling on impaired aged skeletal muscle repair. Int. J. Biol. Sci. 8, 731–760. https://doi.org/10.7150/ijbs.4262

Askew, C.D., Parmenter, B., Leicht, A.S., Walker, P.J., Golledge, J., 2014. Exercise & Sports Science Australia (ESSA) position statement on exercise prescription for patients with peripheral arterial disease and intermittent claudication. J. Sci. Med. Sport 17, 623–629. https://doi.org/10.1016/j.jsams.2013.10.251

Azad, G.K., Singh, V., Mandal, P., Singh, P., Golla, U., Baranwal, S., Chauhan, S., Tomar, R.S., 2014. Ebselen induces reactive oxygen species (ROS)-mediated cytotoxicity in Saccharomyces cerevisiae with inhibition of glutamate dehydrogenase being a target. FEBS Open Bio 4, 77–89. https://doi.org/10.1016/j.fob.2014.01.002

Bailey, G., Meadows, J., Morrison, A.R., 2016. Imaging Atherosclerotic Plaque Calcification: Translating Biology. Curr. Atheroscler. Rep. 18, 51. https://doi.org/10.1007/s11883-016-0601-6

Bakogiannis, C., Sachse, M., Stamatelopoulos, K., Stellos, K., 2019. Platelet-derived chemokines in inflammation and atherosclerosis. Cytokine 122, 154157. https://doi.org/10.1016/j.cyto.2017.09.013

Baragi, V.M., Becher, G., Bendele, A.M., Biesinger, R., Bluhm, H., Boer, J., Deng, H., Dodd, R., Essers, M., Feuerstein, T., Gallagher, B.M., Gege, C., Hochgürtel, M., Hofmann, M., Jaworski, A., Jin, L., Kiely, A., Korniski, B., Kroth, H., Nix, D., Nolte, B., Piecha, D., Powers, T.S., Richter, F., Schneider, M., Steeneck, C., Sucholeiki, I., Taveras, A., Timmermann, A., Van Veldhuizen, J., Weik, J., Wu, X., Xia, B., 2009. A new class of potent matrix metalloproteinase 13 inhibitors for potential treatment of osteoarthritis: Evidence of histologic and clinical efficacy without musculoskeletal toxicity in rat models. Arthritis Rheum. 60, 2008–2018. https://doi.org/10.1002/art.24629

Barbalho, S.M., Prado Neto, E.V., De Alvares Goulart, R., Bechara, M.D., Baisi Chagas, E.F., Audi, M., Guissoni Campos, L.M., Landgraf Guiger, E., Buchaim, R.L., Buchaim, D.V., Cressoni Araujo, A., 2020. Myokines: a descriptive review. J. Sports Med. Phys. Fitness 60, 1583–1590. https://doi.org/10.23736/S0022-4707.20.10884-3

Barbieri, E., Sestili, P., 2012. Reactive oxygen species in skeletal muscle signaling. J. Signal Transduct. 2012, 982794. https://doi.org/10.1155/2012/982794

Barbouti, A., Vasileiou, P.V.S., Evangelou, K., Vlasis, K.G., Papoudou-Bai, A., Gorgoulis, V.G., Kanavaros, P., 2020. Implications of Oxidative Stress and Cellular Senescence in Age-Related Thymus Involution. Oxid. Med. Cell. Longev. 2020, 7986071. https://doi.org/10.1155/2020/7986071

Barlow, J., Sfyri, P.P., Mitchell, R., Verpoorten, S., Scully, D., Andreou, C., Papadopoulos, P., Patel, K., Matsakas, A., 2021. Platelet releasate normalises the compromised muscle regeneration in a mouse model of hyperlipidaemia. Exp. Physiol. 106, 700–713. https://doi.org/10.1113/EP088937

Barnes, P.J., Baker, J., Donnelly, L.E., 2019. Cellular Senescence as a Mechanism and Target in Chronic Lung Diseases. Am. J. Respir. Crit. Care Med. 200, 556–564. https://doi.org/10.1164/rccm.201810-1975TR

Bashiri Dezfouli, A., Salar-Amoli, J., Pourfathollah, A.A., Yazdi, M., Nikougoftar-Zarif, M., Khosravi, M., Hassan, J., 2020. Doxorubicin-induced senescence through NF-κB affected by the age of mouse mesenchymal stem cells. J. Cell. Physiol. 235, 2336–2349. https://doi.org/10.1002/jcp.29140

Batna, A., Fuchs, C., Spiteller, G., 1997. Lipid peroxidation in presence of ebselen. Chem. Phys. Lipids 87, 149–158. https://doi.org/10.1016/s0009-3084(97)00037-6

Beauséjour, C.M., Krtolica, A., Galimi, F., Narita, M., Lowe, S.W., Yaswen, P., Campisi, J., 2003. Reversal of human cellular senescence: roles of the p53 and p16 pathways. EMBO J. 22, 4212–4222. https://doi.org/10.1093/emboj/cdg417

Behroozi, Z., Ramezani, F., Janzadeh, A., Rahimi, B., Nasirinezhad, F., 2021. Platelet-rich plasma in umbilical cord blood reduces neuropathic pain in spinal cord injury by altering the expression of ATP receptors. Physiol. Behav. 228, 113186. https://doi.org/10.1016/j.physbeh.2020.113186

Bejta, F., Moore, E.H., Avella, M., Gough, P.J., Suckling, K.E., Botham, K.M., 2007. Oxidation of chylomicron remnant-like particles inhibits their uptake by THP-1 macrophages by apolipoprotein E-dependent processes. Biochim. Biophys. Acta 1771, 901–910. https://doi.org/10.1016/j.bbalip.2007.04.013

Bellosta, S., Nathan, B.P., Orth, M., Dong, L.M., Mahley, R.W., Pitas, R.E., 1995. Stable expression and secretion of apolipoproteins E3 and E4 in mouse neuroblastoma cells produces differential effects on neurite outgrowth. J. Biol. Chem. 270, 27063–27071. https://doi.org/10.1074/jbc.270.45.27063

Benoit, B., Meugnier, E., Castelli, M., Chanon, S., Vieille-Marchiset, A., Durand, C., Bendridi, N., Pesenti, S., Monternier, P.-A., Durieux, A.-C., Freyssenet, D., Rieusset, J., Lefai, E., Vidal, H., Ruzzin, J., 2017. Fibroblast growth factor 19 regulates skeletal muscle mass and ameliorates muscle wasting in mice. Nat. Med. 23, 990–996. https://doi.org/10.1038/nm.4363

Beyfuss, K., Hood, D.A., 2018. A systematic review of p53 regulation of oxidative stress in skeletal muscle. Redox Rep. Commun. Free Radic. Res. 23, 100–117. https://doi.org/10.1080/13510002.2017.1416773

Bhattacharya, A., Muller, F.L., Liu, Y., Sabia, M., Liang, H., Song, W., Jang, Y.C., Ran, Q., Van Remmen, H., 2009. Denervation induces cytosolic phospholipase A2-mediated fatty acid hydroperoxide generation by muscle mitochondria. J. Biol. Chem. 284, 46–55. https://doi.org/10.1074/jbc.M806311200

Bielack, S.S., Erttmann, R., Winkler, K., Landbeck, G., 1989. Doxorubicin: effect of different schedules on toxicity and anti-tumor efficacy. Eur. J. Cancer Clin. Oncol. 25, 873–882. https://doi.org/10.1016/0277-5379(89)90135-1

Bilgen, E., Persil Çetinkol, Ö., 2020. Doxorubicin exhibits strong and selective association with VEGF Pu22 G-quadruplex. Biochim. Biophys. Acta Gen. Subj. 1864, 129720. https://doi.org/10.1016/j.bbagen.2020.129720

Blaauw, B., Schiaffino, S., Reggiani, C., 2013. Mechanisms modulating skeletal muscle phenotype. Compr. Physiol. 3, 1645–1687. https://doi.org/10.1002/cphy.c130009

Blocquiaux, S., Gorski, T., Van Roie, E., Ramaekers, M., Van Thienen, R., Nielens, H., Delecluse, C., De Bock, K., Thomis, M., 2020. The effect of resistance training, detraining and retraining on muscle strength and power, myofibre size, satellite cells and myonuclei in older men. Exp. Gerontol. 133, 110860. https://doi.org/10.1016/j.exger.2020.110860

Boden, G., 2008. Obesity and free fatty acids. Endocrinol. Metab. Clin. North Am. 37, 635–646, viii–ix. https://doi.org/10.1016/j.ecl.2008.06.007

Boscher, J., Guinard, I., Eckly, A., Lanza, F., Léon, C., 2020. Blood platelet formation at a glance. J. Cell Sci. 133, jcs244731. https://doi.org/10.1242/jcs.244731

Bosutti, A., Degens, H., 2015. The impact of resveratrol and hydrogen peroxide on muscle cell plasticity shows a dose-dependent interaction. Sci. Rep. 5, 8093. https://doi.org/10.1038/srep08093

Bottinelli, R., Reggiani, C., 2000. Human skeletal muscle fibres: molecular and functional diversity. Prog. Biophys. Mol. Biol. 73, 195–262. https://doi.org/10.1016/s0079-6107(00)00006-7

Branco, A.F., Sampaio, S.F., Moreira, A.C., Holy, J., Wallace, K.B., Baldeiras, I., Oliveira, P.J., Sardão, V.A., 2012. Differentiation-dependent doxorubicin toxicity on H9c2 cardiomyoblasts. Cardiovasc. Toxicol. 12, 326–340. https://doi.org/10.1007/s12012-012-9177-8

Bredahl, E.C., Najdawi, W., Pass, C., Siedlik, J., Eckerson, J., Drescher, K., 2021. Use of Creatine and Creatinine to Minimize Doxorubicin-Induced Cytotoxicity in Cardiac and Skeletal Muscle Myoblasts. Nutr. Cancer 73, 2597–2604. https://doi.org/10.1080/01635581.2020.1842893

Bredahl, E.C., Pfannenstiel, K.B., Quinn, C.J., Hayward, R., Hydock, D.S., 2016. Effects of Exercise on Doxorubicin-Induced Skeletal Muscle Dysfunction. Med. Sci. Sports Exerc. 48, 1468–1473. https://doi.org/10.1249/MSS.0000000000000926

Brodsky, S.V., Gealekman, O., Chen, J., Zhang, F., Togashi, N., Crabtree, M., Gross, S.S., Nasjletti, A., Goligorsky, M.S., 2004. Prevention and reversal of premature endothelial cell senescence and vasculopathy in obesity-induced diabetes by ebselen. Circ. Res. 94, 377–384. https://doi.org/10.1161/01.RES.0000111802.09964.EF

Brown, L.A., Lee, D.E., Patton, J.F., Perry, R.A., Brown, J.L., Baum, J.I., Smith-Blair, N., Greene, N.P., Washington, T.A., 2015. Diet-induced obesity alters anabolic signalling in mice at the onset of skeletal muscle regeneration. Acta Physiol. Oxf. Engl. 215, 46–57. https://doi.org/10.1111/apha.12537

Bruusgaard, J.C., Egner, I.M., Larsen, T.K., Dupre-Aucouturier, S., Desplanches, D., Gundersen, K., 2012. No change in myonuclear number during muscle unloading and reloading. J. Appl. Physiol. Bethesda Md 1985 113, 290–296. https://doi.org/10.1152/japplphysiol.00436.2012

Bruusgaard, J.C., Gundersen, K., 2008. In vivo time-lapse microscopy reveals no loss of murine myonuclei during weeks of muscle atrophy. J. Clin. Invest. 118, 1450–1457. https://doi.org/10.1172/JCI34022

Brzoska, E., Kowalewska, M., Markowska-Zagrajek, A., Kowalski, K., Archacka, K., Zimowska, M., Grabowska, I., Czerwińska, A.M., Czarnecka-Góra, M., Stremińska, W., Jańczyk-Ilach, K., Ciemerych, M.A., 2012. Sdf-1 (CXCL12) improves skeletal muscle regeneration via the mobilisation of Cxcr4 and CD34 expressing cells. Biol. Cell 104, 722–737. https://doi.org/10.1111/boc.201200022

Bushby, K., Finkel, R., Birnkrant, D.J., Case, L.E., Clemens, P.R., Cripe, L., Kaul, A., Kinnett, K., McDonald, C., Pandya, S., Poysky, J., Shapiro, F., Tomezsko, J., Constantin, C., DMD Care Considerations Working Group, 2010. Diagnosis and management of Duchenne muscular dystrophy, part 1: diagnosis, and pharmacological and psychosocial management. Lancet Neurol. 9, 77–93. https://doi.org/10.1016/S1474-4422(09)70271-6

Bye, A.P., Unsworth, A.J., Gibbins, J.M., 2016. Platelet signaling: a complex interplay between inhibitory and activatory networks. J. Thromb. Haemost. JTH 14, 918–930. https://doi.org/10.1111/jth.13302

Caiozzo, V.J., Baker, M.J., Baldwin, K.M., 1997. Modulation of myosin isoform expression by mechanical loading: role of stimulation frequency. J. Appl. Physiol. Bethesda Md 1985 82, 211–218. https://doi.org/10.1152/jappl.1997.82.1.211

Calderón, J.C., Bolaños, P., Caputo, C., 2014. The excitation-contraction coupling mechanism in skeletal muscle. Biophys. Rev. 6, 133–160. https://doi.org/10.1007/s12551-013-0135-x

Camera, M., Toschi, V., Brambilla, M., Lettino, M., Rossetti, L., Canzano, P., Di Minno, A., Tremoli, E., 2015. The Role of Tissue Factor in Atherothrombosis and Coronary Artery Disease: Insights into Platelet Tissue Factor. Semin. Thromb. Hemost. 41, 737–746. https://doi.org/10.1055/s-0035-1564041

Carbone, F., Teixeira, P.C., Braunersreuther, V., Mach, F., Vuilleumier, N., Montecucco, F., 2015. Pathophysiology and Treatments of Oxidative Injury in Ischemic Stroke: Focus on the Phagocytic NADPH Oxidase 2. Antioxid. Redox Signal. 23, 460–489. https://doi.org/10.1089/ars.2013.5778

Carvalho, A.N., Firuzi, O., Gama, M.J., Horssen, J. van, Saso, L., 2017. Oxidative Stress and Antioxidants in Neurological Diseases: Is There Still Hope? Curr. Drug Targets 18, 705–718. https://doi.org/10.2174/1389450117666160401120514

Carvalho, C., Santos, R.X., Cardoso, S., Correia, S., Oliveira, P.J., Santos, M.S., Moreira, P.I., 2009. Doxorubicin: the good, the bad and the ugly effect. Curr. Med. Chem. 16, 3267–3285. https://doi.org/10.2174/092986709788803312

Casas, A.I., Dao, V.T.-V., Daiber, A., Maghzal, G.J., Di Lisa, F., Kaludercic, N., Leach, S., Cuadrado, A., Jaquet, V., Seredenina, T., Krause, K.H., López, M.G., Stocker, R., Ghezzi, P., Schmidt, H.H.H.W., 2015. Reactive Oxygen-Related Diseases: Therapeutic Targets and Emerging Clinical Indications. Antioxid. Redox Signal. 23, 1171–1185. https://doi.org/10.1089/ars.2015.6433

Casella, G., Munk, R., Kim, K.M., Piao, Y., De, S., Abdelmohsen, K., Gorospe, M., 2019. Transcriptome signature of cellular senescence. Nucleic Acids Res. 47, 7294–7305. https://doi.org/10.1093/nar/gkz555

Casino, P.R., Kilcoyne, C.M., Quyyumi, A.A., Hoeg, J.M., Panza, J.A., 1994. Investigation of decreased availability of nitric oxide precursor as the mechanism responsible for impaired endothelium-dependent vasodilation in hypercholesterolemic patients. J. Am. Coll. Cardiol. 23, 844–850. https://doi.org/10.1016/0735-1097(94)90628-9

Catani, M.V., Savini, I., Duranti, G., Caporossi, D., Ceci, R., Sabatini, S., Avigliano, L., 2004. Nuclear factor kappaB and activating protein 1 are involved in differentiation-related resistance to oxidative stress in skeletal muscle cells. Free Radic. Biol. Med. 37, 1024–1036. https://doi.org/10.1016/j.freeradbiomed.2004.06.021

Celegato, B., Capitanio, D., Pescatori, M., Romualdi, C., Pacchioni, B., Cagnin, S., Viganò, A., Colantoni, L., Begum, S., Ricci, E., Wait, R., Lanfranchi, G., Gelfi, C., 2006. Parallel protein and transcript profiles of FSHD patient muscles correlate to the D4Z4 arrangement and reveal a common impairment of slow to fast fibre differentiation and a general deregulation of MyoD-dependent genes. Proteomics 6, 5303–5321. https://doi.org/10.1002/pmic.200600056

Centeno, C., Markle, J., Dodson, E., Stemper, I., Hyzy, M., Williams, C., Freeman, M., 2017. The use of lumbar epidural injection of platelet lysate for treatment of radicular pain. J. Exp. Orthop. 4, 38. https://doi.org/10.1186/s40634-017-0113-5

Chambers, M.A., Moylan, J.S., Smith, J.D., Goodyear, L.J., Reid, M.B., 2009. Stretch-stimulated glucose uptake in skeletal muscle is mediated by reactive oxygen species and p38 MAP-kinase. J. Physiol. 587, 3363–3373. https://doi.org/10.1113/jphysiol.2008.165639

Chan, D.C., Watts, G.F., 2006. Apolipoproteins as markers and managers of coronary risk. QJM Mon. J. Assoc. Physicians 99, 277–287. https://doi.org/10.1093/qjmed/hcl027

Chavez, J.A., Summers, S.A., 2003. Characterizing the effects of saturated fatty acids on insulin signaling and ceramide and diacylglycerol accumulation in 3T3-L1 adipocytes and C2C12 myotubes. Arch. Biochem. Biophys. 419, 101–109. https://doi.org/10.1016/j.abb.2003.08.020

Chazaud, B., 2020. Inflammation and Skeletal Muscle Regeneration: Leave It to the Macrophages! Trends Immunol. 41, 481–492. https://doi.org/10.1016/j.it.2020.04.006

Chen, F., Liu, Y., Wong, N.-K., Xiao, J., So, K.-F., 2017. Oxidative Stress in Stem Cell Aging. Cell Transplant. 26, 1483–1495. https://doi.org/10.1177/0963689717735407

Chen, T.T., Wang, J.Y., 2000. Establishment of irreversible growth arrest in myogenic differentiation requires the RB LXCXE-binding function. Mol. Cell. Biol. 20, 5571–5580. https://doi.org/10.1128/MCB.20.15.5571-5580.2000

Cheng, F., Torzewski, M., Degreif, A., Rossmann, H., Canisius, A., Lackner, K.J., 2013. Impact of glutathione peroxidase-1 deficiency on macrophage foam cell formation and proliferation: implications for atherogenesis. PloS One 8, e72063. https://doi.org/10.1371/journal.pone.0072063

Chew, P., Yuen, D.Y.C., Koh, P., Stefanovic, N., Febbraio, M.A., Kola, I., Cooper, M.E., de Haan, J.B., 2009. Site-specific antiatherogenic effect of the antioxidant ebselen in the diabetic apolipoprotein E-deficient mouse. Arterioscler. Thromb. Vasc. Biol. 29, 823–830. https://doi.org/10.1161/ATVBAHA.109.186619

Chew, P., Yuen, D.Y.C., Stefanovic, N., Pete, J., Coughlan, M.T., Jandeleit-Dahm, K.A., Thomas, M.C., Rosenfeldt, F., Cooper, M.E., de Haan, J.B., 2010. Antiatherosclerotic and renoprotective effects of ebselen in the diabetic apolipoprotein E/GPx1-double knockout mouse. Diabetes 59, 3198–3207. https://doi.org/10.2337/db10-0195

Chinzei, N., Hayashi, S., Ueha, T., Fujishiro, T., Kanzaki, N., Hashimoto, S., Sakata, S., Kihara, S., Haneda, M., Sakai, Y., Kuroda, R., Kurosaka, M., 2015. P21 deficiency delays regeneration of skeletal muscular tissue. PloS One 10, e0125765. https://doi.org/10.1371/journal.pone.0125765

Chou, M.-L., Burnouf, T., Wang, T.-J., 2014. Ex vivo expansion of bovine corneal endothelial cells in xeno-free medium supplemented with platelet releasate. PloS One 9, e99145. https://doi.org/10.1371/journal.pone.0099145

Chuang, M.-H., Ho, L.-H., Kuo, T.-F., Sheu, S.-Y., Liu, Y.-H., Lin, P.-C., Tsai, Y.-C., Yang, C.-H., Chu, C.-M., Lin, S.-Z., 2020. Regenerative Potential of Platelet-Rich Fibrin Releasate Combined with Adipose Tissue-Derived Stem Cells in a Rat Sciatic Nerve Injury Model. Cell Transplant. 29, 963689720919438. https://doi.org/10.1177/0963689720919438

Chung, L.-H., Liu, S.-T., Huang, S.-M., Salter, D.M., Lee, H.-S., Hsu, Y.-J., 2020. High phosphate induces skeletal muscle atrophy and suppresses myogenic differentiation by increasing oxidative stress and activating Nrf2 signaling. Aging 12, 21446–21468. https://doi.org/10.18632/aging.103896

Chung, Y.W., Cha, J., Han, S., Chen, Y., Gucek, M., Cho, H.-J., Nakahira, K., Choi, A.M.K., Ryu, J.-H., Yoon, J.-H., 2020. Apolipoprotein E and Periostin Are Potential Biomarkers of Nasal Mucosal Inflammation. A Parallel Approach of In Vitro and In Vivo Secretomes. Am. J. Respir. Cell Mol. Biol. 62, 23–34. https://doi.org/10.1165/rcmb.2018-0248OC

Ciciliot, S., Rossi, A.C., Dyar, K.A., Blaauw, B., Schiaffino, S., 2013. Muscle type and fiber type specificity in muscle wasting. Int. J. Biochem. Cell Biol. 45, 2191–2199. https://doi.org/10.1016/j.biocel.2013.05.016

Ciciliot, S., Schiaffino, S., 2010. Regeneration of mammalian skeletal muscle. Basic mechanisms and clinical implications. Curr. Pharm. Des. 16, 906–914. https://doi.org/10.2174/138161210790883453

Clark, K.A., McElhinny, A.S., Beckerle, M.C., Gregorio, C.C., 2002. Striated muscle cytoarchitecture: an intricate web of form and function. Annu. Rev. Cell Dev. Biol. 18, 637–706. https://doi.org/10.1146/annurev.cellbio.18.012502.105840

Cohen, E., Lee, Y.C., 2015. A Mechanism-Based Approach to the Management of Osteoarthritis Pain. Curr. Osteoporos. Rep. 13, 399–406. https://doi.org/10.1007/s11914-015-0291-y

Cole, L.K., Dolinsky, V.W., Dyck, J.R.B., Vance, D.E., 2011. Impaired phosphatidylcholine biosynthesis reduces atherosclerosis and prevents lipotoxic cardiac dysfunction in ApoE-/- Mice. Circ. Res. 108, 686–694. https://doi.org/10.1161/CIRCRESAHA.110.238691

Collins, C.A., Olsen, I., Zammit, P.S., Heslop, L., Petrie, A., Partridge, T.A., Morgan, J.E., 2005. Stem cell function, self-renewal, and behavioral heterogeneity of cells from the adult muscle satellite cell niche. Cell 122, 289–301. https://doi.org/10.1016/j.cell.2005.05.010

Conley, K.E., Kemper, W.F., Crowther, G.J., 2001. Limits to sustainable muscle performance: interaction between glycolysis and oxidative phosphorylation. J. Exp. Biol. 204, 3189–3194. https://doi.org/10.1242/jeb.204.18.3189

Coppinger, J.A., O'Connor, R., Wynne, K., Flanagan, M., Sullivan, M., Maguire, P.B., Fitzgerald, D.J., Cagney, G., 2007. Moderation of the platelet releasate response by aspirin. Blood 109, 4786–4792. https://doi.org/10.1182/blood-2006-07-038539

Costello, B., Chadwick, C., Saito, A., Chu, A., Maurer, A., Fleischer, S., 1986. Characterization of the junctional face membrane from terminal cisternae of sarcoplasmic reticulum. J. Cell Biol. 103, 741–753. https://doi.org/10.1083/jcb.103.3.741

Costford, S.R., Seifert, E.L., Bézaire, V., F Gerrits, M., Bevilacqua, L., Gowing, A., Harper, M.-E., 2007. The energetic implications of uncoupling protein-3 in skeletal muscle. Appl. Physiol. Nutr. Metab. Physiol. Appl. Nutr. Metab. 32, 884–894. https://doi.org/10.1139/H07-063

Courneya, K.S., Mackey, J.R., Bell, G.J., Jones, L.W., Field, C.J., Fairey, A.S., 2003. Randomized controlled trial of exercise training in postmenopausal breast cancer survivors: cardiopulmonary and quality of life outcomes. J. Clin. Oncol. Off. J. Am. Soc. Clin. Oncol. 21, 1660–1668. https://doi.org/10.1200/JCO.2003.04.093

Couteaux, R., Mira, J.-C., d'Albis, A., 1988. Regeneration of muscles after cardiotoxin injury I. Cytological aspects. Biol. Cell 62, 171–182. https://doi.org/10.1111/j.1768-322X.1988.tb00719.x

Covington, J.D., Tam, C.S., Bajpeyi, S., Galgani, J.E., Noland, R.C., Smith, S.R., Redman, L.M., Ravussin, E., 2016. Myokine Expression in Muscle and Myotubes in Response to Exercise Stimulation. Med. Sci. Sports Exerc. 48, 384–390. https://doi.org/10.1249/MSS.0000000000000787

Crawford, R.S., Albadawi, H., Robaldo, A., Peck, M.A., Abularrage, C.J., Yoo, H.-J., Lamuraglia, G.M., Watkins, M.T., 2013. Divergent systemic and local inflammatory response to hind limb demand ischemia in wild-type and ApoE-/- mice. J. Surg. Res. 183, 952–962. https://doi.org/10.1016/j.jss.2013.02.042

Czerwinska, A.M., Streminska, W., Ciemerych, M.A., Grabowska, I., 2012. Mouse gastrocnemius muscle regeneration after mechanical or cardiotoxin injury. Folia Histochem. Cytobiol. 50, 144–153. https://doi.org/10.2478/18710

da Fonseca, L., Santos, G.S., Huber, S.C., Setti, T.M., Setti, T., Lana, J.F., 2021. Human platelet lysate - A potent (and overlooked) orthobiologic. J. Clin. Orthop. Trauma 21, 101534. https://doi.org/10.1016/j.jcot.2021.101534

Datla, S.R., Peshavariya, H., Dusting, G.J., Mahadev, K., Goldstein, B.J., Jiang, F., 2007. Important role of Nox4 type NADPH oxidase in angiogenic responses in human microvascular endothelial cells in vitro. Arterioscler. Thromb. Vasc. Biol. 27, 2319–2324. https://doi.org/10.1161/ATVBAHA.107.149450

de Mos, M., van der Windt, A.E., Jahr, H., van Schie, H.T.M., Weinans, H., Verhaar, J.A.N., van Osch, G.J.V.M., 2008. Can platelet-rich plasma enhance tendon repair? A cell culture study. Am. J. Sports Med. 36, 1171–1178. https://doi.org/10.1177/0363546508314430

DeFina, L.F., Barlow, C.E., Radford, N.B., Leonard, D., Willis, B.L., 2016. The association between midlife cardiorespiratory fitness and later life chronic kidney disease: The Cooper Center Longitudinal Study. Prev. Med. 89, 178–183. https://doi.org/10.1016/j.ypmed.2016.05.030

DeFronzo, R.A., Tripathy, D., 2009. Skeletal muscle insulin resistance is the primary defect in type 2 diabetes. Diabetes Care 32 Suppl 2, S157-163. https://doi.org/10.2337/dc09-S302

Delaney, K., Kasprzycka, P., Ciemerych, M.A., Zimowska, M., 2017. The role of TGF-β1 during skeletal muscle regeneration. Cell Biol. Int. 41, 706–715. https://doi.org/10.1002/cbin.10725

Dhurat, R., Sukesh, M., 2014. Principles and Methods of Preparation of Platelet-Rich Plasma: A Review and Author's Perspective. J. Cutan. Aesthetic Surg. 7, 189–197. https://doi.org/10.4103/0974-2077.150734

Dickinson, J.M., D'Lugos, A.C., Mahmood, T.N., Ormsby, J.C., Salvo, L., Dedmon, W.L., Patel, S.H., Katsma, M.S., Mookadam, F., Gonzales, R.J., Hale, T.M., Carroll, C.C., Angadi, S.S., 2017. Exercise Protects Skeletal Muscle during Chronic Doxorubicin Administration. Med. Sci. Sports Exerc. 49, 2394–2403. https://doi.org/10.1249/MSS.0000000000001395

Diebold, L., Chandel, N.S., 2016. Mitochondrial ROS regulation of proliferating cells. Free Radic. Biol. Med. 100, 86–93. https://doi.org/10.1016/j.freeradbiomed.2016.04.198

Dimauro, I., Grasso, L., Fittipaldi, S., Fantini, C., Mercatelli, N., Racca, S., Geuna, S., Di Gianfrancesco, A., Caporossi, D., Pigozzi, F., Borrione, P., 2014. Platelet-rich plasma and skeletal muscle healing: a molecular analysis of the early

phases of the regeneration process in an experimental animal model. PloS One 9, e102993. https://doi.org/10.1371/journal.pone.0102993
D'Lugos, A.C., Fry, C.S., Ormsby, J.C., Sweeney, K.R., Brightwell, C.R., Hale, T.M., Gonzales, R.J., Angadi, S.S., Carroll, C.C., Dickinson, J.M., 2019. Chronic doxorubicin administration impacts satellite cell and capillary abundance in a muscle-specific manner. Physiol. Rep. 7, e14052. https://doi.org/10.14814/phy2.14052
do Amaral, R.J., Matsiko, A., Tomazette, M.R., Rocha, W.K., Cordeiro-Spinetti, E., Levingstone, T.J., Farina, M., O'Brien, F.J., El-Cheikh, M.C., Balduino, A., 2015. Platelet-rich plasma releasate differently stimulates cellular commitment toward the chondrogenic lineage according to concentration. J. Tissue Eng. 6, 2041731415594127. https://doi.org/10.1177/2041731415594127
Dragan, A.I., Pavlovic, R., McGivney, J.B., Casas-Finet, J.R., Bishop, E.S., Strouse, R.J., Schenerman, M.A., Geddes, C.D., 2012. SYBR Green I: fluorescence properties and interaction with DNA. J. Fluoresc. 22, 1189–1199. https://doi.org/10.1007/s10895-012-1059-8
D'Souza, D.M., Al-Sajee, D., Hawke, T.J., 2013. Diabetic myopathy: impact of diabetes mellitus on skeletal muscle progenitor cells. Front. Physiol. 4, 379. https://doi.org/10.3389/fphys.2013.00379
D'Souza, D.M., Trajcevski, K.E., Al-Sajee, D., Wang, D.C., Thomas, M., Anderson, J.E., Hawke, T.J., 2015. Diet-induced obesity impairs muscle satellite cell activation and muscle repair through alterations in hepatocyte growth factor signaling. Physiol. Rep. 3, e12506. https://doi.org/10.14814/phy2.12506
Duddy, W., Duguez, S., Johnston, H., Cohen, T.V., Phadke, A., Gordish-Dressman, H., Nagaraju, K., Gnocchi, V., Low, S., Partridge, T., 2015. Muscular dystrophy in the mdx mouse is a severe myopathy compounded by hypotrophy, hypertrophy and hyperplasia. Skelet. Muscle 5, 16. https://doi.org/10.1186/s13395-015-0041-y
Dulhunty, A.F., Wei-LaPierre, L., Casarotto, M.G., Beard, N.A., 2017. Core skeletal muscle ryanodine receptor calcium release complex. Clin. Exp. Pharmacol. Physiol. 44, 3–12. https://doi.org/10.1111/1440-1681.12676
Dumont, N.A., Bentzinger, C.F., Sincennes, M.-C., Rudnicki, M.A., 2015. Satellite Cells and Skeletal Muscle Regeneration. Compr. Physiol. 5, 1027–1059. https://doi.org/10.1002/cphy.c140068
Ebata, T., Mitsui, Y., Sugimoto, W., Maeda, M., Araki, K., Machiyama, H., Harada, I., Sawada, Y., Fujita, H., Hirata, H., Kawauchi, K., 2017. Substrate Stiffness Influences Doxorubicin-Induced p53 Activation via ROCK2 Expression. BioMed Res. Int. 2017, 5158961. https://doi.org/10.1155/2017/5158961
Edelstein, L.C., 2017. The role of platelet microvesicles in intercellular communication. Platelets 28, 222–227. https://doi.org/10.1080/09537104.2016.1257114
Egan, B., Zierath, J.R., 2013. Exercise metabolism and the molecular regulation of skeletal muscle adaptation. Cell Metab. 17, 162–184. https://doi.org/10.1016/j.cmet.2012.12.012
El Bakly, W., Medhat, M., Shafei, M., Tash, R., Elrefai, M., Shoukry, Y., Omar, N.N., 2020. Optimized platelet rich plasma releasate (O-rPRP) repairs galactosemia-induced ovarian follicular loss in rats by activating mTOR signaling and inhibiting apoptosis. Heliyon 6, e05006. https://doi.org/10.1016/j.heliyon.2020.e05006
Ellulu, M.S., Patimah, I., Khaza'ai, H., Rahmat, A., Abed, Y., Ali, F., 2016. Atherosclerotic cardiovascular disease: a review of initiators and protective

factors. Inflammopharmacology 24, 1–10. https://doi.org/10.1007/s10787-015-0255-y
Essex, D.W., Wu, Y., 2018. Multiple protein disulfide isomerases support thrombosis. Curr. Opin. Hematol. 25, 395–402. https://doi.org/10.1097/MOH.0000000000000449
Estevez, B., Du, X., 2017. New Concepts and Mechanisms of Platelet Activation Signaling. Physiol. Bethesda Md 32, 162–177. https://doi.org/10.1152/physiol.00020.2016
Etulain, J., 2018. Platelets in wound healing and regenerative medicine. Platelets 29, 556–568. https://doi.org/10.1080/09537104.2018.1430357
Falk, E., 2006. Pathogenesis of atherosclerosis. J. Am. Coll. Cardiol. 47, C7-12. https://doi.org/10.1016/j.jacc.2005.09.068
Faralli, H., Dilworth, F.J., 2012. Turning on myogenin in muscle: a paradigm for understanding mechanisms of tissue-specific gene expression. Comp. Funct. Genomics 2012, 836374. https://doi.org/10.1155/2012/836374
Farmer, E.E., Mueller, M.J., 2013. ROS-mediated lipid peroxidation and RES-activated signaling. Annu. Rev. Plant Biol. 64, 429–450. https://doi.org/10.1146/annurev-arplant-050312-120132
Ferreira, L.F., Laitano, O., 2016. Regulation of NADPH oxidases in skeletal muscle. Free Radic. Biol. Med. 98, 18–28. https://doi.org/10.1016/j.freeradbiomed.2016.05.011
Förstermann, U., Xia, N., Li, H., 2017. Roles of Vascular Oxidative Stress and Nitric Oxide in the Pathogenesis of Atherosclerosis. Circ. Res. 120, 713–735. https://doi.org/10.1161/CIRCRESAHA.116.309326
Fox, J.E., 1994. Transmembrane signaling across the platelet integrin glycoprotein IIb-IIIa. Ann. N. Y. Acad. Sci. 714, 75–87. https://doi.org/10.1111/j.1749-6632.1994.tb12032.x
Frey, S.P., Jansen, H., Raschke, M.J., Meffert, R.H., Ochman, S., 2012. VEGF improves skeletal muscle regeneration after acute trauma and reconstruction of the limb in a rabbit model. Clin. Orthop. 470, 3607–3614. https://doi.org/10.1007/s11999-012-2456-7
Frontera, W.R., Ochala, J., 2015. Skeletal muscle: a brief review of structure and function. Calcif. Tissue Int. 96, 183–195. https://doi.org/10.1007/s00223-014-9915-y
Fu, J., Wang, H., Deng, L., Li, J., 2016. Exercise Training Promotes Functional Recovery after Spinal Cord Injury. Neural Plast. 2016, 4039580. https://doi.org/10.1155/2016/4039580
Fu, S., Zhao, H., Shi, J., Abzhanov, A., Crawford, K., Ohno-Machado, L., Zhou, J., Du, Y., Kuo, W.P., Zhang, J., Jiang, M., Jin, J.G., 2008. Peripheral arterial occlusive disease: global gene expression analyses suggest a major role for immune and inflammatory responses. BMC Genomics 9, 369. https://doi.org/10.1186/1471-2164-9-369
Fu, X., Zhu, M., Zhang, S., Foretz, M., Viollet, B., Du, M., 2016. Obesity Impairs Skeletal Muscle Regeneration Through Inhibition of AMPK. Diabetes 65, 188–200. https://doi.org/10.2337/db15-0647
Füchtbauer, E.M., Westphal, H., 1992. MyoD and myogenin are coexpressed in regenerating skeletal muscle of the mouse. Dev. Dyn. Off. Publ. Am. Assoc. Anat. 193, 34–39. https://doi.org/10.1002/aja.1001930106
Fujio, Y., Guo, K., Mano, T., Mitsuuchi, Y., Testa, J.R., Walsh, K., 1999. Cell cycle withdrawal promotes myogenic induction of Akt, a positive modulator of

myocyte survival. Mol. Cell. Biol. 19, 5073–5082. https://doi.org/10.1128/MCB.19.7.5073
Fujita, H., Lu, X., Suzuki, M., Ishiwata, S., Kawai, M., 2004. The effect of tropomyosin on force and elementary steps of the cross-bridge cycle in reconstituted bovine myocardium. J. Physiol. 556, 637–649. https://doi.org/10.1113/jphysiol.2003.059956
Galanis, A., Pappa, A., Giannakakis, A., Lanitis, E., Dangaj, D., Sandaltzopoulos, R., 2008. Reactive oxygen species and HIF-1 signalling in cancer. Cancer Lett. 266, 12–20. https://doi.org/10.1016/j.canlet.2008.02.028
García-Prat, L., Martínez-Vicente, M., Perdiguero, E., Ortet, L., Rodríguez-Ubreva, J., Rebollo, E., Ruiz-Bonilla, V., Gutarra, S., Ballestar, E., Serrano, A.L., Sandri, M., Muñoz-Cánoves, P., 2016. Autophagy maintains stemness by preventing senescence. Nature 529, 37–42. https://doi.org/10.1038/nature16187
Gastin, P.B., 2001. Energy system interaction and relative contribution during maximal exercise. Sports Med. Auckl. NZ 31, 725–741. https://doi.org/10.2165/00007256-200131100-00003
Gaudreault, N., Kumar, N., Posada, J.M., Stephens, K.B., Reyes de Mochel, N.S., Eberlé, D., Olivas, V.R., Kim, R.Y., Harms, M.J., Johnson, S., Messina, L.M., Rapp, J.H., Raffai, R.L., 2012. ApoE suppresses atherosclerosis by reducing lipid accumulation in circulating monocytes and the expression of inflammatory molecules on monocytes and vascular endothelium. Arterioscler. Thromb. Vasc. Biol. 32, 264–272. https://doi.org/10.1161/ATVBAHA.111.238964
Getz, G.S., Reardon, C.A., 2018. Apoprotein E and Reverse Cholesterol Transport. Int. J. Mol. Sci. 19, E3479. https://doi.org/10.3390/ijms19113479
Getz, G.S., Reardon, C.A., 2009. Apoprotein E as a lipid transport and signaling protein in the blood, liver, and artery wall. J. Lipid Res. 50 Suppl, S156-161. https://doi.org/10.1194/jlr.R800058-JLR200
Gewirtz, D.A., 1999. A critical evaluation of the mechanisms of action proposed for the antitumor effects of the anthracycline antibiotics adriamycin and daunorubicin. Biochem. Pharmacol. 57, 727–741. https://doi.org/10.1016/s0006-2952(98)00307-4
Gianni-Barrera, R., Butschkau, A., Uccelli, A., Certelli, A., Valente, P., Bartolomeo, M., Groppa, E., Burger, M.G., Hlushchuk, R., Heberer, M., Schaefer, D.J., Gürke, L., Djonov, V., Vollmar, B., Banfi, A., 2018. PDGF-BB regulates splitting angiogenesis in skeletal muscle by limiting VEGF-induced endothelial proliferation. Angiogenesis 21, 883–900. https://doi.org/10.1007/s10456-018-9634-5
Gibson, N.M., Quinn, C.J., Pfannenstiel, K.B., Hydock, D.S., Hayward, R., 2014. Effects of age on multidrug resistance protein expression and doxorubicin accumulation in cardiac and skeletal muscle. Xenobiotica Fate Foreign Compd. Biol. Syst. 44, 472–479. https://doi.org/10.3109/00498254.2013.846489
Gierer, P., Röther, J., Mittlmeier, T., Gradl, G., Vollmar, B., 2010. Ebselen reduces inflammation and microvascular perfusion failure after blunt skeletal muscle injury of the rat. J. Trauma 68, 853–858. https://doi.org/10.1097/TA.0b013e3181b28a18
Gimbrone, M.A., García-Cardeña, G., 2016. Endothelial Cell Dysfunction and the Pathobiology of Atherosclerosis. Circ. Res. 118, 620–636. https://doi.org/10.1161/CIRCRESAHA.115.306301

Girgenrath, M., Kostek, C.A., Miller, J.B., 2005. Diseased muscles that lack dystrophin or laminin-alpha2 have altered compositions and proliferation of mononuclear cell populations. BMC Neurol. 5, 7. https://doi.org/10.1186/1471-2377-5-7

Go, G.-W., Mani, A., 2012. Low-density lipoprotein receptor (LDLR) family orchestrates cholesterol homeostasis. Yale J. Biol. Med. 85, 19–28.

Golebiewska, E.M., Poole, A.W., 2015. Platelet secretion: From haemostasis to wound healing and beyond. Blood Rev. 29, 153–162. https://doi.org/10.1016/j.blre.2014.10.003

Grabiec, K., Majewska, A., Wicik, Z., Milewska, M., Błaszczyk, M., Grzelkowska-Kowalczyk, K., 2016. The effect of palmitate supplementation on gene expression profile in proliferating myoblasts. Cell Biol. Toxicol. 32, 185–198. https://doi.org/10.1007/s10565-016-9324-2

Greenow, K., Pearce, N.J., Ramji, D.P., 2005. The key role of apolipoprotein E in atherosclerosis. J. Mol. Med. Berl. Ger. 83, 329–342. https://doi.org/10.1007/s00109-004-0631-3

Grounds, M.D., Garrett, K.L., Lai, M.C., Wright, W.E., Beilharz, M.W., 1992. Identification of skeletal muscle precursor cells in vivo by use of MyoD1 and myogenin probes. Cell Tissue Res. 267, 99–104. https://doi.org/10.1007/BF00318695

Gu, N., Guo, Q., Mao, K., Hu, H., Jin, S., Zhou, Y., He, H., Oh, Y., Liu, C., Wu, Q., 2015. Palmitate increases musclin gene expression through activation of PERK signaling pathway in C2C12 myotubes. Biochem. Biophys. Res. Commun. 467, 521–526. https://doi.org/10.1016/j.bbrc.2015.10.005

Guigni, B.A., Callahan, D.M., Tourville, T.W., Miller, M.S., Fiske, B., Voigt, T., Korwin-Mihavics, B., Anathy, V., Dittus, K., Toth, M.J., 2018. Skeletal muscle atrophy and dysfunction in breast cancer patients: role for chemotherapy-derived oxidant stress. Am. J. Physiol. Cell Physiol. 315, C744–C756. https://doi.org/10.1152/ajpcell.00002.2018

Gundry, C.N., Vandersteen, J.G., Reed, G.H., Pryor, R.J., Chen, J., Wittwer, C.T., 2003. Amplicon melting analysis with labeled primers: a closed-tube method for differentiating homozygotes and heterozygotes. Clin. Chem. 49, 396–406. https://doi.org/10.1373/49.3.396

Guttridge, D.C., Mayo, M.W., Madrid, L.V., Wang, C.Y., Baldwin, A.S., 2000. NF-kappaB-induced loss of MyoD messenger RNA: possible role in muscle decay and cachexia. Science 289, 2363–2366. https://doi.org/10.1126/science.289.5488.2363

Guven, A., Tunc, T., Topal, T., Kul, M., Korkmaz, A., Gundogdu, G., Onguru, O., Ozturk, H., 2008. Alpha-lipoic acid and ebselen prevent ischemia/reperfusion injury in the rat intestine. Surg. Today 38, 1029–1035. https://doi.org/10.1007/s00595-007-3752-9

Haas, T.L., Lloyd, P.G., Yang, H.-T., Terjung, R.L., 2012. Exercise training and peripheral arterial disease. Compr. Physiol. 2, 2933–3017. https://doi.org/10.1002/cphy.c110065

Haghani, K., Pashaei, S., Vakili, S., Taheripak, G., Bakhtiyari, S., 2015. TNF-α knockdown alleviates palmitate-induced insulin resistance in C2C12 skeletal muscle cells. Biochem. Biophys. Res. Commun. 460, 977–982. https://doi.org/10.1016/j.bbrc.2015.03.137

Halevy, O., Piestun, Y., Allouh, M.Z., Rosser, B.W.C., Rinkevich, Y., Reshef, R., Rozenboim, I., Wleklinski-Lee, M., Yablonka-Reuveni, Z., 2004. Pattern of Pax7 expression during myogenesis in the posthatch chicken establishes a

model for satellite cell differentiation and renewal. Dev. Dyn. Off. Publ. Am. Assoc. Anat. 231, 489–502. https://doi.org/10.1002/dvdy.20151
Hargreaves, M., Spriet, L.L., 2020. Skeletal muscle energy metabolism during exercise. Nat. Metab. 2, 817–828. https://doi.org/10.1038/s42255-020-0251-4
Harrington, E.A., Bruce, J.L., Harlow, E., Dyson, N., 1998. pRB plays an essential role in cell cycle arrest induced by DNA damage. Proc. Natl. Acad. Sci. U. S. A. 95, 11945–11950. https://doi.org/10.1073/pnas.95.20.11945
Harris, J.B., 2003. Myotoxic phospholipases A2 and the regeneration of skeletal muscles. Toxicon Off. J. Int. Soc. Toxinology 42, 933–945. https://doi.org/10.1016/j.toxicon.2003.11.011
Harrison, P., Cramer, E.M., 1993. Platelet alpha-granules. Blood Rev. 7, 52–62. https://doi.org/10.1016/0268-960x(93)90024-x
Hawke, T.J., Meeson, A.P., Jiang, N., Graham, S., Hutcheson, K., DiMaio, J.M., Garry, D.J., 2003. p21 is essential for normal myogenic progenitor cell function in regenerating skeletal muscle. Am. J. Physiol. Cell Physiol. 285, C1019-1027. https://doi.org/10.1152/ajpcell.00055.2003
Hayward, R., Hydock, D., Gibson, N., Greufe, S., Bredahl, E., Parry, T., 2013. Tissue retention of doxorubicin and its effects on cardiac, smooth, and skeletal muscle function. J. Physiol. Biochem. 69, 177–187. https://doi.org/10.1007/s13105-012-0200-0
He, A.-D., Xie, W., Song, W., Ma, Y.-Y., Liu, G., Liang, M.-L., Da, X.-W., Yao, G.-Q., Zhang, B.-X., Gao, C.-J., Xiang, J.-Z., Ming, Z.-Y., 2017. Platelet releasates promote the proliferation of hepatocellular carcinoma cells by suppressing the expression of KLF6. Sci. Rep. 7, 3989. https://doi.org/10.1038/s41598-017-02801-1
Herrington, W., Lacey, B., Sherliker, P., Armitage, J., Lewington, S., 2016. Epidemiology of Atherosclerosis and the Potential to Reduce the Global Burden of Atherothrombotic Disease. Circ. Res. 118, 535–546. https://doi.org/10.1161/CIRCRESAHA.115.307611
Hikida, R.S., Van Nostran, S., Murray, J.D., Staron, R.S., Gordon, S.E., Kraemer, W.J., 1997. Myonuclear loss in atrophied soleus muscle fibers. Anat. Rec. 247, 350–354. https://doi.org/10.1002/(SICI)1097-0185(199703)247:3<350::AID-AR6>3.0.CO;2-Y
Holinstat, M., 2017. Normal platelet function. Cancer Metastasis Rev. 36, 195–198. https://doi.org/10.1007/s10555-017-9677-x
Hoppeler, H., Lüthi, P., Claassen, H., Weibel, E.R., Howald, H., 1973. The ultrastructure of the normal human skeletal muscle. A morphometric analysis on untrained men, women and well-trained orienteers. Pflugers Arch. 344, 217–232. https://doi.org/10.1007/BF00588462
Hu, P., Zhang, K.M., Wright, L.D., Spratt, J.A., Briggs, F.N., 1997. Correlations between MyoD, myogenin, SERCA1, SERCA2 and phospholamban transcripts during transformation of type-II to type-I skeletal muscle fibers. Pflugers Arch. 434, 209–211. https://doi.org/10.1007/s004240050386
Hu, Z., Wang, H., Lee, I.H., Modi, S., Wang, X., Du, J., Mitch, W.E., 2010. PTEN inhibition improves muscle regeneration in mice fed a high-fat diet. Diabetes 59, 1312–1320. https://doi.org/10.2337/db09-1155
Huang, Z., Miao, X., Luan, Y., Zhu, L., Kong, F., Lu, Q., Pernow, J., Nilsson, G., Li, N., 2015. PAR1-stimulated platelet releasate promotes angiogenic activities of endothelial progenitor cells more potently than PAR4-stimulated platelet

releasate. J. Thromb. Haemost. JTH 13, 465–476. https://doi.org/10.1111/jth.12815
Huang, Z.H., Gu, D., Mazzone, T., 2009. Role of adipocyte-derived apoE in modulating adipocyte size, lipid metabolism, and gene expression in vivo. Am. J. Physiol. Endocrinol. Metab. 296, E1110-1119. https://doi.org/10.1152/ajpendo.90964.2008
Huebbe, P., Lodge, J.K., Rimbach, G., 2010. Implications of apolipoprotein E genotype on inflammation and vitamin E status. Mol. Nutr. Food Res. 54, 623–630. https://doi.org/10.1002/mnfr.200900398
Hughes, S.M., Taylor, J.M., Tapscott, S.J., Gurley, C.M., Carter, W.J., Peterson, C.A., 1993. Selective accumulation of MyoD and myogenin mRNAs in fast and slow adult skeletal muscle is controlled by innervation and hormones. Dev. Camb. Engl. 118, 1137–1147. https://doi.org/10.1242/dev.118.4.1137
Hvas, A.-M., 2016. Platelet Function in Thrombosis and Hemostasis. Semin. Thromb. Hemost. 42, 183–184. https://doi.org/10.1055/s-0036-1572329
Hwang, A.B., Brack, A.S., 2018. Muscle Stem Cells and Aging. Curr. Top. Dev. Biol. 126, 299–322. https://doi.org/10.1016/bs.ctdb.2017.08.008
Ikewaki, K., Cain, W., Thomas, F., Shamburek, R., Zech, L.A., Usher, D., Brewer, H.B., Rader, D.J., 2004. Abnormal in vivo metabolism of apoB-containing lipoproteins in human apoE deficiency. J. Lipid Res. 45, 1302–1311. https://doi.org/10.1194/jlr.M400020-JLR200
Imaizumi, K., 2011. Diet and atherosclerosis in apolipoprotein E-deficient mice. Biosci. Biotechnol. Biochem. 75, 1023–1035. https://doi.org/10.1271/bbb.110059
Irshad, M., Dubey, R., 2005. Apolipoproteins and their role in different clinical conditions: an overview. Indian J. Biochem. Biophys. 42, 73–80.
Ishibashi, S., Brown, M.S., Goldstein, J.L., Gerard, R.D., Hammer, R.E., Herz, J., 1993. Hypercholesterolemia in low density lipoprotein receptor knockout mice and its reversal by adenovirus-mediated gene delivery. J. Clin. Invest. 92, 883–893. https://doi.org/10.1172/JCI116663
Ito, J.-I., Nagayasu, Y., Hoshikawa, M., Kato, K.H., Miura, Y., Asai, K., Hayashi, H., Yokoyama, S., Michikawa, M., 2013. Enhancement of FGF-1 release along with cytosolic proteins from rat astrocytes by hydrogen peroxide. Brain Res. 1522, 12–21. https://doi.org/10.1016/j.brainres.2013.05.035
Jakic, B., Carlsson, M., Buszko, M., Cappellano, G., Ploner, C., Onestingel, E., Foti, M., Hackl, H., Demetz, E., Dietrich, H., Wick, C., Wick, G., 2019. The Effects of Endurance Exercise and Diet on Atherosclerosis in Young and Aged ApoE-/- and Wild-Type Mice. Gerontology 65, 45–56. https://doi.org/10.1159/000492571
Jang, Y.C., Sinha, M., Cerletti, M., Dall'Osso, C., Wagers, A.J., 2011. Skeletal muscle stem cells: effects of aging and metabolism on muscle regenerative function. Cold Spring Harb. Symp. Quant. Biol. 76, 101–111. https://doi.org/10.1101/sqb.2011.76.010652
Jaspers, R.T., Feenstra, H.M., van Beek-Harmsen, B.J., Huijing, P.A., van der Laarse, W.J., 2006. Differential effects of muscle fibre length and insulin on muscle-specific mRNA content in isolated mature muscle fibres during long-term culture. Cell Tissue Res. 326, 795–808. https://doi.org/10.1007/s00441-006-0227-z
Jeong, S.-J., Kim, S., Park, J.-G., Jung, I.-H., Lee, M.-N., Jeon, S., Kweon, H.Y., Yu, D.-Y., Lee, S.-H., Jang, Y., Kang, S.W., Han, K.-H., Miller, Y.I., Park, Y.M., Cheong, C., Choi, J.-H., Oh, G.T., 2018. Prdx1 (peroxiredoxin 1) deficiency

reduces cholesterol efflux via impaired macrophage lipophagic flux. Autophagy 14, 120–133. https://doi.org/10.1080/15548627.2017.1327942
Jiang, L., Luan, Y., Miao, X., Sun, C., Li, K., Huang, Z., Xu, D., Zhang, M., Kong, F., Li, N., 2017. Platelet releasate promotes breast cancer growth and angiogenesis via VEGF-integrin cooperative signalling. Br. J. Cancer 117, 695–703. https://doi.org/10.1038/bjc.2017.214
Jin, Q., Qiao, C., Li, Jianbin, Xiao, B., Li, Juan, Xiao, X., 2019. A GDF11/myostatin inhibitor, GDF11 propeptide-Fc, increases skeletal muscle mass and improves muscle strength in dystrophic mdx mice. Skelet. Muscle 9, 16. https://doi.org/10.1186/s13395-019-0197-y
Jin, X., Kim, J.-G., Oh, M.-J., Oh, H.-Y., Sohn, Y.-W., Pian, X., Yin, J.L., Beck, S., Lee, N., Son, J., Kim, H., Yan, C., Wang, J.H., Choi, Y.-J., Whang, K.Y., 2007. Opposite roles of MRF4 and MyoD in cell proliferation and myogenic differentiation. Biochem. Biophys. Res. Commun. 364, 476–482. https://doi.org/10.1016/j.bbrc.2007.10.042
Jing, Y.-Y., Li, D., Wu, F., Gong, L.-L., Li, R., 2017. GDF11 does not improve the palmitate induced insulin resistance in C2C12. Eur. Rev. Med. Pharmacol. Sci. 21, 1795–1802.
Jofre-Monseny, L., de Pascual-Teresa, S., Plonka, E., Huebbe, P., Boesch-Saadatmandi, C., Minihane, A.-M., Rimbach, G., 2007a. Differential effects of apolipoprotein E3 and E4 on markers of oxidative status in macrophages. Br. J. Nutr. 97, 864–871. https://doi.org/10.1017/S0007114507669219
Jofre-Monseny, L., Loboda, A., Wagner, A.E., Huebbe, P., Boesch-Saadatmandi, C., Jozkowicz, A., Minihane, A.-M., Dulak, J., Rimbach, G., 2007b. Effects of apoE genotype on macrophage inflammation and heme oxygenase-1 expression. Biochem. Biophys. Res. Commun. 357, 319–324. https://doi.org/10.1016/j.bbrc.2007.03.150
Jornayvaz, F.R., Samuel, V.T., Shulman, G.I., 2010. The role of muscle insulin resistance in the pathogenesis of atherogenic dyslipidemia and nonalcoholic fatty liver disease associated with the metabolic syndrome. Annu. Rev. Nutr. 30, 273–290. https://doi.org/10.1146/annurev.nutr.012809.104726
Josefs, T., Barrett, T.J., Brown, E.J., Quezada, A., Wu, X., Voisin, M., Amengual, J., Fisher, E.A., 2020. Neutrophil extracellular traps promote macrophage inflammation and impair atherosclerosis resolution in diabetic mice. JCI Insight 5, 134796. https://doi.org/10.1172/jci.insight.134796
Kakudo, N., Morimoto, N., Kushida, S., Ogawa, T., Kusumoto, K., 2014. Platelet-rich plasma releasate promotes angiogenesis in vitro and in vivo. Med. Mol. Morphol. 47, 83–89. https://doi.org/10.1007/s00795-013-0045-9
Kang, J., Albadawi, H., Patel, V.I., Abbruzzese, T.A., Yoo, J.-H., Austen, W.G., Watkins, M.T., 2008. Apolipoprotein E-/- mice have delayed skeletal muscle healing after hind limb ischemia-reperfusion. J. Vasc. Surg. 48, 701–708. https://doi.org/10.1016/j.jvs.2008.04.006
Kannappan, R., Mattapally, S., Wagle, P.A., Zhang, J., 2018. Transactivation domain of p53 regulates DNA repair and integrity in human iPS cells. Am. J. Physiol. Heart Circ. Physiol. 315, H512–H521. https://doi.org/10.1152/ajpheart.00160.2018
Kark, L.R., Karp, J.M., Davies, J.E., 2006. Platelet releasate increases the proliferation and migration of bone marrow-derived cells cultured under osteogenic conditions. Clin. Oral Implants Res. 17, 321–327. https://doi.org/10.1111/j.1600-0501.2005.01189.x

Kattoor, A.J., Pothineni, N.V.K., Palagiri, D., Mehta, J.L., 2017. Oxidative Stress in Atherosclerosis. Curr. Atheroscler. Rep. 19, 42. https://doi.org/10.1007/s11883-017-0678-6

Kelc, R., Trapecar, M., Gradisnik, L., Rupnik, M.S., Vogrin, M., 2015. Platelet-rich plasma, especially when combined with a TGF-β inhibitor promotes proliferation, viability and myogenic differentiation of myoblasts in vitro. PloS One 10, e0117302. https://doi.org/10.1371/journal.pone.0117302

Kennedy, K.A.M., Sandiford, S.D.E., Skerjanc, I.S., Li, S.S.-C., 2012. Reactive oxygen species and the neuronal fate. Cell. Mol. Life Sci. CMLS 69, 215–221. https://doi.org/10.1007/s00018-011-0807-2

Kiani, F.A., Fischer, S., 2016. ATP-dependent interplay between local and global conformational changes in the myosin motor. Cytoskelet. Hoboken NJ 73, 643–651. https://doi.org/10.1002/cm.21333

Kim, B.M., Choi, Y.J., Lee, Y.H., Joe, Y.A., Hong, S.H., 2010. N,N-Dimethyl phytosphingosine sensitizes HL-60/MX2, a multidrug-resistant variant of HL-60 cells, to doxorubicin-induced cytotoxicity through ROS-mediated release of cytochrome c and AIF. Apoptosis Int. J. Program. Cell Death 15, 982–993. https://doi.org/10.1007/s10495-010-0512-x

Kim, H.-S., Lee, Y.-S., Kim, D.-K., 2009. Doxorubicin exerts cytotoxic effects through cell cycle arrest and Fas-mediated cell death. Pharmacology 84, 300–309. https://doi.org/10.1159/000245937

Klos, K., Shimmin, L., Ballantyne, C., Boerwinkle, E., Clark, A., Coresh, J., Hanis, C., Liu, K., Sayre, S., Hixson, J., 2008. APOE/C1/C4/C2 hepatic control region polymorphism influences plasma apoE and LDL cholesterol levels. Hum. Mol. Genet. 17, 2039–2046. https://doi.org/10.1093/hmg/ddn101

Knowles, L.M., Axelrod, F., Browne, C.D., Smith, J.W., 2004. A fatty acid synthase blockade induces tumor cell-cycle arrest by down-regulating Skp2. J. Biol. Chem. 279, 30540–30545. https://doi.org/10.1074/jbc.M405061200

Knudsen, K.E., Booth, D., Naderi, S., Sever-Chroneos, Z., Fribourg, A.F., Hunton, I.C., Feramisco, J.R., Wang, J.Y., Knudsen, E.S., 2000. RB-dependent S-phase response to DNA damage. Mol. Cell. Biol. 20, 7751–7763. https://doi.org/10.1128/MCB.20.20.7751-7763.2000

Koo, J.H., Smiley, M.A., Lovering, R.M., Margolis, F.L., 2007. Bex1 knock out mice show altered skeletal muscle regeneration. Biochem. Biophys. Res. Commun. 363, 405–410. https://doi.org/10.1016/j.bbrc.2007.08.186

Kosmacheva, S.M., Danilkovich, N.N., Shchepen', A.V., Ignatenko, S.I., Potapnev, M.P., 2014. Effect of platelet releasate on osteogenic differentiation of human mesenchymal bone marrow stem cells. Bull. Exp. Biol. Med. 156, 560–565. https://doi.org/10.1007/s10517-014-2396-1

Koutakis, P., Miserlis, D., Myers, S.A., Kim, J.K.-S., Zhu, Z., Papoutsi, E., Swanson, S.A., Haynatzki, G., Ha, D.M., Carpenter, L.A., McComb, R.D., Johanning, J.M., Casale, G.P., Pipinos, I.I., 2015. Abnormal accumulation of desmin in gastrocnemius myofibers of patients with peripheral artery disease: associations with altered myofiber morphology and density, mitochondrial dysfunction and impaired limb function. J. Histochem. Cytochem. Off. J. Histochem. Soc. 63, 256–269. https://doi.org/10.1369/0022155415569348

Koutakis, P., Weiss, D.J., Miserlis, D., Shostrom, V.K., Papoutsi, E., Ha, D.M., Carpenter, L.A., McComb, R.D., Casale, G.P., Pipinos, I.I., 2014. Oxidative damage in the gastrocnemius of patients with peripheral artery disease is

myofiber type selective. Redox Biol. 2, 921–928. https://doi.org/10.1016/j.redox.2014.07.002
Kowalski, K., Kołodziejczyk, A., Sikorska, M., Płaczkiewicz, J., Cichosz, P., Kowalewska, M., Stremińska, W., Jańczyk-Ilach, K., Koblowska, M., Fogtman, A., Iwanicka-Nowicka, R., Ciemerych, M.A., Brzoska, E., 2017. Stem cells migration during skeletal muscle regeneration - the role of Sdf-1/Cxcr4 and Sdf-1/Cxcr7 axis. Cell Adhes. Migr. 11, 384–398. https://doi.org/10.1080/19336918.2016.1227911
Kruse, R., Højlund, K., 2018. Proteomic study of skeletal muscle in obesity and type 2 diabetes: progress and potential. Expert Rev. Proteomics 15, 817–828. https://doi.org/10.1080/14789450.2018.1528147
Kuang, S., Kuroda, K., Le Grand, F., Rudnicki, M.A., 2007. Asymmetric self-renewal and commitment of satellite stem cells in muscle. Cell 129, 999–1010. https://doi.org/10.1016/j.cell.2007.03.044
Kubista, M., Andrade, J.M., Bengtsson, M., Forootan, A., Jonák, J., Lind, K., Sindelka, R., Sjöback, R., Sjögreen, B., Strömbom, L., Ståhlberg, A., Zoric, N., 2006. The real-time polymerase chain reaction. Mol. Aspects Med. 27, 95–125. https://doi.org/10.1016/j.mam.2005.12.007
Kuo, I.Y., Ehrlich, B.E., 2015. Signaling in muscle contraction. Cold Spring Harb. Perspect. Biol. 7, a006023. https://doi.org/10.1101/cshperspect.a006023
Kurabayashi, M., Jeyaseelan, R., Kedes, L., 1994. Doxorubicin represses the function of the myogenic helix-loop-helix transcription factor MyoD. Involvement of Id gene induction. J. Biol. Chem. 269, 6031–6039.
Kurabayashi, M., Jeyaseelan, R., Kedes, L., 1993. Antineoplastic agent doxorubicin inhibits myogenic differentiation of C2 myoblasts. J. Biol. Chem. 268, 5524–5529.
Lach-Trifilieff, E., Minetti, G.C., Sheppard, K., Ibebunjo, C., Feige, J.N., Hartmann, S., Brachat, S., Rivet, H., Koelbing, C., Morvan, F., Hatakeyama, S., Glass, D.J., 2014. An antibody blocking activin type II receptors induces strong skeletal muscle hypertrophy and protects from atrophy. Mol. Cell. Biol. 34, 606–618. https://doi.org/10.1128/MCB.01307-13
Lahoute, C., Sotiropoulos, A., Favier, M., Guillet-Deniau, I., Charvet, C., Ferry, A., Butler-Browne, G., Metzger, D., Tuil, D., Daegelen, D., 2008. Premature aging in skeletal muscle lacking serum response factor. PloS One 3, e3910. https://doi.org/10.1371/journal.pone.0003910
Lai, C.-F., Shao, J.-S., Behrmann, A., Krchma, K., Cheng, S.-L., Towler, D.A., 2012. TNFR1-activated reactive oxidative species signals up-regulate osteogenic Msx2 programs in aortic myofibroblasts. Endocrinology 153, 3897–3910. https://doi.org/10.1210/en.2012-1216
Laumonier, T., Menetrey, J., 2016. Muscle injuries and strategies for improving their repair. J. Exp. Orthop. 3, 15. https://doi.org/10.1186/s40634-016-0051-7
Laursen, J.B., Somers, M., Kurz, S., McCann, L., Warnholtz, A., Freeman, B.A., Tarpey, M., Fukai, T., Harrison, D.G., 2001. Endothelial regulation of vasomotion in apoE-deficient mice: implications for interactions between peroxynitrite and tetrahydrobiopterin. Circulation 103, 1282–1288. https://doi.org/10.1161/01.cir.103.9.1282
Lazar, S., Goldfinger, L.E., 2021. Platelets and extracellular vesicles and their cross talk with cancer. Blood 137, 3192–3200. https://doi.org/10.1182/blood.2019004119

Le Bihan, M.-C., Barrio-Hernandez, I., Mortensen, T.P., Henningsen, J., Jensen, S.S., Bigot, A., Blagoev, B., Butler-Browne, G., Kratchmarova, I., 2015. Cellular Proteome Dynamics during Differentiation of Human Primary Myoblasts. J. Proteome Res. 14, 3348–3361. https://doi.org/10.1021/acs.jproteome.5b00397

Lee, J.E., Park, J.H., Shin, I.C., Koh, H.C., 2012. Reactive oxygen species regulated mitochondria-mediated apoptosis in PC12 cells exposed to chlorpyrifos. Toxicol. Appl. Pharmacol. 263, 148–162. https://doi.org/10.1016/j.taap.2012.06.005

Lee, V.W.S., Harris, D.C.H., 2011. Adriamycin nephropathy: a model of focal segmental glomerulosclerosis. Nephrol. Carlton Vic 16, 30–38. https://doi.org/10.1111/j.1440-1797.2010.01383.x

Lee, Y., Kockx, M., Raftery, M.J., Jessup, W., Griffith, R., Kritharides, L., 2010. Glycosylation and sialylation of macrophage-derived human apolipoprotein E analyzed by SDS-PAGE and mass spectrometry: evidence for a novel site of glycosylation on Ser290. Mol. Cell. Proteomics MCP 9, 1968–1981. https://doi.org/10.1074/mcp.M900430-MCP200

Li, H., Usas, A., Poddar, M., Chen, C.-W., Thompson, S., Ahani, B., Cummins, J., Lavasani, M., Huard, J., 2013. Platelet-rich plasma promotes the proliferation of human muscle derived progenitor cells and maintains their stemness. PloS One 8, e64923. https://doi.org/10.1371/journal.pone.0064923

Li, J., Yi, X., Yao, Z., Chakkalakal, J.V., Xing, L., Boyce, B.F., 2020. TNF Receptor-Associated Factor 6 Mediates TNFα-Induced Skeletal Muscle Atrophy in Mice During Aging. J. Bone Miner. Res. Off. J. Am. Soc. Bone Miner. Res. 35, 1535–1548. https://doi.org/10.1002/jbmr.4021

Li, S., Czubryt, M.P., McAnally, J., Bassel-Duby, R., Richardson, J.A., Wiebel, F.F., Nordheim, A., Olson, E.N., 2005. Requirement for serum response factor for skeletal muscle growth and maturation revealed by tissue-specific gene deletion in mice. Proc. Natl. Acad. Sci. U. S. A. 102, 1082–1087. https://doi.org/10.1073/pnas.0409103102

Li, X., Zhang, S., Zhang, Y., Liu, P., Li, M., Lu, Y., Han, J., 2021. Myoblast differentiation of C2C12 cell may related with oxidative stress. Intractable Rare Dis. Res. 10, 173–178. https://doi.org/10.5582/irdr.2021.01058

Li, Y.-H., Liu, L., 2014. Apolipoprotein E synthesized by adipocyte and apolipoprotein E carried on lipoproteins modulate adipocyte triglyceride content. Lipids Health Dis. 13, 136. https://doi.org/10.1186/1476-511X-13-136

Li, Z., Delaney, M.K., O'Brien, K.A., Du, X., 2010. Signaling during platelet adhesion and activation. Arterioscler. Thromb. Vasc. Biol. 30, 2341–2349. https://doi.org/10.1161/ATVBAHA.110.207522

Li, Z., Mericskay, M., Agbulut, O., Butler-Browne, G., Carlsson, L., Thornell, L.E., Babinet, C., Paulin, D., 1997. Desmin is essential for the tensile strength and integrity of myofibrils but not for myogenic commitment, differentiation, and fusion of skeletal muscle. J. Cell Biol. 139, 129–144. https://doi.org/10.1083/jcb.139.1.129

Lieber, R.L., Roberts, T.J., Blemker, S.S., Lee, S.S.M., Herzog, W., 2017. Skeletal muscle mechanics, energetics and plasticity. J. Neuroengineering Rehabil. 14, 108. https://doi.org/10.1186/s12984-017-0318-y

Liu, G., Mac Gabhann, F., Popel, A.S., 2012. Effects of fiber type and size on the heterogeneity of oxygen distribution in exercising skeletal muscle. PloS One 7, e44375. https://doi.org/10.1371/journal.pone.0044375

Liu, H.-Y., Huang, C.-F., Lin, T.-C., Tsai, C.-Y., Tina Chen, S.-Y., Liu, A., Chen, W.-H., Wei, H.-J., Wang, M.-F., Williams, D.F., Deng, W.-P., 2014. Delayed animal aging through the recovery of stem cell senescence by platelet rich plasma. Biomaterials 35, 9767–9776. https://doi.org/10.1016/j.biomaterials.2014.08.034

Liu, J., Liao, S., Huang, Y., Samuel, R., Shi, T., Naxerova, K., Huang, P., Kamoun, W., Jain, R.K., Fukumura, D., Xu, L., 2011. PDGF-D improves drug delivery and efficacy via vascular normalization, but promotes lymphatic metastasis by activating CXCR4 in breast cancer. Clin. Cancer Res. Off. J. Am. Assoc. Cancer Res. 17, 3638–3648. https://doi.org/10.1158/1078-0432.CCR-10-2456

Liu, S.-T., Huang, S.-M., Ho, C.-L., Yen, L.-C., Huang, C.-J., Lin, W.-S., Chan, J.Y.-H., 2015. The regulatory mechanisms of myogenin expression in doxorubicin-treated rat cardiomyocytes. Oncotarget 6, 37443–37457. https://doi.org/10.18632/oncotarget.5338

Liu, X., Wang, Y., Zhao, S., Li, X., 2017. Fibroblast Growth Factor 21 Promotes C2C12 Cells Myogenic Differentiation by Enhancing Cell Cycle Exit. BioMed Res. Int. 2017, 1648715. https://doi.org/10.1155/2017/1648715

Livak, K.J., Schmittgen, T.D., 2001. Analysis of relative gene expression data using real-time quantitative PCR and the 2(-Delta Delta C(T)) Method. Methods San Diego Calif 25, 402–408. https://doi.org/10.1006/meth.2001.1262

Lopez, M.F., Krastins, B., Ning, M., 2014. The role of apolipoprotein E in neurodegeneration and cardiovascular disease. Expert Rev. Proteomics 11, 371–381. https://doi.org/10.1586/14789450.2014.901892

Luo, Y., Duan, H., Qian, Y., Feng, L., Wu, Z., Wang, F., Feng, J., Yang, D., Qin, Z., Yan, X., 2017. Macrophagic CD146 promotes foam cell formation and retention during atherosclerosis. Cell Res. 27, 352–372. https://doi.org/10.1038/cr.2017.8

Ma, Y., Yang, L., Ma, J., Lu, L., Wang, X., Ren, J., Yang, J., 2017. Rutin attenuates doxorubicin-induced cardiotoxicity via regulating autophagy and apoptosis. Biochim. Biophys. Acta Mol. Basis Dis. 1863, 1904–1911. https://doi.org/10.1016/j.bbadis.2016.12.021

Machlus, K.R., Italiano, J.E., 2013. The incredible journey: From megakaryocyte development to platelet formation. J. Cell Biol. 201, 785–796. https://doi.org/10.1083/jcb.201304054

Mackay, A.D., Marchant, E.D., Louw, M., Thomson, D.M., Hancock, C.R., 2021. Exercise, but Not Metformin Prevents Loss of Muscle Function Due to Doxorubicin in Mice Using an In Situ Method. Int. J. Mol. Sci. 22, 9163. https://doi.org/10.3390/ijms22179163

Mackman, N., 2008. Triggers, targets and treatments for thrombosis. Nature 451, 914–918. https://doi.org/10.1038/nature06797

Maezawa, I., Nivison, M., Montine, K.S., Maeda, N., Montine, T.J., 2006. Neurotoxicity from innate immune response is greatest with targeted replacement of E4 allele of apolipoprotein E gene and is mediated by microglial p38MAPK. FASEB J. Off. Publ. Fed. Am. Soc. Exp. Biol. 20, 797–799. https://doi.org/10.1096/fj.05-5423fje

Mah, L.-J., El-Osta, A., Karagiannis, T.C., 2010. gammaH2AX: a sensitive molecular marker of DNA damage and repair. Leukemia 24, 679–686. https://doi.org/10.1038/leu.2010.6

Mahley, R.W., Huang, Y., Weisgraber, K.H., 2006. Putting cholesterol in its place: apoE and reverse cholesterol transport. J. Clin. Invest. 116, 1226–1229. https://doi.org/10.1172/JCI28632
Mahley, R.W., Innerarity, T.L., Rall, S.C., Weisgraber, K.H., 1984. Plasma lipoproteins: apolipoprotein structure and function. J. Lipid Res. 25, 1277–1294.
Mahley, R.W., Rall, S.C., 2000. Apolipoprotein E: far more than a lipid transport protein. Annu. Rev. Genomics Hum. Genet. 1, 507–537. https://doi.org/10.1146/annurev.genom.1.1.507
Mahley, R.W., Weisgraber, K.H., Huang, Y., 2009. Apolipoprotein E: structure determines function, from atherosclerosis to Alzheimer's disease to AIDS. J. Lipid Res. 50 Suppl, S183-188. https://doi.org/10.1194/jlr.R800069-JLR200
Mahmood, T., Yang, P.-C., 2012. Western blot: technique, theory, and trouble shooting. North Am. J. Med. Sci. 4, 429–434. https://doi.org/10.4103/1947-2714.100998
Marais, A.D., 2019. Apolipoprotein E in lipoprotein metabolism, health and cardiovascular disease. Pathology (Phila.) 51, 165–176. https://doi.org/10.1016/j.pathol.2018.11.002
Marini, J.F., Pons, F., Leger, J., Loffreda, N., Anoal, M., Chevallay, M., Fardeau, M., Leger, J.J., 1991. Expression of myosin heavy chain isoforms in Duchenne muscular dystrophy patients and carriers. Neuromuscul. Disord. NMD 1, 397–409. https://doi.org/10.1016/0960-8966(91)90003-b
Marsh, S., Hanson, B., Wood, M.J.A., Varela, M.A., Roberts, T.C., 2020. Application of CRISPR-Cas9-Mediated Genome Editing for the Treatment of Myotonic Dystrophy Type 1. Mol. Ther. J. Am. Soc. Gene Ther. 28, 2527–2539. https://doi.org/10.1016/j.ymthe.2020.10.005
Martins, R.P., Hartmann, D.D., de Moraes, J.P., Soares, F.A.A., Puntel, G.O., 2016. Platelet-rich plasma reduces the oxidative damage determined by a skeletal muscle contusion in rats. Platelets 27, 784–790. https://doi.org/10.1080/09537104.2016.1184752
Marzetti, E., Calvani, R., Cesari, M., Buford, T.W., Lorenzi, M., Behnke, B.J., Leeuwenburgh, C., 2013. Mitochondrial dysfunction and sarcopenia of aging: from signaling pathways to clinical trials. Int. J. Biochem. Cell Biol. 45, 2288–2301. https://doi.org/10.1016/j.biocel.2013.06.024
Masuda, S., Tanaka, M., Inoue, T., Ohue-Kitano, R., Yamakage, H., Muranaka, K., Kusakabe, T., Shimatsu, A., Hasegawa, K., Satoh-Asahara, N., 2018. Chemokine (C-X-C motif) ligand 1 is a myokine induced by palmitate and is required for myogenesis in mouse satellite cells. Acta Physiol. Oxf. Engl. 222. https://doi.org/10.1111/apha.12975
Masumoto, H., Sies, H., 1996. The reaction of ebselen with peroxynitrite. Chem. Res. Toxicol. 9, 262–267. https://doi.org/10.1021/tx950115u
Matsakas, A., Patel, K., 2009. Skeletal muscle fibre plasticity in response to selected environmental and physiological stimuli. Histol. Histopathol. 24, 611–629. https://doi.org/10.14670/HH-24.611
Mauer, K., Gardner, A.W., Dasari, T.W., Stoner, J.A., Blevins, S.M., Montgomery, P.S., Saucedo, J.F., Exaire, J.E., 2015. Clot strength is negatively associated with ambulatory function in patients with peripheral artery disease and intermittent claudication. Angiology 66, 354–359. https://doi.org/10.1177/0003319714532518
Maulik, N., Yoshida, T., 2000. Oxidative stress developed during open heart surgery induces apoptosis: reduction of apoptotic cell death by ebselen, a glutathione

peroxidase mimic. J. Cardiovasc. Pharmacol. 36, 601–608. https://doi.org/10.1097/00005344-200011000-00009
McClure, M.J., Garg, K., Simpson, D.G., Ryan, J.J., Sell, S.A., Bowlin, G.L., Ericksen, J.J., 2016. The influence of platelet-rich plasma on myogenic differentiation. J. Tissue Eng. Regen. Med. 10, E239-249. https://doi.org/10.1002/term.1755
McDermott, M.M., Guralnik, J.M., Ferrucci, L., Tian, L., Pearce, W.H., Hoff, F., Liu, K., Liao, Y., Criqui, M.H., 2007. Physical activity, walking exercise, and calf skeletal muscle characteristics in patients with peripheral arterial disease. J. Vasc. Surg. 46, 87–93. https://doi.org/10.1016/j.jvs.2007.02.064
McKay, B.R., Ogborn, D.I., Baker, J.M., Toth, K.G., Tarnopolsky, M.A., Parise, G., 2013. Elevated SOCS3 and altered IL-6 signaling is associated with age-related human muscle stem cell dysfunction. Am. J. Physiol. Cell Physiol. 304, C717-728. https://doi.org/10.1152/ajpcell.00305.2012
McLaughlin, M., Gagnet, P., Cunningham, E., Yeager, R., D'Amico, M., Guski, K., Scarpone, M., Kuebler, D., 2016. Allogeneic Platelet Releasate Preparations Derived via a Novel Rapid Thrombin Activation Process Promote Rapid Growth and Increased BMP-2 and BMP-4 Expression in Human Adipose-Derived Stem Cells. Stem Cells Int. 2016, 7183734. https://doi.org/10.1155/2016/7183734
Meftahpour, V., Malekghasemi, S., Baghbanzadeh, A., Aghebati-Maleki, A., Pourakbari, R., Fotouhi, A., Aghebati-Maleki, L., 2021. Platelet lysate: a promising candidate in regenerative medicine. Regen. Med. 16, 71–85. https://doi.org/10.2217/rme-2020-0065
Mehta, J.L., Sanada, N., Hu, C.P., Chen, J., Dandapat, A., Sugawara, F., Satoh, H., Inoue, K., Kawase, Y., Jishage, K., Suzuki, H., Takeya, M., Schnackenberg, L., Beger, R., Hermonat, P.L., Thomas, M., Sawamura, T., 2007. Deletion of LOX-1 reduces atherogenesis in LDLR knockout mice fed high cholesterol diet. Circ. Res. 100, 1634–1642. https://doi.org/10.1161/CIRCRESAHA.107.149724
Merz, K.E., Thurmond, D.C., 2020. Role of Skeletal Muscle in Insulin Resistance and Glucose Uptake. Compr. Physiol. 10, 785–809. https://doi.org/10.1002/cphy.c190029
Meshkani, R., Sadeghi, A., Taheripak, G., Zarghooni, M., Gerayesh-Nejad, S., Bakhtiyari, S., 2014. Rosiglitazone, a PPARγ agonist, ameliorates palmitate-induced insulin resistance and apoptosis in skeletal muscle cells. Cell Biochem. Funct. 32, 683–691. https://doi.org/10.1002/cbf.3072
Metso, S., Nikkilä, M., Laippala, P., Jaakkola, O., Solakivi, T., Lehtimäki, T., 2003. Oxidized LDL autoantibodies are related to apolipoprotein E phenotype, independently of postprandial change in plasma triglycerides and LDL size, among patients with angiographically verified coronary artery disease and healthy controls. J. Biomed. Sci. 10, 345–351. https://doi.org/10.1007/BF02256454
Meyer, J.M., Graf, G.A., van der Westhuyzen, D.R., 2013. New developments in selective cholesteryl ester uptake. Curr. Opin. Lipidol. 24, 386–392. https://doi.org/10.1097/MOL.0b013e3283638042
Meyer, S.U., Thirion, C., Polesskaya, A., Bauersachs, S., Kaiser, S., Krause, S., Pfaffl, M.W., 2015. TNF-α and IGF1 modify the microRNA signature in skeletal muscle cell differentiation. Cell Commun. Signal. CCS 13, 4. https://doi.org/10.1186/s12964-015-0083-0
Meyrelles, S.S., Peotta, V.A., Pereira, T.M.C., Vasquez, E.C., 2011. Endothelial dysfunction in the apolipoprotein E-deficient mouse: insights into the influence

of diet, gender and aging. Lipids Health Dis. 10, 211. https://doi.org/10.1186/1476-511X-10-211
Miller, A.A., Drummond, G.R., Sobey, C.G., 2006. Novel isoforms of NADPH-oxidase in cerebral vascular control. Pharmacol. Ther. 111, 928–948. https://doi.org/10.1016/j.pharmthera.2006.02.005
Mineo, C., 2020. Lipoprotein receptor signalling in atherosclerosis. Cardiovasc. Res. 116, 1254–1274. https://doi.org/10.1093/cvr/cvz338
Miyata, M., Smith, J.D., 1996. Apolipoprotein E allele-specific antioxidant activity and effects on cytotoxicity by oxidative insults and beta-amyloid peptides. Nat. Genet. 14, 55–61. https://doi.org/10.1038/ng0996-55
Moloney, J.N., Cotter, T.G., 2018. ROS signalling in the biology of cancer. Semin. Cell Dev. Biol. 80, 50–64. https://doi.org/10.1016/j.semcdb.2017.05.023
Monis, P.T., Giglio, S., Saint, C.P., 2005. Comparison of SYTO9 and SYBR Green I for real-time polymerase chain reaction and investigation of the effect of dye concentration on amplification and DNA melting curve analysis. Anal. Biochem. 340, 24–34. https://doi.org/10.1016/j.ab.2005.01.046
Moore, D.R., Kelly, R.P., Devries, M.C., Churchward-Venne, T.A., Phillips, S.M., Parise, G., Johnston, A.P., 2018. Low-load resistance exercise during inactivity is associated with greater fibre area and satellite cell expression in older skeletal muscle. J. Cachexia Sarcopenia Muscle 9, 747–754. https://doi.org/10.1002/jcsm.12306
Morales, M.G., Abrigo, J., Acuña, M.J., Santos, R.A., Bader, M., Brandan, E., Simon, F., Olguin, H., Cabrera, D., Cabello-Verrugio, C., 2016. Angiotensin-(1-7) attenuates disuse skeletal muscle atrophy in mice via its receptor, Mas. Dis. Model. Mech. 9, 441–449. https://doi.org/10.1242/dmm.023390
Morgan, J.E., Zammit, P.S., 2010. Direct effects of the pathogenic mutation on satellite cell function in muscular dystrophy. Exp. Cell Res. 316, 3100–3108. https://doi.org/10.1016/j.yexcr.2010.05.014
Morita, S., 2016. Metabolism and Modification of Apolipoprotein B-Containing Lipoproteins Involved in Dyslipidemia and Atherosclerosis. Biol. Pharm. Bull. 39, 1–24. https://doi.org/10.1248/bpb.b15-00716
Morrissey, M.A., Sherwood, D.R., 2015. An active role for basement membrane assembly and modification in tissue sculpting. J. Cell Sci. 128, 1661–1668. https://doi.org/10.1242/jcs.168021
Morton, A.M., Furtado, J.D., Mendivil, C.O., Sacks, F.M., 2019. Dietary unsaturated fat increases HDL metabolic pathways involving apoE favorable to reverse cholesterol transport. JCI Insight 4, 124620. https://doi.org/10.1172/jci.insight.124620
Müller, A., Cadenas, E., Graf, P., Sies, H., 1984. A novel biologically active seleno-organic compound--I. Glutathione peroxidase-like activity in vitro and antioxidant capacity of PZ 51 (Ebselen). Biochem. Pharmacol. 33, 3235–3239. https://doi.org/10.1016/0006-2952(84)90083-2
Murach, K.A., Englund, D.A., Dupont-Versteegden, E.E., McCarthy, J.J., Peterson, C.A., 2018. Myonuclear Domain Flexibility Challenges Rigid Assumptions on Satellite Cell Contribution to Skeletal Muscle Fiber Hypertrophy. Front. Physiol. 9, 635. https://doi.org/10.3389/fphys.2018.00635
Nakasa, T., Ishikawa, M., Shi, M., Shibuya, H., Adachi, N., Ochi, M., 2010. Acceleration of muscle regeneration by local injection of muscle-specific microRNAs in rat skeletal muscle injury model. J. Cell. Mol. Med. 14, 2495–2505. https://doi.org/10.1111/j.1582-4934.2009.00898.x

Nelson, R.H., 2013. Hyperlipidemia as a risk factor for cardiovascular disease. Prim. Care 40, 195–211. https://doi.org/10.1016/j.pop.2012.11.003
Nguyen, M.-H., Cheng, M., Koh, T.J., 2011. Impaired muscle regeneration in ob/ob and db/db mice. ScientificWorldJournal 11, 1525–1535. https://doi.org/10.1100/tsw.2011.137
Noguchi, N., Yoshida, Y., Kaneda, H., Yamamoto, Y., Niki, E., 1992. Action of ebselen as an antioxidant against lipid peroxidation. Biochem. Pharmacol. 44, 39–44. https://doi.org/10.1016/0006-2952(92)90035-h
Nunes, V.S., Cazita, P.M., Catanozi, S., Nakandakare, E.R., Quintão, E.C.R., 2018. Decreased content, rate of synthesis and export of cholesterol in the brain of apoE knockout mice. J. Bioenerg. Biomembr. 50, 283–287. https://doi.org/10.1007/s10863-018-9757-9
Obata, S., Akeda, K., Imanishi, T., Masuda, K., Bae, W., Morimoto, R., Asanuma, Y., Kasai, Y., Uchida, A., Sudo, A., 2012. Effect of autologous platelet-rich plasma-releasate on intervertebral disc degeneration in the rabbit anular puncture model: a preclinical study. Arthritis Res. Ther. 14, R241. https://doi.org/10.1186/ar4084
Oberlohr, V., Lengel, H., Hambright, W.S., Whitney, K.E., Evans, T.A., Huard, J., 2020. Biologics for Skeletal Muscle Healing: The Role of Senescence and Platelet-Based Treatment Modalities. Oper. Tech. Sports Med. 28, 150754. https://doi.org/10.1016/j.otsm.2020.150754
Ochoa, C.D., Wu, R.F., Terada, L.S., 2018. ROS signaling and ER stress in cardiovascular disease. Mol. Aspects Med. 63, 18–29. https://doi.org/10.1016/j.mam.2018.03.002
O'Connell, B., Wragg, N.M., Wilson, S.L., 2019. The use of PRP injections in the management of knee osteoarthritis. Cell Tissue Res. 376, 143–152. https://doi.org/10.1007/s00441-019-02996-x
Omairi, S., Matsakas, A., Degens, H., Kretz, O., Hansson, K.-A., Solbrå, A.V., Bruusgaard, J.C., Joch, B., Sartori, R., Giallourou, N., Mitchell, R., Collins-Hooper, H., Foster, K., Pasternack, A., Ritvos, O., Sandri, M., Narkar, V., Swann, J.R., Huber, T.B., Patel, K., 2016. Enhanced exercise and regenerative capacity in a mouse model that violates size constraints of oxidative muscle fibres. eLife 5, e16940. https://doi.org/10.7554/eLife.16940
Ono, Y., Urata, Y., Goto, S., Nakagawa, S., Humbert, P.O., Li, T.-S., Zammit, P.S., 2015. Muscle stem cell fate is controlled by the cell-polarity protein Scrib. Cell Rep. 10, 1135–1148. https://doi.org/10.1016/j.celrep.2015.01.045
Ottenheijm, C.A.C., Granzier, H., 2010. Lifting the nebula: novel insights into skeletal muscle contractility. Physiol. Bethesda Md 25, 304–310. https://doi.org/10.1152/physiol.00016.2010
Pagel, O., Walter, E., Jurk, K., Zahedi, R.P., 2017. Taking the stock of granule cargo: Platelet releasate proteomics. Platelets 28, 119–128. https://doi.org/10.1080/09537104.2016.1254762
Paik, Y.K., Chang, D.J., Reardon, C.A., Davies, G.E., Mahley, R.W., Taylor, J.M., 1985. Nucleotide sequence and structure of the human apolipoprotein E gene. Proc. Natl. Acad. Sci. U. S. A. 82, 3445–3449. https://doi.org/10.1073/pnas.82.10.3445
Papadopoulou, S.K., 2020. Sarcopenia: A Contemporary Health Problem among Older Adult Populations. Nutrients 12, E1293. https://doi.org/10.3390/nu12051293

Pappas, C.T., Bliss, K.T., Zieseniss, A., Gregorio, C.C., 2011. The Nebulin family: an actin support group. Trends Cell Biol. 21, 29–37. https://doi.org/10.1016/j.tcb.2010.09.005

Park, J.-G., Yoo, J.-Y., Jeong, S.-J., Choi, J.-H., Lee, M.-R., Lee, M.-N., Hwa Lee, J., Kim, H.C., Jo, H., Yu, D.-Y., Kang, S.W., Rhee, S.G., Lee, M.-H., Oh, G.T., 2011. Peroxiredoxin 2 deficiency exacerbates atherosclerosis in apolipoprotein E-deficient mice. Circ. Res. 109, 739–749. https://doi.org/10.1161/CIRCRESAHA.111.245530

Park, J.M., Lee, J.S., Song, J.E., Sim, Y.C., Ha, S.-J., Hong, E.K., 2015. Cytoprotective effect of hispidin against palmitate-induced lipotoxicity in C2C12 myotubes. Mol. Basel Switz. 20, 5456–5467. https://doi.org/10.3390/molecules20045456

Park, Y.M., 2014. CD36, a scavenger receptor implicated in atherosclerosis. Exp. Mol. Med. 46, e99. https://doi.org/10.1038/emm.2014.38

Parsons, M.E.M., Szklanna, P.B., Guerrero, J.A., Wynne, K., Dervin, F., O'Connell, K., Allen, S., Egan, K., Bennett, C., McGuigan, C., Gheveart, C., Ní Áinle, F., Maguire, P.B., 2018. Platelet Releasate Proteome Profiling Reveals a Core Set of Proteins with Low Variance between Healthy Adults. Proteomics 18, e1800219. https://doi.org/10.1002/pmic.201800219

Passaretti, F., Tia, M., D'Esposito, V., De Pascale, M., Del Corso, M., Sepulveres, R., Liguoro, D., Valentino, R., Beguinot, F., Formisano, P., Sammartino, G., 2014. Growth-promoting action and growth factor release by different platelet derivatives. Platelets 25, 252–256. https://doi.org/10.3109/09537104.2013.809060

Passos, J.F., Saretzki, G., von Zglinicki, T., 2007. DNA damage in telomeres and mitochondria during cellular senescence: is there a connection? Nucleic Acids Res. 35, 7505–7513. https://doi.org/10.1093/nar/gkm893

Patel, H.J., Patel, B.M., 2017. TNF-α and cancer cachexia: Molecular insights and clinical implications. Life Sci. 170, 56–63. https://doi.org/10.1016/j.lfs.2016.11.033

Pavlath, G.K., Rich, K., Webster, S.G., Blau, H.M., 1989. Localization of muscle gene products in nuclear domains. Nature 337, 570–573. https://doi.org/10.1038/337570a0

Pawlikowski, B., Vogler, T.O., Gadek, K., Olwin, B.B., 2017. Regulation of skeletal muscle stem cells by fibroblast growth factors. Dev. Dyn. Off. Publ. Am. Assoc. Anat. 246, 359–367. https://doi.org/10.1002/dvdy.24495

Pearson, T., Kabayo, T., Ng, R., Chamberlain, J., McArdle, A., Jackson, M.J., 2014. Skeletal muscle contractions induce acute changes in cytosolic superoxide, but slower responses in mitochondrial superoxide and cellular hydrogen peroxide. PloS One 9, e96378. https://doi.org/10.1371/journal.pone.0096378

Pedersen, B.K., Febbraio, M.A., 2012. Muscles, exercise and obesity: skeletal muscle as a secretory organ. Nat. Rev. Endocrinol. 8, 457–465. https://doi.org/10.1038/nrendo.2012.49

Pellegrin, M., Bouzourène, K., Poitry-Yamate, C., Mlynarik, V., Feihl, F., Aubert, J.-F., Gruetter, R., Mazzolai, L., 2014. Experimental peripheral arterial disease: new insights into muscle glucose uptake, macrophage, and T-cell polarization during early and late stages. Physiol. Rep. 2, e00234. https://doi.org/10.1002/phy2.234

Pereira, S.S., Teixeira, L.G., Aguilar, E.C., Matoso, R.O., Soares, F.L.P., Ferreira, A.V.M., Alvarez-Leite, J.I., 2012. Differences in adipose tissue inflammation

and oxidative status in C57BL/6 and ApoE-/- mice fed high fat diet. Anim. Sci. J. Nihon Chikusan Gakkaiho 83, 549–555. https://doi.org/10.1111/j.1740-0929.2011.00982.x

Pessina, P., Cabrera, D., Morales, M.G., Riquelme, C.A., Gutiérrez, J., Serrano, A.L., Brandan, E., Muñoz-Cánoves, P., 2014. Novel and optimized strategies for inducing fibrosis in vivo: focus on Duchenne Muscular Dystrophy. Skelet. Muscle 4, 7. https://doi.org/10.1186/2044-5040-4-7

Peterson, J.M., Wang, Y., Bryner, R.W., Williamson, D.L., Alway, S.E., 2008. Bax signaling regulates palmitate-mediated apoptosis in C(2)C(12) myotubes. Am. J. Physiol. Endocrinol. Metab. 295, E1307-1314. https://doi.org/10.1152/ajpendo.00738.2007

Petrosino, J.M., Leask, A., Accornero, F., 2019. Genetic manipulation of CCN2/CTGF unveils cell-specific ECM-remodeling effects in injured skeletal muscle. FASEB J. Off. Publ. Fed. Am. Soc. Exp. Biol. 33, 2047–2057. https://doi.org/10.1096/fj.201800622RR

Pette, D., Staron, R.S., 2000. Myosin isoforms, muscle fiber types, and transitions. Microsc. Res. Tech. 50, 500–509. https://doi.org/10.1002/1097-0029(20000915)50:6<500::AID-JEMT7>3.0.CO;2-7

Phillips, M.C., 2014. Apolipoprotein E isoforms and lipoprotein metabolism. IUBMB Life 66, 616–623. https://doi.org/10.1002/iub.1314

Phinikaridou, A., Andia, M.E., Passacquale, G., Ferro, A., Botnar, R.M., 2013. Noninvasive MRI monitoring of the effect of interventions on endothelial permeability in murine atherosclerosis using an albumin-binding contrast agent. J. Am. Heart Assoc. 2, e000402. https://doi.org/10.1161/JAHA.113.000402

Piecha, G., Koleganova, N., Gross, M.-L., Geldyyev, A., Ritz, E., 2008. Oxidative stress after uninephrectomy alters heart morphology in the apolipoprotein E -/- mouse. J. Hypertens. 26, 2220–2229. https://doi.org/10.1097/HJH.0b013e32830ef5e4

Piechota, M., Sunderland, P., Wysocka, A., Nalberczak, M., Sliwinska, M.A., Radwanska, K., Sikora, E., 2016. Is senescence-associated β-galactosidase a marker of neuronal senescence? Oncotarget 7, 81099–81109. https://doi.org/10.18632/oncotarget.12752

Pierre, N., Fernández-Verdejo, R., Regnier, P., Vanmechelen, S., Demeulder, B., Francaux, M., 2016. IRE1α and TRB3 do not contribute to the disruption of proximal insulin signaling caused by palmitate in C2C12 myotubes. Cell Biol. Int. 40, 91–99. https://doi.org/10.1002/cbin.10542

Plump, A.S., Smith, J.D., Hayek, T., Aalto-Setälä, K., Walsh, A., Verstuyft, J.G., Rubin, E.M., Breslow, J.L., 1992. Severe hypercholesterolemia and atherosclerosis in apolipoprotein E-deficient mice created by homologous recombination in ES cells. Cell 71, 343–353. https://doi.org/10.1016/0092-8674(92)90362-g

Pomiès, P., Rodriguez, J., Blaquière, M., Sedraoui, S., Gouzi, F., Carnac, G., Laoudj-Chenivesse, D., Mercier, J., Préfaut, C., Hayot, M., 2015. Reduced myotube diameter, atrophic signalling and elevated oxidative stress in cultured satellite cells from COPD patients. J. Cell. Mol. Med. 19, 175–186. https://doi.org/10.1111/jcmm.12390

Powers, J.D., Malingen, S.A., Regnier, M., Daniel, T.L., 2021. The Sliding Filament Theory Since Andrew Huxley: Multiscale and Multidisciplinary Muscle Research. Annu. Rev. Biophys. 50, 373–400. https://doi.org/10.1146/annurev-biophys-110320-062613

Powers, S.K., Deminice, R., Ozdemir, M., Yoshihara, T., Bomkamp, M.P., Hyatt, H., 2020. Exercise-induced oxidative stress: Friend or foe? J. Sport Health Sci. 9, 415–425. https://doi.org/10.1016/j.jshs.2020.04.001

Powers, S.K., Duarte, J.A., Le Nguyen, B., Hyatt, H., 2019. Endurance exercise protects skeletal muscle against both doxorubicin-induced and inactivity-induced muscle wasting. Pflugers Arch. 471, 441–453. https://doi.org/10.1007/s00424-018-2227-8

Prasanna, P.L., Renu, K., Valsala Gopalakrishnan, A., 2020. New molecular and biochemical insights of doxorubicin-induced hepatotoxicity. Life Sci. 250, 117599. https://doi.org/10.1016/j.lfs.2020.117599

Price, N.L., Rotllan, N., Zhang, X., Canfrán-Duque, A., Nottoli, T., Suarez, Y., Fernández-Hernando, C., 2019. Specific Disruption of Abca1 Targeting Largely Mimics the Effects of miR-33 Knockout on Macrophage Cholesterol Efflux and Atherosclerotic Plaque Development. Circ. Res. 124, 874–880. https://doi.org/10.1161/CIRCRESAHA.118.314415

Proto, J.D., Tang, Y., Lu, A., Chen, W.C.W., Stahl, E., Poddar, M., Beckman, S.A., Robbins, P.D., Nidernhofer, L.J., Imbrogno, K., Hannigan, T., Mars, W.M., Wang, B., Huard, J., 2015. NF-κB inhibition reveals a novel role for HGF during skeletal muscle repair. Cell Death Dis. 6, e1730. https://doi.org/10.1038/cddis.2015.66

Puri, P.L., Medaglia, S., Cimino, L., Maselli, C., Germani, A., De Marzio, E., Levrero, M., Balsano, C., 1997. Uncoupling of p21 induction and MyoD activation results in the failure of irreversible cell cycle arrest in doxorubicin-treated myocytes. J. Cell. Biochem. 66, 27–36. https://doi.org/10.1002/(sici)1097-4644(19970701)66:1<27::aid-jcb4>3.0.co;2-#

Qaisar, R., Bhaskaran, S., Van Remmen, H., 2016. Muscle fiber type diversification during exercise and regeneration. Free Radic. Biol. Med. 98, 56–67. https://doi.org/10.1016/j.freeradbiomed.2016.03.025

Raber, J., Wong, D., Yu, G.Q., Buttini, M., Mahley, R.W., Pitas, R.E., Mucke, L., 2000. Apolipoprotein E and cognitive performance. Nature 404, 352–354. https://doi.org/10.1038/35006165

Rachek, L.I., Musiyenko, S.I., LeDoux, S.P., Wilson, G.L., 2007. Palmitate induced mitochondrial deoxyribonucleic acid damage and apoptosis in l6 rat skeletal muscle cells. Endocrinology 148, 293–299. https://doi.org/10.1210/en.2006-0998

Rajabi, H.N., Takahashi, C., Ewen, M.E., 2014. Retinoblastoma protein and MyoD function together to effect the repression of Fra-1 and in turn cyclin D1 during terminal cell cycle arrest associated with myogenesis. J. Biol. Chem. 289, 23417–23427. https://doi.org/10.1074/jbc.M113.532572

Rajasekaran, N.S., Shelar, S.B., Jones, D.P., Hoidal, J.R., 2020. Reductive stress impairs myogenic differentiation. Redox Biol. 34, 101492. https://doi.org/10.1016/j.redox.2020.101492

Ramaswamy Reddy, S.H., Reddy, R., Babu, N.C., Ashok, G.N., 2018. Stem-cell therapy and platelet-rich plasma in regenerative medicines: A review on pros and cons of the technologies. J. Oral Maxillofac. Pathol. JOMFP 22, 367–374. https://doi.org/10.4103/jomfp.JOMFP_93_18

Rayani, K., Seffernick, J., Li, A.Y., Davis, J.P., Spuches, A.M., Van Petegem, F., Solaro, R.J., Lindert, S., Tibbits, G.F., 2021. Binding of calcium and magnesium to human cardiac troponin C. J. Biol. Chem. 296, 100350. https://doi.org/10.1016/j.jbc.2021.100350

Reddy, K.G., Nair, R.N., Sheehan, H.M., Hodgson, J.M., 1994. Evidence that selective endothelial dysfunction may occur in the absence of angiographic or ultrasound atherosclerosis in patients with risk factors for atherosclerosis. J. Am. Coll. Cardiol. 23, 833–843. https://doi.org/10.1016/0735-1097(94)90627-0

Relaix, F., Zammit, P.S., 2012. Satellite cells are essential for skeletal muscle regeneration: the cell on the edge returns centre stage. Dev. Camb. Engl. 139, 2845–2856. https://doi.org/10.1242/dev.069088

Renault, V., Thornell, L.-E., Eriksson, P.-O., Butler-Browne, G., Mouly, V., Thorne, L.-E., 2002. Regenerative potential of human skeletal muscle during aging. Aging Cell 1, 132–139. https://doi.org/10.1046/j.1474-9728.2002.00017.x

Rendu, F., Brohard-Bohn, B., 2001. The platelet release reaction: granules' constituents, secretion and functions. Platelets 12, 261–273. https://doi.org/10.1080/09537100120068170

Ríos, E., Györke, S., 2009. Calsequestrin, triadin and more: the molecules that modulate calcium release in cardiac and skeletal muscle. J. Physiol. 587, 3069–3070. https://doi.org/10.1113/jphysiol.2009.175083

Ross, J.A., Levy, Y., Svensson, K., Philp, A., Schenk, S., Ochala, J., 2018. SIRT1 regulates nuclear number and domain size in skeletal muscle fibers. J. Cell. Physiol. 233, 7157–7163. https://doi.org/10.1002/jcp.26542

Rotkrua, P., Lohlamoh, W., Watcharapo, P., Soontornworajit, B., 2021. A molecular hybrid comprising AS1411 and PDGF-BB aptamer, cholesterol, and doxorubicin for inhibiting proliferation of SW480 cells. J. Mol. Recognit. JMR 34, e2926. https://doi.org/10.1002/jmr.2926

Roy, A., Sharma, A.K., Nellore, K., Narkar, V.A., Kumar, A., 2020. TAK1 preserves skeletal muscle mass and mitochondrial function through redox homeostasis. FASEB BioAdvances 2, 538–553. https://doi.org/10.1096/fba.2020-00043

Rubenstein, D.A., Yin, W., 2018. Platelet-Activation Mechanisms and Vascular Remodeling. Compr. Physiol. 8, 1117–1156. https://doi.org/10.1002/cphy.c170049

Sabourin, L.A., Rudnicki, M.A., 2000. The molecular regulation of myogenesis. Clin. Genet. 57, 16–25. https://doi.org/10.1034/j.1399-0004.2000.570103.x

Sacks, F.M., 2015. The crucial roles of apolipoproteins E and C-III in apoB lipoprotein metabolism in normolipidemia and hypertriglyceridemia. Curr. Opin. Lipidol. 26, 56–63. https://doi.org/10.1097/MOL.0000000000000146

Salviati, G., Volpe, P., Salvatori, S., Betto, R., Damiani, E., Margreth, A., Pasquali-Ronchetti, I., 1982. Biochemical heterogeneity of skeletal-muscle microsomal membranes. Membrane origin, membrane specificity and fibre types. Biochem. J. 202, 289–301. https://doi.org/10.1042/bj2020289

Sanchez-Encinales, V., Cozar-Castellano, I., Garcia-Ocaña, A., Perdomo, G., 2015. Targeted delivery of HGF to the skeletal muscle improves glucose homeostasis in diet-induced obese mice. J. Physiol. Biochem. 71, 795–805. https://doi.org/10.1007/s13105-015-0444-6

Sandiford, S.D.E., Kennedy, K.A.M., Xie, X., Pickering, J.G., Li, S.S.C., 2014. Dual oxidase maturation factor 1 (DUOXA1) overexpression increases reactive oxygen species production and inhibits murine muscle satellite cell differentiation. Cell Commun. Signal. CCS 12, 5. https://doi.org/10.1186/1478-811X-12-5

Sang, Y., Roest, M., de Laat, B., de Groot, P.G., Huskens, D., 2021. Interplay between platelets and coagulation. Blood Rev. 46, 100733. https://doi.org/10.1016/j.blre.2020.100733

Sawyer, D.B., Peng, X., Chen, B., Pentassuglia, L., Lim, C.C., 2010. Mechanisms of anthracycline cardiac injury: can we identify strategies for cardioprotection? Prog. Cardiovasc. Dis. 53, 105–113. https://doi.org/10.1016/j.pcad.2010.06.007

Schewe, T., 1995. Molecular actions of ebselen--an antiinflammatory antioxidant. Gen. Pharmacol. 26, 1153–1169. https://doi.org/10.1016/0306-3623(95)00003-j

Schiaffino, S., Reggiani, C., 2011. Fiber types in mammalian skeletal muscles. Physiol. Rev. 91, 1447–1531. https://doi.org/10.1152/physrev.00031.2010

Schuh, R.A., Jackson, K.C., Khairallah, R.J., Ward, C.W., Spangenburg, E.E., 2012. Measuring mitochondrial respiration in intact single muscle fibers. Am. J. Physiol. Regul. Integr. Comp. Physiol. 302, R712-719. https://doi.org/10.1152/ajpregu.00229.2011

Schwartz, L.M., Brown, C., McLaughlin, K., Smith, W., Bigelow, C., 2016. The myonuclear domain is not maintained in skeletal muscle during either atrophy or programmed cell death. Am. J. Physiol. Cell Physiol. 311, C607–C615. https://doi.org/10.1152/ajpcell.00176.2016

Scully, D., Naseem, K.M., Matsakas, A., 2018. Platelet biology in regenerative medicine of skeletal muscle. Acta Physiol. Oxf. Engl. 223, e13071. https://doi.org/10.1111/apha.13071

Scully, D., Sfyri, P., Verpoorten, S., Papadopoulos, P., Muñoz-Turrillas, M.C., Mitchell, R., Aburima, A., Patel, K., Gutiérrez, L., Naseem, K.M., Matsakas, A., 2019. Platelet releasate promotes skeletal myogenesis by increasing muscle stem cell commitment to differentiation and accelerates muscle regeneration following acute injury. Acta Physiol. Oxf. Engl. 225, e13207. https://doi.org/10.1111/apha.13207

Scully, D., Sfyri, P., Wilkinson, H.N., Acebes-Huerta, A., Verpoorten, S., Muñoz-Turrillas, M.C., Parnell, A., Patel, K., Hardman, M.J., Gutiérrez, L., Matsakas, A., 2020. Optimising platelet secretomes to deliver robust tissue-specific regeneration. J. Tissue Eng. Regen. Med. 14, 82–98. https://doi.org/10.1002/term.2965

Severinsen, M.C.K., Pedersen, B.K., 2020. Muscle-Organ Crosstalk: The Emerging Roles of Myokines. Endocr. Rev. 41, bnaa016. https://doi.org/10.1210/endrev/bnaa016

Sfyri, P., Matsakas, A., 2017. Crossroads between peripheral atherosclerosis, western-type diet and skeletal muscle pathophysiology: emphasis on apolipoprotein E deficiency and peripheral arterial disease. J. Biomed. Sci. 24, 42. https://doi.org/10.1186/s12929-017-0346-8

Sfyri, P.P., Yuldasheva, N.Y., Tzimou, A., Giallourou, N., Crispi, V., Aburima, A., Beltran-Alvarez, P., Patel, K., Mougios, V., Swann, J.R., Kearney, M.T., Matsakas, A., 2018. Attenuation of oxidative stress-induced lesions in skeletal muscle in a mouse model of obesity-independent hyperlipidaemia and atherosclerosis through the inhibition of Nox2 activity. Free Radic. Biol. Med. 129, 504–519. https://doi.org/10.1016/j.freeradbiomed.2018.10.422

Sharma, V., Tewari, R., Sk, U.H., Joseph, C., Sen, E., 2008. Ebselen sensitizes glioblastoma cells to Tumor Necrosis Factor (TNFalpha)-induced apoptosis through two distinct pathways involving NF-kappaB downregulation and Fas-mediated formation of death inducing signaling complex. Int. J. Cancer 123, 2204–2212. https://doi.org/10.1002/ijc.23771

Shen, L., Sevanian, A., 2001. OxLDL induces macrophage gamma-GCS-HS protein expression: a role for oxLDL-associated lipid hydroperoxide in GSH synthesis. J. Lipid Res. 42, 813–823.
Shi, Y., Liu, J.-P., 2011. Gdf11 facilitates temporal progression of neurogenesis in the developing spinal cord. J. Neurosci. Off. J. Soc. Neurosci. 31, 883–893. https://doi.org/10.1523/JNEUROSCI.2394-10.2011
Sies, H., 1993. Ebselen, a selenoorganic compound as glutathione peroxidase mimic. Free Radic. Biol. Med. 14, 313–323. https://doi.org/10.1016/0891-5849(93)90028-s
Sies, H., de Groot, H., 1992. Role of reactive oxygen species in cell toxicity. Toxicol. Lett. 64-65 Spec No, 547–551. https://doi.org/10.1016/0378-4274(92)90230-h
Silva, E.F., Bazoni, R.F., Ramos, E.B., Rocha, M.S., 2017. DNA-doxorubicin interaction: New insights and peculiarities. Biopolymers 107. https://doi.org/10.1002/bip.22998
Sincennes, M.-C., Brun, C.E., Lin, A.Y.T., Rosembert, T., Datzkiw, D., Saber, J., Ming, H., Kawabe, Y.-I., Rudnicki, M.A., 2021. Acetylation of PAX7 controls muscle stem cell self-renewal and differentiation potential in mice. Nat. Commun. 12, 3253. https://doi.org/10.1038/s41467-021-23577-z
Smith, C.W., 2022. Release of α-granule contents during platelet activation. Platelets 33, 491–502. https://doi.org/10.1080/09537104.2021.1913576
Smith, S.M.E., Min, J., Ganesh, T., Diebold, B., Kawahara, T., Zhu, Y., McCoy, J., Sun, A., Snyder, J.P., Fu, H., Du, Y., Lewis, I., Lambeth, J.D., 2012. Ebselen and congeners inhibit NADPH oxidase 2-dependent superoxide generation by interrupting the binding of regulatory subunits. Chem. Biol. 19, 752–763. https://doi.org/10.1016/j.chembiol.2012.04.015
Snijders, T., Wall, B.T., Dirks, M.L., Senden, J.M.G., Hartgens, F., Dolmans, J., Losen, M., Verdijk, L.B., van Loon, L.J.C., 2014. Muscle disuse atrophy is not accompanied by changes in skeletal muscle satellite cell content. Clin. Sci. Lond. Engl. 1979 126, 557–566. https://doi.org/10.1042/CS20130295
Song, Y.-H., Song, J.L., Delafontaine, P., Godard, M.P., 2013. The therapeutic potential of IGF-I in skeletal muscle repair. Trends Endocrinol. Metab. TEM 24, 310–319. https://doi.org/10.1016/j.tem.2013.03.004
Songbo, M., Lang, H., Xinyong, C., Bin, X., Ping, Z., Liang, S., 2019. Oxidative stress injury in doxorubicin-induced cardiotoxicity. Toxicol. Lett. 307, 41–48. https://doi.org/10.1016/j.toxlet.2019.02.013
Sousa-Victor, P., Gutarra, S., García-Prat, L., Rodriguez-Ubreva, J., Ortet, L., Ruiz-Bonilla, V., Jardí, M., Ballestar, E., González, S., Serrano, A.L., Perdiguero, E., Muñoz-Cánoves, P., 2014. Geriatric muscle stem cells switch reversible quiescence into senescence. Nature 506, 316–321. https://doi.org/10.1038/nature13013
Spallarossa, P., Altieri, P., Aloi, C., Garibaldi, S., Barisione, C., Ghigliotti, G., Fugazza, G., Barsotti, A., Brunelli, C., 2009. Doxorubicin induces senescence or apoptosis in rat neonatal cardiomyocytes by regulating the expression levels of the telomere binding factors 1 and 2. Am. J. Physiol. Heart Circ. Physiol. 297, H2169-2181. https://doi.org/10.1152/ajpheart.00068.2009
Sriram, S., Yuan, C., Chakraborty, S., Tay, W., Park, M., Shabbir, A., Toh, S.-A., Han, W., Sugii, S., 2019. Oxidative stress mediates depot-specific functional differences of human adipose-derived stem cells. Stem Cell Res. Ther. 10, 141. https://doi.org/10.1186/s13287-019-1240-y

Stalker, T.J., Newman, D.K., Ma, P., Wannemacher, K.M., Brass, L.F., 2012. Platelet signaling. Handb. Exp. Pharmacol. 59–85. https://doi.org/10.1007/978-3-642-29423-5_3

Stapleton, P.A., Goodwill, A.G., James, M.E., D'Audiffret, A.C., Frisbee, J.C., 2010. Differential impact of familial hypercholesterolemia and combined hyperlipidemia on vascular wall and network remodeling in mice. Microcirc. N. Y. N 1994 17, 47–58. https://doi.org/10.1111/j.1549-8719.2009.00003.x

Steinbacher, P., Eckl, P., 2015. Impact of oxidative stress on exercising skeletal muscle. Biomolecules 5, 356–377. https://doi.org/10.3390/biom5020356

Su, L.-J., Zhang, J.-H., Gomez, H., Murugan, R., Hong, X., Xu, D., Jiang, F., Peng, Z.-Y., 2019. Reactive Oxygen Species-Induced Lipid Peroxidation in Apoptosis, Autophagy, and Ferroptosis. Oxid. Med. Cell. Longev. 2019, 5080843. https://doi.org/10.1155/2019/5080843

Suess, P.M., Smith, S.A., Morrissey, J.H., 2020. Platelet polyphosphate induces fibroblast chemotaxis and myofibroblast differentiation. J. Thromb. Haemost. JTH 18, 3043–3052. https://doi.org/10.1111/jth.15066

Sugamura, K., Keaney, J.F., 2011. Reactive oxygen species in cardiovascular disease. Free Radic. Biol. Med. 51, 978–992. https://doi.org/10.1016/j.freeradbiomed.2011.05.004

Sui, S.X., Williams, L.J., Holloway-Kew, K.L., Hyde, N.K., Pasco, J.A., 2020. Skeletal Muscle Health and Cognitive Function: A Narrative Review. Int. J. Mol. Sci. 22, E255. https://doi.org/10.3390/ijms22010255

Sun, X., Seidman, J.S., Zhao, P., Troutman, T.D., Spann, N.J., Que, X., Zhou, F., Liao, Z., Pasillas, M., Yang, X., Magida, J.A., Kisseleva, T., Brenner, D.A., Downes, M., Evans, R.M., Saltiel, A.R., Tsimikas, S., Glass, C.K., Witztum, J.L., 2020. Neutralization of Oxidized Phospholipids Ameliorates Non-alcoholic Steatohepatitis. Cell Metab. 31, 189-206.e8. https://doi.org/10.1016/j.cmet.2019.10.014

Sun, Y.-N., Yang, Z.-X., Ren, F.-Z., Fang, B., 2020. FGF19 alleviates palmitate-induced atrophy in C2C12 cells by inhibiting mitochondrial overload and insulin resistance. Int. J. Biol. Macromol. 158, 401–407. https://doi.org/10.1016/j.ijbiomac.2020.04.186

Sunitha, B., Gayathri, N., Kumar, M., Keshava Prasad, T.S., Nalini, A., Padmanabhan, B., Srinivas Bharath, M.M., 2016. Muscle biopsies from human muscle diseases with myopathic pathology reveal common alterations in mitochondrial function. J. Neurochem. 138, 174–191. https://doi.org/10.1111/jnc.13626

Tacar, O., Sriamornsak, P., Dass, C.R., 2013. Doxorubicin: an update on anticancer molecular action, toxicity and novel drug delivery systems. J. Pharm. Pharmacol. 65, 157–170. https://doi.org/10.1111/j.2042-7158.2012.01567.x

Takahashi, A., Ohtani, N., Yamakoshi, K., Iida, S., Tahara, H., Nakayama, K., Nakayama, K.I., Ide, T., Saya, H., Hara, E., 2006. Mitogenic signalling and the p16INK4a-Rb pathway cooperate to enforce irreversible cellular senescence. Nat. Cell Biol. 8, 1291–1297. https://doi.org/10.1038/ncb1491

Takasago, T., Peters, E.E., Graham, D.I., Masayasu, H., Macrae, I.M., 1997. Neuroprotective efficacy of ebselen, an anti-oxidant with anti-inflammatory actions, in a rodent model of permanent middle cerebral artery occlusion. Br. J. Pharmacol. 122, 1251–1256. https://doi.org/10.1038/sj.bjp.0701426

Takemoto, Y., Inaba, S., Zhang, L., Tsujikawa, K., Uezumi, A., Fukada, S.-I., 2019. Implication of basal lamina dependency in survival of Nrf2-null muscle stem

cells via an antioxidative-independent mechanism. J. Cell. Physiol. 234, 1689–1698. https://doi.org/10.1002/jcp.27040
Tallis, J., James, R.S., Seebacher, F., 2018. The effects of obesity on skeletal muscle contractile function. J. Exp. Biol. 221, jeb163840. https://doi.org/10.1242/jeb.163840
Talmud, P.J., Cooper, J.A., Hattori, H., Miller, I.P., Miller, G.J., Humphries, S.E., 2006. The apolipoprotein A-V genotype and plasma apolipoprotein A-V and triglyceride levels: prospective risk of type 2 diabetes. Results from the Northwick Park Heart Study II. Diabetologia 49, 2337–2340. https://doi.org/10.1007/s00125-006-0387-0
Tamilarasan, K.P., Temmel, H., Das, S.K., Al Zoughbi, W., Schauer, S., Vesely, P.W., Hoefler, G., 2012. Skeletal muscle damage and impaired regeneration due to LPL-mediated lipotoxicity. Cell Death Dis. 3, e354. https://doi.org/10.1038/cddis.2012.91
Tan, S.M., Sharma, A., Yuen, D.Y.C., Stefanovic, N., Krippner, G., Mugesh, G., Chai, Z., de Haan, J.B., 2013. The modified selenenyl amide, M-hydroxy ebselen, attenuates diabetic nephropathy and diabetes-associated atherosclerosis in ApoE/GPx1 double knockout mice. PloS One 8, e69193. https://doi.org/10.1371/journal.pone.0069193
Tanaka, R., Ichioka, S., Sekiya, N., Ohura, N., Uchino, S., Ojima, A., Itoh, Y., Ishihara, O., Nakatsuka, T., Ikebuchi, K., 2007. Elastic plasma protein film blended with platelet releasate accelerates healing of diabetic mouse skin wounds. Vox Sang. 93, 49–56. https://doi.org/10.1111/j.1423-0410.2007.00913.x
Tawil, R., van der Maarel, S.M., Tapscott, S.J., 2014. Facioscapulohumeral dystrophy: the path to consensus on pathophysiology. Skelet. Muscle 4, 12. https://doi.org/10.1186/2044-5040-4-12
Taylor-Weiner, H., Grigsby, C.L., Ferreira, D.M.S., Dias, J.M., Stevens, M.M., Ruas, J.L., Teixeira, A.I., 2020. Modeling the transport of nuclear proteins along single skeletal muscle cells. Proc. Natl. Acad. Sci. U. S. A. 117, 2978–2986. https://doi.org/10.1073/pnas.1919600117
Teng, Z., Guo, Z., Zhong, J., Cheng, C., Huang, Z., Wu, Y., Tang, S., Luo, C., Peng, X., Wu, H., Sun, X., Jiang, L., 2017. ApoE Influences the Blood-Brain Barrier Through the NF-κB/MMP-9 Pathway After Traumatic Brain Injury. Sci. Rep. 7, 6649. https://doi.org/10.1038/s41598-017-06932-3
Thom, S.R., Bhopale, V.M., Yang, M., 2014. Neutrophils generate microparticles during exposure to inert gases due to cytoskeletal oxidative stress. J. Biol. Chem. 289, 18831–18845. https://doi.org/10.1074/jbc.M113.543702
Thomas, G.D., 2013. Functional muscle ischemia in Duchenne and Becker muscular dystrophy. Front. Physiol. 4, 381. https://doi.org/10.3389/fphys.2013.00381
Thornton, C.A., 2014. Myotonic dystrophy. Neurol. Clin. 32, 705–719, viii. https://doi.org/10.1016/j.ncl.2014.04.011
Thornton, C.A., Wang, E., Carrell, E.M., 2017. Myotonic dystrophy: approach to therapy. Curr. Opin. Genet. Dev. 44, 135–140. https://doi.org/10.1016/j.gde.2017.03.007
Tidball, J.G., Spencer, M.J., 1993. PDGF stimulation induces phosphorylation of talin and cytoskeletal reorganization in skeletal muscle. J. Cell Biol. 123, 627–635. https://doi.org/10.1083/jcb.123.3.627
Tsai, W.-C., Yu, T.-Y., Chang, G.-J., Lin, L.-P., Lin, M.-S., Pang, J.-H.S., 2018. Platelet-Rich Plasma Releasate Promotes Regeneration and Decreases

Inflammation and Apoptosis of Injured Skeletal Muscle. Am. J. Sports Med. 46, 1980–1986. https://doi.org/10.1177/0363546518771076

Tsai, W.-C., Yu, T.-Y., Lin, L.-P., Lin, M.-S., Wu, Y.-C., Liao, C.-H., Pang, J.-H.S., 2017. Platelet rich plasma releasate promotes proliferation of skeletal muscle cells in association with upregulation of PCNA, cyclins and cyclin dependent kinases. Platelets 28, 491–497. https://doi.org/10.1080/09537104.2016.1227061

Tseng, B.S., Kasper, C.E., Edgerton, V.R., 1994. Cytoplasm-to-myonucleus ratios and succinate dehydrogenase activities in adult rat slow and fast muscle fibers. Cell Tissue Res. 275, 39–49. https://doi.org/10.1007/BF00305374

Tskhovrebova, L., Trinick, J., 2010. Roles of titin in the structure and elasticity of the sarcomere. J. Biomed. Biotechnol. 2010, 612482. https://doi.org/10.1155/2010/612482

Tsuda, M., Sanada, M., Higashi, Y., Hara, Y., Kodama, I., Chayama, K., Yoshizumi, M., Ohama, K., 2004. Apolipoprotein E phenotype affects the malondialdehyde-modified LDL concentration and forearm endothelial function in postmenopausal women. Clin. Endocrinol. (Oxf.) 61, 619–625. https://doi.org/10.1111/j.1365-2265.2004.02145.x

van Buul, G.M., Koevoet, W.L.M., Kops, N., Bos, P.K., Verhaar, J.A.N., Weinans, H., Bernsen, M.R., van Osch, G.J.V.M., 2011. Platelet-rich plasma releasate inhibits inflammatory processes in osteoarthritic chondrocytes. Am. J. Sports Med. 39, 2362–2370. https://doi.org/10.1177/0363546511419278

van der Meer, S.F.T., Jaspers, R.T., Jones, D.A., Degens, H., 2011. The time course of myonuclear accretion during hypertrophy in young adult and older rat plantaris muscle. Ann. Anat. Anat. Anz. Off. Organ Anat. Ges. 193, 56–63. https://doi.org/10.1016/j.aanat.2010.08.004

van der Meijden, P.E.J., Heemskerk, J.W.M., 2019. Platelet biology and functions: new concepts and clinical perspectives. Nat. Rev. Cardiol. 16, 166–179. https://doi.org/10.1038/s41569-018-0110-0

van Leent, M.M.T., Beldman, T.J., Toner, Y.C., Lameijer, M.A., Rother, N., Bekkering, S., Teunissen, A.J.P., Zhou, X., van der Meel, R., Malkus, J., Nauta, S.A., Klein, E.D., Fay, F., Sanchez-Gaytan, B.L., Pérez-Medina, C., Kluza, E., Ye, Y.-X., Wojtkiewicz, G., Fisher, E.A., Swirski, F.K., Nahrendorf, M., Zhang, Bin, Li, Y., Zhang, Bowen, Joosten, L.A.B., Pasterkamp, G., Boltjes, A., Fayad, Z.A., Lutgens, E., Netea, M.G., Riksen, N.P., Mulder, W.J.M., Duivenvoorden, R., 2021. Prosaposin mediates inflammation in atherosclerosis. Sci. Transl. Med. 13, eabe1433. https://doi.org/10.1126/scitranslmed.abe1433

Varu, V.N., Hogg, M.E., Kibbe, M.R., 2010. Critical limb ischemia. J. Vasc. Surg. 51, 230–241. https://doi.org/10.1016/j.jvs.2009.08.073

Vélez, P., Izquierdo, I., Rosa, I., García, Á., 2015. A 2D-DIGE-based proteomic analysis reveals differences in the platelet releasate composition when comparing thrombin and collagen stimulations. Sci. Rep. 5, 8198. https://doi.org/10.1038/srep08198

Verpoorten, S., Sfyri, P., Scully, D., Mitchell, R., Tzimou, A., Mougios, V., Patel, K., Matsakas, A., 2020. Loss of CD36 protects against diet-induced obesity but results in impaired muscle stem cell function, delayed muscle regeneration and hepatic steatosis. Acta Physiol. Oxf. Engl. 228, e13395. https://doi.org/10.1111/apha.13395

Vink, A., Pasterkamp, G., 2002. Atherosclerotic plaque burden, plaque vulnerability and arterial remodeling: the role of inflammation. Minerva Cardioangiol. 50, 75–83.
Vlahovic, H., Bazdaric, K., Marijancic, V., Soic-Vranic, T., Malnar, D., Arbanas, J., 2017. Segmental fibre type composition of the rat iliopsoas muscle. J. Anat. 230, 542–548. https://doi.org/10.1111/joa.12588
Wagner, P.D., 2011. The critical role of VEGF in skeletal muscle angiogenesis and blood flow. Biochem. Soc. Trans. 39, 1556–1559. https://doi.org/10.1042/BST20110646
Wang, J., Perrard, X.D., Perrard, J.L., Mukherjee, A., Rosales, C., Chen, Y., Smith, C.W., Pownall, H.J., Ballantyne, C.M., Wu, H., 2012. ApoE and the role of very low density lipoproteins in adipose tissue inflammation. Atherosclerosis 223, 342–349. https://doi.org/10.1016/j.atherosclerosis.2012.06.003
Wang, L., Lavier, J., Hua, W., Wang, Y., Gong, L., Wei, H., Wang, J., Pellegrin, M., Millet, G.P., Zhang, Y., 2021. High-Intensity Interval Training and Moderate-Intensity Continuous Training Attenuate Oxidative Damage and Promote Myokine Response in the Skeletal Muscle of ApoE KO Mice on High-Fat Diet. Antioxid. Basel Switz. 10, 992. https://doi.org/10.3390/antiox10070992
Wang, Q., Wu, P.C., Roberson, R.S., Luk, B.V., Ivanova, I., Chu, E., Wu, D.Y., 2011. Survivin and escaping in therapy-induced cellular senescence. Int. J. Cancer 128, 1546–1558. https://doi.org/10.1002/ijc.25482
Wang, Q., Zou, M.-H., 2018. Measurement of Reactive Oxygen Species (ROS) and Mitochondrial ROS in AMPK Knockout Mice Blood Vessels. Methods Mol. Biol. Clifton NJ 1732, 507–517. https://doi.org/10.1007/978-1-4939-7598-3_32
Wang, Q.-S., Liang, C., Niu, N., Yang, X., Chen, X., Song, B.-L., Yu, C.-J., Wu, M.-M., Zhang, Z.-R., Ma, H.-P., 2018. Palmitate Stimulates the Epithelial Sodium Channel by Elevating Intracellular Calcium, Reactive Oxygen Species, and Phosphoinositide 3-Kinase Activity. Oxid. Med. Cell. Longev. 2018, 7560610. https://doi.org/10.1155/2018/7560610
Wang, Y.-H., Wang, D.-R., Guo, Y.-C., Liu, J.-Y., Pan, J., 2020. The application of bone marrow mesenchymal stem cells and biomaterials in skeletal muscle regeneration. Regen. Ther. 15, 285–294. https://doi.org/10.1016/j.reth.2020.11.002
Webster, C., Silberstein, L., Hays, A.P., Blau, H.M., 1988. Fast muscle fibers are preferentially affected in Duchenne muscular dystrophy. Cell 52, 503–513. https://doi.org/10.1016/0092-8674(88)90463-1
Wei, C.-D., Li, Y., Zheng, H.-Y., Tong, Y.-Q., Dai, W., 2013. Palmitate induces H9c2 cell apoptosis by increasing reactive oxygen species generation and activation of the ERK1/2 signaling pathway. Mol. Med. Rep. 7, 855–861. https://doi.org/10.3892/mmr.2013.1276
Wei, W., Ji, S., 2018. Cellular senescence: Molecular mechanisms and pathogenicity. J. Cell. Physiol. 233, 9121–9135. https://doi.org/10.1002/jcp.26956
Weisgraber, K.H., 1994. Apolipoprotein E: structure-function relationships. Adv. Protein Chem. 45, 249–302. https://doi.org/10.1016/s0065-3233(08)60642-7
Weisleder, N., Brotto, M., Komazaki, S., Pan, Z., Zhao, X., Nosek, T., Parness, J., Takeshima, H., Ma, J., 2006. Muscle aging is associated with compromised Ca2+ spark signaling and segregated intracellular Ca2+ release. J. Cell Biol. 174, 639–645. https://doi.org/10.1083/jcb.200604166
Weiss, D.J., Casale, G.P., Koutakis, P., Nella, A.A., Swanson, S.A., Zhu, Z., Miserlis, D., Johanning, J.M., Pipinos, I.I., 2013. Oxidative damage and myofiber

degeneration in the gastrocnemius of patients with peripheral arterial disease. J. Transl. Med. 11, 230. https://doi.org/10.1186/1479-5876-11-230
Weist, M.R., Wellington, M.S., Bermudez, J.E., Kostrominova, T.Y., Mendias, C.L., Arruda, E.M., Larkin, L.M., 2013. TGF-β1 enhances contractility in engineered skeletal muscle. J. Tissue Eng. Regen. Med. 7, 562–571. https://doi.org/10.1002/term.551
Westerblad, H., Bruton, J.D., Katz, A., 2010. Skeletal muscle: energy metabolism, fiber types, fatigue and adaptability. Exp. Cell Res. 316, 3093–3099. https://doi.org/10.1016/j.yexcr.2010.05.019
Wilkins, J.T., Krivickas, L.S., Goldstein, R., Suh, D., Frontera, W.R., 2001. Contractile properties of adjacent segments of single human muscle fibers. Muscle Nerve 24, 1319–1326. https://doi.org/10.1002/mus.1150
Witt, R., Weigand, A., Boos, A.M., Cai, A., Dippold, D., Boccaccini, A.R., Schubert, D.W., Hardt, M., Lange, C., Arkudas, A., Horch, R.E., Beier, J.P., 2017. Mesenchymal stem cells and myoblast differentiation under HGF and IGF-1 stimulation for 3D skeletal muscle tissue engineering. BMC Cell Biol. 18, 15. https://doi.org/10.1186/s12860-017-0131-2
Woll, K.A., Van Petegem, F., 2022. Calcium-release channels: structure and function of IP3 receptors and ryanodine receptors. Physiol. Rev. 102, 209–268. https://doi.org/10.1152/physrev.00033.2020
Wu, C., Luo, J., Liu, Y., Fan, J., Shang, X., Liu, R., Ye, C., Yang, J., Cao, H., 2021. Doxorubicin suppresses chondrocyte differentiation by stimulating ROS production. Eur. J. Pharm. Sci. Off. J. Eur. Fed. Pharm. Sci. 167, 106013. https://doi.org/10.1016/j.ejps.2021.106013
Xia, R., Ganther, H.E., Egge, A., Abramson, J.J., 2004. Selenium compounds modulate the calcium release channel/ryanodine receptor of rabbit skeletal muscle by oxidizing functional thiols. Biochem. Pharmacol. 67, 2071–2079. https://doi.org/10.1016/j.bcp.2004.02.018
Xie, L., Zheng, W., Xin, N., Xie, J.-W., Wang, T., Wang, Z.-Y., 2012. Ebselen inhibits iron-induced tau phosphorylation by attenuating DMT1 up-regulation and cellular iron uptake. Neurochem. Int. 61, 334–340. https://doi.org/10.1016/j.neuint.2012.05.016
Xu, P., Werner, J.-U., Milerski, S., Hamp, C.M., Kuzenko, T., Jähnert, M., Gottmann, P., de Roy, L., Warnecke, D., Abaei, A., Palmer, A., Huber-Lang, M., Dürselen, L., Rasche, V., Schürmann, A., Wabitsch, M., Knippschild, U., 2018. Diet-Induced Obesity Affects Muscle Regeneration After Murine Blunt Muscle Trauma-A Broad Spectrum Analysis. Front. Physiol. 9, 674. https://doi.org/10.3389/fphys.2018.00674
Yablonka-Reuveni, Z., Rivera, A.J., 1994. Temporal expression of regulatory and structural muscle proteins during myogenesis of satellite cells on isolated adult rat fibers. Dev. Biol. 164, 588–603. https://doi.org/10.1006/dbio.1994.1226
Yablonka-Reuveni, Z., Seger, R., Rivera, A.J., 1999. Fibroblast growth factor promotes recruitment of skeletal muscle satellite cells in young and old rats. J. Histochem. Cytochem. Off. J. Histochem. Soc. 47, 23–42. https://doi.org/10.1177/002215549904700104
Yakushkin, V.V., Tsibulsky, V.P., 1998. Binding of apoB-containing lipoproteins from unfractionated human blood sera to immobilized LDL receptor. Biochem. Biokhimiia 63, 1164–1171.
Yamaguchi, T., Miki, Y., Yoshida, K., 2007. Protein kinase C delta activates IkappaB-kinase alpha to induce the p53 tumor suppressor in response to oxidative

stress. Cell. Signal. 19, 2088–2097. https://doi.org/10.1016/j.cellsig.2007.06.002
Yang, F., Teves, S.S., Kemp, C.J., Henikoff, S., 2014. Doxorubicin, DNA torsion, and chromatin dynamics. Biochim. Biophys. Acta 1845, 84–89. https://doi.org/10.1016/j.bbcan.2013.12.002
Yang, J., 2019. The role of reactive oxygen species in angiogenesis and preventing tissue injury after brain ischemia. Microvasc. Res. 123, 62–67. https://doi.org/10.1016/j.mvr.2018.12.005
Yang, J., Cao, R.Y., Gao, R., Mi, Q., Dai, Q., Zhu, F., 2017. Physical Exercise Is a Potential “Medicine” for Atherosclerosis. Adv. Exp. Med. Biol. 999, 269–286. https://doi.org/10.1007/978-981-10-4307-9_15
Yang, M., Wei, D., Mo, C., Zhang, J., Wang, X., Han, X., Wang, Z., Xiao, H., 2013. Saturated fatty acid palmitate-induced insulin resistance is accompanied with myotube loss and the impaired expression of health benefit myokine genes in C2C12 myotubes. Lipids Health Dis. 12, 104. https://doi.org/10.1186/1476-511X-12-104
Yang, Z.J.P., Broz, D.K., Noderer, W.L., Ferreira, J.P., Overton, K.W., Spencer, S.L., Meyer, T., Tapscott, S.J., Attardi, L.D., Wang, C.L., 2015. p53 suppresses muscle differentiation at the myogenin step in response to genotoxic stress. Cell Death Differ. 22, 560–573. https://doi.org/10.1038/cdd.2014.189
Yaren, H., Mollaoglu, H., Kurt, B., Korkmaz, A., Oter, S., Topal, T., Karayilanoglu, T., 2007. Lung toxicity of nitrogen mustard may be mediated by nitric oxide and peroxynitrite in rats. Res. Vet. Sci. 83, 116–122. https://doi.org/10.1016/j.rvsc.2006.11.004
Yin, H., Price, F., Rudnicki, M.A., 2013. Satellite cells and the muscle stem cell niche. Physiol. Rev. 93, 23–67. https://doi.org/10.1152/physrev.00043.2011
Yokoyama, S., 1998. Apolipoprotein-mediated cellular cholesterol efflux. Biochim. Biophys. Acta 1392, 1–15. https://doi.org/10.1016/s0005-2760(98)00032-0
Yoshida, T., Delafontaine, P., 2020. Mechanisms of IGF-1-Mediated Regulation of Skeletal Muscle Hypertrophy and Atrophy. Cells 9, E1970. https://doi.org/10.3390/cells9091970
Yu, G., Luo, H., Zhang, N., Wang, Y., Li, Y., Huang, H., Liu, Y., Hu, Y., Liu, H., Zhang, J., Tang, Y., Huang, Y., 2019. Loss of p53 Sensitizes Cells to Palmitic Acid-Induced Apoptosis by Reactive Oxygen Species Accumulation. Int. J. Mol. Sci. 20, E6268. https://doi.org/10.3390/ijms20246268
Yu, T.-Y., Pang, J.-H.S., Lin, L.-P., Cheng, J.-W., Liu, S.-J., Tsai, W.-C., 2021. Platelet-Rich Plasma Releasate Promotes Early Healing in Tendon After Acute Injury. Orthop. J. Sports Med. 9, 2325967121990377. https://doi.org/10.1177/2325967121990377
Yuzefovych, L., Wilson, G., Rachek, L., 2010. Different effects of oleate vs. palmitate on mitochondrial function, apoptosis, and insulin signaling in L6 skeletal muscle cells: role of oxidative stress. Am. J. Physiol. Endocrinol. Metab. 299, E1096-1105. https://doi.org/10.1152/ajpendo.00238.2010
Yuzefovych, L.V., Solodushko, V.A., Wilson, G.L., Rachek, L.I., 2012. Protection from palmitate-induced mitochondrial DNA damage prevents from mitochondrial oxidative stress, mitochondrial dysfunction, apoptosis, and impaired insulin signaling in rat L6 skeletal muscle cells. Endocrinology 153, 92–100. https://doi.org/10.1210/en.2011-1442
Zammit, P.S., 2017. Function of the myogenic regulatory factors Myf5, MyoD, Myogenin and MRF4 in skeletal muscle, satellite cells and regenerative

myogenesis. Semin. Cell Dev. Biol. 72, 19–32. https://doi.org/10.1016/j.semcdb.2017.11.011
Zammit, P.S., Golding, J.P., Nagata, Y., Hudon, V., Partridge, T.A., Beauchamp, J.R., 2004. Muscle satellite cells adopt divergent fates: a mechanism for self-renewal? J. Cell Biol. 166, 347–357. https://doi.org/10.1083/jcb.200312007
Zammit, P.S., Heslop, L., Hudon, V., Rosenblatt, J.D., Tajbakhsh, S., Buckingham, M.E., Beauchamp, J.R., Partridge, T.A., 2002. Kinetics of myoblast proliferation show that resident satellite cells are competent to fully regenerate skeletal muscle fibers. Exp. Cell Res. 281, 39–49. https://doi.org/10.1006/excr.2002.5653
Zammit, P.S., Relaix, F., Nagata, Y., Ruiz, A.P., Collins, C.A., Partridge, T.A., Beauchamp, J.R., 2006. Pax7 and myogenic progression in skeletal muscle satellite cells. J. Cell Sci. 119, 1824–1832. https://doi.org/10.1242/jcs.02908
Zapata, J.C., Cox, D., Salvato, M.S., 2014. The Role of Platelets in the Pathogenesis of Viral Hemorrhagic Fevers. PLoS Negl. Trop. Dis. 8, e2858. https://doi.org/10.1371/journal.pntd.0002858
Zhang, S.H., Reddick, R.L., Piedrahita, J.A., Maeda, N., 1992. Spontaneous hypercholesterolemia and arterial lesions in mice lacking apolipoprotein E. Science 258, 468–471. https://doi.org/10.1126/science.1411543
Zhao, Y., Qu, H., Wang, Y., Xiao, W., Zhang, Y., Shi, D., 2020. Small rodent models of atherosclerosis. Biomed. Pharmacother. Biomedecine Pharmacother. 129, 110426. https://doi.org/10.1016/j.biopha.2020.110426
Zhao, Y., Yang, Y., Xing, R., Cui, X., Xiao, Y., Xie, L., You, P., Wang, T., Zeng, L., Peng, W., Li, D., Chen, H., Liu, M., 2018. Hyperlipidemia induces typical atherosclerosis development in Ldlr and Apoe deficient rats. Atherosclerosis 271, 26–35. https://doi.org/10.1016/j.atherosclerosis.2018.02.015
Zheng, F., Cai, Y., 2019. Concurrent exercise improves insulin resistance and nonalcoholic fatty liver disease by upregulating PPAR-γ and genes involved in the beta-oxidation of fatty acids in ApoE-KO mice fed a high-fat diet. Lipids Health Dis. 18, 6. https://doi.org/10.1186/s12944-018-0933-z
Zheng, M., Wei, J., Tang, Y., Yang, C., Wei, Y., Yin, X., Liu, Q., 2014. ApoE-deficient promotes blood-brain barrier disruption in experimental autoimmune encephalomyelitis via alteration of MMP-9. J. Mol. Neurosci. MN 54, 282–290. https://doi.org/10.1007/s12031-014-0291-x
Zhou, L., Lu, R., Huang, C., Lin, D., 2021. Taurine Protects C2C12 Myoblasts From Impaired Cell Proliferation and Myotube Differentiation Under Cisplatin-Induced ROS Exposure. Front. Mol. Biosci. 8, 685362. https://doi.org/10.3389/fmolb.2021.685362
Zipper, H., Brunner, H., Bernhagen, J., Vitzthum, F., 2004. Investigations on DNA intercalation and surface binding by SYBR Green I, its structure determination and methodological implications. Nucleic Acids Res. 32, e103. https://doi.org/10.1093/nar/gnh101
Zuo, L., Shiah, A., Roberts, W.J., Chien, M.T., Wagner, P.D., Hogan, M.C., 2013. Low Po_2 conditions induce reactive oxygen species formation during contractions in single skeletal muscle fibers. Am. J. Physiol. Regul. Integr. Comp. Physiol. 304, R1009-1016. https://doi.org/10.1152/ajpregu.00563.2012
Zurer, I., Hofseth, L.J., Cohen, Y., Xu-Welliver, M., Hussain, S.P., Harris, C.C., Rotter, V., 2004. The role of p53 in base excision repair following genotoxic stress. Carcinogenesis 25, 11–19. https://doi.org/10.1093/carcin/bgg186